

“If I have seen further, it is by standing on the shoulders of giants.”

-Sir Isaac Newton

University of Alberta

Transcriptional regulation of vascular patterning in *Arabidopsis thaliana*

by

Tyler James Donner

A thesis submitted to the Faculty of Graduate Studies and Research
in partial fulfillment of the requirements for the degree of

Doctor of Philosophy

in

Molecular Biology and Genetics

Department of Biological Sciences

©Tyler Donner
Spring 2013
Edmonton, Alberta

Permission is hereby granted to the University of Alberta Libraries to reproduce single copies of this thesis and to lend or sell such copies for private, scholarly or scientific research purposes only. Where the thesis is converted to, or otherwise made available in digital form, the University of Alberta will advise potential users of the thesis of these terms.

The author reserves all other publication and other rights in association with the copyright in the thesis and, except as herein before provided, neither the thesis nor any substantial portion thereof may be printed or otherwise reproduced in any material form whatsoever without the author's prior written permission.

DEDICATION

This thesis is dedicated to my grandfather, Robert H. Donner (1913-2003), who emphasized the value of education and knowledge, and who fostered my curiosity for the world around me.

ABSTRACT

The plant vascular system is a network of vascular strands that transport nutrients and signals. Some of these signals control the development of non-vascular tissues surrounding vascular strands; some others coordinate the development of new branches, leaves, and flowers with that of new roots. Thus, understanding how vascular strands form may provide understanding of how tissues and organs are formed and how their formation is integrated within the organism. Available evidence implicates the plant signaling molecule auxin in the control of vascular strand formation, but the molecular details of auxin's action in this process remain unclear. Leaves are an attractive system to study the mechanisms controlling vascular strand formation because in leaf development strands of vascular cells appear from within a population of seemingly identical cells. Within this population, however, only vascular precursor cells initiate expression of the *ARABIDOPSIS THALIANA HOMEBOX8 (ATHB8)* gene. Under both normal and experimental conditions, domains of *ATHB8* expression accurately predict sites of vascular strand formation, suggesting that the mechanisms that control vascular strand formation act prior to initiation of *ATHB8* expression. If initiation of *ATHB8* expression identifies the termination of the vascular patterning process, identification of the regulatory elements required for expression of *ATHB8* and similarly expressed genes, and identification of the transcription factors binding to these regulatory elements, should identify transcriptional controls of leaf vascular patterning. Here I identify three *Arabidopsis* genes whose initiation of expression overlaps with initiation of *ATHB8* expression during leaf vascular development.

Further, I show that for three of these four early vascular genes, including *ATHB8*, initiation of expression depends on different regulatory elements, suggesting that early vascular gene expression is controlled by different regulatory pathways. Finally, I identify the regulatory pathway that initiates *ATHB8* expression and contributes to vascular strand formation. My findings define molecular identities of early vascular cells, transcriptional controls of early vascular gene expression, and molecular inputs of auxin signal transduction in leaf vascular patterning.

ACKNOWLEDGEMENTS

This work could not have been accomplished without the contributions of many other people.

I thank Steffen Vanneste and Tom Beeckman for the opportunity to collaborate on the *CYCA2* project and for making it such a pleasant experience. For kindly providing seeds and plasmids, I thank the Arabidopsis Biological Resource Center, Thomas Berleth, Robert Campbell, Taku Demura, David Galbraith, Jim Mattsson, Ben Scheres, Mathias Schuetz, Roger Tsien, and Jian Xu. I thank Dolf Weijers for generously sharing unpublished material and results. I thank Ben Nilsson for technical help. I thank Thomas Berleth, Osama Odat, and Megan Sawchuk for critically reading parts of this thesis. I thank all the authors of the papers derived from this thesis for their kind permission to include here those published works. I thank the Natural Sciences and Engineering Research Council of Canada for Canada Graduate Scholarships at the Master's and Doctoral level and the Alberta Ingenuity Fund (now Alberta Innovates) for a Student Scholarship.

I thank Dr. Enrico Scarpella for giving me the opportunity to join his lab. His guidance and mentoring has made me into the scientist that I am today, and the support, time, and attention to detail that he devotes to all of his students motivates me to strive to follow in his footsteps. I enjoyed our conversations on the many, varied topics that tend to arise in the lab and will miss the stimulating discussions that always followed.

I thank the members of my supervisory committee, Dr Andrew Waskiewicz and Dr. Michael Deyholos, for their support and advice throughout my time at the University of Alberta.

My fellow graduate students in the Scarpella lab have all grown from colleagues to close friends and I thank them for the major roles that they played in helping me to put this thesis together. In alphabetical order: Carla, though we have not had a lot of time to interact, for the enjoyable discussions and pleasant time together in the lab; Ira, for his many long hours working on the *ATHB8*

story, introducing me to the wonders of CBC Radio, and being the wonderfully quirky fellow that always entertained us in the lab; Jason, for his dedication to the *SHR* story and the stories that are still yet to come, for the many laughs on the “Married Man Bench”, and for being a fellow “Grumpy Old Man”; Megan, for the laughs during late nights of potting and for always being willing to listen or lend a hand; and Osama, the third member of the “Married Man Bench”, for his sense of humour and his willingness to listen.

My family has played a tremendous role in my life, and I am grateful for everything that they have done for me. I thank my parents for making me who I am today, always being there to listen, and their love and support. I thank my sister, Jana, for always listening and for her support and advice. I also thank my cousin, Rob, for being the big brother I never had and someone I continue to look up to.

My friends have always been a tremendous source of support, laughter, and insightful discussions during my studies. In alphabetical order: Courtney, Jeremy, Kaleb, Michael, Pearl, Rob, and Ryan. I also thank the Greenwood and Nygren families for always being so welcoming and kind.

During my education I was inspired by many excellent teachers. In particular, I thank Mr. Bob Lanman for his sense of humour and Dr. Pliny Hayes for his intellectual challenges, entertaining conversations, and sage advice.

Finally, I thank my wife, Alison, for being by my side during my studies. Her patience, support, humour, and love have carried me through all of the challenges I faced during the past seven years and made me a better person in the process. This would not have been possible without her, and I look forward to exploring many new challenges with her in the future.

5.2 Materials and methods.....	137
5.2.1 Vector construction.....	137
5.2.2 Plant material and growth conditions.....	137
5.2.3 Microscopy and image analysis.....	137
5.2.4 Bioinformatics.....	137
5.3 Results and discussion.....	142
5.3.1 Early vein expression of <i>CYCA2;1</i> and <i>CYCA2;4</i> in <i>Arabidopsis</i> leaves.....	142
5.3.2 Expression of <i>CYCA2;1</i> and <i>CYCA2;4</i> at preprocambial stages of vein development.....	146
5.3.3 <i>Cis</i> -regulation of <i>CYCA2;1</i> preprocambial expression	148
5.3.4 <i>Cis</i> -regulation of <i>CYCA2;4</i> preprocambial expression	150
5.3.5 Conserved regulatory motifs in preprocambial elements of <i>CYCA2;1</i> and <i>CYCA2;4</i>	150
5.3.6 Transcriptional regulation of preprocambial expression	154
Chapter 6: Conclusions and perspectives.....	157
6.1 Regulatory elements required for gene expression at early stages of leaf vascular development.....	158
6.2 Transcription factors required for gene expression at early stages of leaf vascular development.....	162
6.3 Functions of genes expressed at early stages of leaf vascular development.....	164
Bibliography.....	169

LIST OF TABLES

Chapter 2

Table 2.1	Sequences of primers used in this study.....	20
Table 2.2	Reproducibility indices and the features used as criteria in their calculation.....	31
Table 2.3	Phenotype distribution of mature vein patterns.....	37
Table 2.4	Incidence of leaf fusion.....	39

Chapter 3

Table 3.1	Sequences of primers used in this study.....	75
-----------	--	----

Chapter 4

Table 4.1	Analysis of stomatal phenotypes of various mutant combinations	101
Table 4.2	Sequences of primers used in this study	103

Chapter 5

Table 5.1	Sequences of primers used in this study.....	138
Table 5.2	Origin and nature of lines.....	141

LIST OF FIGURES

Chapter 1

Figure 1.1	The plant vascular system.....	2
Figure 1.2	Cellular auxin transport and the chemiosmotic hypothesis.....	5
Figure 1.3	Auxin-mediated gene expression.....	8

Chapter 2

Figure 2.1	Leaf vascular development in <i>Arabidopsis athb8</i>	29
Figure 2.2	PIN1 expression in wild-type and <i>athb8</i> leaf development.....	30
Figure 2.3	Auxin transport and response in <i>athb8</i> leaves.....	43
Figure 2.4	Responses of vascular patterns to auxin transport inhibition in wild-type and <i>athb8</i> first leaves.....	44
Figure 2.5	<i>ATHB8</i> expression in leaf development.....	46
Figure 2.6	<i>ATHB8</i> expression at the leaf hydathode.....	47
Figure 2.7	Expression of HTA6:EYFP under control of the -47 35S promoter of the cauliflower mosaic virus in 4-DAG seedlings.....	49
Figure 2.8	Scale diagram of <i>ATHB8</i> promoter fragments analyzed in this study.....	50
Figure 2.9	Leaf expression conferred by <i>ATHB8</i> promoter deletions.....	51
Figure 2.10	Leaf expression conferred by mutated versions of the <i>ATHB8</i> promoter.....	54
Figure 2.11	Auxin responsiveness of <i>ATHB8</i> promoter sequences in the leaf.....	55
Figure 2.12	Control of <i>ATHB8</i> leaf preprocambial expression.....	57
Figure 2.13	Genetic interaction between <i>mp</i> and <i>athb8</i>	60
Figure 2.14	Responsiveness of leaves of <i>mp</i> and <i>athb8</i> mutant combinations to auxin transport inhibition.....	62
Figure 2.15	Summary and perspectives.....	70

Chapter 3

Figure 3.1	Vein development in the <i>Arabidopsis</i> first leaf.....	78
------------	--	----

Figure 3.2	Marker expression in seedling organs.....	80
Figure 3.3	Additional expression patterns of J2501 in leaves.....	81
Figure 3.4	<i>ATHB8</i> and <i>SHR</i> expression in first leaf development.....	83
Figure 3.5	Stage-specific <i>SHR</i> expression in leaf vein development.....	85
Figure 3.6	<i>SHR</i> and <i>ATHB8</i> expression in auxin transport-inhibited leaves	88
Figure 3.7	<i>SHR</i> expression in first leaves.....	90
Figure 3.8	<i>SCL29</i> and <i>SCL32</i> expression in first leaves.....	91

Chapter 4

Figure 4.1	Molecular characterisation of <i>cyca2</i> mutant alleles.....	100
Figure 4.2	Expression patterns of <i>CYCA2s</i> in the root.....	109
Figure 4.3	Overview picture of the respective, single, double, triple, and quadraple mutants at the stage of flowering.....	110
Figure 4.4	Root phenotypes of <i>cyca2</i> triple mutants.....	111
Figure 4.5	<i>cyca2</i> triple mutants have defects in cell-cycle progression....	112
Figure 4.6	Quantitative analysis of root apical meristem size.....	113
Figure 4.7	Evolution of <i>CYCA2s</i> expression pattern during early phases of leaf development.....	115
Figure 4.8	Leaf development shows enhanced endoreduplication and slowed down cell-cycle progression in <i>cyca2</i> triple mutants.....	116
Figure 4.9	Evolution of cell number in developing first leaves in WT and <i>cyca2;234</i>	117
Figure 4.10	Expression pattern of <i>CYCA2;2</i> and <i>CYCA2;3</i> in 4-DAG first leaves	119
Figure 4.11	Expression pattern of <i>CYCA2s</i> in serration tips of 8-DAG first leaves.....	120
Figure 4.12	Tissue-specific expression of <i>CYCA2s</i> is required for vascular cell proliferation.....	121
Figure 4.13	Stomatal expression of <i>CYCA2s</i> is required for guard mother cell division.....	123
Figure 4.14	Nuclear contents of guard cells.....	124

Figure 4.15	<i>CYCA2;2</i> , <i>CYCA2;3</i> , <i>CYCA2;4</i> , and <i>CDKB1;1</i> genes synergistically promote guard mother cell symmetric division.....	125
Figure 4.16	Overview picture of Col-0, <i>cdkb1;1</i> , <i>cyca2;234</i> , and <i>cyca2;234 cdkb1;1</i> mutant combinations at the stage of flowering....	126
Figure 4.17	Expression pattern of <i>CYCA2</i> s in the stomatal lineage.....	128
Figure 4.18	FLP/MYB124 and MYB88 are direct repressors of <i>CYCA2;3</i> expression during guard mother cell (GMC) division.....	129
Figure 4.19	Genetic interaction between <i>fama</i> and <i>cyca2;234</i>	130

Chapter 5

Figure 5.1	Expression of <i>CYCA2;1</i> and <i>CYCA2;4</i> in <i>Arabidopsis</i> leaf development.....	143
Figure 5.2	Stage-specific expression of <i>CYCA2;1</i> and <i>CYCA2;4</i> in vein development.....	147
Figure 5.3	Deletion analysis of the <i>CYCA2;1</i> promoter.....	149
Figure 5.4	Deletion analysis of the <i>CYCA2;4</i> promoter.....	151
Figure 5.5	Preprocambial regulatory elements of <i>CYCA2;1</i> and <i>CYCA2;4</i> in <i>Brassicaceae</i> species.....	153
Figure 5.6	Transcriptional regulation of preprocambial expression.....	155

LIST OF ABBREVIATIONS AND NOTATIONS

Abbreviations

2,4-D	2,4-dichlorophenoxyacetic acid
ADP	Adenosine diphosphate
AFB	AUXIN-SIGNALING F-BOX PROTEIN
APC	Anaphase promoting complex
ARE	Auxin Response Element
ARF	AUXIN RESPONSE FACTOR
ARR	ARABIDOPSIS RESPONSE REGULATOR
Asp	Aspartic acid
ATHB	ARABIDOPSIS THALIANA HOMEBOX
AUX/IAA	AUXIN/INDOLE 3-ACETIC ACID
AXR	AUXIN-RESISTANT
BDL	BODENLOS
BES1	BRASSINOSTEROID INSENSITIVE1-ETHYL METHANESULFONATE SUPPRESSOR1
bp	Base pair
CDK	CYCLIN-DEPENDENT KINASE
cDNA	Complementary DNA
ChIP	Chromatin immunoprecipitation
CHS	CHALCONE SYNTHASE
Col	Columbia
CVL	COTYLEDON VASCULAR PATTERN2-LIKE
CVP	COTYLEDON VASCULAR PATTERN
CYC	CYCLIN
DAG	Days After Germination
DAPI	4',6-diamidino-2-phenylindole
DNA	Deoxyribonucleic acid
DOF	DNA-BINDING WITH ONE ZINC FINGER
DR5	Direct Repeat 5

ECFP	ENHANCED CYAN FLUORESCENT PROTEIN
EGFP	ENHANCED GREEN FLUORESCENT PROTEIN
er	Endoplasmic reticulum localization signal
EYFP	ENHANCED YELLOW FLUORESCENT PROTEIN
Fig.	Figure
FLP	FOUR LIPS
G1	Gap1 phase of the cell cycle
G2	Gap2 phase of the cell cycle
GC	Guard cell
GMC	Guard mother cell
Gly	Glycine
GN	GNOM
GR	Glucocorticoid receptor
GRAS	GIBERELIC ACID INSENSITIVE, REPRESSOR OF <i>giberellic acid1-3</i> , and SCARECROW family of transcription factors
GT	GT-ELEMENT BINDING FACTOR
GUS	β -glucuronidase
HD-ZIP	HOMEODOMAIN-LEUCINE ZIPPER
HTA	HISTONE 2A
IAA	Indole-3-acetic acid
<i>Ler</i>	Landsberg <i>erecta</i>
LTI6B	LOW TEMPERATURE INDUCED 6B
LUT	Look-up table
M	Mitosis
mGFP5er	endoplasmic-reticulum-localized mutant GFP variant 5
miR	microRNA
MP	MONOPTEROS
MPF	MITOSIS PROMOTING FACTOR
MS	Murashige and Skoog
MYB	MYELOBLASTOSIS
NPA	1-N-naphthylphthalamic acid

Nuc	Nuclear localization signal
PCR	Polymerase chain reaction
PID	PINOID
PIN	PIN-FORMED
Pro	Proline
qPCR	quantitative PCR
REV	REVOLUTA
RT	reverse transcriptase
S	Synthesis phase of the cell cycle
SBF	SILENCER-BINDING FACTOR
SCL	SCARECROW-LIKE
SGC	Single guard cell
SHR	SHORT-ROOT
SKP	S-PHASE KINASE ASSOCIATED PROTEIN
SMT	STEROLMETHYLTRANSFERASE
ST	Serration tips
TC	Transcription complex
T-DNA	Transfer-DNA
TIR	TRANSPORT INHIBITOR RESPONSE
TMM	TOO MANY MOUTHS
UBQ	UBIQUITIN
VAB	VAN3-BINDING PROTEIN
VAN	VASCULAR NETWORK
VH	Vascular hypertrophy
WOL	WOODEN LEG
WT	Wild-type

Gene and protein notation

MP	Wild-type protein
mp	Mutant protein
<i>MP</i>	Wild-type gene
<i>mp</i>	Mutant gene

Gene fusion notation

Doubled colons (::) are used to indicate transcriptional fusions and single colons (:) are used to indicate translational fusions. *E.g.*, in *ATHB8::HTA6:EYFP*, the *ATHB8* promoter is being used to drive a translational fusion between HTA6 and EYFP.

CHAPTER 1: GENERAL INTRODUCTION

1.1 THE PLANT VASCULAR SYSTEM

The vascular system of plants is a network of continuous vascular strands (Esau, 1965; Fig. 1.1). Mature vascular strands are cylinders of longitudinally juxtaposed xylem and phloem—the two vascular tissues—each composed of specialized vascular cell types. Xylem mainly transports water and minerals from the root, which absorbs them from the soil, to the leaf, where water evaporates creating a negative pressure that drives xylem transport (Taiz and Zeiger, 2006). Phloem mainly transports photosynthesis products from source tissues, such as the leaf, to sink tissues, such as the roots (Taiz and Zeiger, 2006). In addition to water and nutrients, vascular tissues transport signaling molecules with developmental functions from their sites of synthesis to target tissues located either a few cells away or at the opposite side of the plant (Berleth and Sachs, 2001). Finally, in addition to their transport function, vascular tissues provide mechanical support to the plant body (Esau, 1965).

All mature vascular cells derive from the differentiation of procambial cells: elongated vascular-precursor cells characteristically arranged in continuous files (Esau, 1965). Strands of procambial cells are formed *de novo* during embryogenesis and during the post-embryonic formation of lateral organs such as leaves (Sections 1.3 and 1.4, respectively, and references therein). During post-embryonic growth of the plant by lengthening—or primary growth—existing procambial strands are extended either by addition of new vascular cells at one end of the existing strand, as in the root, or by intercalary cell division within the strand, as in the leaf (Larson, 1975). In plants that undergo post-embryonic growth by thickening—or secondary growth—a layer of undifferentiated procambial cells remain between the xylem and phloem of each mature vascular strand (Esau, 1965). During secondary growth, these procambial cells resume division, adding new xylem to one side of the vascular strand and new phloem to the other.

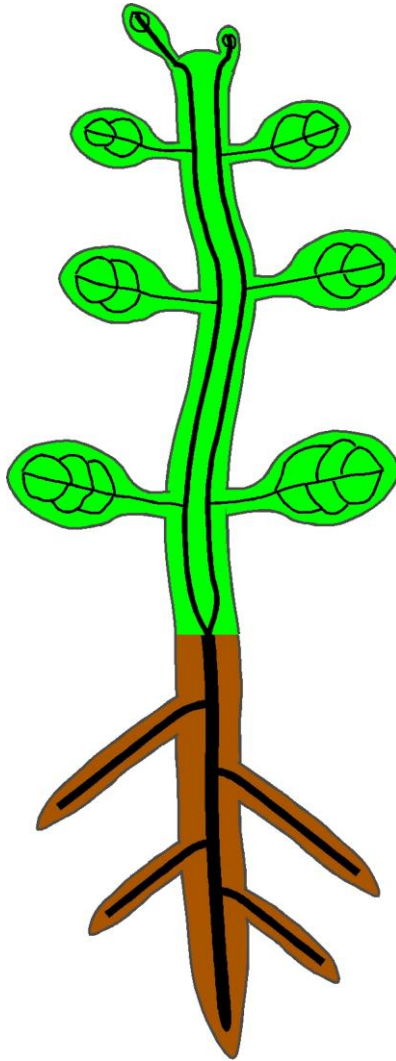


Figure 1.1. The plant vascular system. Plant vascular tissues (black) form a continuous network that extends through the entire body of the plant, innervating all organs of the plant from the shoot (green) to the root (brown).

1.2 AUXIN-INDUCED VASCULAR STRAND FORMATION

The plant signaling molecule auxin is unique among the molecules that promote vascular differentiation because it is the only one that can align such differentiation along continuous lines to form vascular strands, a response with characteristic properties (Berleth *et al.*, 2000; Sachs, 1981). First, the response is local, as auxin-induced vascular strands form in plant tissues at sites of auxin application. Second, it is continuous, as it induces the formation of uninterrupted files of vascular cells. Third, it is radially restricted, as only narrow strips of cells are induced to differentiate into vascular strands. Fourth, it is polar, as auxin-induced vascular strands connect to pre-existing vascular strands located basal to the site of auxin application. Fifth, it is dependent on the transport of auxin, as it is induced by polarly transported auxins and is obstructed by polar auxin transport inhibitors (Berleth *et al.*, 2000; Sachs, 1981). These properties are consistent with predictions made by the canalization hypothesis, which postulates positive feedback between polar auxin transport through a cell and the cell's capacity to transport auxin (Sachs, 1981; Sachs, 1991). According to the canalization hypothesis, upon auxin application, existing vascular strands will drain auxin from the neighbouring cells. As auxin moves through these cells to enter the vascular strands, it feeds back on the cells' capacity to transport auxin, thus making these cells better auxin-transporters. These specialized cells will in turn drain auxin from the cells above them, which will induce them to become better auxin-transporters. Eventually, continuous files of auxin-transporting cells will differentiate into vascular strands connecting the applied auxin to the pre-existing vascular strands (Sachs, 1981; Sachs, 1991). The polarity of auxin-induced vascular differentiation suggests that the underlying mechanism recruits a polar signal already present in plants, and the dependence of auxin-induced vascular differentiation on auxin transport suggests that this polar signal is, in fact, the polar transport of auxin itself.

Auxin is mostly synthesized in young, apical tissues, such as leaf and flower primordia, and is primarily transported basally through vascular strands towards the roots (Michniewicz *et al.*, 2007; Normanly, 2010). The main form of

auxin in plants, indole-3-acetic acid (IAA), is a weak acid (Fig. 1.2). When IAA is in the slightly more acidic intercellular space, it remains protonated and non-polar, allowing it to readily diffuse through the plasma membrane of plant cells. Upon entering the slightly more basic cytoplasm, IAA becomes deprotonated and negatively charged, preventing it from exiting the cytoplasm by diffusion. The chemiosmotic hypothesis predicts that IAA can only leave cells by active transport through membrane-localized auxin-efflux carrier proteins and that the apical-basal direction of polar auxin transport results from the asymmetric localization of these carrier proteins to the basal sides of auxin-transporting cells (Raven, 1975; Rubery and Shelldrake, 1974).

Of the gene families implicated in cellular auxin efflux, the PIN-FORMED (PIN) family has been strongly linked with apical-basal polar auxin transport (Krecek *et al.*, 2009; Okada *et al.*, 1991). In *Arabidopsis*, five *PIN* genes encode plasma-membrane proteins with redundant functions in cellular export of auxin (Petrasek *et al.*, 2006). Because the subcellular localization of PIN proteins labels sites of cellular auxin efflux, the localization of PIN proteins can be used to infer directions of polar auxin transport (Petrasek and Friml, 2009). Consistent with predictions of the canalization hypothesis, local auxin application induces a broad PIN1 expression domain that connects the site of application to existing vascular strands (Sauer *et al.*, 2006). Over time, these broad PIN1-expression domains narrow to individual cell files which mark sites of future vascular strand formation and in which PIN1 localization suggests polar auxin transport from the site of application towards the pre-existing vascular strands.

1.3 VASCULAR STRAND FORMATION DURING EMBRYOGENESIS

The organization of a plant seedling can be viewed as the apical-basal sequence of pattern elements: the shoot meristem, from which all the above-ground structures of the plant—leaves, stem and branches, flowers and fruits—form; the embryonic leaves, or cotyledons; the embryonic stem, or hypocotyl; the root; and the root meristem, from which the entire root system of the plant forms (Capron *et al.*, 2009). The elements of the seedling pattern are all present for the first time in the

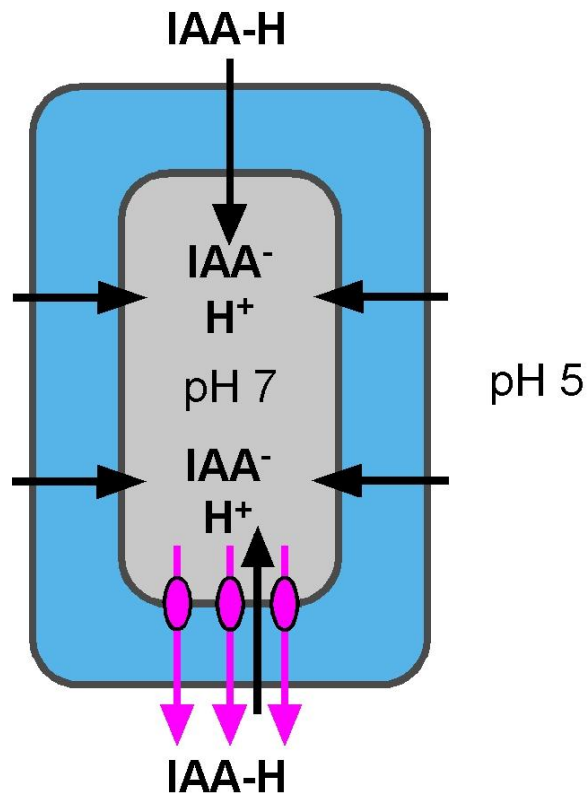


Figure 1.2. Cellular auxin transport and the chemiosmotic hypothesis. At the lower pH of the intercellular space in plants, indole-3-acetic acid (IAA) is protonated (IAA-H), which allows it to easily diffuse across the plasma membrane of the cell (black arrows). Once inside the cell (gray rectangle), the higher pH results in IAA becoming deprotonated (IAA⁻ and H⁺). Because charged IAA⁻ molecules cannot diffuse across the plasma membrane, IAA⁻ can only leave cells by active transport (magenta arrows) through carrier proteins (magenta ovals), and the asymmetric localization of these carrier proteins to the basal side of the cell results in the apical-basal transport of auxin on a tissue and organismal level. See text for additional details. Blue band, cell wall.

heart-stage embryo. However, the centrally located vascular strand visible in the heart-stage embryo—the first vascular strand of the plant—is already present in the centre of the lower half of the early-globular embryo (Capron *et al.*, 2009). The formation of this vascular strand and of the apical-basal sequence of embryo pattern elements appear to be two intimately linked processes that depend on polar auxin transport and auxin signal transduction.

The role of polar auxin transport in regulation of embryonic vascular strand formation and apical-basal embryo patterning was first derived from the results of experiments in which wild-type embryos were cultured in the presence of polar auxin transport inhibitors: in the most severe cases, inhibition of polar auxin transport during embryogenesis led to ball-shaped seedlings completely lacking apical-basal polarity (Friml *et al.*, 2003; Hadfi *et al.*, 1998; Liu *et al.*, 1993). Similar defects were later observed in embryos simultaneously lacking multiple members of the PIN family of auxin transporters (Friml *et al.*, 2003). If embryo apical-basal polarity depends on polar auxin transport (Friml *et al.*, 2003; Hadfi *et al.*, 1998; Liu *et al.*, 1993) and if polar auxin transport depends on polar localization of PIN proteins (Wisniewska *et al.*, 2006), then disruption of polar PIN localization would be expected to lead to defects in embryo apical-basal polarity. The ADP-ribosylation-factor guanine-nucleotide-exchange-factor EMBRYO DEFECTIVE30/GNOM/VASCULAR NETWORK7 (GN hereafter) controls PIN protein localization by regulating the endocytosis of PIN-protein-containing vesicles from the plasma membrane to endosomes that recycle PIN proteins back to the plasma membrane (Geldner *et al.*, 2003; Steinmann *et al.*, 1999). Consistent with predictions based on GN biochemical function, PIN1 proteins are mislocalized in *gn* embryos, and the most severe *gn* seedlings are ball-shaped, similar to those resulting from chemical or genetic disruption of polar auxin transport (Geldner *et al.*, 2003; Mayer *et al.*, 1993; Shevell *et al.*, 1994; Steinmann *et al.*, 1999); moreover, in these ball-shaped seedlings, vascular cells are not arranged in continuous strands but are disconnected from one another and randomly positioned in the innermost region of the seedling (Mayer *et al.*, 1991; Mayer *et al.*, 1993).

The role of auxin signal transduction in embryonic vascular strand formation and apical-basal embryo patterning became first apparent with the isolation of the *auxin-resistant6* (*axr6*), *bodenlos* (*bdl*), and *monopteros* (*mp*) mutants of *Arabidopsis* (Berleth and Jurgens, 1993; Hamann *et al.*, 1999; Hobbie *et al.*, 2000). Mutation of *AXR6*, *BDL*, or *MP* results in embryos in which the central vascular strand is missing and the hypocotyl, root, and root meristem are replaced by an undifferentiated ‘basal peg’ (Berleth and Jurgens, 1993; Hamann *et al.*, 1999; Hobbie *et al.*, 2000). Mutation of these three genes is also associated with defective auxin responses, and the products of all three genes are directly linked to auxin signal transduction (Hamann *et al.*, 1999; Hamann *et al.*, 2002; Hartdke and Berleth, 1998; Hobbie *et al.*, 2000; Mattsson *et al.*, 2003). Auxin signaling is initiated by the binding of intracellular auxin to members of the TIR1/AFB (for TRANSPORT INHIBITOR RESPONSE1/AUXIN SIGNALING F-BOX PROTEIN) family of F-box proteins, which are part of the SKP (for S-PHASE KINASE ASSOCIATED PROTEIN)—AXR6/CULLIN1—F-BOX protein poly-ubiquitination complex (SCF^{TIR1/AFB} hereafter) (Mockaitis and Estelle, 2008; Fig. 1.3). This complex ubiquitinates target proteins to be degraded by the 26S proteasome. The main targets of SCF^{TIR1/AFB}-dependent degradation are members of the AUXIN/INDOLE-3-ACETIC ACID (AUX/IAA) family of transcriptional repressors, of which BDL/IAA12 is a member, and which act as auxin co-receptors with TIR1/AFB proteins (Dharmasiri *et al.*, 2005a; Dharmasiri *et al.*, 2005b; Kepinski and Leyser, 2005; Tan *et al.*, 2007). Auxin acts as a ‘molecular glue’ that strengthens the interaction between TIR1/AFBs and AUX/IAAs which leads to the ubiquitination and degradation of AUX/IAAs (Tan *et al.*, 2007). The auxin-dependent degradation of AUX/IAAs relieves their binding partners, the members of the AUXIN RESPONSE FACTOR (ARF) family of transcription factors—among them, ARF5/MP—from AUX/IAA-mediated repression, thus allowing auxin-responsive gene expression (Tiwari *et al.*, 2003; Ulmasov *et al.*, 1997a; Ulmasov *et al.*, 1997b; Worley *et al.*, 2000). In the absence of auxin, on the other hand, AUX/IAAs repress ARF-mediated gene transcription (Tiwari *et al.*, 2003; Ulmasov *et al.*, 1997b). This repression is

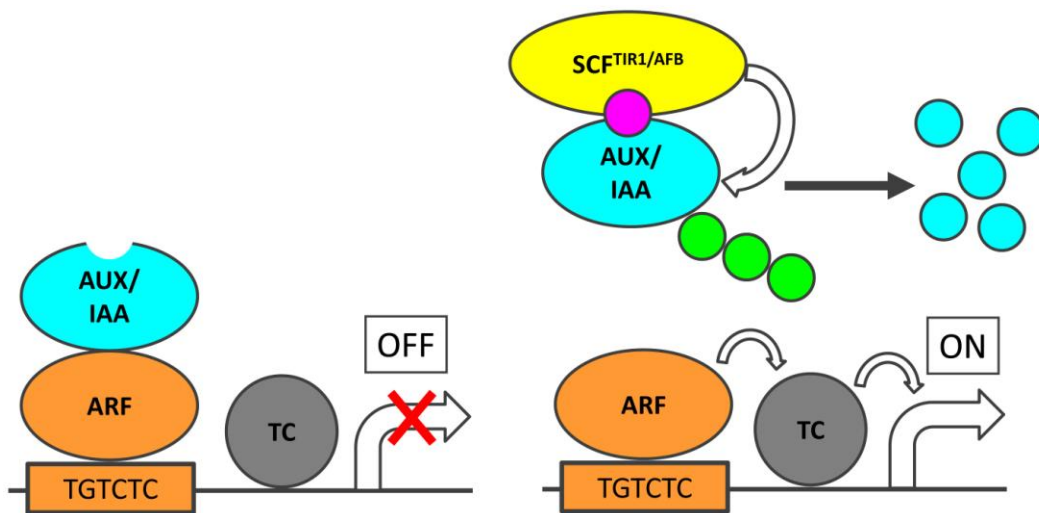


Figure 1.3. Auxin-mediated gene expression. (Left) In the absence of auxin, members of the auxin response factor family of transcription factors (ARF, orange ovals) bind to TGTCTC auxin response elements (orange box) in the promoters of target genes but are prevented from activating gene expression by AUX/IAA repressor proteins (cyan oval). (Right) In the presence of auxin (pink circle), ARF proteins can still bind to auxin response elements, but AUX/IAA repressor proteins act as a co-receptor for auxin with the SCF^{TIR1/AFB} poly-ubiquitination complex (yellow oval). This receptor complex adds ubiquitin molecules (green circles) to the AUX/IAA repressor protein, resulting in the degradation of the AUX/IAA repressor protein and activation of auxin-mediated gene expression through ARF transcription factors. TC, transcription complex.

dependent on four conserved domains—domains I-IV—shared among most of the 29 AUX/IAA proteins of *Arabidopsis* (Reed, 2001). Domain I interacts with TOPLESS and related proteins, which are members of the Groucho/Leunig family of transcriptional co-repressors and recruit chromatin modification complexes to repress gene expression (Long *et al.*, 2006, Szemenyei *et al.*, 2008). Domain II is responsible for the stability of AUX/IAAs, and mutation of a conserved sequence within this domain increases AUX/IAA stability by preventing ubiquitination and subsequent degradation (Mockaitis and Estelle, 2008). Finally, domains III and IV mediate protein-protein interaction between AUX/IAAs and ARFs, which too share these domains (Mockaitis and Estelle, 2008). In addition to mediating interaction with AUX/IAAs, domains III and IV mediate interaction among ARFs (Hardtke *et al.*, 2004; Li *et al.*, 2011; Ulmasov *et al.*, 1999b; Vernoux *et al.*, 2011; and reviewed in Guilfoyle and Hagen, 2012). ARF function depends on two other conserved domains: the first is a DNA-binding domain that binds to Auxin Response Elements (ARE) in the regulatory sequences of target genes (Tiwari *et al.*, 2003; Ulmasov *et al.*, 1999b); the second is a transcriptional activation or repression domain (Tiwari *et al.*, 2003; Ulmasov *et al.*, 1999a). Five of the 22 ARFs in *Arabidopsis*, including MP, behave as transcriptional activators in cell culture assays, while the remaining 17 family members behave as transcriptional repressors (Okushima *et al.*, 2005; Tiwari *et al.*, 2003; Ulmasov *et al.*, 1999a). However, some direct targets of the ‘activating’ ARFs seem to be repressed *in vivo* by these ARFs, suggesting that the results of the cell culture assays have to be interpreted with caution (Zhao *et al.*, 2010).

In summary, available evidence suggests that formation of the central vascular strand of the embryo and of apical-basal embryo polarity is controlled by polar auxin transport and signal transduction.

1.4 VASCULAR STRAND FORMATION IN LEAVES

The vascular network of the leaf is a continuous network of vascular strands that innervates the entire organ (Candela *et al.*, 1999; reviewed in Dengler and Kang, 2001; Nelson and Dengler, 1997). In *Arabidopsis*, the leaf vascular network is

typically composed of a central midvein that extends from the leaf base to its tip; a series of loops that extend from the midvein towards the margin of the leaf and connect to more distal vascular strands; and a reticulum of higher-order vascular strands that extend from pre-existing strands, and can either connect two strands or end freely within the leaf (Nelson and Dengler, 1997). Each of these vascular strands can be first recognized anatomically as continuous files of procambial cells that form from within a seemingly homogeneous population of isodiametric, polygonal ‘ground’ cells (Esau, 1943; Esau, 1965; Foster, 1952); ground cells that will elongate into procambial cells (‘preprocambial’ cells) can be recognized by their selective expression of the *ARABIDOPSIS THALIANA HOMEBOX8* (*ATHB8*) and *SHORT-ROOT* (*SHR*) genes (Gardiner *et al.*, 2011; Kang and Dengler, 2004; Scarpella *et al.*, 2004; Chapter 3). If onset of expression of *ATHB8* and *SHR* defines a reproducible, preprocambial stage of leaf vascular development, experimentally induced alterations of leaf vascular patterns should be foreshadowed by similar alterations in the expression of these genes. Genetic or pharmacological manipulation of leaf development induces alterations in vascular patterns that are preceded by corresponding alterations in expression of *ATHB8* and *SHR*, suggesting that onset of expression of these genes does mark a reproducible, preprocambial stage in leaf vascular development (Alonso-Peral *et al.*, 2006; Carland and Nelson, 2004; Cnops *et al.*, 2006; Gardiner *et al.*, 2010; Gardiner *et al.*, 2011; Hou *et al.*, 2010; Koizumi *et al.*, 2000; Mattsson *et al.*, 1999; Petricka and Nelson, 2007; Pineau *et al.*, 2005; Pullen *et al.*, 2010; Robles *et al.*, 2010; Scarpella *et al.*, 2006; Sieburth, 1999; Chapter 3). Because procambial stages of leaf vascular development seem irresponsive to attempts to manipulate leaf vascular patterns (Mattsson *et al.*, 1999), leaf vascular patterning is likely occurring prior to, and terminating with, the initiation of *ATHB8* and *SHR* expression. The molecular details of the mechanisms that position leaf vascular strands and thus pattern the leaf vascular network are not fully known; however, a growing body of evidence suggests that auxin, particularly its polar transport and signal transduction, plays a central role in leaf vascular strand formation and vascular patterning.

Treatment with polar auxin transport inhibitors induces characteristic changes in leaf vascular patterns (Mattsson *et al.*, 1999, Sieburth, 1999). First, the midvein frequently bifurcates near the leaf tip. Second, more loops are formed and these loops either connect to the midvein at a more acute angle or fail to connect to the midvein altogether and instead run parallel to it, thus giving the impression of a wide midvein. Third, these supernumerary loops merge near the leaf margin to form a broad vascular differentiation band. Fourth, cells within vascular strands are misaligned. Similar, though weaker, vascular pattern defects have been observed in the leaves of *pin1* mutants (Bilsborough *et al.*, 2011; Guenot *et al.*, 2012; Mattsson *et al.*, 1999; Okada *et al.*, 1991), and expression of PIN1 during leaf development is consistent with its function in leaf vascular patterning. Broad, auxin-responsive PIN1-expression domains narrow to sites of vascular strand formation in an auxin-transport-dependent fashion, and patterns of PIN1 expression suggest that vascular strands form through one of two basic ontogenies (Scarpella *et al.*, 2006; Wenzel *et al.*, 2007). The midvein and the lower part of each loop originate in association with convergent points of PIN1 polarity in the epidermis of the leaf. Localization of PIN1 in the epidermis suggests that auxin is transported towards single epidermal cells, in which PIN1 localization is directed towards the centre of the leaf. Broad PIN1-expression domains connect these epidermal convergence points of PIN1 polarity to pre-existing vascular strands. These broad domains eventually narrow to files of PIN1 expressing cells which mark sites of vascular strand formation and in which PIN1 localization is directed towards pre-existing vascular strands. On the other hand, higher-order vascular strands and the upper part of each loop are generated by PIN1 expression domains that form in association with pre-existing vascular strands. These PIN1 expression domains are also initially broad but eventually narrow to sites of vascular strand formation in which PIN1 localization is directed towards pre-existing vascular strands. These domains can end freely within the leaf or connect two existing vascular strands, as in the case of the upper part of each loop, which connects the lower part of the loop to a pre-existing vascular strand (Scarpella *et al.*, 2006; Wenzel *et al.*, 2007).

Continuity of vascular strands is a stringent requirement for the long-distance transport of water, nutrients and signaling molecules carried out by the plant vascular system. In leaves, vascular strand continuity depends on the function of the ADP-ribosylation-factor GTPase-activating-protein FORKED2/SCARFACE/VASCULAR NETWORK3 (VAN3 hereafter) (Carland and Nelson, 2009; Deyholos *et al.*, 2000; Koizumi *et al.*, 2000; Koizumi *et al.*, 2005; Naramoto *et al.*, 2009; Sieburth *et al.*, 2006; Steynen and Schultz, 2003). In *van3* mutants, PIN1 expression domains form normally but become fragmented, consistent with fragmented domains of *ATHB8* expression and sites of vascular strand formation (Deyholos *et al.*, 2000; Koizumi *et al.*, 2000; Naramoto *et al.*, 2009; Scarpella *et al.*, 2006; Sieburth *et al.*, 2006). Similar continuity defects in domains of PIN1 expression and sites of vascular strand formation are also observed in leaves of plants simultaneously mutated in the inositol polyphosphate 5'-phosphatase COTYLEDON VASCULAR PATTERN2 (CVP2) and in the closely related CVP2-LIKE1 (CVL1) (Carland and Nelson 2009; Naramoto *et al.*, 2009). The defects of *cvp2 cvl1* double mutants are enhanced by mutation of *FORKED1/VAN3-BINDING PROTEIN* (VAB hereafter) (Carland and Nelson, 2009; Naramoto *et al.*, 2009), which encodes a protein of unknown biochemical function (Hou *et al.*, 2010; Naramoto *et al.*, 2009). VAN3 is mis-localized in *cvp2 cvl1* and *cvp2 cvl1 vab*, suggesting that CVP2, CVL1, and VAB maintain continuous domains of PIN1 expression through regulation of VAN3 localization (Carland and Nelson, 2009; Koizumi *et al.*, 2005; Naramoto *et al.*, 2009). Continuity of leaf vascular strand seems to depend also on plant sterols as *hydra1* (*hyd1*) or *fackel/hyd2* single mutants and *cvp1/sterol methyltransferase2* (*smt2* hereafter) *smt3* double mutants—all impaired in sterol synthesis—have fragmented leaf vascular strands (Carland *et al.*, 2010; Pullen *et al.*, 2010; Souter *et al.*, 2002); however, it is unknown whether sterols control continuity of PIN1 expression domains.

A role for auxin signal transduction in leaf vascular strand formation can be inferred from the defects of plants in which components of the auxin signaling machinery are disrupted. Loss-of-function mutations in genes predicted to

regulate formation and function of the SCF^{TIR1} complex result in simpler leaf-vascular-networks (Alonso-Peral *et al.*, 2006; Deyholos *et al.*, 2003; reviewed in Mockaitis and Estelle, 2008). Furthermore, *MP*, which is required for the formation of the first vascular strand in the embryo (Berleth and Jurgens, 1993; Hardtke and Berleth, 1998; Section 1.3), is also required for vascular strand formation in leaves: *mp* leaves form fewer and incompletely differentiated vascular strands (Donner *et al.*, 2009; Przemeck *et al.*, 1996; Chapter 2). Conversely, gain-of-function mutations in *MP* that prevent interaction with the repressing AUX/IAA proteins lead to expansion of expression domains of PIN1 and *ATHB8* and hyperproliferation of vascular tissues (Garrett *et al.*, 2012; Krogan *et al.*, 2012). During leaf development, the dynamics of MP expression domains resemble those of PIN1: initially broad but eventually narrowing to sites of vascular strand formation (Donner *et al.*, 2009; Scarpella *et al.*, 2006; Wenzel *et al.*, 2007; Chapter 2). Within broad domains of its expression, MP directly controls initiation of *ATHB8* expression at preprocambial stages of leaf vascular development by binding to an ARE in the *ATHB8* promoter (Donner *et al.*, 2009; Chapter 2).

In summary, the formation of leaf vascular strands and the patterning of the leaf vascular network crucially depend on polar auxin transport and auxin signal transduction.

1.5 SCOPE OF THE THESIS

The purpose of my Ph. D. thesis is to understand the transcriptional controls that underlie vascular patterning. Vascular strands have important regulatory roles in the developmental patterning of plants on both organismal and local levels (Berleth and Sachs, 2001), therefore understanding how vascular strands form can provide insights into how vascular strands pattern the tissues that surround them, how these tissues are integrated into organs, and how the resulting organs are integrated within the organism. Leaves are an attractive system for the study of vascular strand formation development as vascular strands form *de novo* during the growth of the leaf, unlike the extension of root vascular strands by addition of

new vascular cells or of mature leaf vascular strands by intercalary cell divisions within the vascular strand (Larson, 1975). During leaf development, initiation of *ATHB8* expression in isodiametric cells identifies the transition to a preprocambial stage of leaf vascular development, and files of *ATHB8*-expressing preprocambial cells mark sites of vascular strand formation (Kang and Dengler, 2004; Scarpella *et al.*, 2004). Moreover, alterations of leaf vascular patterns by either genetic or chemical means are foreshadowed by corresponding defects in the expression pattern of *ATHB8* (Alonso-Peral *et al.*, 2006; Carland and Nelson, 2004; Cnops *et al.*, 2006; Gardiner *et al.*, 2010; Gardiner *et al.*, 2011; Hou *et al.*, 2010; Koizumi *et al.*, 2000; Mattsson *et al.*, 1999; Petricka and Nelson, 2007; Pineau *et al.*, 2005; Pullen *et al.*, 2010; Robles *et al.*, 2010; Scarpella *et al.*, 2006; Sieburth, 1999; Chapter 3). Therefore, it seems likely that initiation of *ATHB8* expression and the transition to preprocambial stages of leaf vascular development are the first indicators of the final vascular pattern of the leaf and that the mechanisms positioning leaf vascular strands are acting prior to preprocambial stages of vascular development. If termination of the patterning process is marked by initiation of *ATHB8* expression, identification of the regulatory elements required for preprocambial expression and of the transcription factors binding to these elements should identify transcriptional controls of leaf vascular patterning. Therefore, to transcriptional controls of leaf vascular patterning, I set out to identify regulatory elements required for preprocambial expression and the transcription factors that bind them.

To this aim, I first identified new genes expressed at preprocambial stages of leaf vascular development (Donner *et al.*, 2009; Gardiner *et al.*, 2011; Vanneste *et al.*, 2011; Chapters 2, 3, and 4). *ATHB8* expression is initiated in narrow files of preprocambial cells, remains on in procambial cells, and eventually disappears at later stages of leaf vascular development (Donner *et al.*, 2009; Kang *et al.*, 2004, Scarpella *et al.*, 2004; Chapter 2). Like *ATHB8*, *SHR* expression is initiated in narrow files of preprocambial cells and remains on in procambial cells, but unlike that of *ATHB8*, *SHR* expression remains on at later stages of leaf vascular development (Gardiner *et al.*, 2011). Two members of the *CYCA2* gene family,

CYCA2;1 and *CYCA2;4*, are also expressed in preprocambial cells of the leaf (Vanneste *et al.*, 2011; Chapter 4), though their expression differs slightly from that of *ATHB8* and *SHR*. At their initiation, domains of *CYCA2;4* expression are broader than those of *ATHB8*, and *CYCA2;4* expression domains become restricted to narrow cell files and eventually disappears at later stages of leaf vascular development (Donner and Scarpella, 2013; Vanneste *et al.*, 2011; Chapters 4 and 5). *CYCA2;1* expression, on the other hand, is initiated in narrow cell files that already express *ATHB8*, suggesting that *CYCA2;1* expression is initiated after that of *ATHB8*, though like *SHR*, *CYCA2;1* expression remains on at later stages of leaf vascular development (Donner and Scarpella, 2013; Vanneste *et al.*, 2011; Chapters 4 and 5).

In addition to analyzing their expression, I identified functions for three of these four preprocambial genes during leaf vascular development. *ATHB8* is required for stabilizing preprocambial cell specification against the effects of auxin transport inhibition and restricting this specification to narrow fields (Donner *et al.*, 2009; Chapter 2). Further, *ATHB8* coordinates formation of procambium within individual vascular strands (Donner *et al.*, 2009; Chapter 2). *CYCA2;1* and *CYCA2;4* are required redundantly with *CYCA2;2* and *CYCA2;3* for the formation of serration tips and the proliferation of vascular cells at these serration tips (Vanneste *et al.*, 2011; Chapter 4).

For *ATHB8*, *CYCA2;1*, and *CYCA2;4*, I proceeded to identify regulatory elements required for their preprocambial expression. I found that preprocambial expression of *CYCA2;4* requires a 76-bp regulatory element that contains conserved, putative binding sites for transcription factors of the DNA-BINDING WITH ONE ZINC FINGER (DOF), ARABIDOPSIS RESPONSE REGULATOR (ARR), and SILENCER-BINDING FACTOR-1 (SBF-1) families (Donner and Scarpella, 2013; Chapter 5). Further, preprocambial expression of *CYCA2;1* requires a 77-bp regulatory element that contains a conserved, putative binding site for the DOF family of transcription factors. Finally, I identified an ARF binding site in the *ATHB8* promoter that is required for the preprocambial

expression of *ATHB8* and I determined that this element is bound by the ARF transcription factor MP.

In summary, my work has contributed to define the molecular identity of cells at preprocambial stages of leaf vascular development, the function of genes expressed in preprocambial cells, and a transcriptional pathway that controls initiation of gene expression at preprocambial stages of vascular development. These discoveries reveal transcriptional controls of vascular patterning and provide a foundation to understand the central role of vascular tissues in integrating tissue patterning and organ formation during plant growth and development.

CHAPTER 2: REGULATION OF PREPROCAMBIAL CELL STATE ACQUISITION BY AUXIN SIGNALING IN *ARABIDOPSIS* LEAVES ¹

2.1 INTRODUCTION

The vascular system of plants is composed of bundles of cell files that extend and intersect throughout all organs (Esau, 1965). Vascular bundles differentiate from procambial cells: narrow, cytoplasm-dense cells, characteristically arranged in continuous strands (Esau, 1943), which in leaves seem to emerge *de novo* from within the morphologically homogeneous population of apparently naïve ground cells (Foster, 1952; Pray, 1955). Although the molecular details are not entirely clear, a role for the polarly transported plant signaling molecule auxin in the selection of leaf ground cells that will elongate to acquire procambial cell identity has increasingly gained experimental support (Mattsson *et al.*, 1999; Mattsson *et al.*, 2003; Sachs, 1981; Sachs, 1989; Scarpella *et al.*, 2006; Sieburth, 1999; Wenzel *et al.*, 2007). During leaf development, polygonal, isodiametric ground cells are shunted towards procambial fate through induction of broad domains of expression of the PIN-FORMED1 (PIN1) auxin exporter (Scarpella *et al.*, 2006; Wenzel *et al.*, 2007). Decay of PIN1 expression and associated relapse to ground state occur in some of the cells initially expressing PIN1, and domains of PIN1 expression are eventually curtailed to individual files of cells that will stretch into procambial cells (Scarpella *et al.*, 2006; Wenzel *et al.*, 2007). Because formation of leaf vascular bundles, or veins, is reiteratively propagated in leaf development

¹ A version of this chapter has been published. (1) T. J. Donner, I. Sherr, E. Scarpella. (2009). Regulation of preprocambial cell state acquisition by auxin signaling in *Arabidopsis* leaves. *Development*. **136**: 3235-3246. doi: <http://dx.doi.org/10.1242/dev.037028>. Adapted with the kind permission of Development and the Company of Biologists.

Conceived and designed the experiments: TJD, ES. Performed the experiments: TJD, IS, ES. Analyzed the data: TJD, IS, ES. Wrote the paper: TJD, IS, ES.

(2) T. J. Donner, I. Sherr, E. Scarpella. (2010). Auxin signal transduction in *Arabidopsis* vein formation. *Plant Signal Behav.* **5**: 70-72. doi: <http://dx.doi.org/10.4161/psb.5.1.10233>. Reproduced with the kind permission of Plant Signaling and Behavior and Landes Bioscience. Conceived and wrote the paper: TJD, IS, ES.

I generated the data that gave rise to figures: 2.3, 2.5, 2.6, 2.7, 2.8, 2.9, 2.10, 2.11, 2.12, and 2.15.

(Nelson and Dengler, 1997), cells that have reverted to ground state may have other opportunities to assume procambial identity before adopting the alternative mesophyll fate (Scarpella *et al.*, 2004; Scarpella *et al.*, 2006; Wenzel *et al.*, 2007).

While onset of PIN1 expression marks an unstable and reversible state in vein formation, files of PIN1-expressing ground cells that are stabilized towards procambial fate initiate expression of the HOMEODOMAIN-LEUCINE ZIPPER (HD-ZIP) III gene *ARABIDOPSIS THALIANA HOMEODOMAIN-LEUCINE ZIPPER* (*ATHB8*) (Baima *et al.*, 1995; Kang and Dengler, 2004; Sawchuk *et al.*, 2007; Scarpella *et al.*, 2004). Available evidence suggests that *ATHB8* expression identifies a crucial and typically irreversible stage in procambial cell fate acquisition: under both undisturbed and perturbed conditions, adoption of the *ATHB8* ‘preprocambial’ cell state accurately predicts sites of vascular differentiation (Alonso-Peral *et al.*, 2006; Carland and Nelson, 2004; Cnops *et al.*, 2006; Kang and Dengler, 2004; Koizumi *et al.*, 2000; Petricka and Nelson, 2007; Pineau *et al.*, 2005; Sawchuk *et al.*, 2007; Scarpella *et al.*, 2004; Scarpella *et al.*, 2006), and the *ATHB8* preprocambial state is mutually exclusive with a ‘premesophyll’ cell state that presages mesophyll fate assignment (Sawchuk *et al.*, 2008). Whereas the preprocambial state is defined by the onset of *ATHB8* expression, differential *ATHB8* expression is only the object of a cell state transition and therefore does not necessarily provide information about the underlying patterning mechanism. Instead, knowledge of the set of transcription factors that determine initiation of *ATHB8* expression at the correct spatiotemporal coordinates in leaf development might provide insight into how the preprocambial cell state arises at defined positions and stages during leaf development.

Here, we show that *ATHB8* is required to stabilize preprocambial cell specification against auxin transport perturbations, to constrict preprocambial cell state acquisition to narrow zones and to synchronize procambial cell identity assignment within and between veins. Further, we show that *ATHB8* preprocambial expression is directly and positively controlled by the auxin-response transcription factor MONOPTEROS (MP) through an auxin response element in the *ATHB8* promoter. Finally, we show that *ATHB8* functions in vein

formation strictly depend on *MP* activity. Our results suggest a molecular mechanism through which general auxin signal transduction is specifically translated into leaf vascular patterning inputs.

2.2 MATERIALS AND METHODS

2.2.1 Vector construction

Sequences of primers used in this study can be found in Table 2.1. To generate the DR5Rev(9x)::ECFP-Nuc construct, nine copies of the Direct Repeat 5 Reverse sequence (DR5Rev; GAGACAAAAGG) (Ulmasov *et al.*, 1997b) upstream of the -46 cauliflower mosaic virus 35S promoter (Fang *et al.*, 1989) were recombined into the pBGCN (Kubo *et al.*, 2005). To generate the ATHB8::ATHB8:mCherry construct, the mCherry coding sequence (Shaner *et al.*, 2004) was cloned downstream of the fragment of the *ATHB8* gene from -1997 to +4233. Functionality of the construct was tested by transformation into homozygous *athb8-11* plants and by assessing normalization of sensitivity towards 5 μ M NPA (Sigma Aldrich, St Louis, MO, USA) in two independent, single insertion transgenic lines. To generate the *ATHB8* promoter deletion and mutation constructs, amplified fragments were recombined into the pFYTAG vector (Zhang *et al.*, 2005). To generate the MP::MP:ECFP construct, the ECFP coding sequence (Clontech Laboratories, Mountain View, CA, USA) was cloned at position +3815 of the fragment of the *MP* gene from -3311 to +4301. Functionality of the construct was tested by crossing two independent, single-insertion lines to heterozygous *mp*^{U55} plants and by assessing rescue of the root phenotype in the F2 generation. To generate the UBQ10::MP:GR construct, the sequence encoding amino acids 508-795 of the rat glucocorticoid receptor (Sablowski and Meyerowitz, 1998) was cloned downstream of the fragment of the *MP* complementary DNA (cDNA) (Hardtke and Berleth, 1998) from +1 to +2696 and controlled by the *UBIQUITIN10* (*UBQ10*) promoter (Sawchuk *et al.*, 2008).

Table 2.1. Sequences of primers used in this study.

Translational fusion primers

mCherry KpnI Fwd	ataggtaccgtgagcaagggcgaggag
mCherry SacI Rev	attgagctcttactgtacagctcgtcc
Athb8 SalI Forw	agtgtcgacgacgataatgatgataactac
Athb8 gORF KpnI Rev	ctcggtagctataaaagaccagttgaggaac
MP prom SalI Forward	cccgtcgacgtatatataaacaataccacctataac
MP KpnI Reverse	catggtacctgcagaattagcataccacac
ECFP Forward AflII	ttacttaaggtgagcaagggcgaggagc
ECFP Reverse AflII	agacttaagattgtacagctcgtccatgcc
MP 3kb SalI Fwd	tctgtcgactccgggtaatcagtattattac
MP 3kb XhoI Rev	attctcgagttaagagttaagaccacctcc
GR BsrGI Fwd	atatgtacatcgctcgaaaaacaagaaaaaatc
GR BsrGI Rev	acgtgtacagtcattttgatgaaacagaagc
MP cDNA KpnI Fwd	agaggtaacatgatggcttcattgtcttg
MP cDNA AgeI Rev	aggaccgggtcttaagatcgttaatgc

Deletion construct primers

[-1997,-1]	Forward - ggggacaagttgtacaaaaagcaggctgacgataatgatgataactac
	Reverse - ggggaccactttgtacaagaaagctgggtctttgatcctctccgatctctc

[-1513,-1] Forward - ggggacaagtttgatacaaaaaagcaggctcccaagtttaaaccttgctgatgtc
Reverse - ggggaccactttgtacaagaaagctgggtctttgatcctctccgatctctc

[-964,-1] Forward - ggggacaagtttgatacaaaaaagcaggctgtgagaagtgggtggtgtctgg
Reverse - ggggaccactttgtacaagaaagctgggtctttgatcctctccgatctctc

[-501,-1] Forward - ggggacaagtttgatacaaaaaagcaggcttcctttgctccagagaccagcg
Reverse - ggggaccactttgtacaagaaagctgggtctttgatcctctccgatctctc

[-964,-776] Forward - ggggacaagtttgatacaaaaaagcaggctgtgagaagtgggtggtgtctgg
Reverse - ggggaccactttgtacaagaaagctgggtgtagtgggatgagagag

[-927,-1] Forward - ggggacaagtttgatacaaaaaagcaggctcttctctctttcaacacagc
Reverse - ggggaccactttgtacaagaaagctgggtctttgatcctctccgatctctc

[-957,-1] Forward - ggggacaagtttgatacaaaaaagcaggctgtggtggtgtctggtattaagg
Reverse - ggggaccactttgtacaagaaagctgggtctttgatcctctccgatctctc

[-953,-1] Forward - ggggacaagtttgatacaaaaaagcaggcttggtgtctggtattaagg
Reverse - ggggaccactttgtacaagaaagctgggtctttgatcctctccgatctctc

[-940,-1] Forward - ggggacaagtttgatacaaaaaagcaggcttaagggtactcacttctc
Reverse - ggggaccactttgtacaagaaagctgggtctttgatcctctccgatctctc

[-907,-1] Forward - ggggacaagtttgatacaaaaaagcaggctgcccacacacatgtctc
Reverse - ggggaccactttgtacaagaaagctgggtctttgatcctctccgatctctc

[-876,-1] Forward - ggggacaagtttgatacaaaaaagcaggctcatacacacatttctatttattag
Reverse - ggggaccactttgtacaagaaagctgggtctttgatcctctccgatctctc

[-864,-1] Forward - ggggacaagtttgatacaaaaaagcaggcttctatttattagtttcctaaataa
Reverse - ggggaccactttgtacaagaaagctgggtctttgatcctctccgatctctc

[-864,-776] Forward - ggggacaagtttgatacaaaaaagcaggcttctatttattagtttcctaaataa

Reverse - ggggaccactttgtacaagaaagctgggtttagtgggatgagagag
mMYB Forward - ggggacaagtttgtacaaaaagcaggcttgactgtctggattaaggg
Reverse - ggggaccactttgtacaagaaagctgggtctttgatcctctccgatctctc
mARF Forward - ggggacaagtttgtacaaaaagcaggcttggttacctggattaaggg
Reverse - ggggaccactttgtacaagaaagctgggtctttgatcctctccgatctctc
mGT Forward - ggggacaagtttgtacaaaaagcaggcttggttctctgacattaaggg
Reverse - ggggaccactttgtacaagaaagctgggtctttgatcctctccgatctctc
CaMV35S -47 Forward - ggggacaagtttgtacaaaaagcaggctcaggaaacagctatgac
Reverse - ggggaccactttgtacaagaaagctgggtgctctccaatgaaatgaac

Genotyping primers

athb8-11 WT

ATHB8-0.5 ggggacaagtttgtacaaaaagcaggcttcctttgcttccagagaccagcg

ATHB8-R ggggaccactttgtacaagaaagctgggtctttgatcctctccgatctctc

athb8-11 mutant

pD991-RB aaaacctggcgttacccaact

athb8 -5944 ggtttggcataaaagtgcgg

athb8-12 WT

athb8-12F tcctttgcttccagagacca

athb8-12R ctttgatcctctccgatctctc

athb8-12 mutant

pROK-LB ggaaccaccatcaaacagga

athb8-12R ctttgatcctctccgatctctct

arf5-2 WT

arf5-2 LP cctggaaactgatgagctgac

arf5-2 RP ccttcttcactcatctgctgg

arf5-2 mutant

LBb1.3 attttgccgatttcggaac

arf5-2 RP ccttcttcactcatctgctgg

Chromatin immunoprecipitation primers

ATHB8 Forward – gaaaggaaggctaaacgaatttgc

Reverse – gtgtcgggctgtgttgaaaag

UBQ10 Forward – caaattccctcccttaagcacc

Reverse – aacttatccggctctagatcatcag

2.2.2 Plant material and growth conditions

The origins of the PIN1::PIN1:EYFP, J1721::mGFP5er, Q0990::mGFP5er, ATHB8::HTA6:EYFP, UBQ10::EGFP:LTI6B, ATHB8::ECFP-Nuc, *athb8-11*, and *athb8-12* lines have been published (Prigge *et al.*, 2005; Sawchuk *et al.*, 2007; Sawchuk *et al.*, 2008; Xu *et al.*, 2006). The *mp*^{U55} line contains a G-to-A transition at position +1237 that disrupts the splicing acceptor site of the sixth intron and is predicted to result in loss of sequences strictly required for DNA binding (Ulmasov *et al.*, 1999b). The proportion of *mp*^{U55} seedlings with single cotyledons (55/116, 47%), fused cotyledons (27/116, 23%) and two cotyledons (34/116, 29%) meet established criteria that define strong *mp* alleles (Berleth and Jurgens, 1993). Therefore, both molecular and morphological evidence indicate the extreme severity of the *mp*^{U55} mutation. The SALK_021319 line was confirmed to contain a single transfer-DNA (T-DNA) insertion at position +3422 of the *ARF5/MP* gene and was therefore renamed *arf5-2*. Sequences of primers used for genotyping are in Table 2.1.

Seeds were surface sterilized for 1 min in 70 % ethanol and 20 min in sterilization solution with shaking (15 % v/v commercial bleach; 0.01 % Triton X-100 (Sigma Aldrich)). Sterilized seeds were rinsed 6-10 times in sterile water and germinated on sealed plates containing germination medium (half-strength Murashige and Skoog (MS) salts (Sigma Aldrich); 15 g l⁻¹ sucrose (Bioshop Canada Inc. Burlington ON, Canada); 0.5 mg l⁻¹ 2-(n-morpholino)-ethanesulfonic acid (Bioshop Canada); 0.8 % w/v agar (Bioshop Canada); pH 5.7) at an approximate density of 1 seed cm⁻². Sealed plates were stratified for 3-5 d in the dark at 4 °C and then placed under continuous fluorescent lights at 25 °C, which defined the beginning of growth, as measured in 'days after germination' (DAG). Between 4 and 6 DAG, seedlings were transferred to PRO-MIX BX soil (Premier Tech Horticulture, Riviere-du-Loup, QC, Canada) in 7- x 7- x 8-cm pots at a density of 0.1 seedlings cm⁻² and plants were grown under long day conditions (16-h-light, 8-h-dark) at 22 °C under fluorescent lights.

For plant transformations, *Arabidopsis* seeds (ecotype Col-0) were suspended in 0.1 % agar (Bioshop Canada) at a density of ~5 seeds ml⁻¹, stratified

in the dark at 4 °C for 3-5 d, and germinated on soil-filled pots (as above) at a density of 0.5 seedlings cm⁻². Flowering plants were transformed by the floral dip method (Clough and Bent, 1998). Primary transformants were selected on growth medium (see above) supplemented with 200 µg ml⁻¹ carbenicillin (Thermo Fisher Scientific, Waltham, MA, USA), 50 µg ml⁻¹ nystatin (Bioshop Canada), and either 10 µg ml⁻¹ glufosinate ammonium (Sigma Aldrich), 15 µg ml⁻¹ hygromycin, or 1 µg ml⁻¹ d-Serine (Sigma Aldrich). At least ten independent transgenic lines were inspected to identify the most representative expression pattern for each construct. Successive expression analysis was performed on the progeny of at least three lines per construct, which were selected because of strong fluorescent protein expression that was emblematic of the expression profile observed across the entire series of transgenic lines and that resulted from single insertion of the transgene. In genetic crosses, the progeny of at least two independent transgenic lines per construct were examined.

For auxin transport inhibition, seeds were germinated on growth medium supplemented with NPA. For auxin or dexamethasone induction, seeds were germinated on growth medium, transferred at 3.5 days after germination (DAG) to liquid growth medium supplemented with 10 µM 2,4-dichlorophenoxyacetic acid (Sigma Aldrich) or 30 µM dexamethasone (Sigma Aldrich) and incubated with shaking at 50 rpm under normal growth conditions for 16 hours prior to imaging.

2.2.3 Microscopy

Dissected leaves were mounted in water with a 0.17-mm coverslip (Thermo Fisher Scientific, Waltham, MA, USA) and imaged with the 10x/0.8 Plan-Apochromat, 20x/0.8 Plan-Apochromat, or 40x/1.2W C-Apochromat objective of an Axio Imager.M1/LSM 510 META confocal microscope (Carl Zeiss, Oberkochen, Germany). CFP was excited with the 458-nm line of a 30-mW Argon laser and was detected with a BP475-525 filter. GFP was excited with the 488-nm line of the Argon laser and was detected with a BP505-530 filter. mCherry was excited with a 543-nm Helium Neon laser and was detected with a BP575-620 filter. YFP was excited with the 514-nm line and was detected with a

BP520-555 filter. For simultaneous visualization of CFP and YFP, CFP was excited with the 458-nm line of the Argon laser and was detected with a BP475-525 filter; YFP was excited with the 514-nm line of the Argon laser and was detected with a BP520-555 filter. For simultaneous visualization of GFP and mCherry, GFP was excited with the 488-nm line of the Argon laser and was detected with a BP505-530 filter; mCherry was excited by the 543-nm Helium Neon laser and was detected with a BP575-620 filter. For simultaneous visualization of GFP and YFP, GFP was excited with the 458-nm line of the Argon laser and was detected with a BP475-525 filter; YFP was excited with the 514-nm line of the Argon laser and was detected with a BP560-615 filter. For simultaneous visualization of mCherry and xylem auto-fluorescence, mCherry was excited with the 543-nm Helium Neon laser and was detected with a BP575-620 filter; xylem autofluorescence was excited with a 405 nm diode laser and detected with a BP420-480 filter. For simultaneous visualization of mCherry and YFP, mCherry was excited by the 543 nm Helium-Neon laser and was detected with a BP575-620 filter; YFP was excited with the 514-nm line of the Argon laser and was detected with a BP520-555 filter. For simultaneous visualization of xylem auto-fluorescence and YFP, xylem autofluorescence was excited with the 405 nm diode laser and detected with a BP420-480 filter; YFP was excited with the 514-nm line of the Argon laser and was detected with a BP520-555 filter. 512x512-pixel frames were scanned unidirectionally at 8-bit depth with 6.39- μ sec pixel dwell time and 4-fold averaging. Scanning zoom was adjusted to set pixel size to no less than half the objective lateral resolving power. Emission was collected from ~1- to 10- μ m-thick (single-fluorophore imaging) or ~2- to 3- μ m-thick (multi-fluorophore imaging) optical slices. Amplifier gain was set at 1; detector gain at ~50-65%. Laser transmission and offset value were adjusted to match signal to detector's input range. For multi-fluorophore imaging, sequential excitation and collection of emission were performed in line-by-line channel-switching mode. Under these conditions, signal bleed-through across different photomultiplier channels was not observed.

To visualize xylem patterns, leaves were cleared in ethanol:acetic acid (3:1, v/v), dehydrated in 70 % ethanol (v/v), rehydrated in water, mounted in chloral hydrate:glycerol:water (8:3:1, w/v/v/), and viewed under darkfield illumination with an Olympus SZ61TR stereomicroscope (Olympus Corporation, Tokyo, Japan). Images were captured with an AxioCam HR camera (Carl Zeiss, Oberkochen, Germany).

2.2.4 Image analysis

Brightness and contrast were not altered for images of mock treatments and induced gene expression. For all other images, brightness and contrast were adjusted through linear stretching of the histogram in ImageJ (National Institutes of Health, <http://rsb.info.nih.gov/ij>). Signal levels were visualized by applying look-up tables. Signal colocalization was visualized with an extended dual channel look-up table from magenta to cyan through red, orange, yellow and green (Demandolx and Davoust, 1997). Fluorescence from each detection channel was displayed in either magenta or cyan and combined using the differential operator in Adobe Photoshop 7.0 (Adobe Systems Incorporated). As a result, higher levels of cyan signal with respect to co-localized magenta signal is encoded in green, opposite in red and orange, and co-localized signals of equal intensity in yellow. Images were cropped in Adobe Photoshop 7.0 (Adobe Systems Incorporated, San Jose, CA, USA) and were labeled and assembled into figures in Canvas 8.0 (ACD Systems International Inc., Seattle, WA, USA).

2.2.5 Chromatin immunoprecipitation

Chromatin immunoprecipitation was performed essentially as described (Jackson, 1978; Nagaki *et al.*, 2003; Palma *et al.*, 2007; Ponnusamy *et al.*, 2008). Briefly, nuclei were isolated from ~2000 4-DAG seedlings (equivalent to ~2.5 g) per genotype per biological replicate, nuclear proteins were crosslinked to DNA with formaldehyde, chromatin was digested with micrococcal nuclease, and DNA-crosslinked fluorescent proteins were isolated using the μ MACS GFP Isolation Kit (Miltenyi Biotec, Bergisch Gladbach, Germany). Enrichment of DNA of putative target regions in the *ATHB8* promoter was determined as described

(Schubert *et al.*, 2006) using a sequence of the *UBQ10* promoter to normalize results (Martin-Trillo *et al.*, 2006). Sequences of primers are in Table 2.1.

2.3 RESULTS

2.3.1 Vascular development in *Arabidopsis athb8* leaves

Null mutants of *ATHB8* display no obvious alterations in the vein patterns of mature leaves (Baima *et al.*, 2001; Prigge *et al.*, 2005). We first asked whether *ATHB8* could be assigned to any distinct function in vein formation or whether *ATHB8* activity is completely dispensable for this process. In *Arabidopsis*, veins of subsequent orders become recognizable progressively later in the same area of the developing leaf primordium, and veins of the same order appear in a tip-to-base sequence during leaf development (Candela *et al.*, 1999; Kang and Dengler, 2002; Kang and Dengler, 2004; Kinsman and Pyke, 1998; Mattsson *et al.*, 1999; Mattsson *et al.*, 2003; Scarpella *et al.*, 2004; Scarpella *et al.*, 2006; Sieburth, 1999; Steynen and Schultz, 2003; Telfer and Poethig, 1994; Wenzel *et al.*, 2007). Fig. 2.1A-D schematically depict the temporal sequence of vascular development events in *Arabidopsis* leaf primordia and define the stages and terminology to which we refer throughout this study.

Selection of ground cells that will acquire a preprocambial state, visualized through the dynamics of PIN1 expression (Scarpella *et al.*, 2006; Wenzel *et al.*, 2007), proceeded similarly in leaf primordia of wild type and of the null *athb8-11* mutant (Fig. 2.2). However, we observed distinct anomalies in the assignment of the preprocambial cell state and procambial cell identity, marked by J1721::mGFP5er and Q0990::mGFP5er expression, respectively (Sawchuk *et al.*, 2007), during *athb8-11* leaf development (for the attributes used to assess the representative nature of all displayed features and derived reproducibility quotients, see Table 2.2).

In wild type, J1721::mGFP5er expression is initiated in files of individual ground cells of the leaf primordium that coexpress *ATHB8* and that will successively elongate to acquire procambial cell identity (Sawchuk *et al.*, 2007). Whereas at all stages of wildtype leaf development, J1721::mGFP5er expression

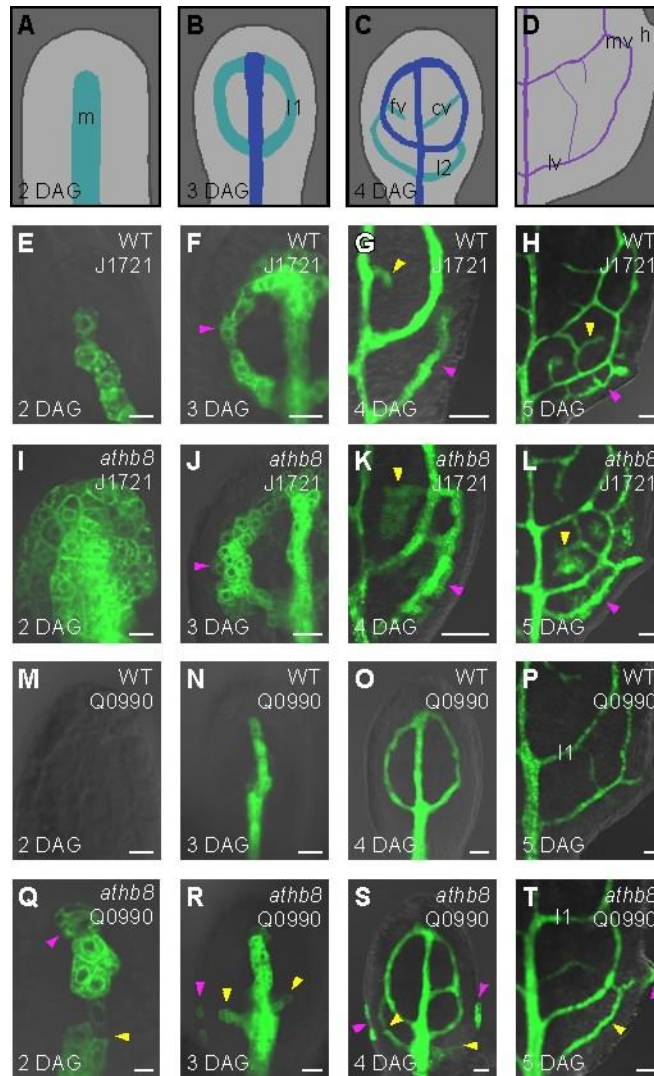


Figure 2.1. Leaf vascular development in *Arabidopsis athb8*. (A-T) First leaf primordia, lateral (A,E,I,M,Q) or abaxial (B-D,F-H,J-L,N-P,R-T) view. Genotypes (WT, wild type) and markers are shown above, the age in days after germination (DAG) below. (A-D) Illustrations depicting the spatiotemporal course of vein formation in *Arabidopsis* first leaf development as inferred from published works (see text for references), and definition of terms used in this study. (A-C) Whole leaves. (D) Detail of the lower-right region of a mature leaf; note the smooth integration of lateral veins (lv) and marginal veins (mv) into vein loops. Cyan, preprocambial stages; blue, procambial stages; purple, mature veins; cv, connecting vein; fv, freely ending vein; h, hydathode; l1, first loop; l2; second loop; m, midvein. (E-T) Overlay of confocal-laser-scanning microscopy and transmitted light images. (E-L) Preprocambium labeling by J1721:mGFP5er expression (green). Note the expanded expression domains in *athb8* leaves during formation of midvein (I), first, second and third loop (magenta arrowheads in J,K,L, respectively), and higher order veins (yellow arrowheads in K,L); compare with wild type (E-H). (M-T) Procambium labeling by Q0990:mGFP5er expression (green). Note the epidermal foci of expression in *athb8* leaves during formation of midvein (magenta arrowhead in Q), first, second and third loop (magenta arrowheads in R,S,T, respectively). Furthermore, note the prematurely emerging expression domains marking development of midvein (yellow arrowhead in Q), first and second loop-forming lateral veins (yellow arrowheads in R,S, respectively), and entire second and third loops in *athb8* leaves (yellow arrowheads in S,T, respectively); compare with wild type (M-P). Scale bars: 5 μ m (E,I,M,Q); 10 μ m (F,J,N,R); 20 μ m (G,H,K,L,O,P,S,T).

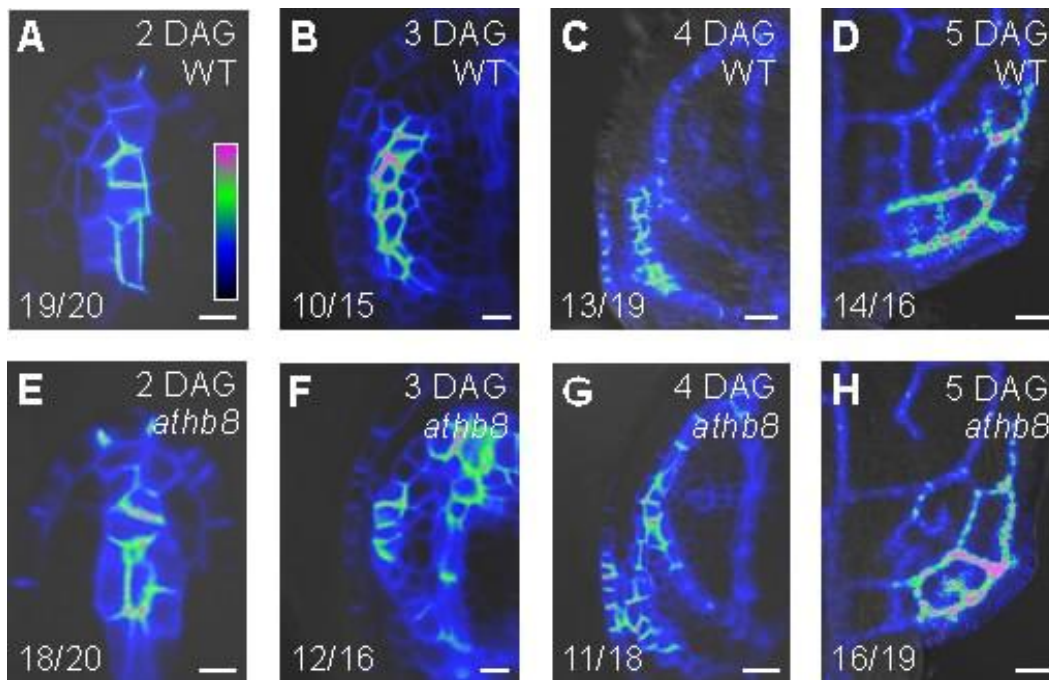


Figure 2.2. PIN1 expression in wild-type and *athb8* leaf development. (A-H) First leaf primordia. Age in DAG and genotypes are shown above, reproducibility indices below. Overlay of confocal-laser-scanning microscopy and differential-interference-contrast images. (A,E) Lateral view. (B-D,F-H) Abaxial view. PIN1::PIN1:EYFP expression is color-coded with an Look-Up Table (LUT) (shown in A) in which black was used to encode background, and blue, green and magenta to encode increasing signal intensities. Scale bars: 5 μm (A,B,E,F); 10 μm (C,G); 25 μm (D,H).

Table 2.2. Reproducibility indices and the features used as criteria in their calculation.

Figure 2.1

E	14/18	narrow GFP expression domain in m
F	11/14	narrow GFP expression domains in m and l1
G	21/22	narrow GFP expression domains in m, l1, l2, and higher-order veins (hv)
H	19/19	narrow GFP expression domains in m, l1, l2, third loops (l3), and hv
I	20/20	expanded GFP expression domain in m
J	13/17	narrow GFP expression domain in m; expanded GFP expression domains in l1
K	28/28	narrow GFP expression domains in m and l1; expanded GFP expression domains in l2 and hv
L	15/18	narrow GFP expression domains in m, l1, and l2; expanded GFP expression domains in l3 and hv
M	8/10	No GFP expression
N	10/10	GFP expression in m
O	11/15	GFP expression in m and l1
P	21/21	GFP expression in m, l1, l2, and hv
Q	13/16	GFP expression in m and epidermal cells at the leaf tip

- R 10/14 GFP expression in m, l1 extending from mv, and epidermal cells at the leaf margin
- S 13/14 GFP expression in m, l1, l2 extending from mv, or entire l2 and epidermal cells at the leaf margin
- T 14/18 GFP expression in m, l1, l2, and l3 and epidermal cells at the leaf margin
-

Figure 2.3

- A-D See Figure 2.4
- E 14/18 YFP expression in m, l1, l2, l3, and hv
- F 14/19 YFP expression in m, l1, l2, l3, and hv
- G 11/12 Expanded and induced proximal domains of YFP expression
- H 16/22 Expanded and strongly induced subepidermal domains of YFP expression
- I 18/20 Erratic CFP expression at tip and in l1, l2, and hv
- J 12/12 Erratic CFP expression at tip and in l1, l2, and hv
- K 12/14 Near-ubiquitous YFP expression
- L 30/33 Near-ubiquitous YFP expression
-

Figure 2.5

- A 10/10 YFP expression in isodiametric, polygonal cells

- B 19/19 Co-expression of GFP with YFP
- C 10/10 Mutually exclusive expression of YFP and xylem autofluorescence
- D 16/16 YFP expression in m and leaf tip
- E 14/16 YFP expression in m and l1
- F 51/51 YFP expression in m, l1, and l2
- G 10/10 mCherry expression in isodiametric, polygonal cells
- H 12/13 Co-expression of GFP with mCherry
- I 10/10 Mutually exclusive expression of mCherry and xylem autofluorescence
- J 24/29 mCherry expression in m
- K 26/29 mCherry expression in m and l1
- L 25/33 mCherry expression in m, l1, and l2
- M-O 11/11 Co-expression of mCherry and YFP

Figure 2.9

- A 10/10 YFP expression in m, l1, l2, and GFP expression in m and l1
- B 51/51 YFP expression in m, l1, and l2
- C 10/10 YFP expression in isodiametric, polygonal cells
- D 19/19 Co-expression of YFP and CFP
- E 33/33 YFP expression in m, l1, and l2 and 24/39 additional trichome expression
- F 54/55 YFP expression in m, l1, and l2

G	19/19	YFP expression in isodiametric, polygonal cells
H	20/20	Co-expression of CFP and YFP
I	33/40	No YFP expression
J	51/51	YFP expression in m, l1, and l2
K	16/16	YFP expression in isodiametric, polygonal cells
L	11/11	Co-expression of CFP and YFP
M	50/55	YFP expression in m and l1
N-P	15/15	Co-expression of YFP with GFP
Q	66/73	YFP expression in m, l1, and l2
R	64/68	YFP expression in m, l1, and l2
S	12/12	YFP expression in isodiametric, polygonal cells
T	18/18	Co-expression of CFP and YFP
U	77/91	YFP expression in m and l1
V-W	19/20	Co-expression of YFP with GFP

Figure 2.10

A	64/68	YFP expression in m, l1, and l2
B	71/91	YFP expression in m and l1
C	47/49	YFP expression in m, l1, and l2
D	44/52	YFP expression in m, l1, and l2
E	37/43	YFP expression in m and l1
F-H	21/21	Co-expression of YFP with GFP

Figure 2.11

- A 20/20 YFP expression in m, l1 and l2
 - B 19/19 Near-ubiquitous YFP expression
 - C 12/12 YFP expression in m, l1 and l2
 - D 14/14 Near-ubiquitous YFP expression
 - E 14/14 YFP expression in m and l1
 - F 10/10 YFP expression in m and l1
 - G 15/15 YFP expression in m and l1
 - H 11/11 YFP expression in m and l1
 - I 12/12 YFP expression in m, l1, and l2
 - J 16/17 Near-ubiquitous YFP expression
 - K 10/10 YFP expression in m, l1, and l2
 - L 10/10 Near-ubiquitous YFP expression
-

Figure 2.12

- A 18/20 Near-ubiquitous CFP expression
- B 17/20 CFP expression in wide domains along leaf margin
- C 18/20 CFP expression in wide domains along basal leaf margin and in narrow domains along apical leaf margin
- D 10/10 Co-expression of YFP with CFP

E	51/51	YFP expression in m, l1, and l2
F	64/68	YFP expression in m, l1, and l2
G	77/91	YFP expression in m and l1
H	37/43	YFP expression in m and l1
I	28/32	YFP expression in m and l1
J	35/46	YFP expression in m and l1
K	18/20	YFP expression in m and l1
L	12/16	YFP expression in m and l1
M	7/12	Vein-associated YFP expression
N	10/13	Near-ubiquitous YFP expression
O	12/12	Vein-associated YFP expression
P	11/11	Vein-associated YFP expression

Figure 2.13

A-I See Table 2.3

Figure 2.14

A-H See Table 2.4

Table 2.3. Phenotype distribution of mature vein patterns.

Genotype	Class I	Class II	Class III	Class IV	Class V	Class VI	Class VII	Class VIII	Total
WT	43 (100)	0	0	0	0	0	0	0	43
<i>athb8-11</i>	51 (100)	0	0	0	0	0	0	0	51
<i>arf5-2</i> (rooted)	0	21 (38.9)	28 (51.9)	1 (1.9)	4 (7.3)	0	0	0	54
<i>arf5-2</i> <i>athb8-11</i> (rooted)	0	18 (20.9)	57 (66.3)	3 (3.5)	8 (9.3)	0	0	0	86

<i>arf5-2</i> (rootless)	0	12 (17.4)	20 (29)	16 (23.2)	21 (30.4)	0	0	0	69
<i>arf5-2</i> <i>athb8-11</i> (rootless)	0	3 (6.5)	13 (28.3)	6 (13.0)	22 (47.8)	2 (4.4)	0	0	46
<i>mp</i> ^{U55}	0	0	0	0	0	10 (22.8)	32 (72.7)	2 (4.5)	44
<i>mp</i> ^{U55} <i>athb8-11</i>	0	0	0	0	0	24 (27.0)	64 (71.9)	1 (1.1)	89

See text and Figure 2.13, respectively, for description and illustration of phenotypic classes.

Values in parentheses indicate percentage contribution of each class.

Table 2.4. Incidence of leaf fusion.

Genotype	Treatment	Separated leaves	Fused leaves	Total
WT	Control	27 (100)	0	27
WT	1 μ M NPA	25 (100)	0	25
<i>athb8-11</i>	Control	24 (100)	0	24
<i>athb8-11</i>	1 μ M NPA	25 (100)	0	25
<i>arf5-2</i> (rootless)	Control	60 (100)	0	60

<i>arf5-2</i> (rootless)	1 μ M NPA	26 (90)	3 (10)	29
<i>arf5-2</i> <i>athb8-11</i> (rootless)	Control	49 (100)	0	49
<i>arf5-2</i> <i>athb8-11</i> (rootless)	1 μ M NPA	17 (63)	10 (37)	27

Values in parentheses indicate percentage contribution of each class. See also Figure 2-14.

was invariably constrained to narrow zones (Sawchuk *et al.*, 2007) (Fig. 2.1E-H), newly emerged J1721::mGFP5er expression domains encompassed wide fields of cells in *athb8* leaf primordia (Fig. 2.1I-L). At later stages of vein development in *athb8* leaves, J1721::mGFP5er expression was, nevertheless, confined to strands of one or very few cell files (Fig. 2.1J-L).

In wild-type leaf development, Q0990::mGFP5er expression first emerges in files of elongated, *ATHB8*-expressing procambial cells, and all cells initiate Q0990::mGFP5er expression simultaneously throughout the length of a developing vein (Sawchuk *et al.*, 2007). During unperturbed development, Q0990::mGFP5er expression is activated in a coordinated fashion in loop-forming lateral and marginal veins, such that expression appears simultaneously along entire vein loops (Sawchuk *et al.*, 2007) (Fig. 2.1O,P). In *athb8* leaf development, however, Q0990::mGFP5er expression was switched on separately in lateral and marginal veins, and ectopic foci of transient epidermal expression were detected at the leaf margin during the development of the midvein and all loops (Fig. 2.1Q-T).

In summary, our results suggest that *ATHB8* is required to circumscribe preprocambial cell state assignment to narrow domains of ground cells and to integrate procambium identity acquisition within and between veins.

2.3.2 Auxin transport and response in *athb8* leaves

The appearance of expanded zones of J1721::mGFP5er expression and the asynchronous emergence of Q0990::mGFP5er expression domains observed during *athb8* leaf development are reminiscent of marker behavior under conditions of mild auxin transport inhibition (Sawchuk *et al.*, 2007). Therefore, we next asked whether *athb8* leaves displayed altered sensitivity to the auxin transport inhibitor 1-N-naphthylphthalamic acid (NPA). Leaves of plants germinated and grown in the presence of auxin transport inhibitors are characterized by a number of distinct anomalies in vascular organization (Mattsson *et al.*, 1999; Sieburth, 1999), most evident as great numbers of broad lateral veins and fusion of marginal veins to give rise to a continuous wide zone of vascular differentiation that extends along the entire margin of the leaf (Fig.

2.3C). Because these responses are quantifiable and NPA concentration dependent (Mattsson *et al.*, 1999; Sieburth, 1999) (Fig. 2.4), they can be used to assess sensitivity to auxin transport inhibition. At low concentrations of NPA, *athb8-11* leaves showed greater numbers of lateral veins, and a higher fraction of *athb8-11* leaves displayed the formation of a marginal vascular differentiation zone than wild-type leaves (Fig. 2.3A-D; 2.4), suggesting that vein development in *athb8-11* is more susceptible to auxin transport inhibition. Similarly, leaves of the weaker *athb8-12* allele (Prigge *et al.*, 2005) displayed hypersensitivity to NPA (Fig. 2.4).

Wild-type leaves developing under conditions of reduced auxin transport display an expansion of PIN1 expression domains proportional to the level of auxin transport inhibition (Scarpella *et al.*, 2006; Wenzel *et al.*, 2007). We therefore asked whether the exaggerated response of vein patterns to auxin transport inhibition in *athb8* was associated with enhanced broadening of PIN1 expression fields under the same conditions. Concentrations of NPA that evoked a maximum differential response of vein patterns in *athb8* versus wild type resulted in higher levels and wider domains of PIN1::PIN1:EYFP expression in *athb8-11* than in wild-type leaves (Fig. 2.3E-H). Because PIN1 expression in leaves is auxin inducible (Scarpella *et al.*, 2006; Wenzel *et al.*, 2007), we asked whether the exaggerated response of PIN1 expression to auxin transport inhibition in *athb8* could be attributable to abnormal auxin sensitivity. In leaves, the synthetic DR5 promoter (Ulmasov *et al.*, 1997b) serves as a cell type-independent reporter of auxin response (Mattsson *et al.*, 2003). Levels and patterns of DR5Rev(9x)::ECFP-Nuc expression in *athb8-11* leaves, either under control conditions or upon treatment with exogenous auxin, were comparable to those in wild type (Fig. 2.3I-L).

We conclude that *ATHB8* is required for normal sensitivity of PIN1 expression and vascular patterns to auxin transport inhibition in the leaf, but that *ATHB8* appears expendable for leaf auxin response.

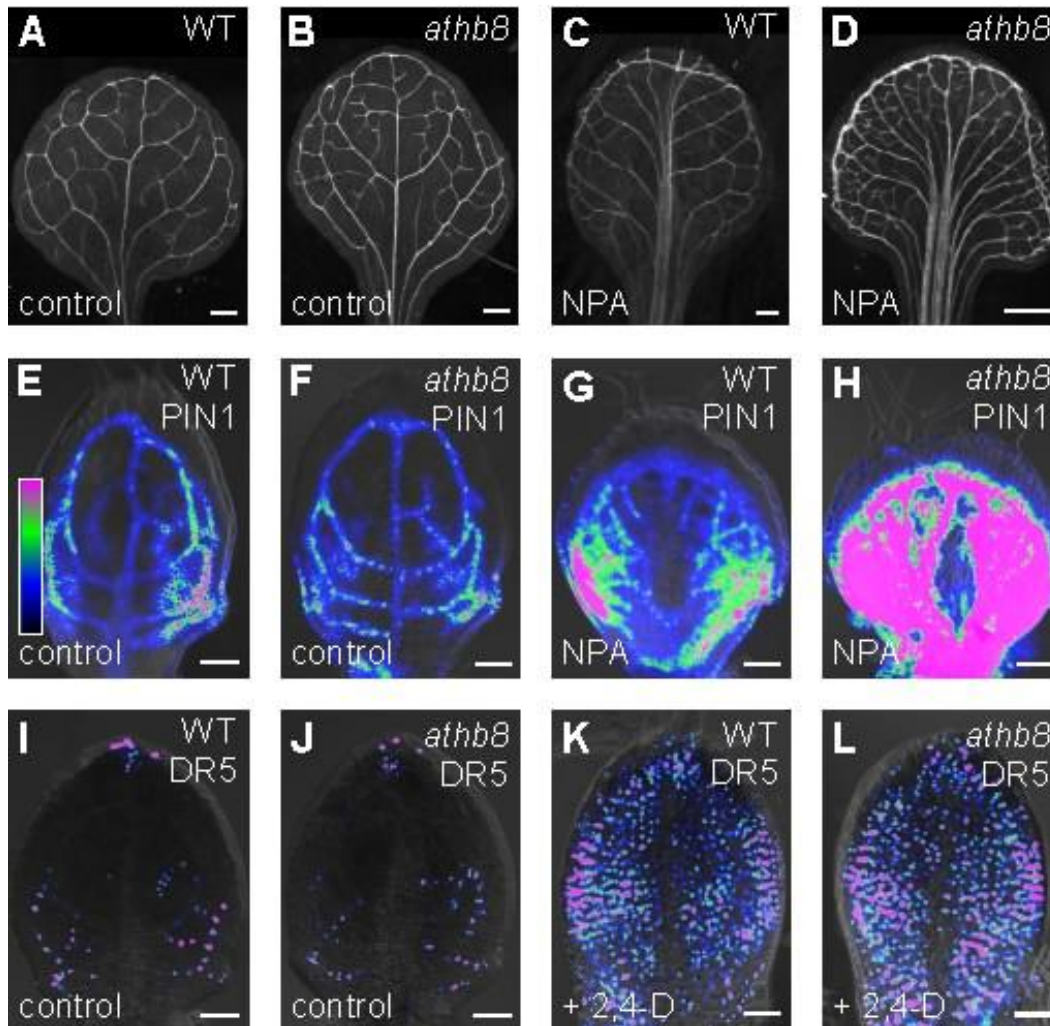


Figure 2.3. Auxin transport and response in *athb8* leaves. (A-L) First leaves, abaxial view. Genotypes and markers are shown above, treatment (2.5 μ M NPA or 10 μ M 2,4-D) below. (A-D) Dark-field illumination of cleared mature leaves. (E-L) Overlay of confocal-laser-scanning microscopy and transmitted light images. Images for each marker series were taken at an identical setting and are color-coded with an intensity LUT (as shown in E and described in Fig. 2.2) encode increasing PIN1::PIN1::EYFP (E-H) or DR5Rev(9x)::ECFP-Nuc (I-L) signal levels. Scale bars: 0.5 mm (A-D); 25 μ m (E-L).

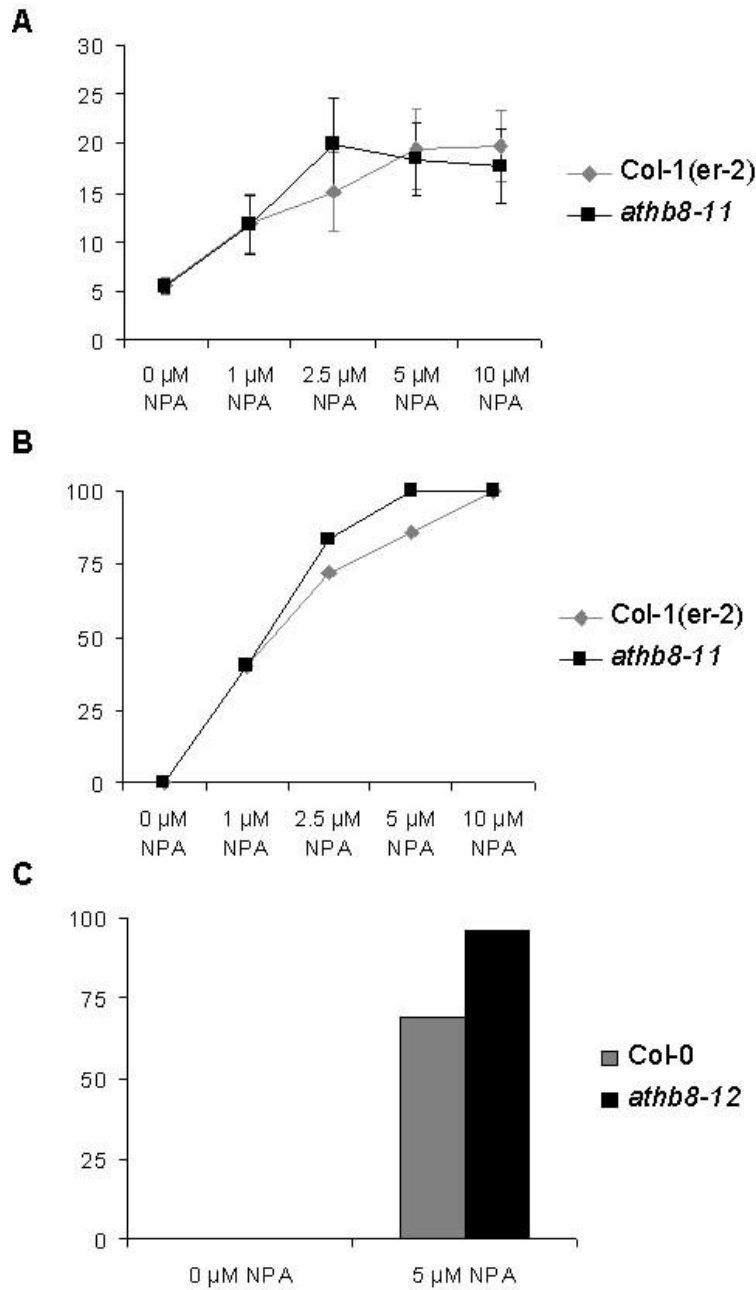


Figure 2.4. Responses of vascular patterns to auxin transport inhibition in wild-type and *athb8* first leaves. (A) Number of lateral veins formed at different concentrations of 1-N-naphthylphthalamic acid (NPA). Values are the average \pm s.d. (B,C) Percentage of leaves displaying formation of a marginal vascular differentiation zone. Sample population sizes as follows. Col-1(*er-2*): 0 μ M NPA, 26; 1 μ M NPA, 25; 2.5 μ M NPA, 36; 5 μ M NPA, 28; 10 μ M NPA, 25. *athb8-11*: 0 μ M NPA, 24; 1 μ M NPA, 25; 2.5 μ M NPA, 41; 5 μ M NPA, 31; 10 μ M NPA, 25. Col-0: 0 μ M NPA, 14; 5 μ M NPA, 26. *athb8-12*: 0 μ M NPA, 15; 5 μ M NPA, 25.

2.3.3 Expression of *ATHB8* in leaf development

In agreement with previous observations (Baima *et al.*, 1995; Kang and Dengler, 2004; Sawchuk *et al.*, 2007; Scarpella *et al.*, 2004), we found that the 2.0 kb sequence upstream of the *ATHB8* translational start site is sufficient to drive expression of a nuclear-localized yellow fluorescent protein (HTA6:EYFP) (Zhang *et al.*, 2005) in isodiametric cells of the leaf primordium that have been recruited towards Q0990::mGFP5er-labeled procambium formation (Fig. 2.5A,B) and that have therefore been designated as preprocambial cells (Mattsson *et al.*, 2003). In leaf development, the intensity of *ATHB8*::HTA6:EYFP signals was sustained in elongated procambial cells and eventually declined during late stages of vascular differentiation (Fig. 2.5B,C). As previously reported (Kang and Dengler, 2002; Scarpella *et al.*, 2004), we additionally observed ephemeral activity of the *ATHB8* promoter at the leaf tip and hydathodes, where not all *ATHB8*-expressing cells will differentiate into vasculature (Fig. 2.5D; 2.6).

Post-transcriptional regulation has been shown to spatially constrain fields of *ATHB8* expression in the root (Lee *et al.*, 2006). To test whether post-transcriptional control impinges on domains of *ATHB8* expression in the leaf, we first visualized expression of a functional (see Section 2.2.1) translational fusion of *ATHB8* with the red fluorescent protein mCherry (Shaner *et al.*, 2004) during leaf development. Expression of *ATHB8*::*ATHB8*:mCherry was initiated in polygonal cells of the leaf primordium (Fig. 2.5G), maintained in elongated Q0990::mGFP5er-marked procambial cells (Fig. 2.5H), extinguished during terminal vascular differentiation (Fig. 2.5I), and was always absent at the leaf tip and hydathodes (Fig. 2.5J; 2.6). Therefore, with the exception of the leaf tip and hydathode nonvascular areas, *ATHB8*:mCherry accumulation profiles are accurately recapitulated by *ATHB8* promoter-driven expression dynamics. We next asked whether imaging patterns of *ATHB8* promoter activity and tagged *ATHB8* protein localization within the same sample could reveal subtle differences that would go unnoticed in comparative analyses performed on separate samples. Covisualization of *ATHB8*::HTA6:EYFP and *ATHB8*::*ATHB8*:mCherry signals showed coincident expression of the two

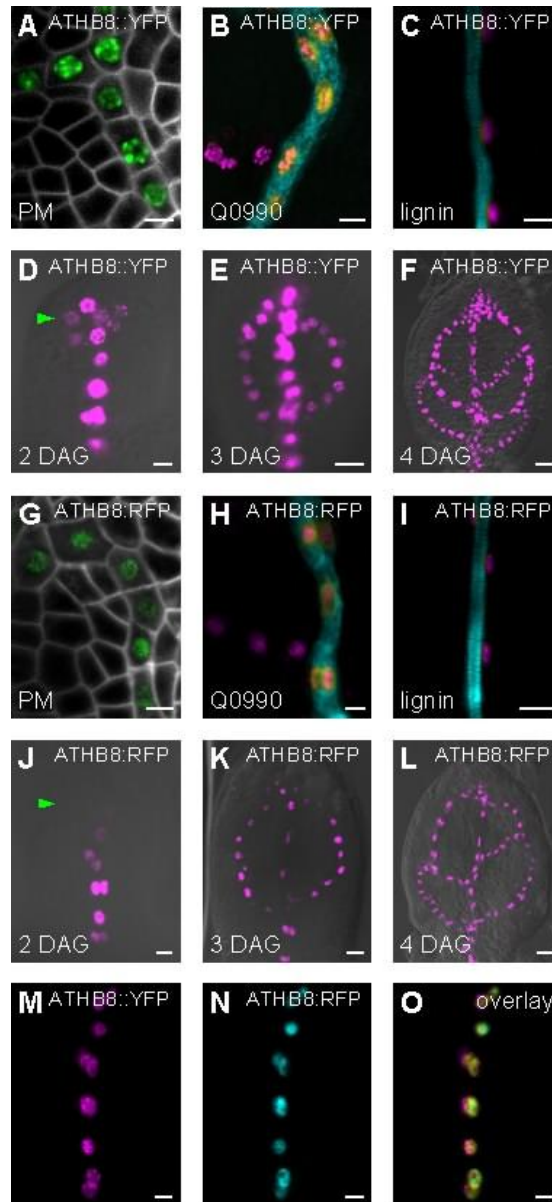


Figure 2.5. *ATHB8* expression in leaf development. (A-O) First leaf primordia, abaxial (A-C, E-I, K-O) or lateral (D, J) view. Markers are shown above, age (DAG) (D-F, J-L) or additional markers (A-C, G-I, M-O) below. (A-C, G-I, M-O) Confocal-laser-scanning microscopy images. (D-F, J-L) Overlay of confocal-laser-scanning microscopy and transmitted light images. (A, G) Plasma membrane (PM) labeling by UBQ10::EGFP:LT16B expression (white). (A) *ATHB8*::HTA6:EYFP (*ATHB8*::YFP) expression (green). (B, H) Procambium labeling by Q0990:mGFP5er expression (cyan). (B-F, M, O) *ATHB8*::HTA6:EYFP expression (magenta). (C, I) Xylem labeling by lignin autofluorescence (cyan). (G) *ATHB8*::*ATHB8*:mCherry (*ATHB8*:mCherry) expression (green). (H-L) *ATHB8*::*ATHB8*:mCherry expression (magenta). (J) Note the confined expression domain at the leaf tip (green arrowhead); compare with D. (N, O) *ATHB8*::*ATHB8*:mCherry expression (cyan). (B, C, H, I, O) Images are color-coded with a dual-channel LUT from cyan to magenta through green, yellow and red (Demandolx and Davoust, 1997). Fluorescence in each detection channel was displayed in either magenta or cyan. Single-fluorophore images were then merged using a differential operator. As a result, a preponderance of cyan signal over colocalized magenta signal is encoded in green, opposite in red, and colocalized cyan and magenta signals of equal intensity in yellow. Scale bars: 5 μ m (A, B, D, G, H, J, M-O); 10 μ m (C, E, I, K); 20 μ m (F, L).

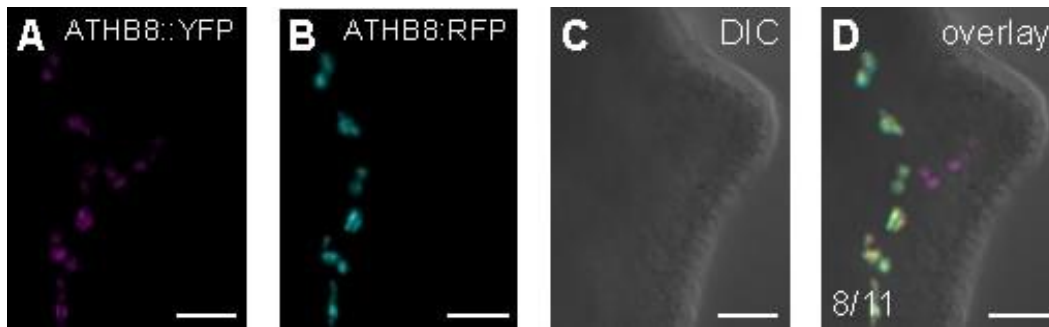


Figure 2.6. *ATHB8* expression at the leaf hydathode. (A-D) First leaf, abaxial view. Markers are shown above, reproducibility indices below. (A,B) Confocal-laser-scanning microscopy images. (C) Differential-interference-contrast image. (D) Overlay of confocal-laser-scanning microscopy and differential-interference-contrast images. (A) *ATHB8*::HTA6:YFP expression (magenta). (B) *ATHB8*::*ATHB8*:mCherry expression (cyan). (D) Single-fluorophore images were merged using a differential operator. As a result, a preponderance of cyan signal over colocalized magenta signal is encoded in green, opposite in red, and colocalized cyan and magenta signals of equal intensity in yellow (for further details, see legend to Fig. 2.5). Note *ATHB8*::HTA6:YFP signals in excess of *ATHB8*::*ATHB8*:mCherry expression at the hydathode. Scale bars: 25 μ m.

fluorescent proteins (Fig. 2.5M-O), suggesting that *ATHB8* promoter activity parallels *ATHB8* protein expression in vascular cells and that post-transcriptional regulation does not revise vein-associated domains of *ATHB8* expression in the leaf.

2.3.4 Expression conferred by deletions of the *ATHB8* promoter

Because *ATHB8* expression is predicted by the activity of its upstream non-coding sequences, to identify regulatory elements required for preprocambial expression, we generated a series of *ATHB8* promoter variants. All the promoter fragments were fused to the nuclear-localized HTA6:EYFP in the context of the pFYTAG binary vector (Zhang *et al.*, 2005). HTA6:EYFP driven by the cauliflower mosaic virus 35S -47 minimal promoter (Fang *et al.*, 1989) was not able to generate detectable levels of YFP fluorescence in transgenic plants (Fig. 2.7), suggesting that the T-DNA in the pFYTAG binary vector does not contain cryptic regulatory elements. Three criteria were sequentially adopted to test preprocambial expression of the promoter fragments: (1) stereotypical expression in leaves 4 days after germination (DAG), as inferred by comparison with expression directed by the 2.0 kb promoter fragment; (2) isodiametric shape of cells first expressing the promoter fragments, as determined by simultaneous visualization of ubiquitously expressed plasma membrane-localized Green Fluorescent Protein (UBQ10::EGFP:LTI6B) (Sawchuk *et al.*, 2008); (3) colocalization of the onset of expression with that of a nuclear-localized CFP driven by the 2.0 kb *ATHB8* promoter fragment (*ATHB8*::ECFP-Nuc) (Sawchuk *et al.*, 2007). Finally, vascular expression at stages later than preprocambial, as suggested by failure to satisfy criterion 1, was independently tested by simultaneous visualization of the procambial marker Q0990::mGFP5er (Sawchuk *et al.*, 2007).

To initially demarcate the regulatory sequences that are required for *ATHB8* preprocambial expression, we generated a series of 0.5 kb 5' deletions of the 2.0 kb *ATHB8* promoter (Fig. 2.8). All deletions were designed so as not to interrupt putative *cis*-acting elements identified by available bioinformatics resources. The sequence of the *ATHB8* promoter between -964 and -1 was the shortest promoter fragment able to direct preprocambial expression (Fig. 2.9A-H),

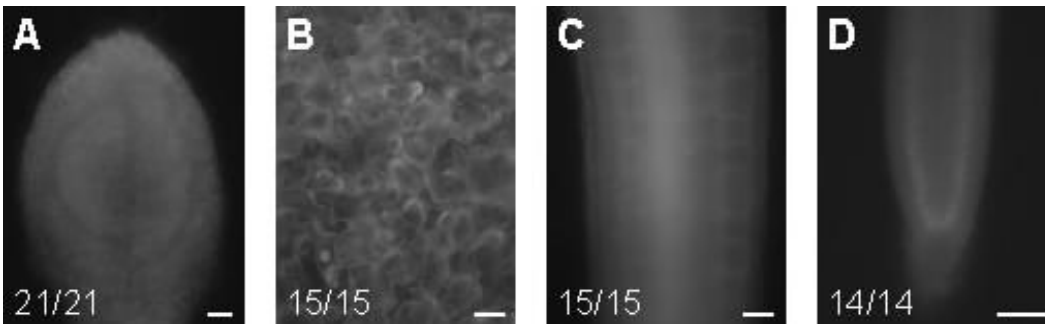


Figure 2.7. Expression of HTA6:EYFP under control of the -47 35S promoter of the cauliflower mosaic virus in 4-DAG seedlings. (A-D) Wide-field epifluorescence microscopy images. Reproducibility indices are shown below. (A,B) Abaxial view. (C,D) Lateral view. (A) First leaf. (B) Cotyledon. (C) Hypocotyl. (D) Root tip. Scale bars: 25 μm (A); 50 μm (B-D).

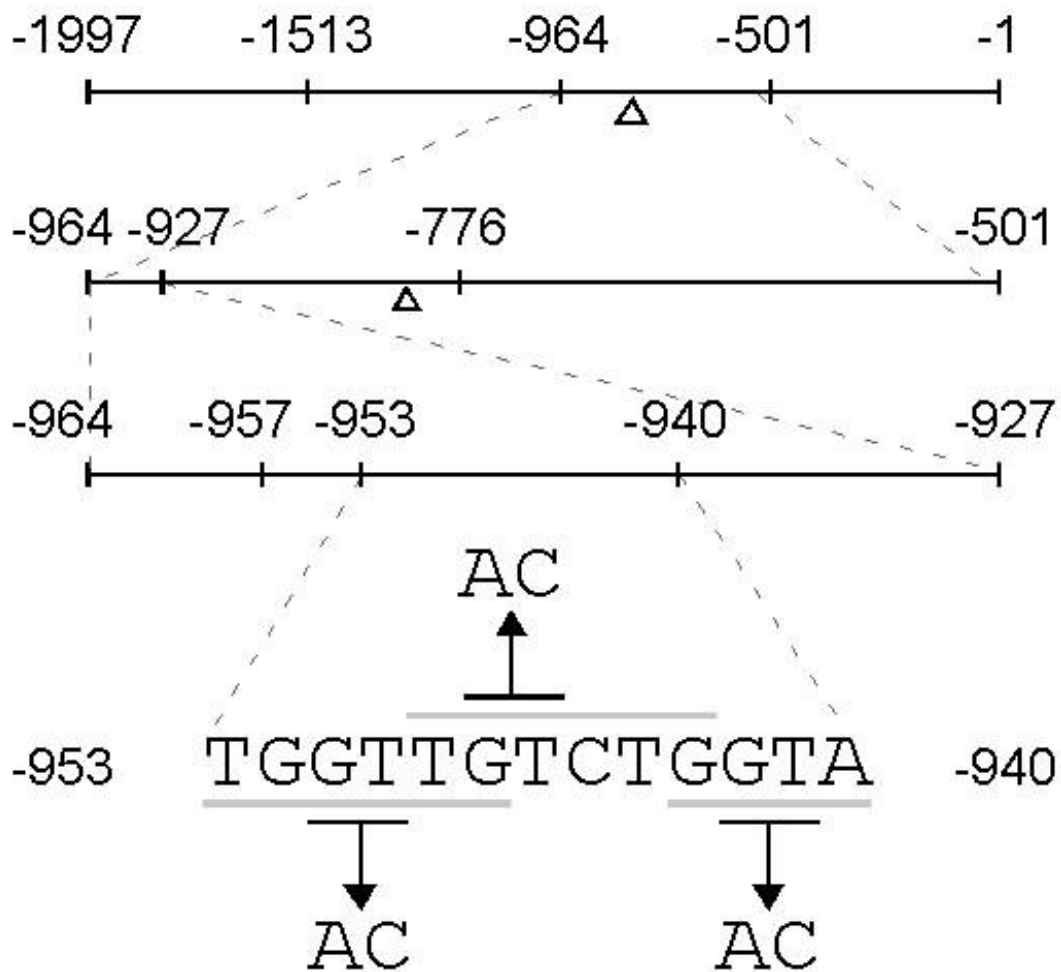


Figure 2.8. Scale diagram of *ATHB8* promoter fragments analyzed in this study. Numbers indicate position relative to the start codon (+1). Open triangles, predicted transcription start site. Gray lines, putative transcription-factor binding sites: MYB (TGGTTG), ARF (TGTCTG), GT1 (GGTA). Black lines with arrows, nucleotides targeted for site-directed mutagenesis and respective mutant variants.

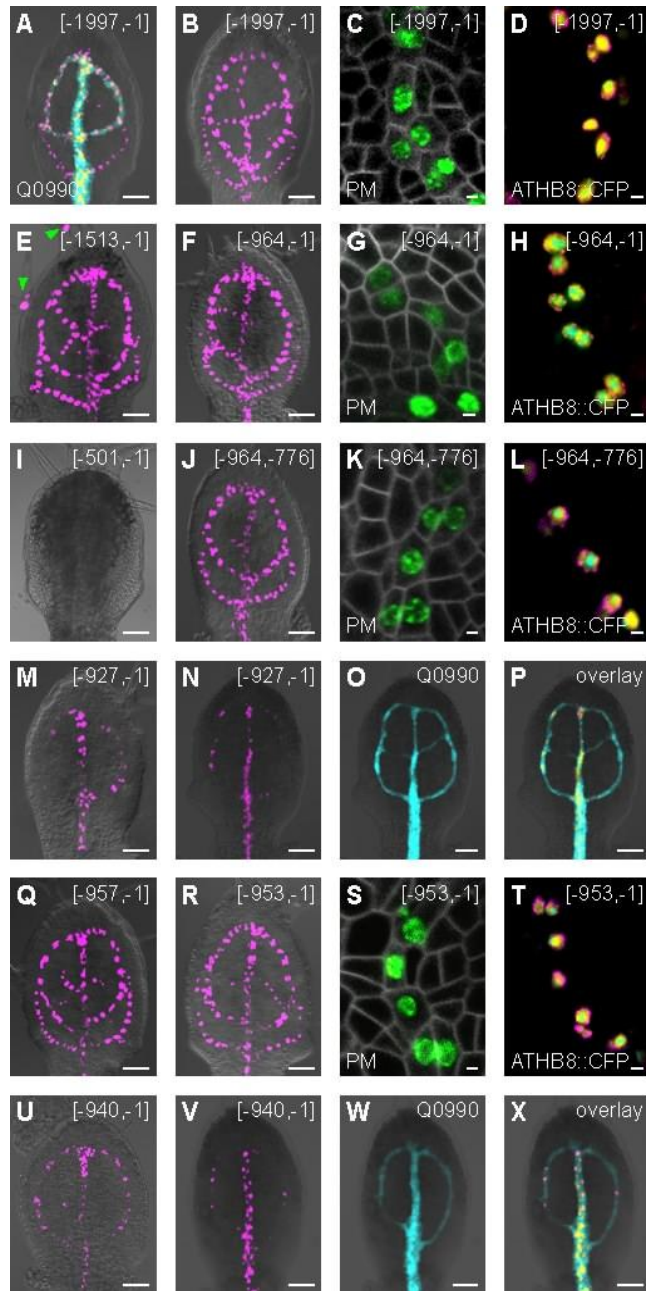


Figure 2.9. Leaf expression conferred by *ATHB8* promoter deletions. (A-X) First leaves, abaxial view. Promoter variants (A-N,Q-V) or markers (O,P,W,X) are shown above, additional markers below. (A,B,E,F,I,J,M-R,U-X) Overlay of confocal-laser-scanning microscopy and transmitted light images. (C,D,G,H,K,L,S,T) Confocal-laser-scanning microscopy images. (A,D,H,L,P,T,X) Image color-coded with a dual-channel LUT as described for Fig. 2.5. (A,O,P,W,X) Procambium labeling by Q0990:mGFP5er expression (cyan). (A,B,D-F,H-J,L-N,P-R,T-V,X) HTA6:EYFP expression (magenta). (C,G,K,S) HTA6:EYFP expression (green) and plasma membrane (PM) labeling by UBQ10::EGFP:LTI6B expression (white). (D,H,L,T) *ATHB8*::ECFP-Nuc expression (cyan). (P,X) Overlay of images in N, O and V, W, respectively. (E) Note expression in trichomes (green arrowheads), which is absent with the -1997 to -1 and -964 to -1 promoter fragments, suggesting the presence of a suppressor of trichome expression in the -1997 to -1513 promoter region and the presence of an inducer of trichome expression in the -1513 to -964 promoter region. Scale bars: 25 μ m (A,B,E,F,I,J,M-R,U-X); 2.5 μ m (C,D,G,H,K,L,S,T).

as the -501 to -1 fragment did not promote any leaf expression (Fig. 2.9I). This suggests that the 463-base-pair (bp) region of the *ATHB8* promoter between -964 and -501 is necessary for *ATHB8* preprocambial expression.

To test whether the *ATHB8* 5' untranslated region in the -964 to -1 promoter fragment is essential to drive preprocambial expression, we deleted the sequence immediately downstream of the *ATHB8* transcriptional start site, as predicted by sequence alignment with the furthest upstream expressed sequence tag available (AV830211), while conserving a putative initiator sequence (Smale and Kadonaga, 2003) centered around the predicted transcription start site (Fig. 2.8). The resulting 188-bp region of the *ATHB8* promoter between -964 and -776 was still able to impart preprocambial expression (Fig. 2.9J-L), suggesting that the *ATHB8* leader sequence is dispensable for preprocambial expression. To further define the regulatory sequences required for *ATHB8* preprocambial expression, we generated a 5' deletion of the -964 to -776 region at position -927 (Fig. 2.8). The -927 to -1 promoter fragment was not able to drive vascular expression at preprocambial stages (Fig. 2.9M-P), suggesting that the 37-bp region of the *ATHB8* promoter from -964 to -927 is necessary for preprocambial expression.

Finally, to more precisely map the sequences essential for *ATHB8* preprocambial expression, we generated progressive 5' deletions of the -964 to -927 region (Fig. 2.8). Because the -940 to -1 promoter fragment was not able to direct vascular expression at preprocambial stages (Fig. 2.9U-X), the region from -953 to -1 constitutes the shortest fragment that still promoted preprocambial expression (Fig. 2.9R-T). This suggests that the 13 bp sequence between -953 and -940 of the *ATHB8* promoter is indispensable for *ATHB8* preprocambial expression.

2.3.5 Expression triggered by mutated variants of the *ATHB8* promoter

Interrogation of available databases of regulatory elements predicted the presence of core binding sites for MYELOBLASTOSIS (MYB) and GT-ELEMENT BINDING FACTOR (GT1) transcription factors in the -953 to -940 *ATHB8* promoter fragment that is required for preprocambial expression (Fig. 2.8). By manual inspection, we further identified a TGTCTG motif, which is a variant of

the TGTCTC auxin-response element (ARE) (Li *et al.*, 1994; Liu *et al.*, 1994) (Fig. 2.8). To test whether any of these putative regulatory elements are necessary for *ATHB8* preprocambial expression, we generated variants of the -953 to -1 *ATHB8* promoter fragment in which each of the three elements was individually mutated so as to abolish binding of the predicted transcription factor as previously determined experimentally (Gubler *et al.*, 1999; Ouwerkerk *et al.*, 1999; Ulmasov *et al.*, 1997a; Ulmasov *et al.*, 1997b) (Fig. 2.8). As shown in Fig. 2.10, mutations in the MYB or GT1 presumed binding sites had no effect on the activity of the -953 to -1 *ATHB8* promoter fragment (Fig. 2.10A,C,D). However, mutation in the hypothetical ARE resulted in loss of expression at preprocambial stages (Fig. 2.10E-H). Furthermore, the expression induced by the -953 to -1 *ATHB8* promoter fragment containing the mutated TGTCTG element was indistinguishable from that induced by the -940 to -1 fragment, which deleted the entire region containing the MYB and GT1 core recognition sequences and the putative ARE (Fig. 2.10B,E). This suggests that the TGTCTG sequence in the -953 to -940 region of the *ATHB8* promoter is required for *ATHB8* preprocambial expression.

2.3.6 Auxin responsiveness of *ATHB8* promoter sequences

The TGTCTG element that we identified as being indispensable for *ATHB8* preprocambial expression is very similar to the TGTCTC element necessary for the auxin response (Li *et al.*, 1994; Liu *et al.*, 1994), and *ATHB8* expression is auxin inducible (Baima *et al.*, 1995). To test whether *ATHB8* auxin responsiveness depends on the TGTCTG element and whether such a sequence therefore represents a functional ARE, we monitored patterns of HTA6:EYFP fluorescence conferred by *ATHB8* promoter variants in 4-DAG leaves after their exposure to the synthetic auxin 2,4-dichlorophenoxyacetic acid (2,4-D), comparing them to HTA6:EYFP expression in mock-treated samples. Auxin inducibility of the 2.0 kb *ATHB8* promoter (Fig. 2.11A,B) was largely retained by the -953 to -1 promoter fragment (Fig. 2.11C,D), suggesting that the region of the *ATHB8* promoter between -1997 and -953 does not contribute significantly to auxin-regulated *ATHB8* expression. Conversely, auxin responsiveness was lost in the -940 to -1 *ATHB8* promoter fragment (Fig. 2.11E,F), suggesting that the

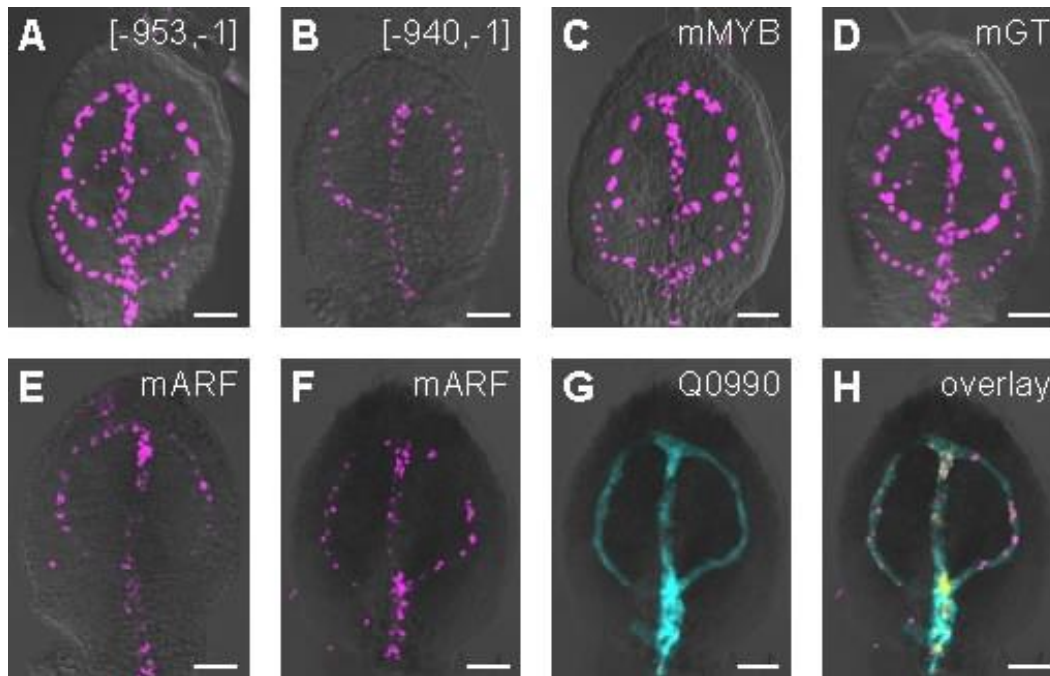


Figure 2.10. Leaf expression conferred by mutated versions of the *ATHB8* promoter. (A-H) First leaves, abaxial view. Promoter variants are shown above. Overlay of confocal-laser-scanning microscopy and transmitted light images. (A-F,H) HTA6:EYFP expression (magenta). (G,H) Procambium labeling by Q0990:mGFP5er expression (cyan). (H) Overlay of images in F,G. Image color-coded with a dual-channel LUT as described for Fig. 2.5. Scale bars: 25 μ m.

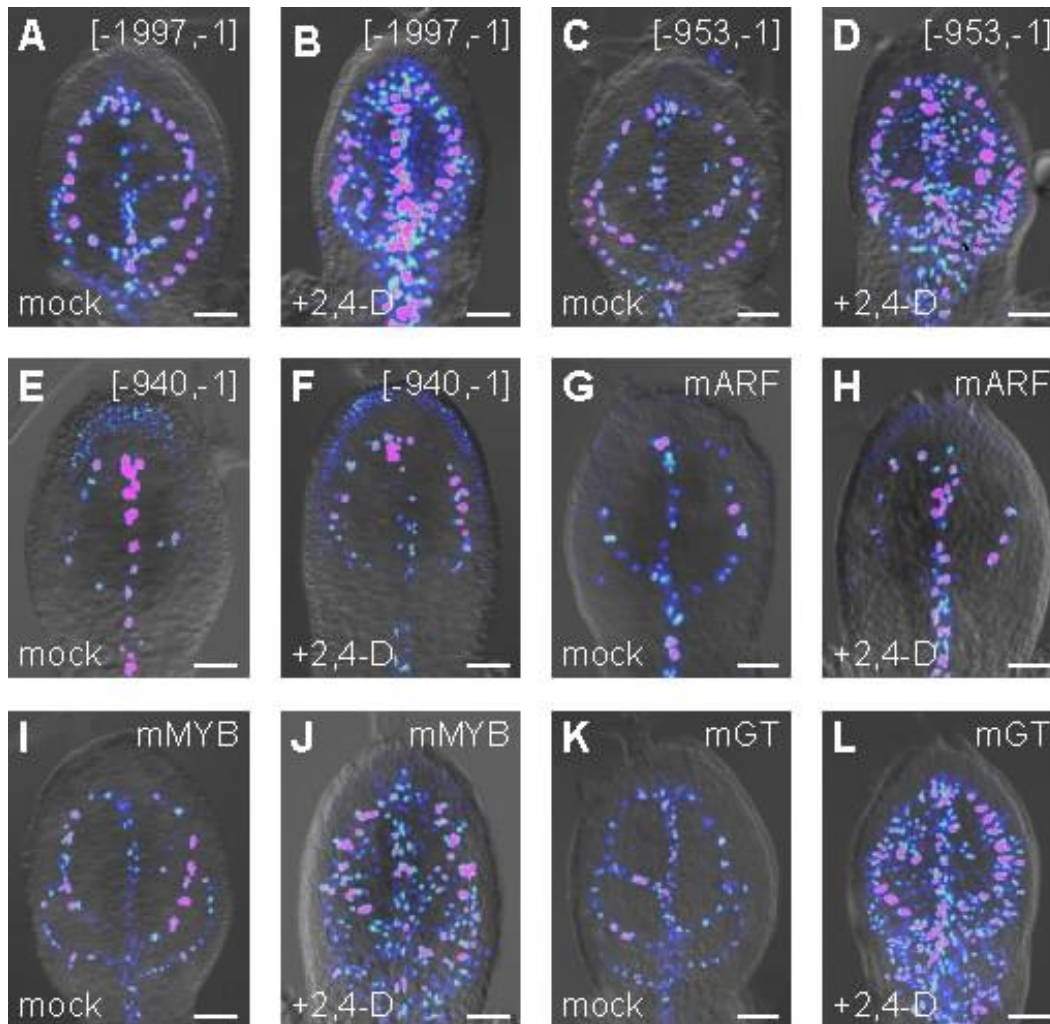


Figure 2.11. Auxin responsiveness of *ATHB8* promoter sequences in the leaf. (A-L) First leaves, abaxial view. Promoter variants are shown above, treatment below. Overlay of confocal-laser-scanning microscopy and transmitted light images. Images of mock and 2,4-dichlorophenoxyacetic acid (2,4-D)-treated leaves were taken at an identical setting and color-coded with an intensity LUT as described for Fig. 2.2. Scale bars: 25 μ m.

region of the *ATHB8* promoter between -953 and -940 is responsible for auxin inducibility. Within this region of the *ATHB8* promoter, mutation in the TGTCTG element, but not in the putative MYB and GT1 binding sites, eliminated auxinresponsiveness (Fig. 2.11G-L). Therefore, we conclude that the TGTCTG element in the *ATHB8* promoter is a functional ARE and that this sequence is required for both *ATHB8* preprocambial expression and auxin inducibility.

2.3.7 Regulators of *ATHB8* preprocambial expression

Transcription factors of the auxin-response factor (ARF) family have been shown to bind AREs *in vitro* (Guilfoyle and Hagen, 2001). Twenty-two ARFs have been identified in *Arabidopsis* (Guilfoyle and Hagen, 2007), and the TGTCTG element in the *ATHB8* promoter could be the target of several, if not all, of these ARFs (see below and Section 2.4). We focused on ARF5/MONOPTEROS (MP hereafter) because of the reduced vascularization of *mp* leaves (Przemeck *et al.*, 1996) and the decreased *ATHB8* transcript abundance in *mp* seedlings (Mattsson *et al.*, 2003).

If MP is a regulator of *ATHB8* preprocambial expression, one would expect it to be at least partially coexpressed with *ATHB8*. To test this, we first monitored expression of a functional (see Section 2.2.1) translational fusion of MP with ECFP in leaf development. Unlike *ATHB8*, MP::MP:ECFP expression was initiated in wide domains (Fig. 2.12A-C), but during leaf development these broad fields of expression resolved into narrower domains before subsiding to undetectable levels (Fig. 2.12B,C). To test whether MP expression domains represent locations of *ATHB8* expression, we visualized fluorescence in leaves simultaneously harboring *ATHB8*::HTA6:EYFP and MP::MP:ECFP, and invariantly observed overlap of *ATHB8*::HTA6:EYFP signals with MP::MP:ECFP expression (Fig. 2.12D).

If MP is a positive regulator of *ATHB8* expression at preprocambial stages, mutations in MP should at least reduce levels of *ATHB8* preprocambial expression. Expression of *ATHB8*::HTA6:EYFP, and of HTA6:EYFP when driven by the -953 to -1 fragment of the *ATHB8* promoter, was initiated in preprocambial cells of wild-type leaves (Fig. 2.9A-D,R-T; 2.12E,F). However, the

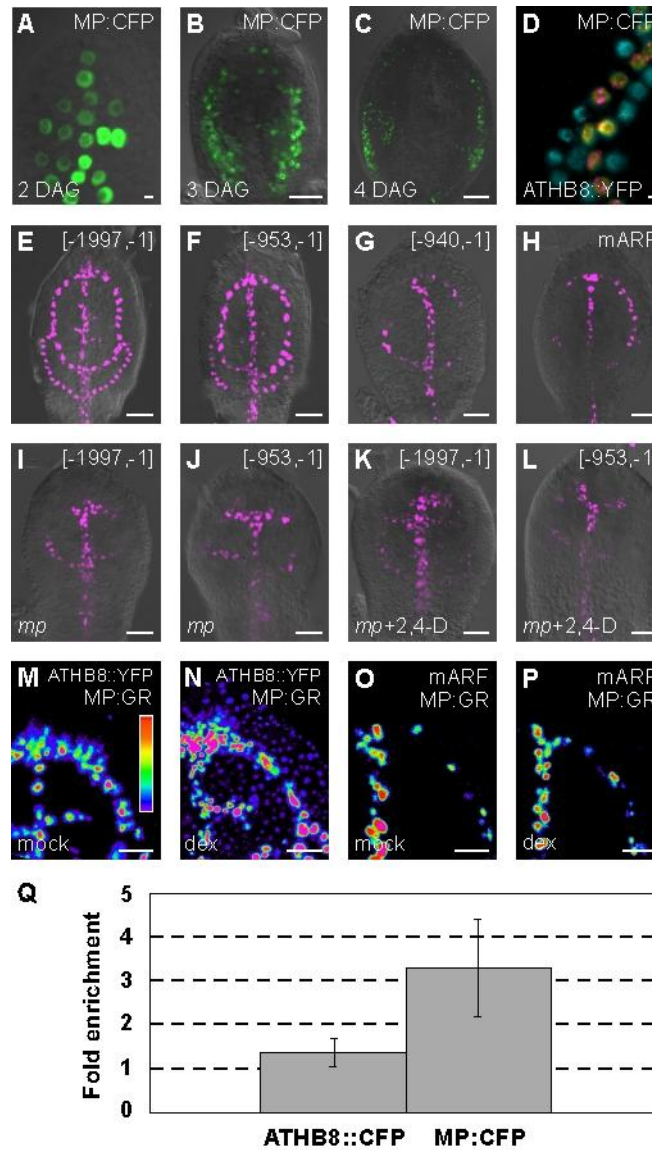


Figure 2.12. Control of *ATHB8* leaf preprocambial expression. (A-P) First leaf primordia, lateral (A) or abaxial (B-P) view. Markers (A-D), promoter variants (E-P) and genotypes (M-P) are shown above, age (DAG) (A-C), additional markers (D), genotypes (I-L) and treatments (I-P) below. (A-C,E-L) Overlay of confocal laser microscopy and transmitted light images. (D,M-P) Confocal laser microscopy images. (A-C) MP::MP:ECFP (MP:CFP) expression (green). (D)MP::MP:ECFP expression (cyan). (D-L) HTA6:EYFP expression (magenta). (D) Image color-coded with a dual-channel LUT as described for Fig. 2.5. (M-P) Images of mock and dexamethasone-treated leaves were taken at an identical setting and color-coded with a spectral LUT (shown in M) in which black and magenta were used to encode zero-value and saturated pixels, respectively, and violet, blue, green, yellow, orange and red to encode increasing HTA6:EYFP signal levels. (Q) Enrichment of TGTCTG containing *ATHB8* promoter fragments in chromatin immunoprecipitation assays performed on *ATHB8*::ECFP-Nuc and MP::MP:ECFP 4-DAG seedlings. Values indicate mean \pm s.d. of three technical replicates for each of three (*ATHB8*::ECFP-Nuc) or four (MP::MP:ECFP) biological replicates. The difference between *ATHB8*::ECFP-Nuc and MP::MP:ECFP populations was analyzed with two-tailed unpaired *t*-test and was significant at $P < 0.001$. For details, see Section 2.2.5. Scale bars: 2.5 μ m (A,D); 25 μ m (B,C,E-L); 10 μ m (M-P).

early stages of expression of these constructs were abolished in the background of the strong (Section 2.2.2) *mp* mutant allele U55 (Fig. 2.12I,J). Furthermore, their expression in *mp* leaves was remarkably similar to that conferred in wild type by loss or mutation of the TGTCTG element in the *ATHB8* promoter (Fig. 2.12G,H). Finally, expression of neither construct could be induced by exogenous 2,4-D in the *mp* mutant background (Fig. 2.12K,L). This suggests that MP is required for both *ATHB8* preprocambial expression and auxin inducibility, and that MP function at the *ATHB8* promoter is mediated by the TGTCTG element.

If MP activity is a limiting factor for *ATHB8* expression, ubiquitous MP expression should result in expansion of *ATHB8* expression domains. To test this, we visualized fields of *ATHB8::HTA6:EYFP* activity in dexamethasone-exposed *UBQ10::MP:GR* leaves and compared them with those in mock-treated leaves. Broadened *ATHB8::HTA6:EYFP* expression domains were only detected in dexamethasone-treated samples (Fig. 2.12M,N), and this response was dependent on the presence of the TGTCTG element in the *ATHB8* promoter (Fig. 2.12O,P).

Finally, we asked whether MP directly regulates *ATHB8* expression. To test this, we immunoprecipitated chromatin-crosslinked ECFP in *MP::MP:ECFP* and *ATHB8::ECFP-Nuc* seedlings; we then assayed levels of co-precipitated *ATHB8* promoter regions in *MP::MP:ECFP* and, to control for the binding of nuclear ECFP to the *ATHB8* promoter, in *ATHB8::ECFP-Nuc* samples. We detected a statistically significant ($P < 0.001$) 2.5-fold enrichment in the *ATHB8* promoter fragment that contains the TGTCTG element in *MP::MP:ECFP* versus *ATHB8::ECFP-Nuc* chromatin immunoprecipitates (Fig. 2.12Q), suggesting that MP resides *in vivo* at the *ATHB8* promoter.

In conclusion, our results suggest that the ARF MP is an essential, direct, and positive regulator of *ATHB8* preprocambial expression and auxin responsiveness.

2.3.8 Genetic interaction between *mp* and *athb8*

Recognizable effects of loss of *ATHB8* function in leaf vascular development are restricted to transient or conditional defects, but any additional regulatory potential of *ATHB8* might be masked by wild-type *MP* activity in *athb8* mutants.

To test this, we compared vascular defects in mature leaves of the weak *mp* mutant allele *arf5-2* with those of the *arf5-2 athb8-11* double mutant. The *arf5-2* allele carries a single T-DNA insertion at the 3' end of the *MP* coding region (see Section 2.2.2) and displayed ~40% penetrance of the rootless phenotype (85/871 seedlings segregating from *arf5-2* heterozygous parents). *arf5-2* homozygous seedlings could form an embryonic root and be grown on soil, but they were invariably sterile (44/44 *arf5-2* homozygous individuals found among 350 genotyped wild-type-looking plants segregating from *arf5-2* heterozygous parents). Most of the mature first leaves of rooted *arf5-2* seedlings (49/54) showed a vascular pattern complexity similar to that of wild-type or *athb8-11* first leaves (Fig. 2.13A,B,I). However, vein loops in *arf5-2* leaves were located further away from the leaf margin than in wild-type or *athb8-11* leaves ('centralized vasculature') (Fig. 2.13A,B,I). At maturity, approximately half of the first leaves of rootless *arf5-2* seedlings (32/69) were characterized by a normally complex, but centralized vein pattern, whereas the remaining half of the leaves displayed a simpler vascular organization (Fig. 2.13D,E,I). Finally, in ~60 % of the leaves of either rooted or rootless *arf5-2* seedlings (32/54 and 41/69, respectively), the midvein bifurcated at the leaf tip (Fig. 2.13C,E,I). The overall complexity of vein pattern was only slightly reduced by additional loss of *ATHB8* function in the *arf5-2* background (Fig. 2.13I). However, ~80 % of the leaves of either rooted (65/86) or rootless (35/46) *arf5-2 athb8-11* seedlings developed a terminally branched midvein (Fig. 2.13I), suggesting an enhancement of *arf5-2* leaf vascular defects in the double mutant, irrespective of its root phenotype.

If *ATHB8* preprocambial expression is contingent on any ARF activity additional to *MP*, the consequences of strongly reduced or complete loss of *MP* function on leaf vascular development should be further aggravated by additional deprivation of *ATHB8* activity. To test this, we compared patterns of vascularization in leaves of *mp^{U55}* with those of the *mp^{U55} athb8-11* double mutant. First leaves of the invariably rootless *mp^{U55}* seedlings displayed a dramatically simplified vascular organization, typically characterized by a bifurcated midvein and few additional

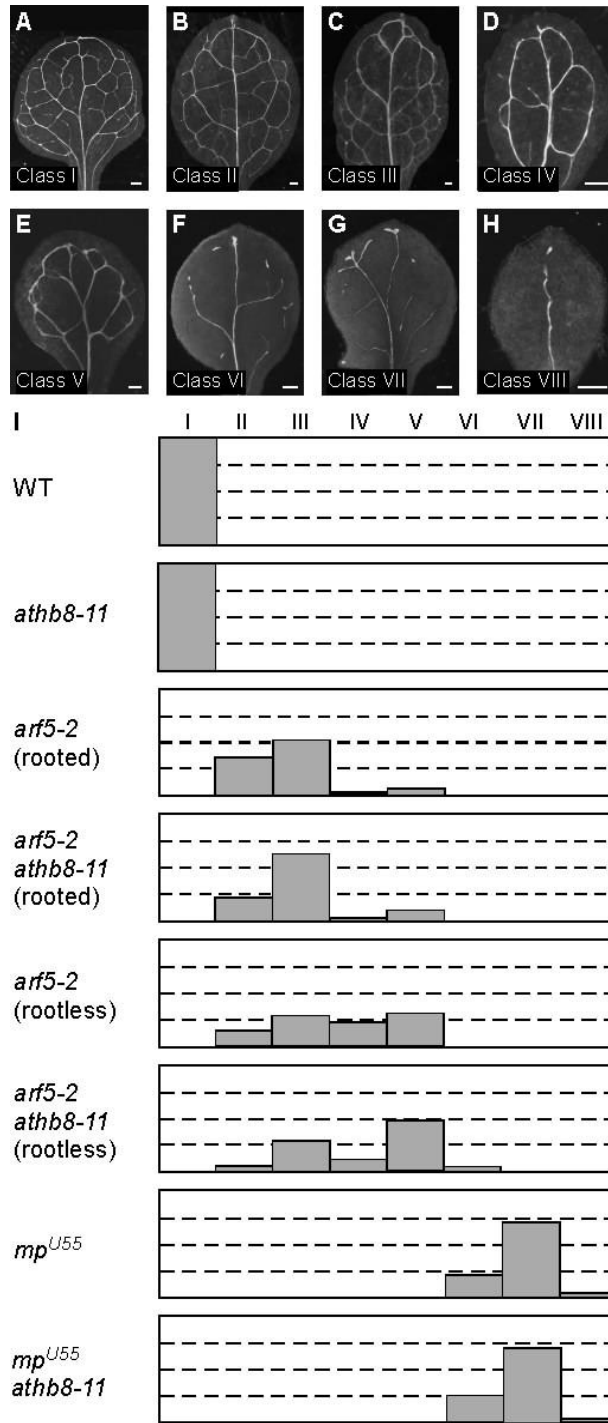


Figure 2.13. Genetic interaction between *mp* and *athb8*. (A-H) Dark-field illumination of cleared mature leaves illustrating phenotypic classes: normal vasculature (A), centralized vasculature with unbranched midvein (B), centralized vasculature with bifurcated midvein (C), reduced vasculature with unbranched midvein (D), reduced vasculature with bifurcated midvein (E), fragmented vasculature with unbranched midvein (F), fragmented vasculature with bifurcated midvein (G), and solitary midvein (H). For details, see text. (I) Percentage of each phenotypic class in wild type, single mutants and double mutant combinations of *athb8-11* with weak (*arf5-2*) and strong (*mp^{U55}*) *mp* alleles. Dashed lines indicate 25, 50 and 75%. See also Table 2.3. Scale bars: 0.25 mm.

vein fragments scattered across the lamina, and this phenotypic spectrum was not appreciably altered by supplemental loss of *ATHB8* function (Fig. 2.13I).

Like *athb8*, *mp* seedlings display enhanced sensitivity to auxin transport inhibition (Schuetz *et al.*, 2008). Because loss of *ATHB8* function augments the effects of diminished *MP* activity on vein patterning, we asked whether the elevated response of *athb8* to auxin transport inhibitors could be further exacerbated in a background of reduced *MP* function. To test this, we assessed the sensitivity to NPA of single and double mutant combinations of *arf5-2* and *athb8-11*. Reduction in auxin transport frequently results in leaf fusion (Okada *et al.*, 1991; Schuetz *et al.*, 2008; Sieburth, 1999; Wang *et al.*, 2005a), a response that we first observed in wild type at 10 μ M NPA (2/95) and in *athb8-11* at 5 μ M NPA (2/33). Approximately 10 % (3/29) of *arf5-2* seedlings displayed leaf fusion at 1 μ M NPA, consistent with strong NPA hypersensitivity of *mp* mutants. At the same concentration of NPA, nearly 40 % (10/27) of *arf5-2 athb8-11* double mutants displayed leaf fusion (Fig. 2.14H). Because loss of *ATHB8* function by itself did not result in leaf fusion at this concentration of NPA (Fig. 2.14F), we conclude that leaf separation defects elicited by reduced auxin transport in *arf5-2* are strongly enhanced by additional *athb8* mutation.

In summary, our results suggest that non-conditional and conditional contributions of *ATHB8* to leaf vascular patterning are covered by *MP* activity. Furthermore, our data suggest that any unique role of *ATHB8* in vein patterning becomes largely inconsequential upon severe loss of *MP* function and, therefore, that *MP* is the primary regulator of *ATHB8* non-redundant activities in leaf vascular patterning (see Discussion).

2.4 DISCUSSION

The molecular details of the mechanisms controlling the recruitment of ground cells in the leaf towards procambium formation are largely unknown. Substantial evidence has, however, been accumulating that implicates polarly transported auxin signals in leaf vascular patterning (Berleth *et al.*, 2000; Sachs, 1981). Near ubiquitous expression of the auxin exporter PIN1 narrows to files of procambial

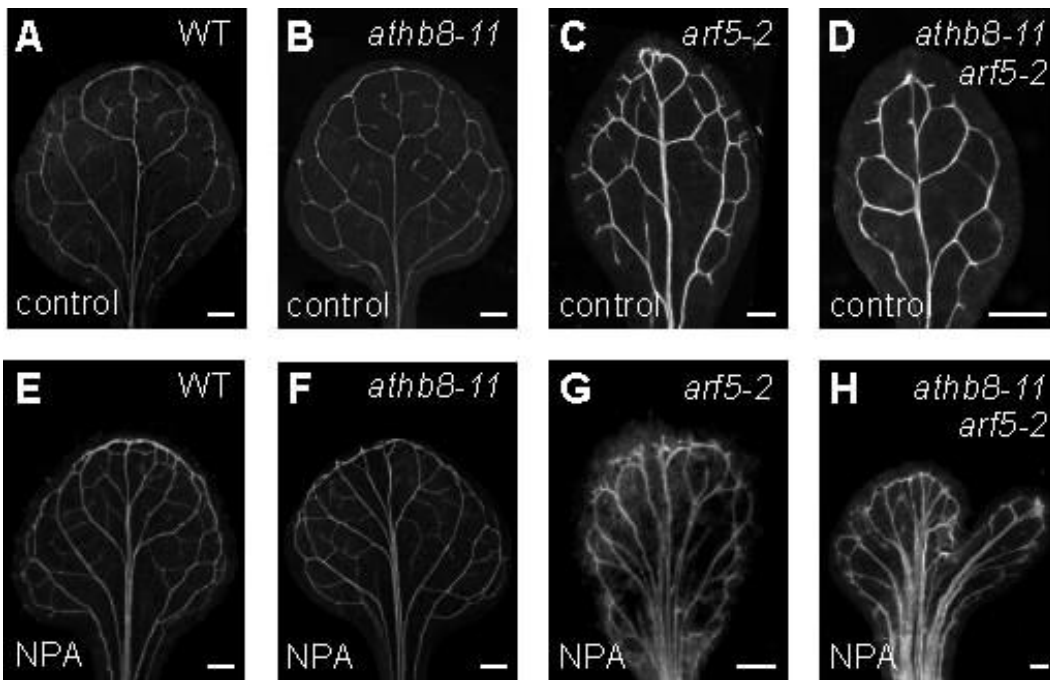


Figure 2.14. Responsiveness of leaves of *mp* and *athb8* mutant combinations to auxin transport inhibition. (A-H) Dark-field illumination of cleared mature first leaves, abaxial view. Genotypes are shown above, treatments (1 μM NPA) below. See also Table 2.4. Scale bars: 0.5 mm.

cells during leaf development (Scarpella *et al.*, 2006; Wenzel *et al.*, 2007), but how cells that will acquire procambial identity are selected among the population of PIN1-expressing cells is not known. Nevertheless, these anatomically inconspicuous ‘preprocambial’ cells can be identified by expression of the *HD-ZIPIII* gene *ATHB8*.

In this study, we have explored biological functions of *ATHB8* in leaf vascular development and searched for regulatory elements and *trans*-acting factors required for *ATHB8* preprocambial expression. We show that *ATHB8* is necessary to stabilize preprocambial cell specification against perturbations in auxin transport, to confine preprocambial cell state acquisition to narrow regions, and to coordinate procambial cell identity assignment within and between veins. Further, we find that *ATHB8* expression in preprocambial cells depends on the presence of an ARE in its promoter. Finally, we show that the *ATHB8* preprocambial regulatory element is a direct target of the transcriptional regulator MP.

2.4.1 Non-redundant roles of *ATHB8* in leaf vascular development

Loss of *ATHB8* function leads to expanded expression of the preprocambial marker J1721 and asynchronous expression of the procambial marker Q0990. Expression of these reporters is strictly associated with zones of vascular differentiation in a variety of genetic backgrounds and under a number of experimental conditions (*e.g.*, Dello Ioio *et al.*, 2007; Leroy *et al.*, 2007; Levesque *et al.*, 2006; Sawchuk *et al.*, 2007; Song *et al.*, 2008; Weijers *et al.*, 2005; Weijers *et al.*, 2006), implicating *ATHB8* in constraining preprocambial state acquisition to narrow fields of cells and in coordinating procambial cell identity assignment within and between veins. Although premature differentiation of procambial strands in *athb8* leaves could simply represent a read-out of preprocambial defects, it is consistent with a proposed role for *ATHB8* in maintaining the meristematic potential of vascular cells (Baima *et al.*, 2001; Kang and Dengler, 2002).

The behavior of J1721 and Q0990 in *athb8* strongly resembles that in wild type under conditions of reduced auxin transport (Sawchuk *et al.*, 2007),

suggesting a role for *ATHB8* in promoting auxin flow during early stages of vein formation. According to this interpretation, loss of *ATHB8* function would be expected to confer an enhanced response to auxin transport inhibitors. In the absence of alterations in auxin sensitivity, PIN1-labeled preprocambial cell specification and vein patterning are more sensitive to chemical obstruction of auxin flow in *athb8* than in wild type, suggesting the presence of auxin transport defects in the mutant. Alternatively, or additionally, the enhanced response of *athb8* leaves could suggest a function for *ATHB8* in stabilizing auxin flow against perturbations, consistent with the observed insensitivity of procambial strands to auxin transport inhibition (Mattsson *et al.*, 1999).

Genetic or pharmacological interference with auxin flow generates broad areas of vascular differentiation (Mattsson *et al.*, 1999; Sieburth, 1999), while it is difficult to explain, based on current knowledge, how exuberant preprocambial state acquisition and incongruent procambial identity assignment would per se result in hypersensitivity to auxin transport inhibition. Nevertheless, because of feedback between auxin flow and vascular development (Sachs, 1981), it is not currently possible to assign a fixed position to either of these processes in a linear cause-effect relationship. As such, the exaggerated response of *athb8* to auxin transport interference might underlie the altered marker behavior, or be a consequence of it, or the two might point to unrelated functions of *ATHB8* in vein formation. Although the assignment of a role for *ATHB8* in leaf vascular development at the molecular level will have to await the identification of its targets, the enhanced sensitivity of PIN1 expression and vascular patterns to obstruction of auxin flow in *athb8* leaves suggests that *ATHB8* is required to stabilize the selection of ground cells that will acquire a preprocambial state against perturbations in auxin transport.

2.4.2 Masked functions of *ATHB8* in vein patterning

Irregular vein formation in *athb8* leaves is corrected and eventually resolves into a normal leaf vascular pattern (Baima *et al.*, 2001; Prigge *et al.*, 2005).

Amelioration of early vascular defects during organ development is not unprecedented (*e.g.*, Scarpella *et al.*, 2003), and responses of the vascular system

to local auxin application or auxin transport inhibition are more severe when evaluated at early stages of vein development (Scarpella *et al.*, 2006; Wenzel *et al.*, 2007). How are defects at early stages of vein formation normalized during *athb8* leaf development? One possibility is that *ATHB8* has an ephemeral role that is confined to early stages of vascular strand formation and that it has an inconsequential function at later stages. Alternatively, or in addition, functional compensation among members of the *HD-ZIPIII* family could rectify defects due to loss of *ATHB8* activity.

If transience is an intrinsic property of the biological role of *ATHB8*, effects of loss of *ATHB8* function should not be expected to have long-lasting consequences in conditions of reduced activity of one of its regulators. The enhancement of vein pattern defects in *arf5-2 athb8-11* double mutants as compared with those in the weak *mp* allele *arf5-2* suggests, however, that *ATHB8* can have permanent effects on vein patterning. In leaves of *arf5-2*, the midvein frequently bifurcates at the leaf apex, a response that is commonly evoked by defective auxin transport (Mattsson *et al.*, 1999; Sieburth, 1999). The fraction of leaves displaying this phenotype increases in the strong *mp*^{U55} allele, suggesting that the defect directly depends on *MP* function. In double-mutant combinations of *athb8-11* with *arf5-2*, no new phenotype class is observed; rather, the fraction of leaves displaying midvein bifurcation is increased to closely match that in the *mp*^{U55} allele. Strong *arf5/mp* alleles display an exaggerated response to auxin transport interference that results in obstruction of leaf formation (Schuetz *et al.*, 2008), whereas enhanced sensitivity to defective auxin flow in the weak *mp* allele *arf5-2* most conspicuously manifests in leaf fusion at very low concentrations of auxin transport inhibitors. Under these conditions, leaves of *athb8* mutants show normal sensitivity to auxin flow inhibition, but additional loss of *ATHB8* function greatly increases the occurrence of leaf separation defects in auxin transport-inhibited *arf5-2* seedlings. Therefore, *ATHB8* has functions in vein formation that extend beyond the evanescent contribution revealed by marker analysis and the moderate input exposed by auxin flow obstruction, but the regulatory potential of

ATHB8 is concealed in the *athb8* mutant background by the presence of functional *MP* activity.

If transience is not necessarily an inherent property of *ATHB8* function in leaf vascular development, then defects at early stages of vein formation in *athb8* could be amended at successive stages of development through the overlapping activities of other members of the *HD-ZIPIII* family, as shown for other aspects of plant development (Prigge *et al.*, 2005). Because correction of *athb8* leaf vascular defects occurs to a lesser extent in the *arf5-2* background, one function of *MP* in vein development could be the regulation of the entire *HD-ZIPIII* family. Post-transcriptional downregulation of all members of the *HD-ZIPIII* family through overexpression of the *microRNA165* (*miR165*) results in cotyledon vascular defects that are remarkably similar to those displayed by strong *mp* alleles (Zhou *et al.*, 2007), and expression of other members of the *HD-ZIPIII* family in addition to *ATHB8* is reduced in the *mp* background (Mattsson *et al.*, 2003). If functional redundancy underlies amelioration of *athb8* vascular defects, the inability of the *athb8* mutation to shift the vein pattern complexity of *arf5-2* towards the severe distribution typical of *mp*^{U55} does not exclude a broader role for *ATHB8* in the regulation of leaf vascular patterning. However, further studies will be required to unravel the overlapping and redundant roles of *HD-ZIPIII* genes in vein formation.

2.4.3 Regulatory elements in preprocambial cell state acquisition

The *ATHB8* promoter is activated in files of ground cells that are stabilized towards the procambial fate (Kang and Dengler, 2004; Scarpella *et al.*, 2004). Additionally, the *ATHB8* promoter induces transient expression at the tip of the leaf and at the hydathodes, where not all *ATHB8*-expressing cells will differentiate into vascular cells (Kang and Dengler, 2004; Scarpella *et al.*, 2004). Expression of a functional *ATHB8* translational fusion recapitulates all aspects of *ATHB8* promoter activity with the exception of the non-vascular expression in the leaf tip and hydathode cells, suggesting the presence of post-transcriptional mechanisms that downregulate *ATHB8* expression at those locations. *ATHB8* transcripts are predicted to be targets of *miR165*-mediated degradation (Rhoades

et al., 2002), and *miR165* is more abundantly expressed at the leaf tip (Li *et al.*, 2005), suggesting that *miR165*-dependent posttranscriptional regulation of *ATHB8* expression might occur at locations of non-overlap between *ATHB8* promoter activity and expression of the *ATHB8* translational fusion.

Expression of *ATHB8* in preprocambial cells is strictly dependent on the presence of a TGTCTG element in its promoter. This element is a variant of the TGTCTC ARE (Li *et al.*, 1994; Liu *et al.*, 1994) and is required for auxin-induced *ATHB8* expression. That both preprocambial expression of *ATHB8* under unperturbed conditions and responsiveness of *ATHB8* to auxin signals are contingent on the activity of a single regulatory element is uncommon. In fact, the presence of a functional ARE in the promoter is not usually necessary for tissue- or stage-specific gene expression, only for a ubiquitous response to auxin signals (Li *et al.*, 1994; Liu *et al.*, 1994). Nevertheless, a synthetic promoter composed of repeats of the TGTCTC ARE coupled to a minimal viral promoter (DR5) (Ulmasov *et al.*, 1997b) is sufficient to drive expression in developing veins (Mattsson *et al.*, 2003). Furthermore, fields of DR5 promoter activity in leaf primordia seem to overlap with *ATHB8* preprocambial expression domains, although DR5 promoter-driven expression displays greater heterogeneity in onset, decay and level along individual veins (Mattsson *et al.*, 2003; Scarpella *et al.*, 2004). These observations suggest that in most auxin-responsive promoters, tissue-specific regulatory elements constrain the activity of AREs solely to auxin inducibility, whereas *ATHB8* preprocambial expression might be the unrestrained read-out of auxin signal transduction.

A confounding multitude of genes in *Arabidopsis* (~5000) contain a TGTCTG element in the 500-bp region immediately upstream of their coding sequence. This list includes genes expressed at early stages of vein development [*e.g.*, *CYCLINA2;1* (Bursens *et al.*, 2000), *SCARECROW-LIKE3* (Ckurshumova *et al.*, 2009), *CELLULOSE SYNTHASEA2* (Beeckman *et al.*, 2002)] and those with a proposed role in vascular development [*e.g.*, *SCARFACE/VASCULAR NETWORK3* (Deyholos *et al.*, 2000; Koizumi *et al.*, 2000), *VASCULAR ASSOCIATED DEATH1* (Lorrain *et al.*, 2004), *VASCULAR-RELATED NAC*

DOMAIN PROTEIN4 (Kubo *et al.*, 2005)] or auxin response [*e.g.*, *ARF2* (Li *et al.*, 2004), *AUXIN/INDOLE 3-ACETIC ACID17/AUXIN RESISTANT3* (Rouse *et al.*, 1998), *HOMEBOX FROM ARABIDOPSIS THALIANA2* (Sawa *et al.*, 2002)]. However, not all AREs present in promoters can bind ARFs *in vitro* (Inukai *et al.*, 2005), and additional regulatory elements may constrain the regulatory potential of AREs to sole auxin responsiveness (Li *et al.*, 1994; Liu *et al.*, 1994). Therefore, we consider it unlikely that all these genes are expressed in preprocambial cells. If the presence of a TGTCTG element in the promoter is unlikely to be sufficient to predict expression in preprocambial cells, what other requirements are necessary for preprocambial expression? Nucleotides flanking the TGTCTC ARE seem to act as modifiers of ARE activity (Ulmasov *et al.*, 1995; Ulmasov *et al.*, 1997a; Ulmasov *et al.*, 1997b). Vast systematic efforts will be necessary to test *in vivo* what, if any, boundary conditions are required for TGTC-containing elements to promote preprocambial expression.

2.4.4 Regulation of preprocambial cell state acquisition by ARF proteins

Transcription factors of the ARF family have been shown to bind AREs *in vitro* (Guilfoyle and Hagen, 2001). Deletion or mutation of the TGTCTG ARE in the *ATHB8* promoter eliminates preprocambial expression but does not induce expression in non-vascular cells. This observation suggests that the TGTCTG element is not the target of a repressor that normally extinguishes *ATHB8* expression outside of the vasculature, but rather that an activator binds to the TGTCTG element and induces *ATHB8* expression in vascular cells. In *Arabidopsis*, the ARF family is encoded by 22 genes, of which five [*ARF5/MP*, *ARF6*, *ARF7*, *ARF8* and *ARF19*] function as transcriptional activators in transfected protoplasts, whereas the remaining 17 behave as repressors in a similar experimental context (Guilfoyle and Hagen, 2007 and references therein). *ATHB8* preprocambial expression is under the direct control of MP, which is consistent with reduced *ATHB8* transcript levels in an *mp* background (Mattsson *et al.*, 2003). None of these observations, however, excludes the involvement of other ARFs in the control of *ATHB8* preprocambial expression. At least three of the four remaining activating ARFs are expressed in domains that may overlap

with those of *ATHB8* (Hardtke *et al.*, 2004; Li *et al.*, 2006; Okushima *et al.*, 2005; Tian *et al.*, 2004; Wilmoth *et al.*, 2005), and the class of activating ARFs is characterized by a high level of functional redundancy among its members (Hardtke *et al.*, 2004; Nagpal *et al.*, 2005; Okushima *et al.*, 2005; Wilmoth *et al.*, 2005). Further, because the tests for activation and repression of transcription by members of the ARF family rely upon transient expression assays in leaf mesophyll or suspension cell culture protoplasts, it remains possible that an ARF classified as a repressor could function as an activator, and vice versa, in certain cell types or environments (*e.g.*, Okushima *et al.*, 2005). Conditional manipulation of gene activity will be required to expose the overlapping and non-redundant roles of ARFs in the regulation of *ATHB8* preprocambial expression, as any further reduction of ARF activity than that residual in strong *mp* backgrounds is likely to directly impinge on leaf primordium formation (Hardtke *et al.*, 2004). However, deletion or mutation of the TGTCTG element in the *ATHB8* promoter confers expression in wild type that is indistinguishable from that of the full-length *ATHB8* promoter in the strong *mp*^{U55} allele. Moreover, leaf vascular defects in *mp*^{U55} cannot be further enhanced by additional loss of *ATHB8* function. Therefore, the contribution of ARFs other than MP to the control of *ATHB8* preprocambial expression is probably subtle.

A functional *MP* translational fusion is at first detected in nearly all subepidermal cells of the young leaf primordium, and its expression is only subsequently confined to sites of vein formation. This is strikingly different from the activity of the *ATHB8* promoter, which is initiated in single cell files before expression of the *MP* fusion protein has been restricted to the narrow sites of vein formation. Further, ubiquitous *MP* expression results in expanded domains of *ATHB8* expression, which do not, however, extend to include all cells in the leaf. As the TGTCTG element in the *ATHB8* promoter is a direct target of *MP* activity, why is *ATHB8* transcription not promoted in all *MP*-expressing cells? At least three formally different possibilities are conceivable (Fig. 2.15). The first is that *MP* is not sufficient to activate *ATHB8* transcription and requires the simultaneous presence of a preprocambial-specific coactivating signal. The

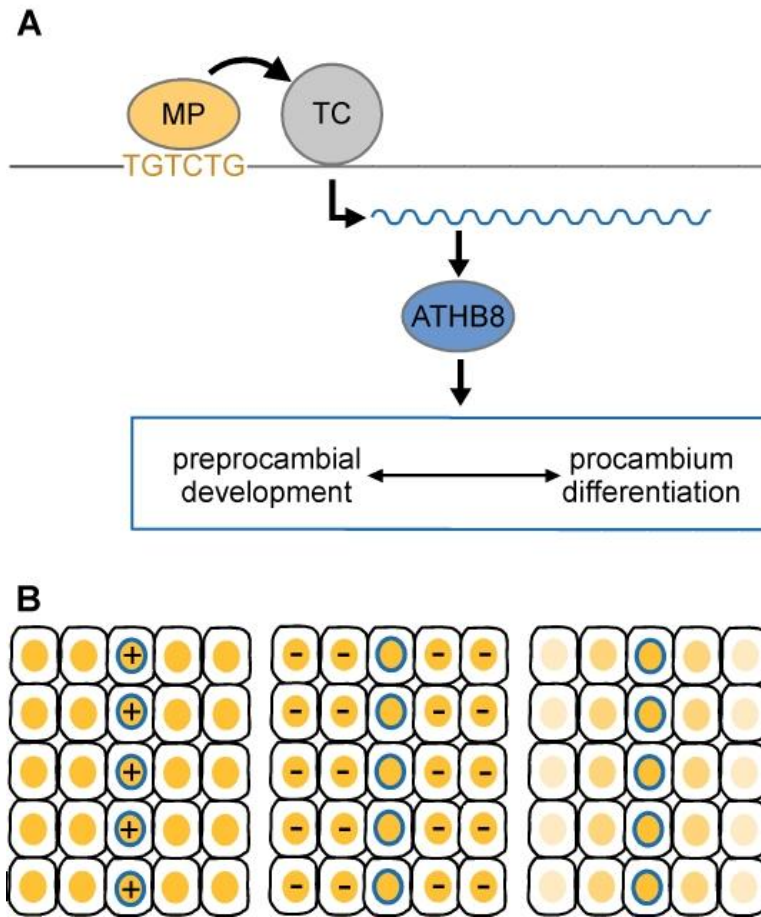


Figure 2.15. Summary and perspectives. (A) Molecular events in early vein formation. In *Arabidopsis* leaf primordia, MP binds to a TGTCTG sequence motif in the *ATHB8* promoter and initiates *ATHB8* transcription (wavy line). *ATHB8*, in turn, controls preprocambial development and procambium differentiation. These two activities could represent completely separated and self sufficient functions of *ATHB8* in leaf vascular development; they could overlap to various extents; or they could simply correspond to different readouts of the same regulatory potential. While the schematic nature of the relations presented here should be emphasized, the diagram illustrates how MP-dependent global auxin signaling inputs are molecularly partitioned into defined patterning events in leaf vascular development. TC, transcription complex. (B) Mechanisms for restriction of *ATHB8* transcription to a subpopulation of MP-expressing cells. At least three formally different scenarios can be envisaged. According to the first (left), expression of *ATHB8* (ring) in a subset of the cells expressing MP (circle) would depend on the presence of an activating signal (plus sign) in preprocambial cells. This cue may not depend on the transcriptional regulatory properties of MP and does not necessarily implicate sequence-specific DNA binding activities, but could reflect, for example, different chromatin configurations at the *ATHB8* promoter in different cells (Kwon *et al.*, 2006; Wagner and Meyerowitz, 2002). In the second scenario (central), confined activation of *ATHB8* expression within wide fields of MP expression would rely upon removal of an inhibiting signal (minus sign) in preprocambial cells, such as transcription-independent degradation of repressors of the Aux/IAA family (Guilfoyle and Hagen, 2007). Finally, according to the third scenario, MP protein would be present in an instructive gradient in leaf primordia with maximum expression in cells that initiate *ATHB8* transcription. Because the *ATHB8* preprocambial element is expected to be suboptimal for MP binding (Ulmasov *et al.*, 1997a), activation of *ATHB8* expression would only occur where MP levels are sufficiently high.

second is that MP activity depends on the specific removal of an inhibiting cue in preprocambial cells. Finally, the third is that MP protein is present in an instructive gradient in leaf primordia, with maximal expression in cells that will activate *ATHB8* transcription. It should be emphasized that these scenarios do not necessarily exclude one another, but that they could all, to varying extents, co-exist. Although it will be interesting in the future to understand how broad patterns of *MP* expression are translated into narrow sites of *ATHB8* activation, the identification of regulators of early vein development and of the transcription factors controlling their expression already assists in defining the contribution of auxin signal transduction to leaf vascular patterning at the molecular level.

CHAPTER 3: SIMULTANEOUS ACTIVATION OF *SHR* AND *ATHB8* EXPRESSION DEFINES SWITCH TO PREPROCAMBIAL CELL STATE IN *ARABIDOPSIS* LEAF DEVELOPMENT ²

3.1 INTRODUCTION

The vascular system of plants is a network of veins that extends throughout all organs (Esau, 1965). Veins transport water and nutrients, and are a source of signals that act locally, to assign identity to surrounding cells, and systemically, to coordinate initiation of new shoot organs with that of new roots (Berleth and Sachs, 2001). Sites of vein formation are foreshadowed by the appearance of files of elongated procambial cells, which in leaf development seem to emerge *de novo* from within a homogeneous population of isodiametric ground cells (Esau, 1943; Foster, 1952; Louis, 1935).

The molecular events that lead to acquisition of procambial cell identity during leaf development are not entirely clear, but available evidence supports a decisive role for transport and transduction of the plant signaling molecule auxin in specifying paths of leaf vein formation. Auxin application to leaf primordia induces formation of new veins (Sachs, 1975; Sachs, 1989; Scarpella *et al.*, 2006), and chemical inhibition of auxin transport during leaf development severely disturbs vein patterning (Mattsson *et al.*, 1999; Sieburth, 1999). Consistent with these observations, mutants impaired in auxin biosynthesis, response, or transport display diagnostic alterations in leaf vein patterns (Alonso-Peral *et al.*, 2006; Cheng *et al.*, 2006; Mattsson *et al.*, 1999; Przemeck *et al.*, 1996). During leaf development, ground cells are directed toward procambial fate through induction

² A version of this chapter has been published. Copyright © 2010 Wiley. Used with permission from J. Gardiner, T. J. Donner, E. Scarpella. (2011). Simultaneous activation of *SHR* and *ATHB8* expression defines switch to preprocambial cell state in *Arabidopsis* leaf development. *Developmental Dynamics*. 2011. **240**(1): 261-270. Wiley-Liss, Inc. doi: <http://dx.doi.org/10.1002/dvdy.22516>.

Conceived and designed the experiments: JG, TJD, ES. Performed the experiments: JG, TJD, ES. Analyzed the data: JG, TJD, ES. Wrote the paper: JG, TJD, ES. I generated the data that gave rise to figures: 3.1, 3.4, 3.5, and 3.7.

with that of *ATHB8* during undisturbed leaf development. Parallel initiation of expression of *SHR* and *ATHB8* persisted under conditions of experimentally manipulated leaf vascular patterning, suggesting that synchronous activation of expression of *SHR* and *ATHB8* operationally defines a reproducible cell state that presages vein appearance. While the *ATHB8* protein remained confined to leaf vascular cells, however, the *SHR* protein additionally localized to adjacent, periveinal positions, suggesting functions of preprocambial cells beyond vein formation. Our observations assist in the molecular characterization of cell state at morphologically indistinguishable, preprocambial stages of leaf vein formation.

3.2 MATERIALS AND METHODS

3.2.1 Terminology and notation

We apply the generic term “subepidermal” to all positions of the leaf beneath the epidermis. We refer to “ground cells” as polygonal, isodiametric, subepidermal cells of the leaf. We use the terms “procambial” and “procambium” to indicate morphologically identifiable vascular cell precursors. We designate as “preprocambial” all stages of vein development before procambium formation. We adopt the “:” symbol to denote translational fusions and the “::” symbol to denote transcriptional fusions.

3.2.2 Vector construction

All amplifications were performed on *Arabidopsis* (*Arabidopsis thaliana*) ecotype Col-0 genomic DNA using Finnzymes Phusion high-fidelity DNA polymerase (New England Biolabs Inc., Ipswich, MA) and gene-specific primers (Table 3.1). To generate the *SHR::HTA6:EYFP* construct, the 2490-bp region from -2505 to -16 of the *SHR* gene (AT4G37650) was recombined into the pFYTAG vector (Zhang *et al.*, 2005). To generate the *SHR::mCherry-Nuc* construct, the 2494-bp region of the *SHR* gene from -2504 to -10 was cloned upstream of a translational fusion of the mCherry coding sequence (Shaner *et al.*, 2004) to the 3xSV40 nuclear localization signal (Nuc) from pEYFP-Nuc (Clontech Laboratories, Mountain View, CA). To generate the *SHR::SHR:EYFP* construct, the 4107-bp

Table 3.1. Sequences of primers used in this study.

Construct name	Primer sequences
SHR::HTA6 :EYFP	SHR-2.5 ggggacaagttgtacaaaaagcaggctggacaaagaagcagagcgtgg SHR-R ggggaccactttgtacaagaaagctgggtaataagaaaatgaatagaagaaagggagacc
SHR:: mCherry- Nuc	SHR HindIII F gagaagcttgacaaagaagcagagcgtgg SHR Sali R tgggtcgacttaatgaataagaaaatgaatagaagaaaggg
SHR::SHR: EYFP	SHR prom Sali Forw2 aaagtcgaccgaagaaagggacaaagaagc SHR gDNA BamHI Rev2 ataggatccgtaggtcgccacgcactag
SCL32:: HTA6: EYFP	SCL32 Transcriptional FWD ggggacaagttgtacaaaaagcaggcttagaatcacgttcctatcgg SCL32 Transcriptional REV ggggaccactttgtacaagaaagctgggtgagtctggttttagagagaaatg
SCL32:: SCL32: EYFP	SCL32 Translational FWD agagtcgacatcttagtagaaataagcgaac SCL32 Translational REV tgcggatccaaggaacccaacggtagc
SCL29:: HTA6: EYFP	SCL29 Transcriptional FWD ggggacaagttgtacaaaaagcaggctgaacaagcgattgacggtag SCL29 Transcriptional REV ggggaccactttgtacaagaaagctgggtatgatgaaaaggtataatttgtagtagg
SCL29:: SCL29: EYFP	SCL29 Translational FWD accgtcgactaccaagagaggaacaagcg SCL29 Translational REV actgatatcctccacaatgaacaaaaggaaactg

region of the *SHR* gene from -2514 to +1593 was cloned upstream of the EYFP coding sequence (Clontech) using an Asp-Pro-Gly linker, as described in Gallagher *et al.*, 2004. To generate the SCL29::HTA6:EYFP construct, the 1679-bp region from -1686 to -7 of the *SCARECROW-LIKE29* (*SCL29*) gene (AT3G13840) was recombined into the pFYTAG vector (Zhang *et al.*, 2005). To generate the SCL29::SCL29:EYFP construct, the 3227-bp region of the *SCL29* gene from -1697 to +1530 was cloned upstream of the EYFP coding sequence (Clontech) using a Pro-Asp-Pro-Gly linker. To generate the SCL32::HTA6:EYFP construct, the 2886-bp region from -2888 to -2 of the *SCL32* gene (AT3G49950) was recombined into the pFYTAG vector (Zhang *et al.*, 2005). To generate the SCL32::SCL32:EYFP construct, the 4169-bp of the *SCL32* gene from -2940 to +1229 was cloned upstream of the EYFP coding sequence (Clontech) using an Asp-Pro-Gly linker.

3.2.3 Plant material and growth conditions

The J2501 and Q0990::mGFP5er enhancer-trap lines of the Haseloff collection (Haseloff, 1999) were obtained from the *Arabidopsis* Biological Resource Center. The WOL::HTA6:EGFP line was a generous gift of David Galbraith. The origins of the ATHB8::HTA6:EYFP, UBQ10::EGFP:LTI6B, ATHB8::ECFP-Nuc, and ATHB8::ATHB8:mCherry lines have been described (Donner *et al.*, 2009; Sawchuk *et al.*, 2007; Sawchuk *et al.*, 2008; Chapter 2). Seeds were sterilized and germinated, and seedlings and plants were grown, transformed, and selected as described in Section 2.2.2. For SHR::HTA6:EYFP, SHR::mCherry-Nuc, SCL29::HTA6:EYFP, SCL32::HTA6:EYFP, SHR::SHR:EYFP, SCL29::SCL29:EYFP and SCL32::SCL32:EYFP, the progeny of 10 to 26 independent transgenic lines were inspected to identify the most representative expression pattern. Successive expression analysis was performed on the progeny of at least three lines per construct, which were selected because of strong fluorescent protein expression that was emblematic of the expression profile observed across the entire series of transgenic lines and that resulted from single insertion of the transgene. In genetic crosses, the progeny of at least two independent lines per construct were examined. For auxin transport inhibition,

seeds were germinated on growth medium supplemented with 2.5 μM 1-N-naphthylphthalamic acid NPA (Chem Service Inc., West Chester, PA). We define “days after germination” (DAG) as days following exposure of imbibed seeds to light.

3.2.4 Microscopy and image analysis

Dissected seedling organs were mounted and imaged as described in Section 2.2.3. Brightness and contrast were adjusted through linear stretching of the histogram in ImageJ (National Institutes of Health, <http://rsb.info.nih.gov/ij>). Signal levels and colocalization were visualized as described in Section 2.2.4. Images were cropped and figures were assembled as described in Section 2.2.4.

3.3 RESULTS

In *Arabidopsis* leaves, veins are arranged in a ramified pattern that largely reflects the shape of the leaf (Candela *et al.*, 1999; Dengler and Kang, 2001; Nelson and Dengler, 1997) (Fig. 3.1A). Lateral veins depart from either side of a conspicuous central vein (midvein), extend along the leaf margin, and connect to distal veins to form prominent closed loops. A series of higher-order veins branch from midvein and loops, and can either terminate in the lamina or join two veins. Veins of succeeding orders become recognizable progressively later in the same area of the developing leaf primordium, and veins of the same order appear in a tip-to-base sequence during leaf development (Candela *et al.*, 1999; Kang and Dengler, 2002; Kang and Dengler, 2004; Kinsman and Pyke, 1998; Mattsson *et al.*, 1999; Scarpella *et al.*, 2004; Sieburth, 1999; Steynen and Schultz, 2003; Telfer and Poethig, 1994) (Fig. 3.1B-D). The illustrations in Figure 3.1 (Fig. 3.1A-D) schematically depict the temporal sequence of vein formation events in *Arabidopsis* leaf development, and define stages and terminology to which we refer throughout this study (for additional details on nomenclature, see Section 3.2.1).

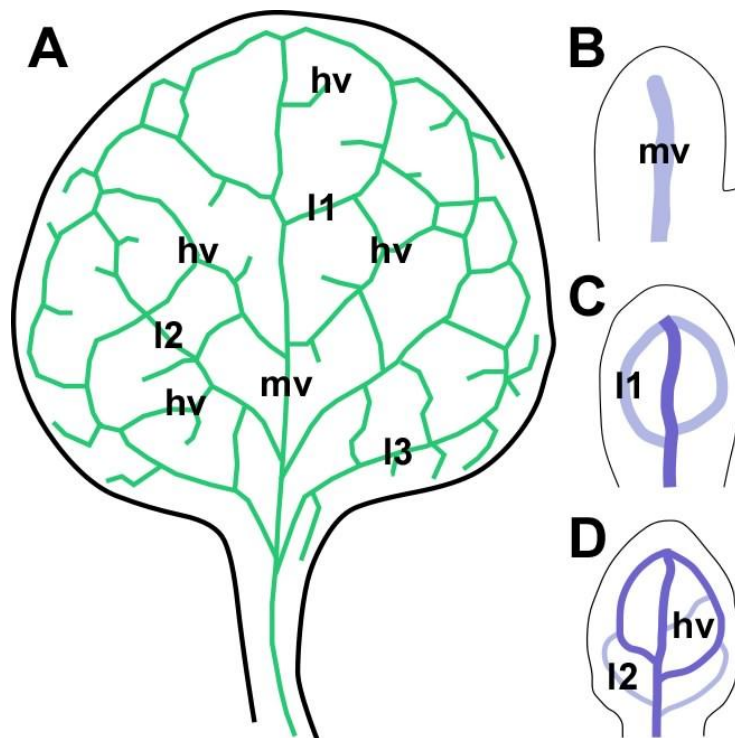


Figure 3.1. Vein development in the *Arabidopsis* first leaf. (A,C,D) Abaxial (*i.e.*, ventral) view. (B) Lateral view (abaxial side to the left). (A-D): Illustrations depicting the vein pattern of the mature first leaf (A) and the spatiotemporal course of vein formation in first leaf development (B-D) as inferred from published works (see text for references), and definition of terms used in this study; see also Section 3.2.1. (B) Two days after germination (DAG). (C) Three DAG. (D) Four DAG. Green, mature veins; indigo, procambial stages; lavender, preprocambial stages; hv, higher-order vein; l1, l2, and l3, first, second and third loop, respectively; mv, midvein.

3.3.1 Leaf expression of root vascular markers

All the genes whose expression has previously been assigned to early stages of leaf vein development have also been reported to be expressed in the root procambium (*e.g.*, Alonso-Peral *et al.*, 2006; Baima *et al.*, 1995; Carland and Nelson, 2009; Gardiner *et al.*, 2010; Hardtke and Berleth, 1998; Kang and Dengler, 2004; Konishi and Yanagisawa, 2007; Scarpella *et al.*, 2004; Scarpella *et al.*, 2006; Steinmann *et al.*, 1999; Wenzel *et al.*, 2007), and identification of leaf vascular gene expression profiles based on root procambial expression has proved to be an effective strategy (Gardiner *et al.*, 2010). Reporter gene expression in the J2501 and Q0990::mGFP5er enhancer-trap lines and in transcriptional fusions to *SHR* or to *ARABIDOPSIS HISTIDINE KINASE4/CYTOKININ RESPONSE1/WOODEN LEG* (*WOL* hereafter) (Inoue *et al.*, 2001; Mahonen *et al.*, 2000; Suzuki *et al.*, 2001) has consistently been used as reliable markers of root procambial cells (*e.g.*, Benkova *et al.*, 2003; Birnbaum *et al.*, 2003; Dello Ioio *et al.*, 2007; Hirota *et al.*, 2007; Mustroph *et al.*, 2009; Petersson *et al.*, 2009; Wang *et al.*, 2005b; Zhang *et al.*, 2005) (Fig. 3.2A-D). Activation of Q0990::mGFP5er expression in the leaf coincides with acquisition of procambial cell identity (Sawchuk *et al.*, 2007) (Fig. 3.2E), further supporting the value of root procambial expression filtering for discovery of leaf vascular expression patterns. Therefore, to identify new preprocambial expression profiles, we asked whether reporter gene expression in J2501::mGFP5er and in transcriptional fusions to *SHR* or *WOL* retained, like Q0990::mGFP5er, vascular specificity in the leaf. To address this question, we visualized fluorescence protein activity in J2501::mGFP5er and in transcriptional fusions of *SHR* or *WOL* to nuclear localized YFP or GFP (HTA6:EYFP or HTA6:EGFP; Zhang *et al.*, 2005), and compared it with that of Q0990::mGFP5er, in first leaves of seedlings 4 days after germination (DAG) as their venation is predominantly preprocambial and procambial (Donner *et al.*, 2009; Sawchuk *et al.*, 2007; Chapter 2) (Fig. 3.1D).

While, in agreement with previous observations (Donner *et al.*, 2009; Sawchuk *et al.*, 2007; Chapter 2), Q0990::mGFP5er signals in 4-DAG leaves were restricted to procambial midvein and first loops (Fig. 3.2E), expression of

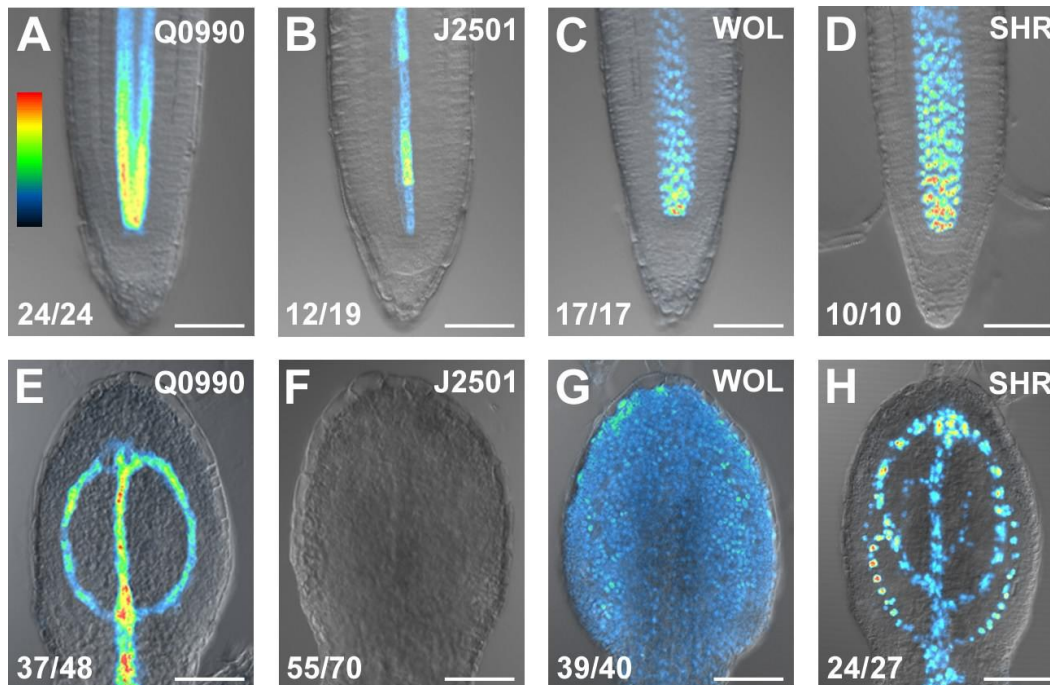


Figure 3.2. Marker expression in seedling organs. (A-H) Overlay of confocal-laser-scanning and differential-interference-contrast microscopy, subepidermal focal plane. A look-up-table (LUT) (displayed in A), in which black was used to encode background, and cyan, green, yellow, orange, and red to encode increasing signal intensities (Sawchuk *et al.*, 2008), was applied to eight-bit gray scaled images to generate color-coded images. Top right, marker identity. Bottom left, fraction of samples showing the displayed features. (A-D) Four-DAG root tips. (E-H) Four-DAG first leaves, abaxial view. (F) See Fig. 3.3 for additional expression patterns and their frequencies. Scale bars: 50 μ m.

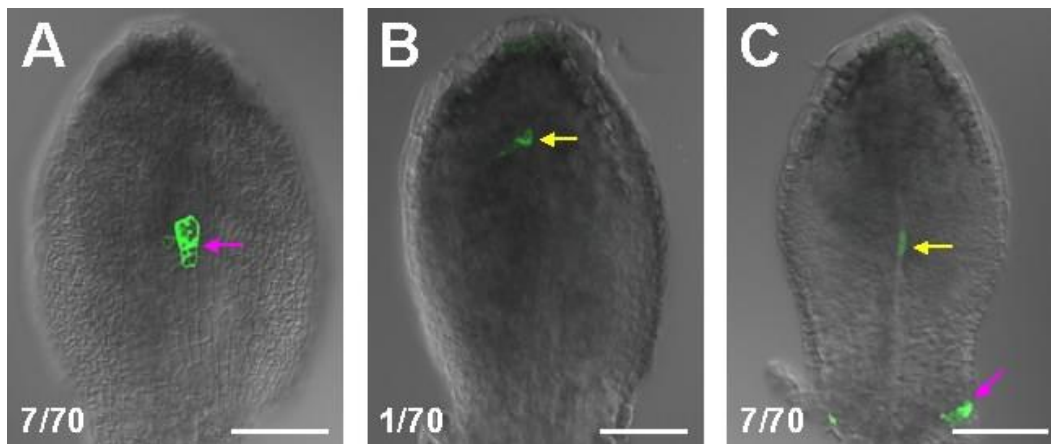


Figure 3.3. Additional expression patterns of J2501 in leaves. (A-C) Four-DAG first leaves, abaxial view. Overlay of confocal-laser-scanning and differential-interference-contrast microscopy. Green, J2501::mGFP5er expression. Bottom left, fraction of samples showing the displayed features. (A) Epidermal focal plane. (B,C) Subepidermal focal plane. Note erratic expression in epidermal cells (A, magenta arrow), in subepidermal cells (B, yellow arrow), or in both positions (C). Scale bars: 50 μ m.

J2501::mGFP5er was not detected (Fig. 3.2F), and weak WOL::HTA6:EGFP fluorescence was observed in nearly all cells (Fig. 3.2G). However, territories of SHR::HTA6:EYFP activity were associated with sites of formation of midvein, first and second loops, and higher-order veins (Fig. 3.2H). Because neither expression of J2501::mGFP5er nor that of WOL::HTA6:EGFP displayed leaf vascular bias, successive characterization focused on SHR::HTA6:EYFP.

3.3.2 Expression of *SHR* during leaf development

Expression of *SHR* in second loops of 4-DAG leaves (Fig. 3.2H; compare with Fig. 3.1D and Fig. 3.2E), suggests that, like *ATHB8* (Kang and Dengler, 2004; Scarpella *et al.*, 2004), *SHR* is expressed in ground cells that have shifted to preprocambial state. However, patterns of initiation, progression and termination of *SHR* expression could be dramatically different from those of *ATHB8*, even if the two genes are expressed similarly at a single stage of leaf development. Therefore, to visualize dynamics of *SHR* expression in leaf vein formation, we monitored activity of SHR::HTA6:EYFP and of the reference preprocambial marker ATHB8::HTA6:EYFP (Donner *et al.*, 2009; Sawchuk *et al.*, 2007; Chapter 2) in first leaf primordia at 2, 3, 4, and 5 DAG.

At 2 DAG, SHR::HTA6:EYFP and ATHB8::HTA6:EYFP signals were confined to a single cell file along the midline of the leaf primordium (Fig. 3.4A,E). At 3 DAG, *SHR* and *ATHB8* transcriptional fusions were expressed in narrow domains at sites of midvein and first loop formation (Fig. 3.4B,F). At 4 DAG, slender zones of SHR::HTA6:EYFP and ATHB8::HTA6:EYFP activity marked appearance of midvein, first and second loops, and higher-order veins (Fig. 3.4C,G). Finally, at 5 DAG, *SHR* and *ATHB8* promoters directed expression in developing midvein, first, second, and third loops, and higher-order veins (Fig. 3.4D,H). However, while ATHB8::HTA6:EYFP expression had subsided from the apical portion of midvein and first loops (Fig. 3.4D), the *SHR* transcriptional fusion was evenly active throughout the leaf vasculature (Fig. 3.4H).

In summary, expression of *SHR* seemed to be tightly associated with regions of *ATHB8*-labeled vein formation throughout leaf development.

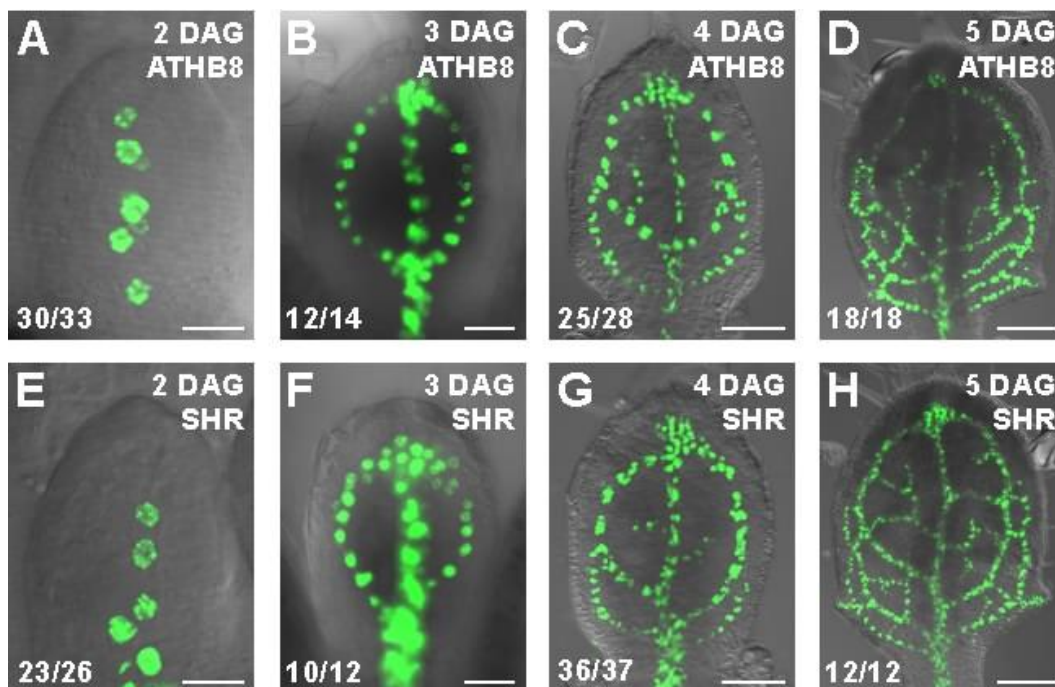


Figure 3.4. *ATHB8* and *SHR* expression in first leaf development. (A-H) Overlay of confocal-laser-scanning and differential-interference-contrast microscopy, subepidermal focal plane. Top right, leaf primordium age and gene identity. Bottom left, fraction of samples showing the displayed features. (A,E) Lateral view (abaxial side to the left). (B-D,F-H) Abaxial view. (A-D) Green, *ATHB8*::HTA6:EYFP expression. (E-H) Green, *SHR*::HTA6:EYFP expression. Scale bars: 10 μm (A,E); 20 μm (B,F); 50 μm (C,G); 75 μm (D,H).

3.3.3 Stage-specific *SHR* expression in leaf vein formation

Comparison between *SHR* and *ATHB8* expression profiles during leaf development (Fig. 3.4) suggests that expression of *SHR* is initiated as early as that of *ATHB8*, and that therefore *SHR* expression could be assigned to ground cells that have switched to preprocambial state. We adopted two criteria to test such a hypothesis: (1) visualization of shape of cells expressing *SHR*; (2) detection of *SHR* and *ATHB8* expression within the same sample.

Simultaneous imaging of activity of *SHR* transcriptional fusions and plasma-membrane-localized GFP (Sawchuk *et al.*, 2008) in basal regions of 4-DAG first leaves showed that, like *ATHB8* (Kang and Dengler, 2004; Scarpella *et al.*, 2004) (Fig. 3.5A), *SHR* is expressed in isodiametric cells (Fig. 3.5B,C), suggesting that *SHR* expression is initiated in ground cells.

Covisualization of signals of *SHR*::HTA6:EYFP and *ATHB8*::ECFP-Nuc (Sawchuk *et al.*, 2007) in second loops of 4-DAG first leaves showed matching expression of fluorescent reporters (Fig. 3.5G-I), suggesting that expression of *SHR* is initiated simultaneously with that *ATHB8*. To test for possible artifacts induced by fluorophore intrinsic properties (*e.g.*, different maturation times and stabilities of HTA6:EYFP and ECFP-Nuc) or detection parameters (*e.g.*, suboptimal excitation wavelengths and emission intervals), we visualized extent of co-expression between *SHR*::mCherry-Nuc and *ATHB8*::HTA6:EYFP signals. The reproducible coincidence of fluorescence in reciprocal permutations of *SHR* and *ATHB8* regulatory regions with YFP and CFP, or mCherry (compare Fig. 3.5M-O to Fig. 3.5G-I), suggests that our covisualization data are fluorophore independent, further supporting that expression of *SHR* and *ATHB8* is simultaneously activated in ground cells that have transitioned to preprocambial state.

3.3.4 *SHR* expression in auxin transport-inhibited leaves

Domains of *SHR* expression may be rigidly specified in leaf development and only incidentally matching with zones of vein appearance. Therefore, we asked whether fields of *SHR* expression remained associated with areas of leaf vein formation upon experimental interference with vascular patterning. Auxin

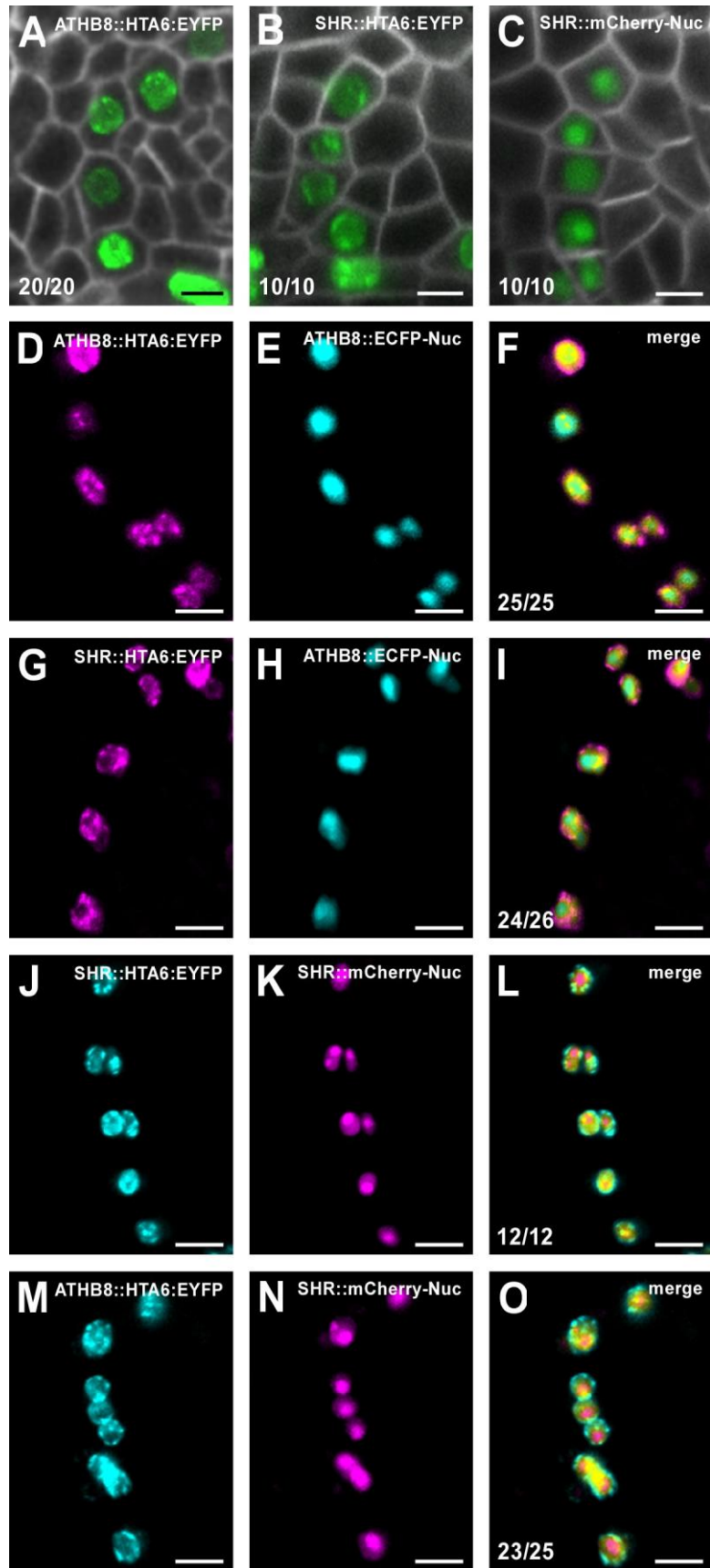


Figure 3.5. Stage-specific *SHR* expression in leaf vein development. (A-O) Details of basal regions (A-C) or second loops (D-O) of 4-DAG first leaves, abaxial view. Confocal–laser-scanning microscopy, subepidermal focal plane. Top right, marker identity. Bottom left, fraction of samples showing the displayed features. (A-C) White, UBQ10::EGFP:LTI6B expression. (A) Green, ATHB8::HTA6:EYFP expression. (B) Green, SHR::HTA6:EYFP expression. (C) Green, SHR::mCherry-Nuc expression. (D,F) Magenta, ATHB8::HTA6:EYFP expression. (E,F,H,I) Cyan, ATHB8::ECFP-Nuc expression. (G,I) Magenta, SHR::HTA6:EYFP expression. (J,L) Cyan, SHR::HTA6:EYFP expression. (K,L,N,O) Magenta, SHR::mCherry-Nuc expression. (M,O) Cyan, ATHB8::HTA6:EYFP expression. (F,I,L,O) Merge of images in D and E, G and H, J and K, and M and N, respectively. Images are color-coded with a dual-channel LUT from cyan to magenta through green, yellow and red (Demandolx and Davoust, 1997). Fluorescence in each detection channel was displayed in either magenta or cyan. Single-fluorophore images were then merged using a differential operator. As a result, preponderance of cyan signal over colocalized magenta signal is encoded in green, opposite in red, and colocalized cyan and magenta signals of equal intensity in yellow. Scale bars: 5 μ m (A-C), 10 μ m (D-O).

transport has been shown to define sites of vein appearance in developing leaf primordia (Mattsson *et al.*, 1999; Sieburth, 1999). Therefore, we grew seedlings harboring the *SHR* and *ATHB8* transcriptional fusions in the presence of the auxin transport inhibitor 1-N-naphthylphthalamic acid (NPA) and imaged fluorescent protein expression in first leaves at 3, 4, and 5 DAG.

Leaves of plants germinated and grown in the presence of auxin transport inhibitors are characterized by several reproducible, distinct abnormalities in vein network configuration; most conspicuously, great numbers of broad vein loops that fuse along the entire edge of the leaf, to give rise to a wide marginal zone of vascular differentiation, and that extend parallel to one another at the centre of the leaf, to give rise to a laterally expanded midvein (Mattsson *et al.*, 1999; Sieburth, 1999). As shown in Figure 3.5, domains of *SHR::mCherry-Nuc* and *ATHB8::HTA6:EYFP* expression retained their tight relation to sites of vein formation throughout development of auxin transport-inhibited leaves (Fig. 3.6A-F). Furthermore, strict congruence between regions of *SHR* and *ATHB8* promoter activity was preserved under conditions of reduced auxin transport (Fig. 3.6G-I). However, as observed in undisturbed leaf development, *SHR::mCherry-Nuc* signals persisted at later stages of vein differentiation, while expression of the *ATHB8* transcriptional fusion had declined (Fig. 3.6H,I).

In conclusion, association between *SHR* expression domains with areas of *ATHB8*-marked vein formation observed under undisturbed conditions persisted in auxin transport-inhibited leaves, suggesting non-circumstantial correlation between *SHR* expression and leaf vein emergence.

3.3.5 *SHR* expression in leaf vein development

In the root, *SHR* transcription is restricted to the procambium, but *SHR* protein is additionally localized to the cell layer surrounding the root vasculature (Helariutta *et al.*, 2000; Nakajima *et al.*, 2001). We therefore asked whether *SHR* displayed similar behavior in the leaf. To address this question, we visualized expression of a translational fusion of *SHR* to YFP in 4-DAG first leaves, and compared it to expression of the non-mobile *ATHB8::ATHB8:mCherry* translational fusion (Donner *et al.*, 2009; Chapter 2).

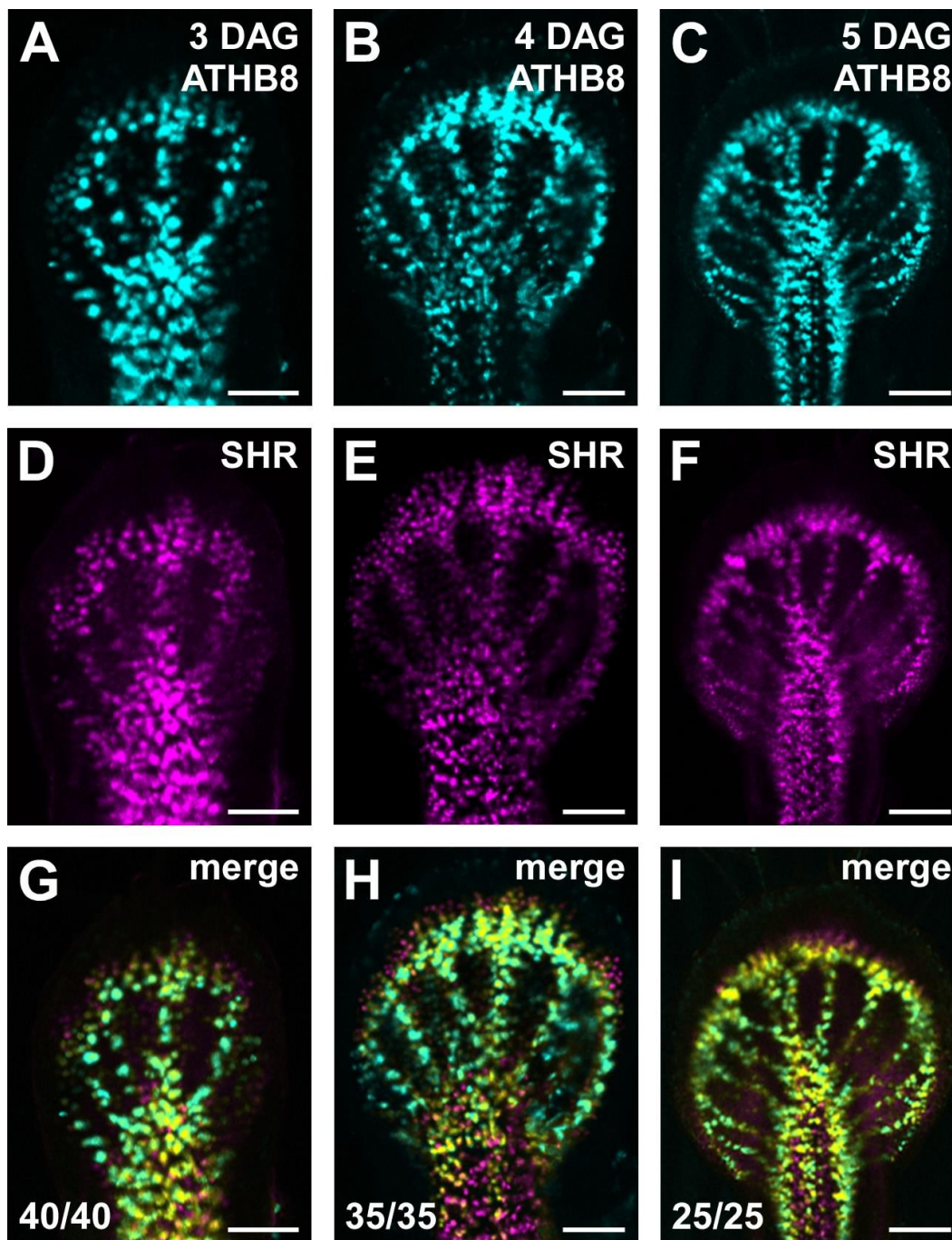


Figure 3.6. *SHR* and *ATHB8* expression in auxin transport-inhibited leaves. (A-I) First leaves, abaxial view, developing in the presence of 2.5 μM 1-N-naphthylphthalamic acid (NPA). Confocal-laser-scanning microscopy, subepidermal focal plane. Top right, leaf primordium age and gene identity. Bottom left, fraction of samples showing the displayed features. (A-C) Cyan, *ATHB8*::HTA6:EYFP expression. (D-F) Magenta, *SHR*::mCherry-Nuc expression. (G-I) Merge of images in A and D, B and E, and C and F, respectively. Images color-coded with a dual-channel LUT as described for Fig. 3.5. Scale bars: 50 μm .

In agreement with previous observations (Donner *et al.*, 2009), expression of the fluorescently tagged *ATHB8* protein mimicked *ATHB8* promoter activity in leaf vascular cells (Fig. 3.7A-C). In contrast, *SHR::SHR:EYFP* signals were further detected in cells adjacent the preprocambial and procambial domains of expression of the *SHR* transcriptional fusion (Fig. 3.7D-I). However, while *SHR::SHR:EYFP* fluorescence was distributed in both nucleus and cytoplasm of cells within the vascular expression territory, fusion protein localization in the periveinal cell layer was markedly nuclear (Fig. 3.7D-I).

3.3.6 Leaf expression of *SHR*-related genes

SHR belongs to a small clade of GRAS genes that includes *SCARECROW-LIKE29* (*SCL29*) and *SCL32* (Bolle, 2004; Lee *et al.*, 2008). Therefore, we asked whether *SCL29* and *SCL32* were expressed in the leaf in a pattern similar to that of *SHR*. To address this question, we visualized expression of transcriptional and translational fusions of *SCL29* or *SCL32* to YFP in 4-DAG first leaves.

While expression of *SCL29* fusions was confined to epidermal cells (Fig. 3.8A,D), activity of *SCL32* fusions was detected at nearly all subepidermal positions (Fig. 3.8B,E). We therefore asked whether the expression domain of *SCL32* in the leaf comprised vascular cells. To address this question, we imaged degree of signal overlap in leaves simultaneously expressing *SHR::mCherry-Nuc* and transcriptional or translational fusions of *SCL32*. We observed separate activity of *SCL32* fusions and of *SHR::mCherry-Nuc* (Fig. 3.8C,F), suggesting non-vascular expression of *SCL32* in the leaf.

3.4 DISCUSSION

While the molecular events that control recruitment of ground cells toward procambium formation in leaf development are largely unknown, available evidence suggests that the selection process culminates with initiation of expression of the *HD-ZIPIII* gene *ATHB8* (Alonso-Peral *et al.*, 2006; Carland and Nelson, 2004; Carland *et al.*, 2010; Cnops *et al.*, 2006; Donner *et al.*, 2009; Kang

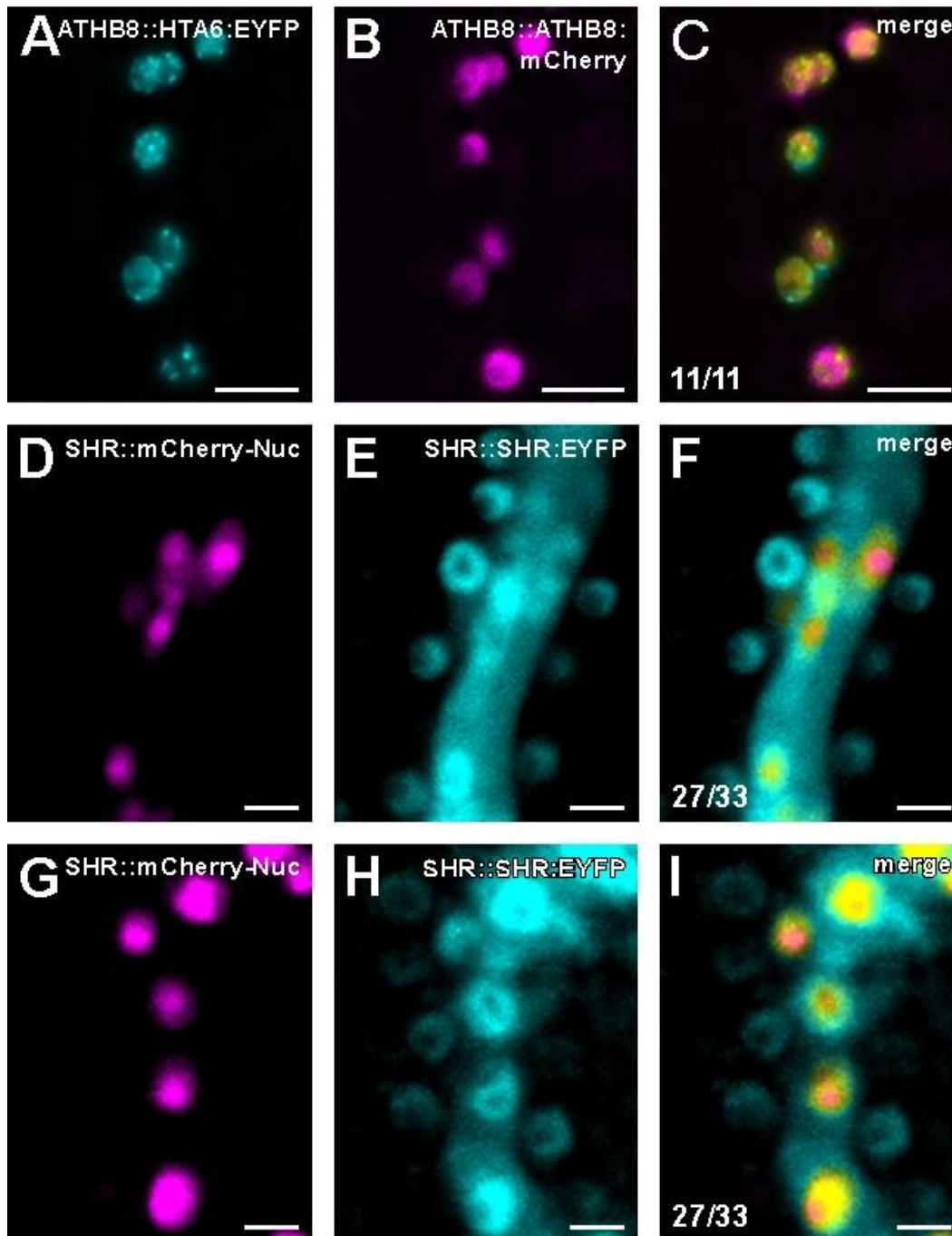


Figure 3.7. SHR expression in first leaves. (A-I) Four-DAG first leaves, abaxial view. Confocal laser scanning microscopy, subepidermal focal plane. Top right, marker identity. Bottom left, fraction of samples showing the displayed features. (A-C,G-I) Details of second loops. (D-F) Details of first loops. (A,C) Cyan, ATHB8::HTA6::EYFP expression. (B,C) Magenta, ATHB8::ATHB8::mCherry expression. (D,F,G,I) Magenta, SHR::mCherry-Nuc expression. (E,F,H,I) Cyan, SHR::SHR::EYFP expression. (C,F,I) Merge of images in A and B, D and E, and G and H, respectively. Images color-coded with a dual-channel LUT as described for Figure 3.5. Scale bars: 10 μm (A-C); 50 μm (D-F); 5 μm (G-I).

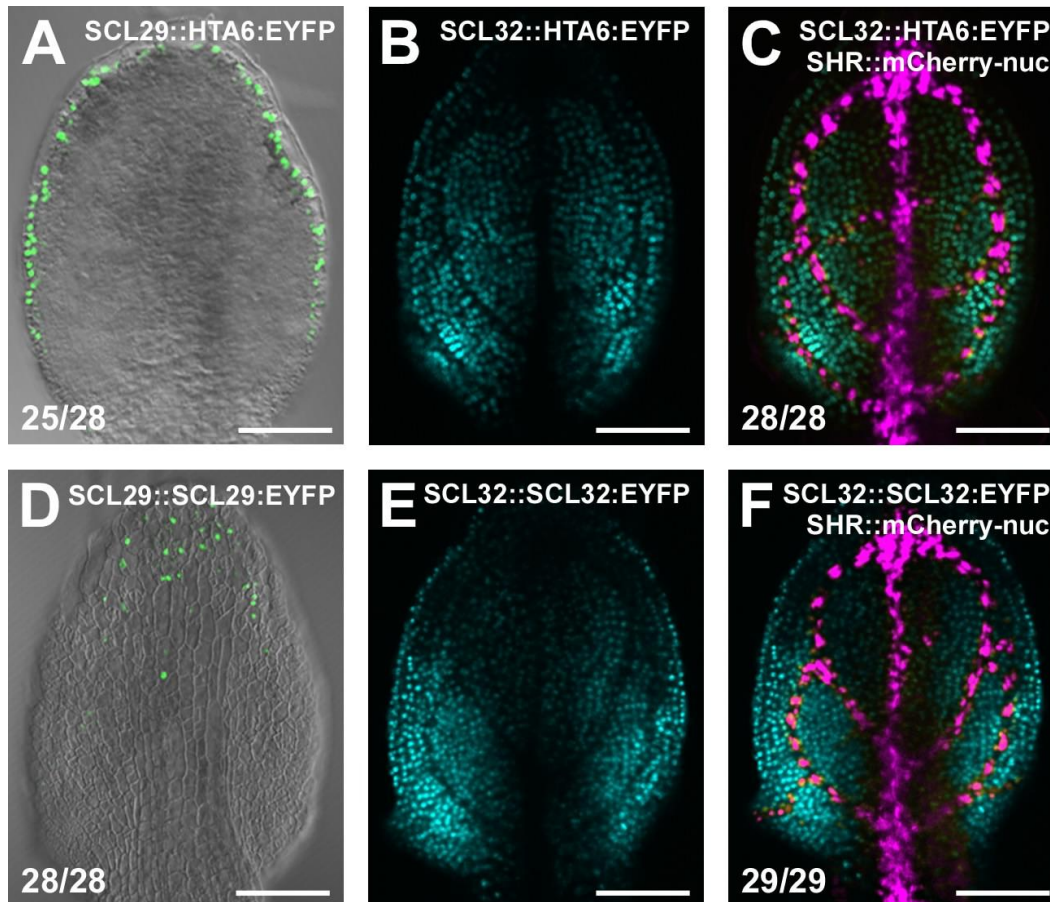


Figure 3.8. SCL29 and SCL32 expression in first leaves. (A-F) Four-DAG, first leaves, abaxial view. Top right, marker identity. Bottom left, fraction of samples showing the displayed features. (A,D) Overlay of confocal-laser-scanning and differential-interference-contrast microscopy. (B,C,E,F) Confocal-laser-scanning microscopy. (A-C,E,F) Subepidermal focal plane. (D) Epidermal focal plane. (A) Green, SCL29::HTA6:EYFP expression. (B,C) Cyan, SCL32::HTA6:EYFP expression. (C,F) Magenta, SHR::mCherry-Nuc expression. Images color-coded with a dual-channel LUT as described for Fig. 3.5. (D) Green, SCL29::SCL29:EYFP expression. (E,F) Cyan, SCL32::SCL32:EYFP expression. Scale bars: 50 μ m.

and Dengler, 2004; Koizumi *et al.*, 2000; Petricka and Nelson, 2007; Pineau *et al.*, 2005; Sawchuk *et al.*, 2007; Sawchuk *et al.*, 2008; Scarpella *et al.*, 2004; Scarpella *et al.*, 2006). Activation of *ATHB8* expression defines transition to a morphologically inconspicuous preprocambial cell state that preludes to procambium appearance. Therefore, characterization of the molecular identity of ground cells that have switched to preprocambial state would be particularly informative as it may provide insight into the molecular circuits controlling vein formation.

In this study, we searched for gene expression profiles associated with preprocambial stages of vein development in *Arabidopsis* leaves. We found that expression of *SHR*, which encodes a member of the GRAS family of plant-specific transcription factors (Di Laurenzio *et al.*, 1996; Helariutta *et al.*, 2000; Pysh *et al.*, 1999), emerges in synchrony with that of *ATHB8* in leaf development, suggesting that parallel activation of expression of *SHR* and *ATHB8* identifies a preprocambial cell state that announces vein formation. However, while *ATHB8* protein expression remained confined to developing veins, the *SHR* protein expression domain further included a contiguous, perivascular cell layer, suggestive of activities of procambium-precursor cells beyond vein formation.

3.4.1 Transition to preprocambial cell state

During leaf development, *SHR* and *ATHB8* were expressed in seemingly overlapping subepidermal domains and with amazingly comparable dynamics. Expression of both *SHR* and *ATHB8* was initiated in narrow domains that became associated with sites of vein formation. Further, vein-associated expression fields of *SHR* and *ATHB8* emerged in the same temporal sequence: midvein, first loops, second loops and higher-order veins, third loops. Finally, vein order-specific expression domains of *SHR* and *ATHB8* became apparent at the same stage of leaf development. However, expression of *SHR* was sustained at all stages of vein formation, while that of *ATHB8* became dissipated at later stages of vascular differentiation, in agreement with previous reports (Kang and Dengler, 2002, 2004; Scarpella *et al.*, 2004). Expression of both *SHR* and *ATHB8* was initiated in files of polygonal, isodiametric ground cells, and positions of activation of *SHR*

expression overlapped with sites of initiation of *ATHB8* expression, suggesting that *SHR* is expressed at preprocambial stages of vein development. Moreover, that *SHR* and *ATHB8* preprocambial expression domains reproducibly coincided with one another suggests that expression of *SHR* is initiated concurrently with transition to *ATHB8* preprocambial cell state.

If coincidence between expression of *SHR* and *ATHB8* were merely circumstantial, one would not expect such association to endure under conditions of manipulated *ATHB8* expression. Behavior of *SHR* expression in leaves developing under conditions of reduced auxin transport, which dramatically changes the architecture of *ATHB8* expression domains and of vein networks (Gardiner *et al.*, 2010; Mattsson *et al.*, 1999; Sieburth, 1999), was comparable to that observed under undisturbed vein patterning. All aspects of *SHR* expression, including relation to *ATHB8* expression and association with positions of vein formation, proved to be highly reproducible under all experimental conditions. We therefore suggest that, together with *ATHB8*, activation of expression of *SHR* defines switch to a morphologically inconspicuous transcriptional state that foreshadows procambial development.

Unlike *ATHB8*, the *SHR* protein is additionally localized to a layer of non-vascular cells that surrounds leaf veins. This observation is consistent with events occurring in root development, where *SHR* movement from vascular to neighboring cells is required for the formation of the cell sheath that envelops the single vein (Gallagher *et al.*, 2004; Helariutta *et al.*, 2000; Nakajima *et al.*, 2001). Leaf veins have long been suspected to provide positional cues that control differentiation of adjoining photosynthetic cell types (Langdale and Nelson, 1991), and the pattern of *SHR* expression in the leaf suggests that such organizing influence may arise simultaneously with transition to preprocambial cell state.

Correct initiation of *ATHB8* expression at preprocambial stages of leaf vein development strictly depends on the presence of a TGTCTG regulatory element in the *ATHB8* promoter (Donner *et al.*, 2009; Chapter 2). The *SHR* promoter does not contain any TGTCTG element, suggesting an independent mechanism controlling onset of *SHR* expression. It will be interesting to

understand the molecular basis of *SHR* preprocambial expression; nevertheless, our findings already contribute to molecularly define cells at incipient stages of leaf vascular development.

3.4.2 Complementary leaf expression profiles of SHR-related genes

Members of gene families frequently display overlapping expression profiles (*e.g.*, Mason *et al.*, 2004; Sawchuk *et al.*, 2008; Tsuchisaka and Theologis, 2004). In contrast, the expression of the related *SHR*, *SCL29*, and *SCL32* genes defines complementary territories of cells in the leaf.

Epidermal domains of *SCL29* promoter activity become further compartmentalized by presence of the intronless *SCL29* coding sequence. Reports of regulatory elements within the coding region are not unprecedented (*e.g.*, Ito *et al.*, 2003), and various post-transcriptional control mechanisms have been described that could account for the differential behavior of *SCL29* transcriptional and translational fusions, including regulated nuclear export (Bailey-Serres *et al.*, 2009), mRNA decay (Belostotsky and Sieburth, 2009), and intercellular mRNA trafficking (Ueki and Citovsky, 2000).

Subepidermal cells that express either type of *SCL32* fusion lack expression of the preprocambial marker gene *SHR*, and mutual exclusivity of *SCL32* and *SHR* expression domains is consistent with the view that photosynthetic and vascular cell identity acquisition represent antagonistic pathways in leaf subepidermal tissue ontogeny (Kang *et al.*, 2007; Sawchuk *et al.*, 2008; Scarpella *et al.*, 2004).

Tissue-specific expression data are available for 21 of the 32 *GRAS* genes in *Arabidopsis*, but function is only known for 10 of them (Bolle *et al.*, 2000; Di Laurenzio *et al.*, 1996; Dill and Sun, 2001; Dill *et al.*, 2001; Fode *et al.*, 2008; Fu *et al.*, 2004; Greb *et al.*, 2003; Lee *et al.*, 2002; Lee *et al.*, 2008; Peng *et al.*, 1997; Pysh *et al.*, 1999; Silverstone *et al.*, 1998; Torres-Galea *et al.*, 2006; Tyler *et al.*, 2004; Wen and Chang, 2002). While it will be interesting to learn whether the non-overlapping expression patterns of *SHR*, *SCL29*, and *SCL32* are associated with equally distinct functions, our results already assist in the characterization of a family of plant-specific transcription factors in leaf development.

CHAPTER 4: DEVELOPMENTAL REGULATION OF *CYCA2s* CONTRIBUTES TO TISSUE-SPECIFIC PROLIFERATION IN *ARABIDOPSIS*³

4.1 INTRODUCTION

After germination, the minimal body plan of the seedling is elaborated by iterative organ development that will shape the adult plant. Each new organ is formed according to a predictable pattern, which reflects a complex interplay between plant hormones and developmental programs (De Veylder *et al.*, 2007). One of the targets of morphogenetic cues is the modulation of local cell proliferation and differentiation. Because plant cells cannot move within the plant body due to their rigid cell walls, cell proliferation must be highly controlled in time and space. While recent studies provide insights into the coordination of plant development and cell-cycle regulation, only a few connections between these processes have been identified at the molecular level (Brownfield *et al.*, 2009; Sozzani *et al.*, 2010; Xie *et al.*, 2010).

Cell proliferation is characterized by consecutive cycles of DNA replication (Synthesis; S-phase) and cell division (Mitosis; M-phase). S-phase is preceded by Gap1-phase (G1), when cells prepare for DNA synthesis, and M-phase by Gap2-phase (G2), when cells prepare to divide. The orderly transition between phases depends largely on oscillations of Cyclin-Dependent Kinase (CDK) activity. Recently, it was shown that thresholds of CDK activity delineate

³ A version of this chapter has been published. S. Vanneste, F. Coppens, E. Lee, T. J. Donner, Z. Xie, G. Van Isterdael, S. Dhondt, F. De Winter, B. De Rybel, M. Vuylsteke, L. De Veylder, J. Friml, D. Inze, E. Grotewold, E. Scarpella, F. D. Sack, G. T. S. Beemster, and T. Beeckman, (2011). Developmental regulation of *CYCA2s* contributes to tissue-specific proliferation in *Arabidopsis*. *EMBO J.* **30**: 3430-3441. doi: <http://dx.doi.org/10.1038/emboj.2011.240>. Reproduced with permission of EMBO Journal and the authors.

Conceived the general idea, isolated higher order mutants, and performed cell division-related experiments: SV, FC, GVI, FDW, BDR, JF, GTSB, TB. Generated and provided promoter:GUS:GFP lines: SD, LDV, DI. Conceived and performed vascular-related experiments: TJD, ES. Conceived and performed the stomatal-related experiments: SV, EL, FDS, TB. Conceived and performed ChIP-PCR: ZX, EG. Statistical analyses of the data: MV. Wrote the paper: SV, FC, TB (with input from all authors). I generated the data that gave rise to figures: 4.10 and 4.12.

independent cell-cycle phases (Coudreuse and Nurse, 2010), providing support for a quantitative model of cell-cycle progression. Importantly, CDK activity is modulated at multiple levels. As monomers, CDKs are usually inactive due to a steric blockage of their catalytic cleft. Binding to a cyclin partner removes this block, and thus represents a major regulatory switch of CDK activity (Jeffrey *et al.*, 1995). Further fine-tuning of CDK activity is achieved by phosphorylation, dephosphorylation, and binding to several cofactors and/or inhibitors (Inze and De Veylder, 2006; Morgan, 1995; Morgan, 1997).

Compared with the relatively simple cell-cycle regulatory module in yeast, which includes just one major CDK and a few cyclins (CYC), higher eukaryotes harbour an elaborate repertoire of CDKs and cyclins. Here, the specialized phase- and tissue-specific expression of multiple CDKs and cyclins provide a wide combinatorial range that allow for the increased complexity associated with multicellularity (De Veylder *et al.*, 2007; Satyanarayana and Kaldis, 2009).

Animals utilize well-characterized D- and E-type cyclins which are expressed at the onset of cell division (G1-to-S phase) and which connect extracellular signals with the cell cycle (Koff *et al.*, 1992; Matsushime *et al.*, 1991; Motokura and Arnold, 1993; Payton and Coats, 2002). Moreover, A- and B-type cyclins are primarily restricted to G2-to-M phase, with A-type cyclins being more broadly expressed, starting as early as S-phase (Fung and Poon, 2005; Pines and Hunter, 1990). Such expression patterns suggest that they function specifically in respective phases of the cell cycle. However, in some cases the loss of one cyclin type can be compensated for by the expression of another cyclin type (Fisher and Nurse, 1996).

Based on sequence homology and conserved motifs, many core cell-cycle regulators have been annotated in plant genomes (Vandepoele *et al.*, 2002). Interestingly, plants have many more cyclins compared with animals. As an example, the *Arabidopsis* genome encodes 10 A-type, 11 B-type and 10 D-type cyclins, but no E-type cyclins, whereas animal genomes usually code for 1 or 2 of each type. In plants, D-type and A3-type cyclins have been implicated in G1-to-S phase regulation (Dewitte *et al.*, 2003, Dewitte *et al.*, 2007; Takahashi *et al.*,

2010), while subgroups of A- and B-type cyclins likely act in G2-to-M phase regulation (Boudolf *et al.*, 2009; Imai *et al.*, 2006; Ishida *et al.*, 2010; Schnittger *et al.*, 2002). The expanded number of cyclins in plants, compared with animals, might represent a mechanism that integrates a broader range of signals to control of proliferation. However, much of what is known about cyclins and plant cell-cycle regulation derives from gain-of-function analyses (Boudolf *et al.*, 2009; Dewitte *et al.*, 2003; Schnittger *et al.*, 2002; Takahashi *et al.*, 2010; Yu *et al.*, 2003). Quantitative models suggest that the timing of cyclin expression controls differences in cell-cycle regulation (Coudreuse and Nurse, 2010; Fisher and Nurse, 1996), including in plants (Schnittger *et al.*, 2002). Therefore, it is essential to define the phenotypic effects of loss of cyclin gene functions to understand their role in plant development.

Although there have been many advances in understanding the regulation of the plant cell cycle, it is still unclear how cell cycling is coordinated with differentiation during development. Components of the G1-to-S transition have been shown to control cell proliferation and differentiation events in shoots (Dewitte *et al.*, 2003; Dewitte *et al.*, 2007) and roots (Caro *et al.*, 2007; Sozzani *et al.*, 2010; Wildwater *et al.*, 2005), which emphasizes the key role of this transition in the cell's decision to exit the cell cycle and activate differentiation. In addition, some differentiated plant cell types are known to undergo multiple rounds of DNA duplication without mitosis (endoreduplication) (Melaragno *et al.*, 1993), suggesting that cyclin downregulation at the G2-to-M transition could be part of a developmental mechanism that coordinates the switch between proliferation and endoreduplication.

Among putative G2-to-M phase regulatory cyclins, A2-type cyclins are poorly characterized in plants. In synchronized cell suspensions, their expression starts in S-phase and peaks during the G2-to-M phase transition (Menges *et al.*, 2005; Reichheld *et al.*, 1996; Shaul *et al.*, 1996). Plant A2 cyclins have been shown to rescue the growth of yeast cyclin-deficient mutants (Setiady *et al.*, 1995), and also induced *Xenopus* oocyte maturation (Renaudin *et al.*, 1994), suggesting they act during entry into mitosis. Developmentally, CYCA2

expression is not obligately associated with cell proliferation, as it is also expressed in seemingly differentiated cells, such as the vascular tissues (BursSENS *et al.*, 2000) and developing trichomes (Imai *et al.*, 2006). In the vascular tissues, it was proposed that *CYCA2;1* expression reflects a competence to divide, while in trichomes *CYCA2;3* acts to terminate endoreduplication. Indeed, *cyca2;1*, *cyca2;3*, and *increased level of polyploidy1-ID (ilp1)* mutants displaying reduced *CYCA2* expression, exhibit increased ploidy levels (Imai *et al.*, 2006; Yoshizumi *et al.*, 2006), whereas overexpression of *CYCA2;3* shows lower ploidy levels, combined with increased proliferation (Boudolf *et al.*, 2009; Imai *et al.*, 2006). Recently, auxin signalling has been implicated in the switch from proliferation to endoreduplication as it stimulates *CYCA2;3* expression (Ishida *et al.*, 2010). However, it is not clear if this is a direct or indirect effect.

Biochemical interaction studies revealed that plant *CYCA2*s can interact with a diverse set of CDKs as well as other cell-cycle regulatory proteins (Boruc *et al.*, 2010b; Boudolf *et al.*, 2009; Imai *et al.*, 2006), suggesting that *CYCA2*s contribute to multiple CDK complexes that might reflect a broad array of biochemical events. Importantly, different *CYCA2*s have distinct and overlapping expression patterns (BursSENS *et al.*, 2000; Imai *et al.*, 2006) corroborating the idea that tissue-specific co-expression with interaction partners is key to their function. Besides transcriptional regulation, *CYCA2*s' degradation is an equally important regulatory mechanism. The Anaphase Promoting Complex (APC) regulates *CYCA* and *CYCB* turnover via their destruction boxes (Marrocco *et al.*, 2009). Moreover, CELL CYCLE SWITCH PROTEIN52A1-dependent activation of the APC mediates proteolysis of *CYCA2;3* during the switch to endoreduplication (Boudolf *et al.*, 2009). These complex regulatory mechanisms highlight the importance of tight control over the cell cycle.

Here, we address the functional requirement of the subfamily of plant A2-type cyclins in plant cell-cycle regulation in different developmental contexts and report a novel transcriptional repression mechanism that acts during terminal differentiation of guard cells.

4.2 MATERIALS AND METHODS

4.2.1 Plant material and growth conditions

We used *Arabidopsis* seedlings of the accession Col-0 and Landsberg *erecta* (*Ler*) and mutants for the various A2-type cyclins from publicly available collections (SALK (Alonso *et al.*, 2003), GABI-KAT (Rosso *et al.*, 2003), and EXOn Trapping Insert Consortium (EXOTIC)

(<http://www.jic.bbsrc.ac.uk/science/cdb/exotic/index.htm>)), and stomatal lineage mutant alleles *four lips-1* (*flp-1*) *myeloblastosis88* (*myb88*), *flp-7 myb88* (Lai *et al.*, 2005), and *fama-1* (Ohashi-Ito and Bergmann, 2006). Cyclin mutant alleles used are *cyca2;1-1* (SALK_121077) (Yoshizumi *et al.*, 2006), *cyca2;1-2* (SALK_123348), *cyca2;2-1* (GABI_120D03), *cyca2;3-1* (SALK_092515) (Imai *et al.*, 2006), *cyca2;3-2* (SALK_086463) (Imai *et al.*, 2006), *cyca2;3-3* (SALK_043246), *cyca2;4-1* (SALK_070301) and *cyca2;4-2* (GAT_5.10009) (Fig. 4.1). For multiple *cyca2* mutant nomenclature, see Table 4.1.

Promoter::reporter lines for FLP (Lai *et al.*, 2005), CDKB1;1 (Xie *et al.*, 2010), and CYCA2;1 (Bursens *et al.*, 2000) have been reported previously. For detection of T-DNA inserts, we used primers specific to the left border of the T-DNAs used for mutagenesis (LBC1, LB_GABI, and LB_EXOTIC) in combination with gene-specific primers (Table 4.2). The alleles *cyca2;1-1*, *cyca2;2-1*, *cyca2;3-1*, and *cyca2;4-1* are representative knockout alleles and have been used for generating triple mutants. Seeds were sterilized and germinated, and seedlings and plants were grown as described in Section 2.2.2. Plant transformations were performed as described in Section 2.2.2.

4.2.2 Immunofluorescence localization

One-week-old seedlings, grown on germination medium (Section 2.2.2) under continuous illumination, were fixed in paraformaldehyde. Immunolocalization was performed as described (Sauer *et al.*, 2006). The rabbit anti-*knolle* antibody (1:2000) (Lauber *et al.*, 1997) and the fluorochrome-conjugated secondary antibody anti-rabbit-Cy3 (1:600; Dianova) were used. Fluorescence detection was done with a confocal-laser-scanning microscope Zeiss 710.

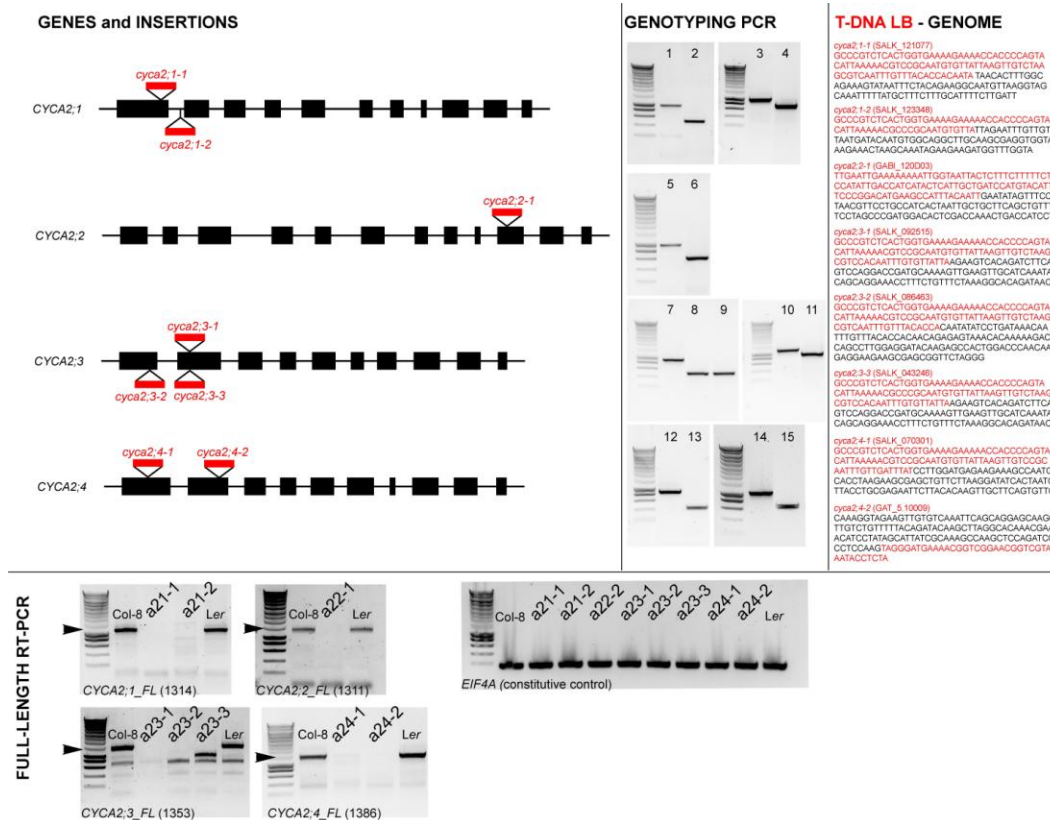


Figure 4.1. Molecular characterisation of *cyca2* mutant alleles. (GENES and INSERTIONS) Intron-exon structure of the respective *CYCA2* genes. The relative position of T-DNA insertions is indicated by triangles with indication of the alleles highlighted in red. **(GENOTYPING PCR)** For each allele a representative gel is included of genotyping reactions showing the expected amplicons for wild-type (WT) (numbered 1, 3, 5, 7, 10, 12, and 14) and insert-genome junction (numbered 2, 4, 6, 8, 9, 11, 13, and 15). **(T-DNA LB – GENOME)** For each allele the insert-genome junction was determined by sequencing respectively reactions 2, 4, 6, 8, 9, 10, 11, 13, and 15; in black the sequence that exactly matches the genome, in red sequence of respective T-DNA left borders. Note that *cyca2;3-1* and *cyca2;3-3* are inserted at exact the same position in the genome. **(FULL-LENGTH REVERSE TRANSCRIPTASE PCR (RT-PCR))** For none of the alleles a full-length transcript could be detected, while these could be easily detected at correct sizes in Col-8 and *Ler* (Arrow heads indicate the expected size of the respective full-length amplicon). Note that in *cyca2;3-3* a smaller band is efficiently amplified. All cDNAs were derived from comparable amounts of mRNA as there were no major differences in *EUKARYOTIC TRANSLATION INITIATION FACTOR4A* levels (constitutive control) among genotypes. This suggests that the respective mutant alleles are null-mutants.

Table 4.1. Analysis of stomatal phenotypes of various mutant combinations.

Genotype	Counts	Normal	SGC	Normal (%)	SGC (%)
Col-8	501	501	0	100	0
<i>cyca2;1-1</i> (SALK_121077)	501	501	0	100	0
<i>cyca2;1-2</i> (SALK_123348)	478	478	0	100	0
<i>cyca2;2-1</i> (GABI_120D03)	965	965	0	100	0
<i>cyca2;3-1</i> (SALK_092515)	845	830	15	98	2
<i>cyca2;3-2</i> (SALK_086463)	960	939	21	98	2
<i>cyca2;3-3</i> (SALK_043246)	988	975	13	99	1
<i>cyca2;4-1</i> (SALK_070301)	805	805	0	100	0
<i>cyca2;4-2</i> (GAT_5.10009)	824	824	0	100	0
<i>cyca2;12</i> (<i>cyca2;1-1 cyca2;2-1</i>)	546	546	0	100	0
<i>cyca2;14</i> (<i>cyca2;1-1 cyca2;4-1</i>)	464	464	0	100	0
<i>cyca2;24</i> (<i>cyca2;2-1 cyca2;4-1</i>)	474	474	0	100	0
<i>cyca2;23</i> (<i>cyca2;2-1 cyca2;3-1</i>)	831	699	132	84	16
<i>cyca2;34</i> (<i>cyca2;3-1 cyca2;4-1</i>)	1149	913	236	79	21

<i>cyca2;3-2 cyca2;4-2</i>	1286	899	387	70	30
<i>cyca2;3-3 cyca2;4-2</i>	964	681	283	71	29
<i>cyca2;124</i> (<i>cyca2;1-1 cyca2;2-1</i> <i>cyca24-1</i>)	529	529	0	100	0
<i>cyca2;134</i> (<i>cyca2;1-1 cyca2;3-1</i> <i>cyca2;4-1</i>)	744	457	287	61	39
<i>cyca2;234</i> (<i>cyca2;2-1 cyca2;3-1</i> <i>cyca2;4-1</i>)	734	42	692	6	94

Table 4.2. Sequences of primers used in this study.

Name	Sequence
<i>Genotyping</i>	
CYCA2;1_1LP	CAATGATTTGATCACGGAAAC
CYCA2;1_1RP	TTTGAGAAACAAACACTCTGG
CYCA2;1_2LP	GCTTGTTGAATCAGTGGAGTG
CYCA2;1_2RP	TGTATTCCTACCTCCACGAGC
CYCA2;2_1LP	GAACAGCATTTCATCACTGG
CYCA2;2_1RP	GAAATGTACCTTTGGTTGGTTG
CYCA2;3_1LP	AACATTTTTATATGCATGGTTGC
CYCA2;3_1RP	TCGATGTCTACAAATTTTGGG
CYCA2;3_2_LP	TTCTGCATTACTGTTTGCATTG
CYCA2;3_2_RP	ACCTCTGAAACACGCAAATTG
CYCA2;4_1LP	CTCCCGTCTTTGCTAAAATTG
CYCA2;4_1RP	CTTGTGAAGTAGCCGAAGAAG
CYCA2;4_2_LP	TCTATACCAATCCATGGTCGC
CYCA2;4_2_RP	TTCCTCTGAGACCTGAAATTTT
LB_GABI-KAT	CCCATTTGGACGTGAATGTAGACAC
LB_SALK	GTGGACCGCTTGCTGCAACTCTCT
LB_EXOTIC	CCGTCCCGCAAGTTAAATATG
<i>Cloning</i>	
CYCA2;1Pro_FW	GGGGACAAGTTTGTACAAAAAAGCAGGCTGGAA- GTGACTAGCAGGATTCG
CYCA2;1Pro_RW	GGGGACCACTTTGTACAAGAAAGCTGGGTCACTC- CACTGATTCAACAAG
CYCA2;4Pro_FW	GGGGACAAGTTTGTACAAAAAAGCAGGCTAAAG- ACCACGGGAGCGTCGT
CYCA2;4Pro_RW	GGGGACCACTTTGTACAAGAAAGCTGGGTGATTG- AAACCCTTTGACAC
MYB88Pro_FW	GGGGACAAGTTTGTACAAAAAAGCAGGCTAAATT- TCTTCTAACTTGGCTCTGATA
MYB88Pro_RW	GGGGACCACTTTGTACAAGAAAGCTGGGTAAAA- AGTTTTGGCCTTCTCTCTCTC
<i>Chromatin immunoprecipitation-quantitative PCR (ChIP-qPCR)</i>	
CYCA2;3-P1-FW	GCTGGACAAGATCTCTGC
CYCA2;3-P1-RW	GAGATCTGGGGTTATTATTTGTCTAC
CYCA2;3-P2-FW	CGTCCATCTCTCGTTAGTATTTTAGAG
CYCA2;3-P2-RW	CCAGCTTCGTCTTCTTGC
CYCA2;3-P3-FW	TACTCACGTGATTGTACTGTAG
CYCA2;3-P3-RW	CTCTAAAATACTAACGAGAGATGGAC
PDF2-FW	GACGATTCTTCGTGCAGTATCGCTT
PDF2-RW	GATACGGCCATGCTTGGTGGAGCTA

4.2.3 Vector construction

Promoter::GUS-GFP fusions of *MYB88*, *CYCA2;2*, *CYCA2;3*, and *CYCA2;4* were generated through Gateway cloning of promoter fragments into pKGWFS7.

PCR fragments of *CYCA2;2*, *CYCA2;3*, and *CYCA2;4* promoters were described previously (Benhamed *et al.*, 2008). To generate the *CYCA2;1* and *CYCA2;4* transcriptional fusions (*CYCA2;1::HTA6:EYFP* and *CYCA2;4::HTA6:EYFP*, respectively), 1808 bp upstream of the *CYCA2;1* start codon and 1963 bp upstream of the *CYCA2;4* start codon were amplified from *Arabidopsis* (*Arabidopsis thaliana*) ecotype Col-0 genomic DNA and cloned into the Gateway-adapted pFYTAG binary vector, which contains a translational fusion between the coding region of HISTONE 2A (HTA6; AT5G59870) and that of enhanced yellow fluorescent protein (EYFP) (Zhang *et al.*, 2005).

4.2.4 Vascular expression analysis

The origin of the *ATHB8::HTA6:EYFP* and the *ATHB8::ECFP-Nuc* has been described (Sawchuk *et al.*, 2007). Seeds were sterilized and germinated, and seedlings and plants were grown, transformed and selected as described in Section 2.2.2. For *CYCA2;1::HTA6:EYFP* and *CYCA2;4::HTA6:EYFP*, the progeny of eight independent, single insertion transgenic lines were inspected to identify the most representative expression pattern. We define ‘days after germination’ (DAG) as days following exposure of imbibed seeds to light. Dissected seedling organs were mounted and imaged as described in Section 2.2.3. Brightness and contrast were adjusted through linear stretching of the histogram in ImageJ (National Institutes of Health; <http://rsb.info.nih.gov/ij>). Signal levels and colocalization were visualized as described in Section 2.2.4.

4.2.5 Histochemical staining and anatomical analysis

Seedlings were permeabilized for 1 h in 90 % acetone at -20 °C, washed twice for 5 min each in 100 mM phosphate buffer (pH 7.7) at room temperature, and stained at 37 °C in freshly prepared GUS staining buffer (100 mM phosphate buffer pH 7.7; 10 mM sodium EDTA (Bioshop Canada); 2 mM 5-bromo-4-chloro-3-indolyl-beta-D-glucuronic acid (Bioshop Canada); and either 2 mmol l⁻¹

(CYCA2;2::GUS) or 5 mmol l⁻¹ (CYCA2;3::GUS) of each potassium ferrocyanide and potassium ferricyanide) for 6 h (CYCA2;2::GUS) or 16 h (CYCA2;3::GUS). For microscopic analysis, chlorophyll was removed by ethanol treatment and further cleared by mounting in 90 % lactic acid (Acros Organics, Brussels, Belgium). All samples were analysed by differential-interference-contrast microscopy.

For anatomical sections, samples were fixed overnight in 1 % glutaraldehyde and 4 % paraformaldehyde in 50 mM phosphate buffer (pH 7). Samples were dehydrated and embedded in Technovit 7100 resin (Heraeus Kulzer, Wehrheim, Germany) according to the manufacturer's protocol. Sections of 5 µm were cut with a microtome (Minot 1212; Leitz, Wetzlar, Germany), dried on Vectabond-coated object glasses, stained with Toluidine Blue for 8 min (Fluka Chemica, Buchs, Switzerland), and rinsed in tap water for 30 s. After drying, the sections were mounted in DePex medium (British Drug House, Poole, UK).

4.2.6 Flow cytometry

Primary leaves of 3-week-old seedlings were chopped with a razor blade in 300 µl of buffer (45 mM MgCl₂; 30 mM sodium citrate; 20 mM 3-[N-morpholino]propanesulphonic acid, pH 7; and 1% Triton X-100). To the supernatants, 1 µl of 4',6-diamidino-2-phenylindole from a stock of 1 mg/ml was added, which was filtered over a 30-mm mesh. The nuclei were analysed with a CyFlows ML (Partec) flow cytometer.

4.2.7 Guard cell nuclear content measurement

Nuclei were stained fluorescently by fixing 3-week-old cotyledons in a mixture of 9:1 ethanol:acetic acid (v/v). After the samples had been rinsed, they were stained for 24 h with 0.1 mg/ml of 4',6-diamidino-2-phenylindole (DAPI), mounted in Vectashield mounting medium (Vector Laboratories, Burlingame, CA), and observed under a 63x oil immersion objective on a Zeiss Axioskop equipped with an AxioCam charge-coupled device camera (Zeiss). Images were obtained using the Axiovision software and analysed in grey scale with the public domain image analysis program ImageJ (version 1.28; <http://rsb.info.nih.gov/ij/>). Relative

fluorescence units were reported as integrated density, which are the product of the area and the average fluorescence of the selected nucleus.

4.2.8 Kinematic analysis of leaf development

Plants of the wild-type and the *cyca2* triple mutants were sown in quarter sections of round 12 cm Petri dishes filled with 100 ml of half-strength Murashige and Skoog medium (Duchefa, Haarlem, The Netherlands) and 0.6 % plant tissue culture agar (Lab M, Bury, UK). At relevant time points after sowing, plants or primary leaves (depending on the size) of the respective genotypes were harvested. All healthy plants were placed in methanol overnight to remove chlorophyll, and subsequently they were cleared and stored in lactic acid for microscopy.

The following parameters were determined: total area of all cells in the drawing, total number of cells, and number of guard cells. From these data, we calculated the average cell area. We estimated the total number of cells per leaf by dividing the leaf area by the average cell area (averaged between the apical and basal positions). Finally, average cell division rates for the whole leaf were determined as the slope of the log₂-transformed number of cells per leaf, which was done using five-point differentiation formulas (Erickson, 1976).

4.2.9 FLP/MYB88 chromatin immunoprecipitation (ChIP) experiment

Polyclonal antibodies against the FLP/MYB88 proteins were generated by inoculating rabbits with Ni-NTA affinity purified NHis6-MYB88. ChIP experiments were performed essentially as before (Xie *et al.*, 2010). In brief, 10-day-old shoots of wild-type and *flp-1 myb88* (200 mg fresh weight for each) were crosslinked in 1 % formaldehyde for 20 min by vacuum filtration, and the crosslinking reaction was stopped by the addition of 0.1 M glycine (final concentration) for an additional 5 min. Tissues were ground to a fine powder in liquid nitrogen using mortar and pestle and then suspended in 300 ml of lysis buffer (50 mM HEPES, pH 7.5; 150 mM NaCl; 1 mM EDTA, pH 8.0; 1 % Triton X-100; 0.1 % sodium deoxycholate; 0.1 % SDS; 1 mM phenylmethanesulphonylfluoride; 10 mM sodium butyrate; 1x protein protease

inhibitor (Sigma)), and sonicated to achieve an average DNA size of 0.3-1 kb. The sonication conditions using the Bioruptor (Diagenode) were as follows: at high power; 30 s of sonication followed by 30 s of break; change ice every 10 min; 30 min in total. After clearing using 30 ml salmon sperm DNA/protein-A agarose (Upstate) at 41 °C for at least 1 h, the supernatant fractions were incubated, respectively, with 1 µl FLP/MYB88 rabbit polyclonal antibody or 1 µg rabbit IgG (Abcam) at 41 °C overnight. At the same time, 10 % of the supernatant was saved as the input fraction. The chromatin-antibody complex was incubated with salmon sperm DNA/protein-A agarose (Upstate) at 41 °C for at least 3 h, washed with lysis buffer, LNDET buffer (0.25 M lithium chloride; 1 % NP40; 1 % sodium deoxycholate; and 1 mM EDTA, pH 8.0), and TE buffer (10 mM Tris-Cl, pH 7.5; 1 mM EDTA, pH 8.0) twice, respectively, and the complex was reverse crosslinked in elution buffer (1 % SDS; 0.1 M NaHCO₃; 1 mg/ml proteinase K) overnight at 65 °C. DNA was extracted using the PCR Cleaning Kit (Qiagen). The presence of the promoter of *CYCA2;3* gene was examined by real-time PCR using SYBR-Green chemistry. The housekeeping gene *PROTEIN PHOSPHATASE 2A SUBUNIT A3* (AT1G13320) was used as an internal control for normalization. The fold enrichment was normalized to the internal control *PROTEIN PHOSPHATASE 2A SUBUNIT A3* using the $2^{-\Delta\Delta C_t}$ method. Two biological replicates were conducted for each real-time PCR experiment. The ChIP-PCR primers used are listed in Table 4.2.

4.3 RESULTS

Sequence similarity (Vandepoele *et al.*, 2002), co-regulation during the cell cycle (Menges *et al.*, 2005), subcellular colocalization (Boruc *et al.*, 2010a), common interaction partners (Boruc *et al.*, 2010b), and mild phenotypes in single mutants (Imai *et al.*, 2006; Yoshizumi *et al.*, 2006) collectively suggest redundancy among the four *CYCA2*s in the *Arabidopsis* genome obscuring their functional analysis. To circumvent this obstacle, phenotypic effects of various combinations of multiple *cyca2* loss-of-function mutants were analysed (Fig. 4.1; Table 4.1).

4.3.1 CYCA2s regulate the G2/M transition in roots

Since *CYCA2* expression is strongly associated with proliferative tissues, such as primary and lateral root meristems (Fig. 4.2), we probed the impact of their loss of function on root growth. Growth defects were apparent when three out of the four *CYCA2s* were mutated. Because the postembryonic growth of the quadruple mutant was extremely slow, we preferentially analysed triple mutant combinations (Fig. 4.3; for multiple mutant nomenclature, see Table 4.1). Triple mutants *cyca2;134* and *cyca2;234* had shorter roots and were impaired in lateral root formation compared with WT (Fig. 4.4). To determine whether these growth defects arose from an abnormal cell proliferation, root meristem phenotypes were analysed. Primary root meristems of *cyca2;134* and *cyca2;234* were smaller (Fig. 4.5A; 4.6A,B) and contained fewer dividing cells than WT, as detected by antibodies to the cytokinesis-specific syntaxin KNOLLE (Lauber *et al.*, 1997) (Fig.4.5B; 4.6C). Similarly, developing lateral root primordia in *cyca2;234* contained fewer cells than WT (Fig. 4.5C), suggesting that cell proliferation defects underlie both reduced root length and lateral root formation.

To determine at which cell-cycle stage *CYCA2s* are prominently involved, cell-cycle progression was compared during synchronized lateral root initiation in WT versus *cyca2;234* triple mutants (Fig. 4.5D). In WT, expression of both auxin signalling and G1-to-S phase regulatory genes preceded the expression of G2-to-M phase regulatory genes (Fig. 4.5D), as previously reported (Himanen *et al.*, 2002, Himanen *et al.*, 2004; Vanneste *et al.*, 2005). By contrast, expression of mitotic regulators, such as B-type cyclins, was no longer induced within the same time course in *cyca2;234* mutants, whereas the expression of auxin signalling and G1-to-S regulatory genes was unaffected (Fig. 4.5D). This delay in activation of mitotic regulators indicates that plant *CYCA2s* function early in the G2-to-M phase transition, as was predicted based on sequence homology (Vandepoele *et al.*, 2002) and on expression patterns in synchronized cell suspensions (Menges *et al.*, 2005). Moreover, it is likely that *CYCA2s* also function in S-phase, given that *CYCA2;2/CDKA;1* can phosphorylate the S-phase regulator E2

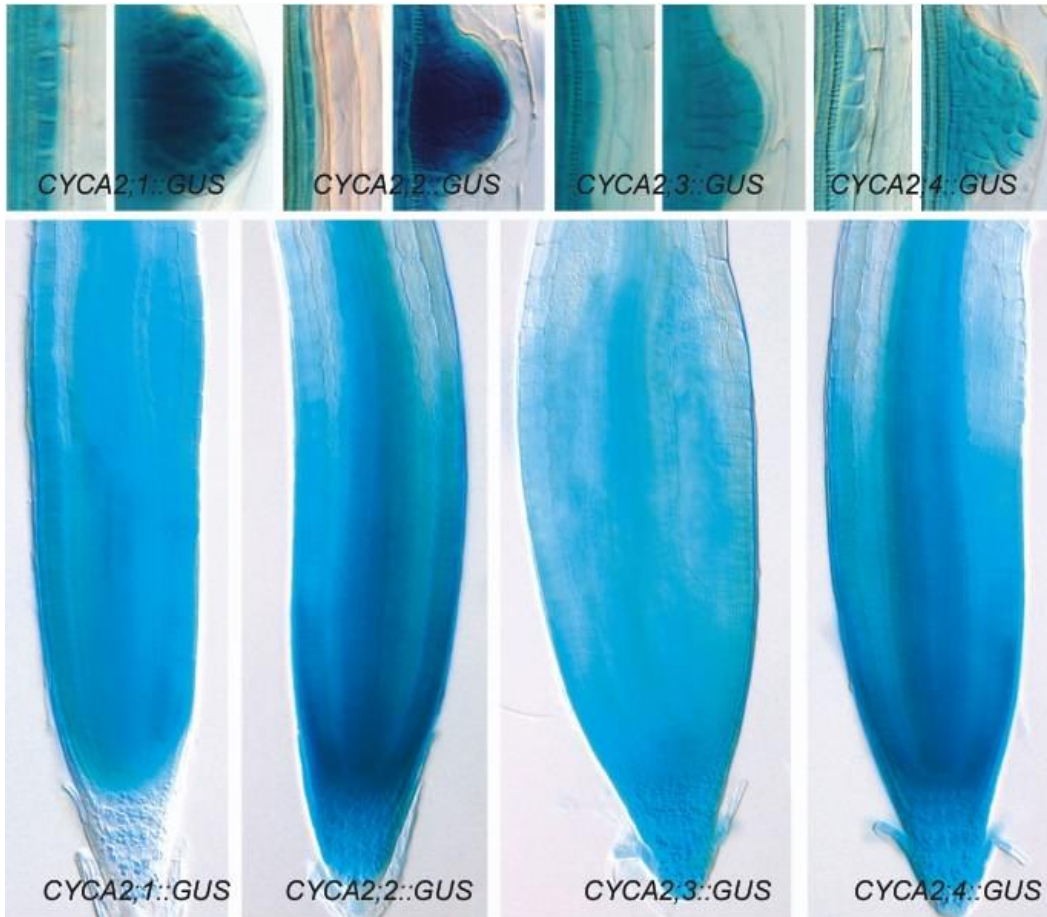


Figure 4.2. Expression patterns of CYCA2s in the root. Expression analysis of CYCA2;1::GUS, CYCA2;2::GUS:GFP, CYCA2;3::GUS:GFP, and CYCA2;4::GUS:GFP in developing lateral root primordia (top row) and root apical meristems (bottom row).

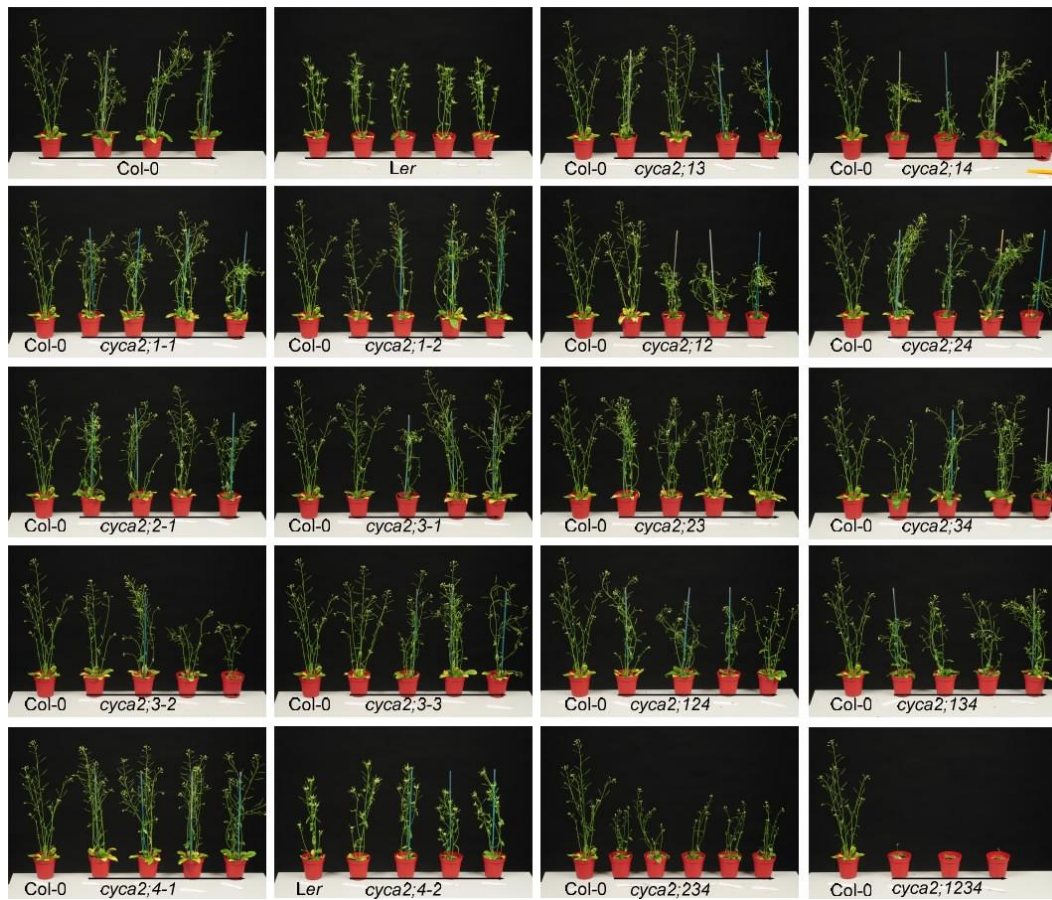


Figure 4.3. Overview picture of the respective single, double, triple, and quadruple mutants at the stage of flowering.

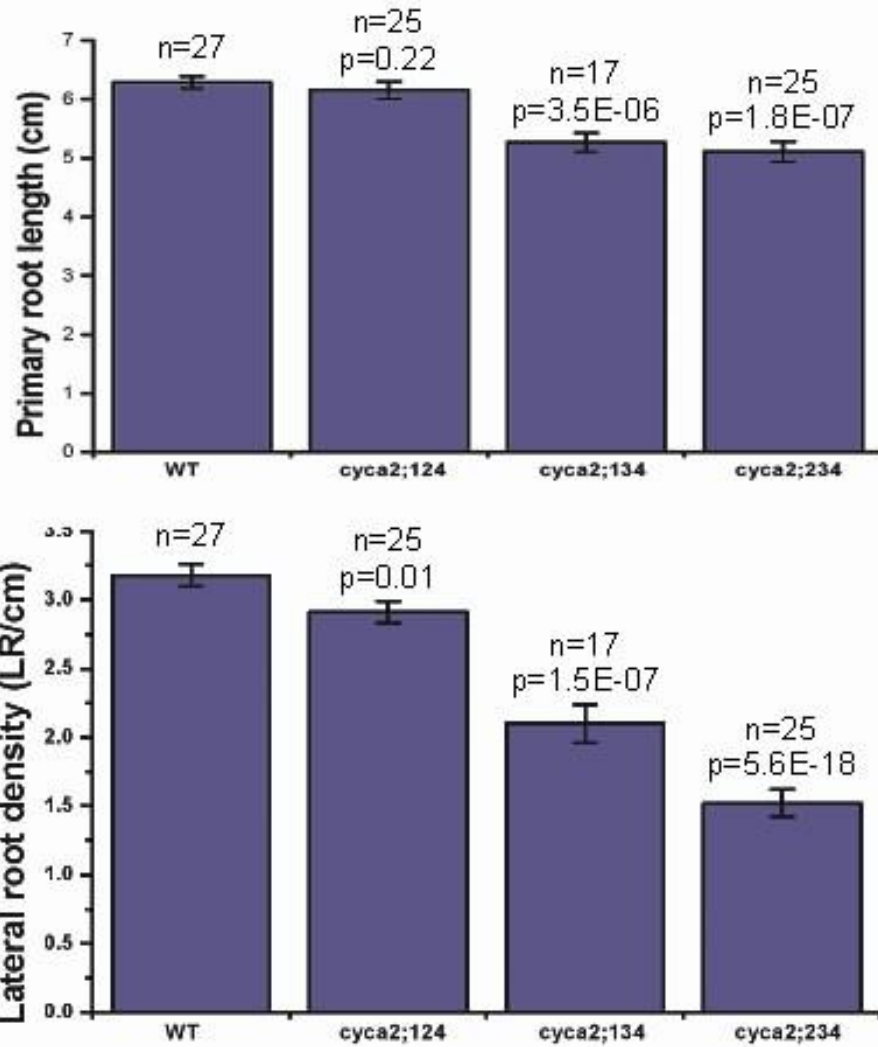


Figure 4.4. Root phenotypes of *cyca2* triple mutants. Primary root lengths and lateral root densities of 10 day old seedlings of WT, *cyca2;124*, *cyca2;134*, and *cyca2;234*. Data are presented as mean +/- S.E.M. (Student's *t*-test).

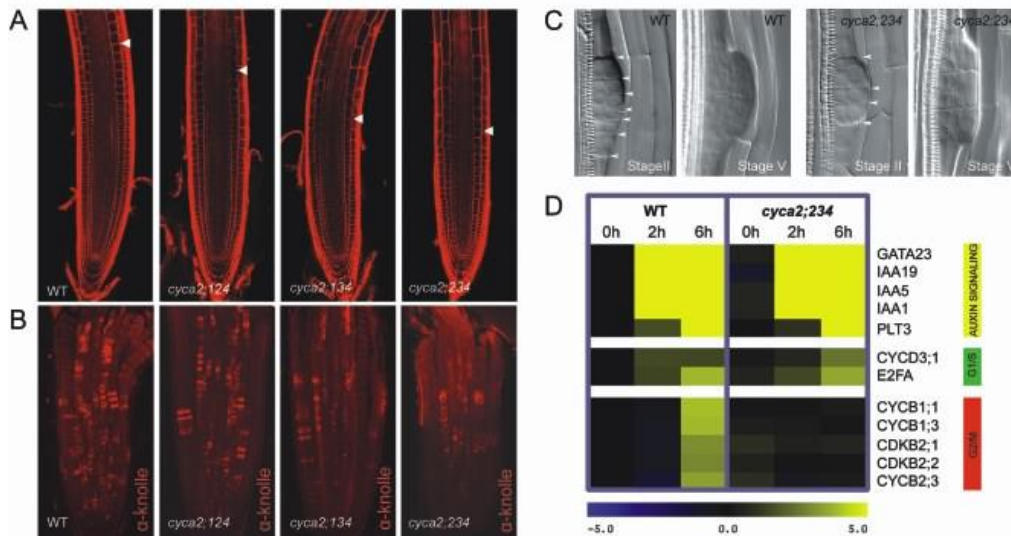


Figure 4.5. *cyca2* triple mutants have defects in cell-cycle progression. (A) Propidium iodide stained root meristems of WT, *cyca2;124* (*cyca2;1-1 cyca2;2-1 cyca2;4-1*), *cyca2;134* (*cyca2;1-1 cyca2;3-1 cyca2;4-1*) and *cyca2;234* (*cyca2;2-1 cyca2;3-1 cyca2;4-1*) 10 days after germination. Arrowheads indicate the ends of meristems, defined as the position where cells start elongating. (B) Immunolocalization of the cytokinesis-specific syntaxin, KNOLLE, labelling cells undergoing cytokinesis in roots of 7-day-old WT, *cyca2;124*, *cyca2;134*, and *cyca2;234*. (C) Stage II and stage V lateral root primordia of WT and *cyca2;234* cleared with chloral hydrate. Lateral root primordia of *cyca2;234* are composed of fewer cells than WT. Arrowheads indicate periclinal cell walls. Stages as defined previously (Malamy and Benfey, 1997). (D) Transcriptional responses of auxin signalling genes, G1-to-S phase, and G2-to-M phase regulators in WT and *cyca2;234* root segments during auxin-induced lateral root initiation. In all, 0, 2, and 6 h correspond to time of auxin treatment (10 μ M) after being germinated in presence of the auxin transport inhibitor 1-N-naphthylphthalamic acid (NPA) (10 μ M). Range indicator from blue to yellow represents expression levels on a log₂ scale relative to NPA germinated WT (0 h).

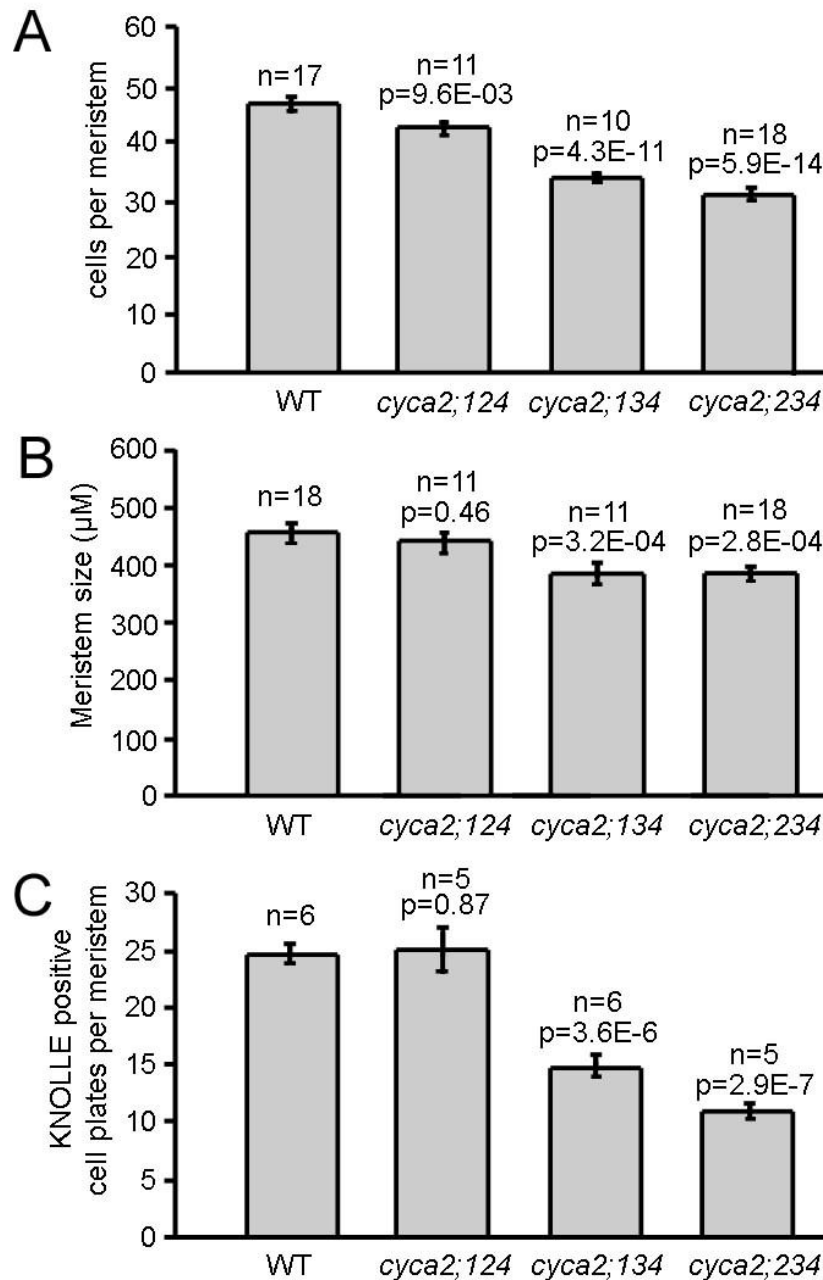


Figure 4.6. Quantitative analysis of root apical meristem size. (A) Comparison of number of cells per meristem in WT, *cyca2;124*, *cyca2;134*, and *cyca2;234*. The number of cortex cells between the quiescent centre and the first elongated cortex cell is taken as a measure of root meristem size. (B) Comparison of meristem sizes of WT, *cyca2;124*, *cyca2;134*, and *cyca2;234*. The meristems defined as in (A) were measured in μm. (C) Comparison of number of KNOLLE-positive cell plates per meristem of WT, *cyca2;124*, *cyca2;134*, and *cyca2;234*. A cell was counted when there was a clear labeling of the cell plate. Cells with KNOLLE expression not at the cell plate were not considered. Data are means +/- S.E.M. (Student's *t*-test).

TRANSCRIPTION FACTOR *c* *in vitro* (del Pozo *et al.*, 2002). However, the lack of appropriate markers hampers such determination.

4.3.2 CYCA2s drive proliferation in leaves, while repressing endoreduplication

To obtain its characteristic final size and shape, leaf morphogenesis depends upon a tight coordination between cell proliferation, cell-cycle exit, and differentiation. Early leaf development displays high cell division activity that is followed by a gradual tip-to-base deceleration of proliferation and the start of differentiation-associated endoreduplication and cell expansion (Beemster *et al.*, 2006; Donnelly *et al.*, 1999). The expression pattern of several *CYCA2s* also showed a comparable and dynamic gradient of expression (Fig. 4.7) (Imai *et al.*, 2006). Dramatic increases in ploidy levels and cell sizes were observed in the mature first true leaves of *cyca2* triple mutants (Fig. 4.8A,B). To address the mechanism driving enhanced ploidy levels and cell sizes, the development of *cyca2;234* leaves was analysed in greater detail. Kinematic analysis of leaf growth showed lower cell division rates in *cyca2;234* leaves compared with the WT (Fig. 4.8C; 4.9). In addition, as soon as the first leaf pair became macroscopically visible (8 DAG, Stage 1.02) (Boyes *et al.*, 2001), DNA content was already dramatically higher than the WT (Fig. 4.8D; % 2C, % 4C and % 8C). Moreover, ploidy levels continued to rise in *cyca2;234* (14 DAG), a period when endoreduplication had already stopped in the WT (Fig. 4.8D; % 16C and % 32C). Thus, enhanced ploidy levels in *cyca2;234* are the combined result of an early onset and extended duration of endoreduplication. Collectively, these phenotypic and molecular analyses in roots and shoots of *cyca2* triple mutants demonstrate that plant *CYCA2s* are fundamental elements of the plant cell cycle, and, like their animal counterparts, function in early G2-to-M phase transition. Furthermore, the enhanced endoreduplication in these mutants is consistent with the observation that low CDK activity allows yeast cells in G2 to (re)enter the G1-to-S phase program without undergoing mitosis (Coudreuse and Nurse, 2010), suggesting that plant *CYCA2s* contribute to CDK activities that are required for mitosis.

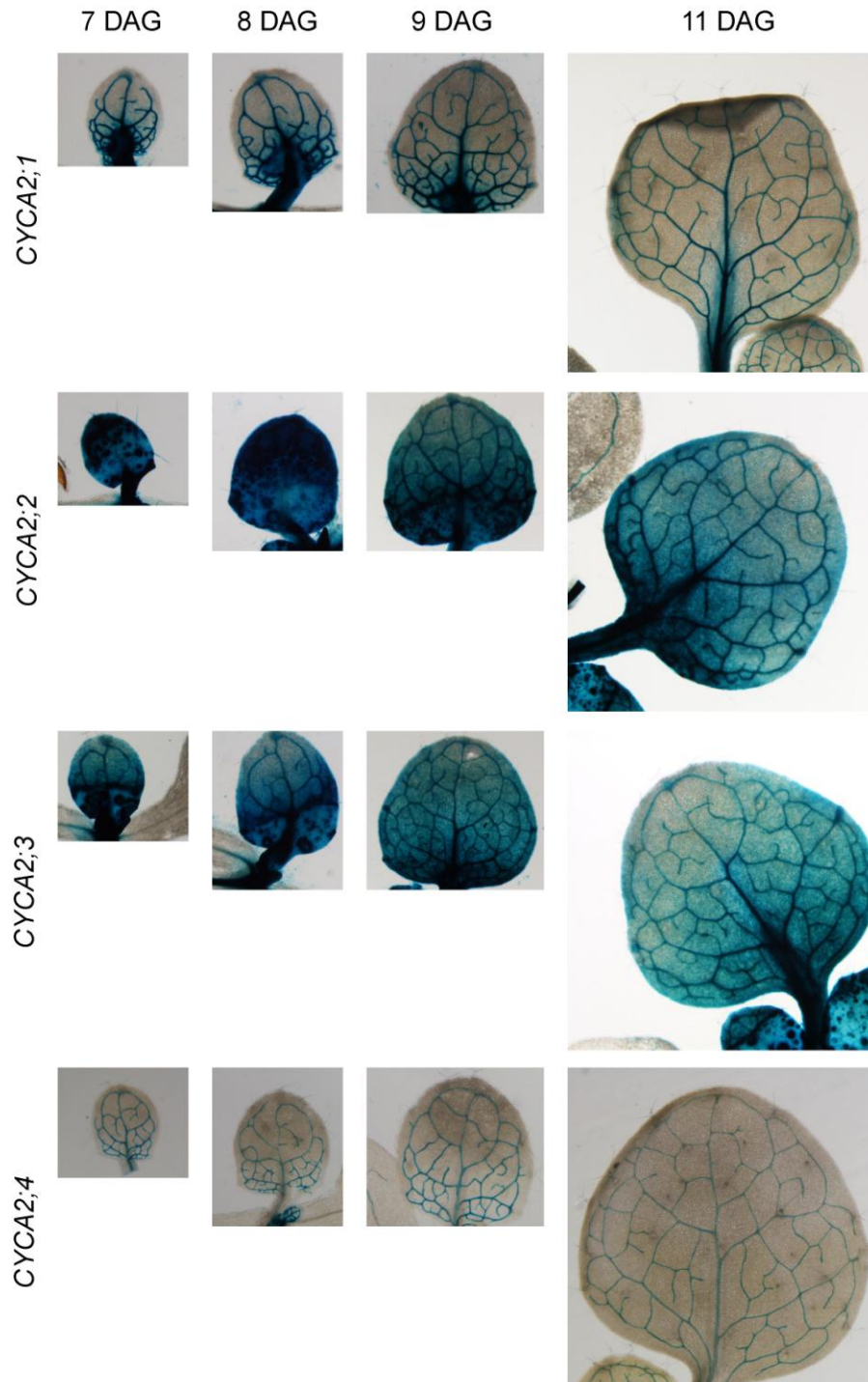


Figure 4.7. Evolution of *CYCA2s* expression pattern during early phases of leaf development. Time series of *CYCA2;1::GUS*, *CYCA2;2::GUS:GFP*, *CYCA2;3::GUS:GFP*, and *CYCA2;4::GUS:GFP* at different stages of leaf development. At 7 Days After Germination (DAG), the expression of *CYCA2;2* and *CYCA2;3* was ubiquitous in the proximal part of the leaf. At later stages this ubiquitous expression was lost and became restricted to specific cell types such as vascular tissues and the stomatal lineage. The switch between a ubiquitous expression pattern to a more restricted expression pattern resembled the gradual tip-to-base deceleration of proliferation associated with the onset of differentiation.

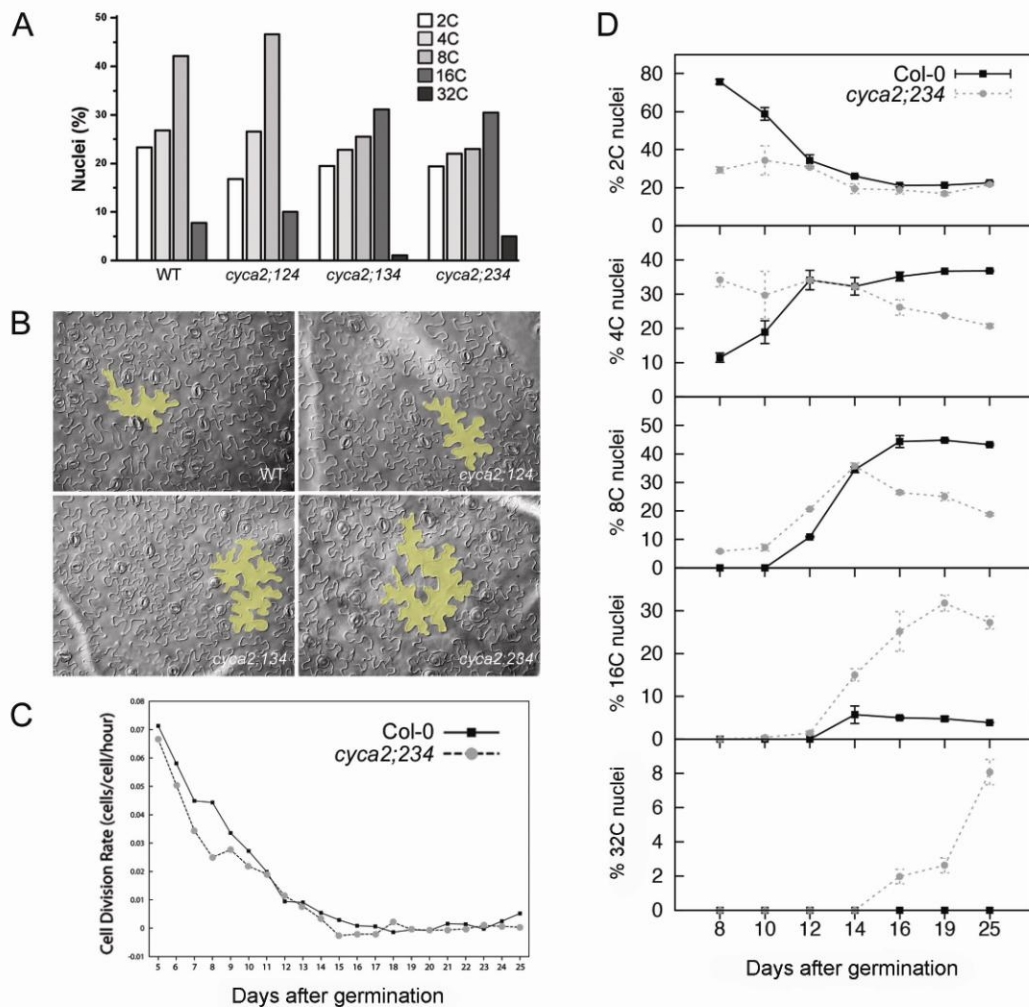


Figure 4.8. Leaf development shows enhanced endoreduplication and slowed down cell-cycle progression in *cyca2* triple mutants. (A) Distribution of nuclear ploidy in mature primary leaves of WT, *cyca2;124*, *cyca2;134*, and *cyca2;234*. Triple mutants *cyca2;134* and *cyca2;234* show highest ploidy levels. (B) Pavement cell size in mature primary leaves of WT, *cyca2;124*, *cyca2;134*, and *cyca2;234*. Yellow overlays highlight representative cells. (C) Kinematic analysis reveals a slowdown in cell division rates in developing primary leaves of *cyca2;234* when compared with WT. (D) Evolution of ploidy levels during the development of WT and *cyca2;234* primary leaves. In early stages, WT has predominantly 2C nuclei and a low 4C fraction. Later, the 2C fraction drops rapidly, while higher ploidy fractions increase until ~16 DAG. In *cyca2;234*, the 2C fraction is already low at the earliest stage analysed, while the 4C fraction is already high and even a small fraction 8C nuclei can be detected. At later stages, higher ploidy fractions continue to increase, and do not saturate within the time frame of our analysis. Data are represented as mean \pm standard error.

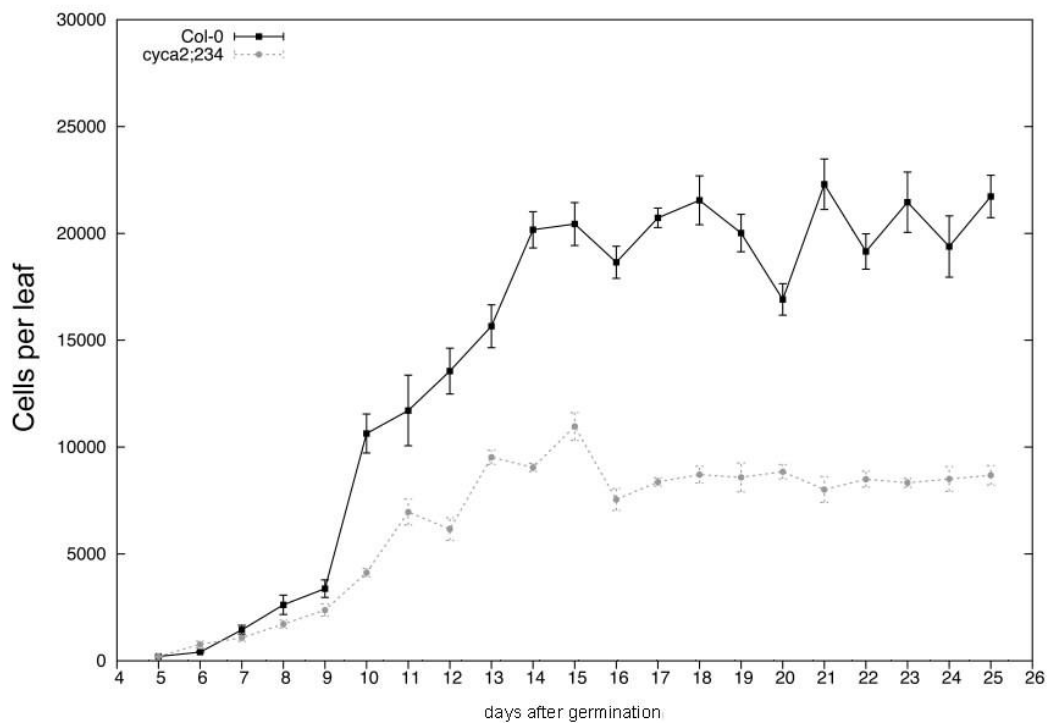


Figure 4.9. Evolution of cell number in developing first leaves in WT and *cyca2;234*. WT seedlings rapidly increase the total number of cells per leaf up to about 14 DAG. Later, the total number cells in a first leaf stabilised, suggesting that the cell division stopped or slowed down. In *cyca2;234* the total number of cells per leaf increases more steadily, and stabilises at about 12-13 DAG. Note that the total number of cells in a mature leaf is about half of the number of cells in a WT leaf. Data are presented as mean \pm standard error ($n = 5$).

4.3.3 Tissue-specific *CYCA2* expression contributes to vascular proliferation near hydathodes

In addition to their expression in meristems, *CYCA2*s were expressed in the leaf; however, while *CYCA2;2* and *CYCA2;3* were expressed throughout the organ (Fig. 4.7; 4.10; 4.11), the expression pattern of *CYCA2;1* and *CYCA2;4* remarkably mimicked the reticulate vein pattern of the leaf (Fig. 4.11; 4.12A). Moreover, the promoter activities of these two genes in the leaf overlapped with one of the earliest hallmarks of the vascular precursor ('preprocambial') cell state (Fig. 4.12B), the promoter activity of the *HOMEODOMAIN-LEUCINE ZIPPER* (*HD-ZIP*) III gene, *ATHB8* (Donner *et al.*, 2009; Kang and Dengler, 2004; Scarpella *et al.*, 2004; Chapter 2). The tissue-specific expression of *CYCA2;1* and *CYCA2;4* suggests that these *CYCA2* genes function in leaf vascular development. Indeed, *cyca2;234* leaves showed fewer vascular hypertrophy zones than the WT (Fig. 4.12C,D); however, vascular defects in *cyca2;234* were seemingly associated with changes in leaf shape resulting in leaves with fewer serration tips (Fig. 4.12C,E). Additional mutation of the vascular-specific *CYCA2;1* in the *cyca2;234* background further reduced the number of vascular hypertrophy zones without additional effects on the number of serration tips (Fig. 4.12D,E), data which are consistent with the tissue-specific expression pattern of *CYCA2;1*. Thus, vascular cell proliferation defects in *cyca2* mutants likely derive from tissue-specific modulation of *CYCA2* levels, rather than being secondary consequences of disrupted leaf growth.

4.3.4 Stomatal formation requires *CYCA2* activity

Stomata consist of two guard cells around a pore whose regulation controls gas exchange between the shoot and the atmosphere. Their development requires at least one asymmetric division as well as a single symmetric division. After the latter division, which occurs in a guard mother cell (GMC) precursor, stomatal differentiation and morphogenesis take place (Bergmann and Sack, 2007). The leaf epidermis of *cyca2;134* and *cyca2;234*, but not those of WT and *cyca2;124*, showed frequent occurrence of unpaired oval cells, displaying cell wall thickenings, and plastid accumulations, trait characteristics of wild-type guard

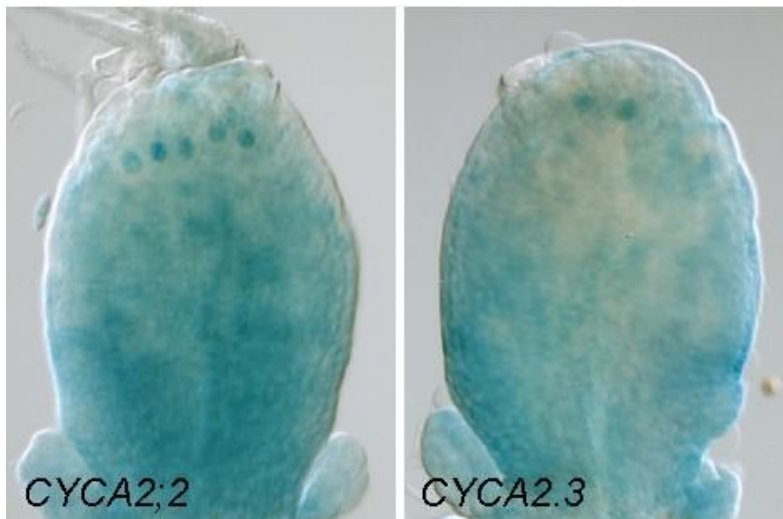


Figure 4.10. Expression pattern of *CYCA2;2* and *CYCA2;3* in 4-DAG first leaves. *CYCA2;2* and *CYCA2;3* are expressed in the stomatal lineage in the distal region of the leaf and more ubiquitously in subepidermal cells of the proximal region of the leaf.

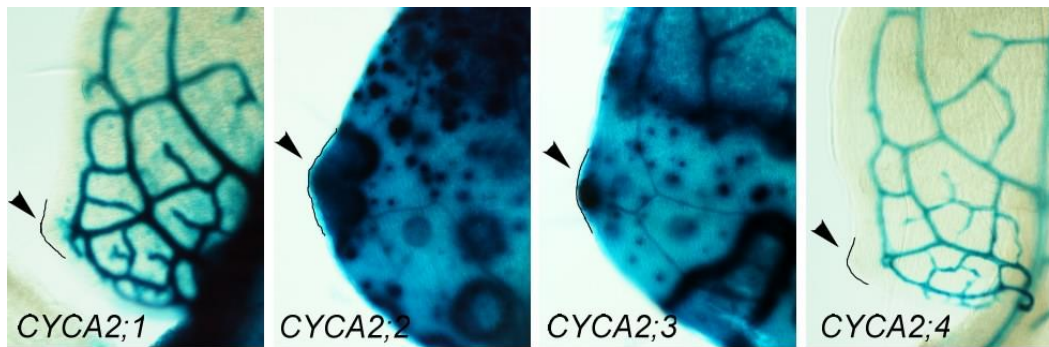


Figure 4.11. Expression pattern of *CYCA2*s in serration tips of 8-DAG first leaves. *CYCA2;2* and *CYCA2;3* are broadly expressed in the margin of developing serration tips, while *CYCA2;1* and *CYCA2;4* are restricted to the vascular tissues in this area. Arrowheads indicate serration tips. Outer edge of the serration tips is indicated by black free-hand line.

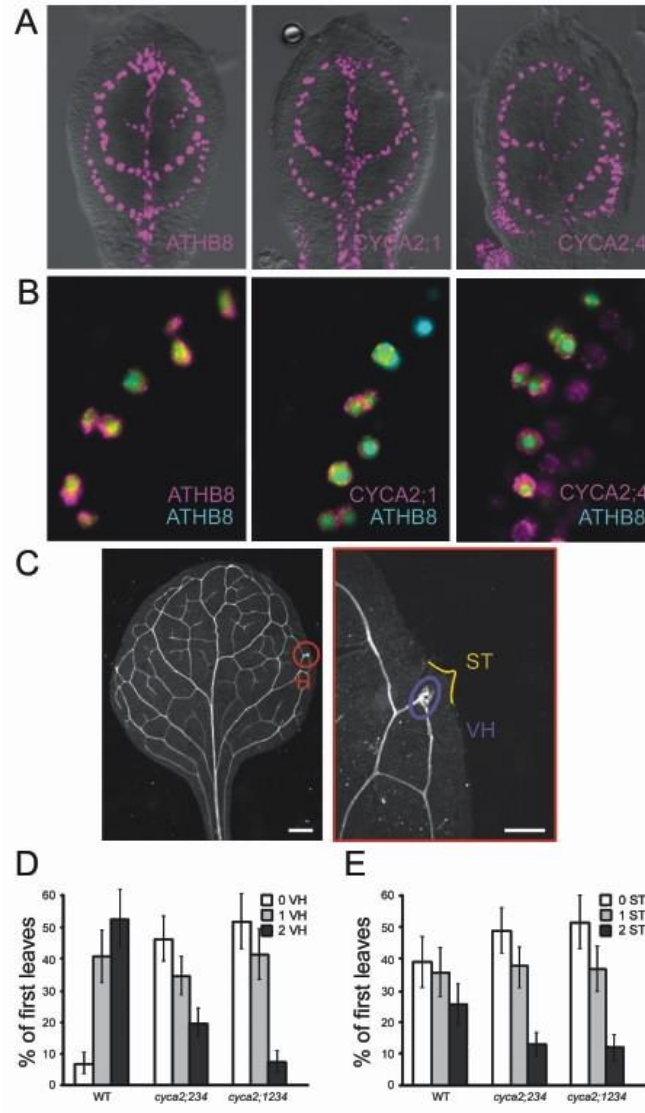


Figure 4.12. Tissue-specific expression of *CYCA2s* is required for vascular cell proliferation. (A) Expression patterns of *CYCA2;1::HTA6:EYFP* and *CYCA2;4::HTA6:EYFP* in 4-DAG first leaves resemble that of *ATHB8::HTA6:EYFP*, which is an early hallmark of vascular development. (B) Co-expression of *ATHB8::HTA6:EYFP*, *CYCA2;1::HTA6:EYFP*, and *CYCA2;4::HTA6:EYFP* with *ATHB8::ECFP-Nuc* in 4-DAG first leaves. Note how *CYCA2;4* expression is initiated slightly earlier than *ATHB8*, and in wider expression domains that over time narrow to single cell files. In contrast, *CYCA2;1* expression is initiated slightly later than *ATHB8*, but its expression is always confined to single cell files. Images colour-coded with a dual-channel LUT from cyan to magenta through green, yellow, and red (Demandolx and Davoust, 1997). Preponderance of cyan signal over colocalized magenta signal is encoded in green, opposite in red, and colocalized cyan and magenta signals of equal intensity in yellow. (C) Overview of cleared, mature first leaf, and detail of hydathode (H) that shows vascular hypertrophy (VH) and serration tip (ST). (D,E) Percentage of mature first leaves showing zero, one, or two zones of vascular hypertrophy (VH) (D) and serration tips (STs) (E). Plots represent mean \pm standard error. Experiments were done in triplicate, and VH and ST were counted on the primary leaves ($19 \leq n \leq 37$) of each of the three genotypes.

cells (Fig. 4.13A). As in normal stomatal guard cells, these single cells were positioned above large intercellular spaces in the subjacent mesophyll (Fig. 4.13B). Moreover, they expressed mature guard cell identity markers, *KAT1::GUS* (Nakamura *et al.*, 1995) and *ET1728* (Gardner *et al.*, 2009) (Fig. 4.13C). Thus, these cells correspond to aberrant, single guard cells (SGCs) that are located where stomata would normally be found. These SGCs had twice the nuclear-DNA content (4C) of normal guard cells (2C) (Fig. 4.14), suggesting they are arrested in G2-phase. Yet, the aberrant cells attained a guard cell identity and formed SGCs instead of a pair.

Strikingly, SGCs could only be found in *cyca2;3* mutant alleles and derived higher order *cyca2* mutant combinations (Table 4.1), suggesting that *CYCA2;3* is a major contributing factor to this phenotype. However, while in single mutants the frequency of SGC formation is very low, additional mutations of other *CYCA2* members resulted in dramatic increases in SGC frequencies (Table 4.1). Collectively, these data demonstrate that *CYCA2*s are synergistically required for the symmetric division that is a prerequisite for stomatal formation, and that acquisition of guard cell identity occurs independently from GMC division.

4.3.5 *CYCA2*s and *CDKB1*s synergistically promote GMC division

SGCs were previously reported in transgenic plants harbouring a *CDKB1;1-N161* dominant-negative construct (Boudolf *et al.*, 2004), as well as *cdkb1;1 cdkb1;2* double mutants (Xie *et al.*, 2010). Moreover, *CDKB1;1* can form a functional complex with *CYCA2;3* (Boudolf *et al.*, 2009) and *CDKB1;1* is expressed around the time of GMC symmetric division (Boudolf *et al.*, 2004), suggesting that *CYCA2*s and *CDKB1*s directly interact in promoting the formation of a two-celled stoma. Indeed, while *cdkb1;1* single mutants only had normal stomata, *cyca2;234 cdkb1;1* quadruple mutants displayed even fewer SGCs than *cyca2;234* triple mutants (Fig. 4.15;4.16). Thus, all four genes act synergistically in promoting GMC symmetric division, and thus stomatal morphogenesis.

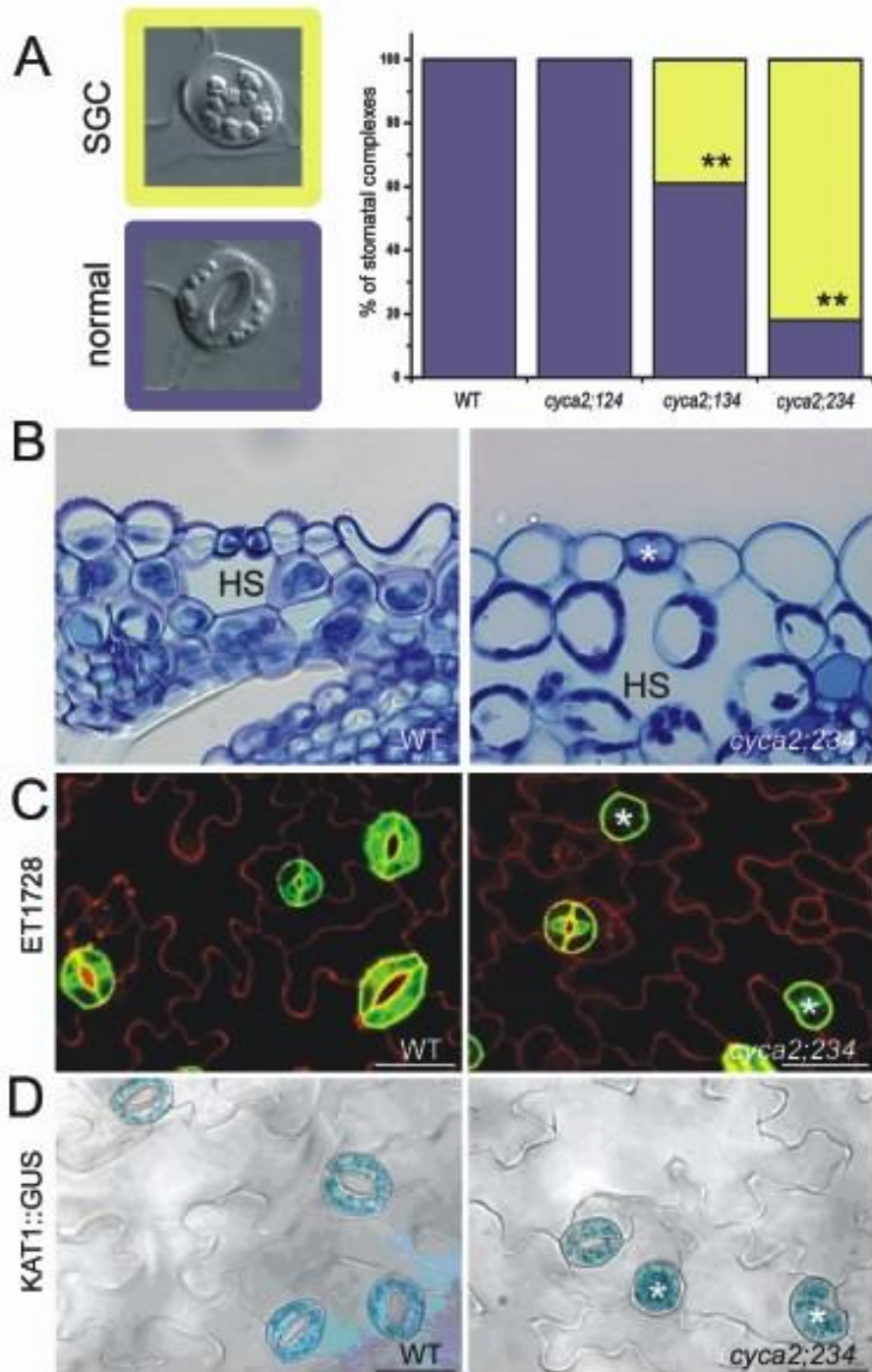


Figure 4.13. Stomatal expression of *CYCA2s* is required for guard mother cell division. (A) Stomatal phenotypes (left) of WT and representative triple mutant. Bar chart: quantification of stomatal phenotypes. Asterisks indicate $P < 0.001$; Fisher's exact test (comparison with WT). The *cyca2;234* triple mutant displays the highest frequency of single guard cells (SGCs). Blue = normal stoma; yellow = SGC. (B) Anatomical section through a WT stomatal complex and a *cyca2;234* SGC showing correct placement of abnormal SGC (asterisk) over a hypostomatal space (HS). (C,D) Expression of mature guard cell identity markers. (C) ET1728 (GFP) and (D) KAT1::GUS in WT and *cyca2;234* (asterisks indicate SGCs).

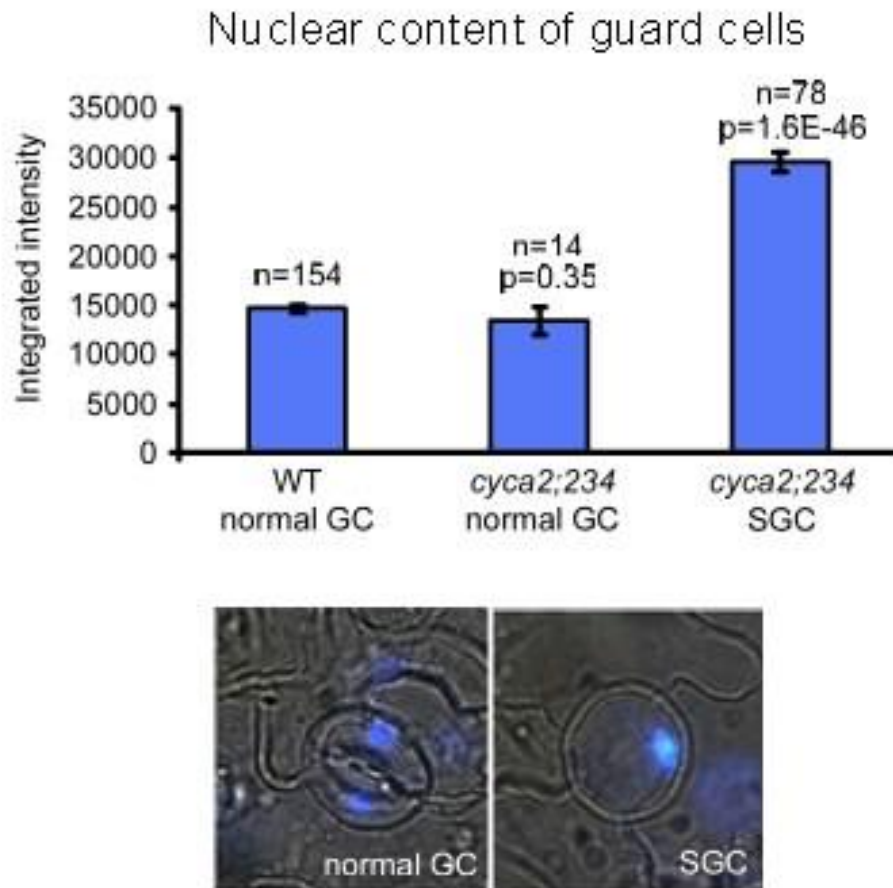


Figure 4.14. Nuclear contents of guard cells. Nuclear content of guard cells (GC) and SGCs in epidermal peels of WT and *cyca2;234*, estimated by integrated intensity of 4',6-diamidino-2-phenylindole (DAPI) fluorescence. SGCs have double nuclear contents relative to normal guard cells in both WT and *cyca2;234*. Data are presented as mean \pm standard error. Comparison to WT GC was done using Student's *t*-test.

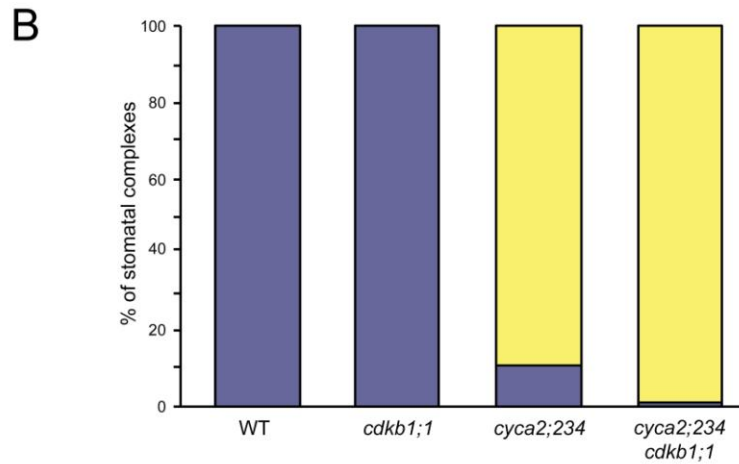
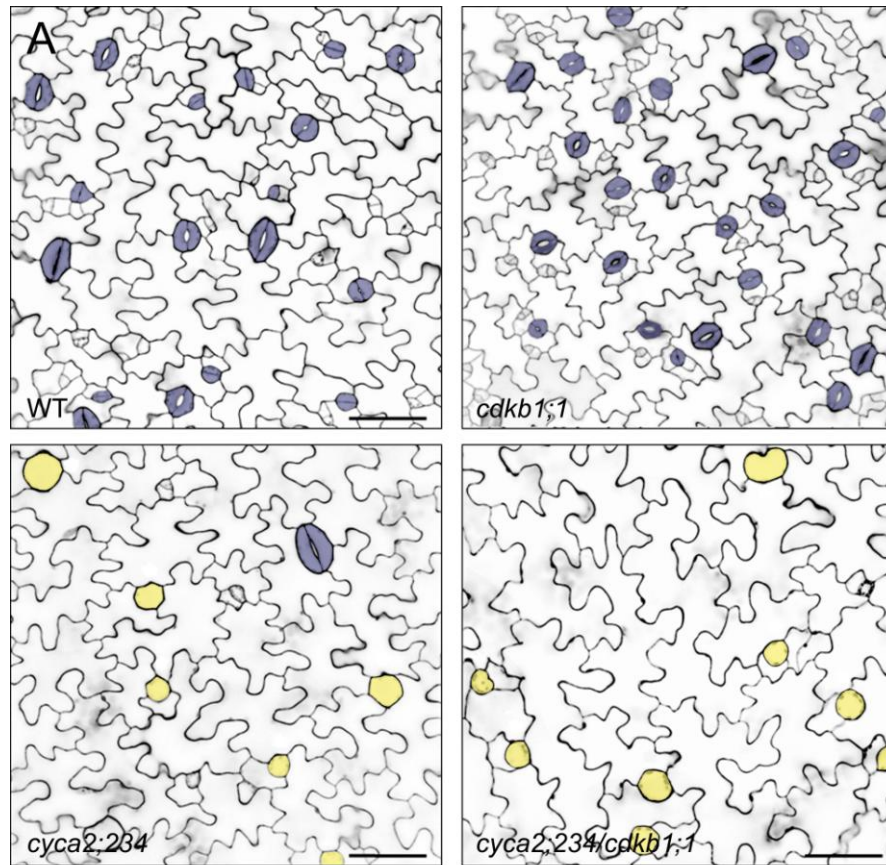


Figure 4.15. *CYCA2;2*, *CYCA2;3*, *CYCA2;4*, and *CDKB1;1* genes synergistically promote guard mother cell symmetric division. (A) Micrographs of WT, *cdkb1;1*, *cyca2;234*, and quadruple *cyca2;234 cdkb1;1* cotyledons of 4-DAG seedlings. Cell walls in 4-DAG cotyledons were visualized using propidium iodide and confocal-laser-scanning microscopy. False colouring highlights stomatal complexes: blue = normal stoma; yellow = SGC. (B) Quantification of stomatal phenotypes. Quadruple *cyca2;234 cdkb1;1* mutant displays more SGCs than *cyca2;234* (Fisher's exact test, $P = 0.0004$).

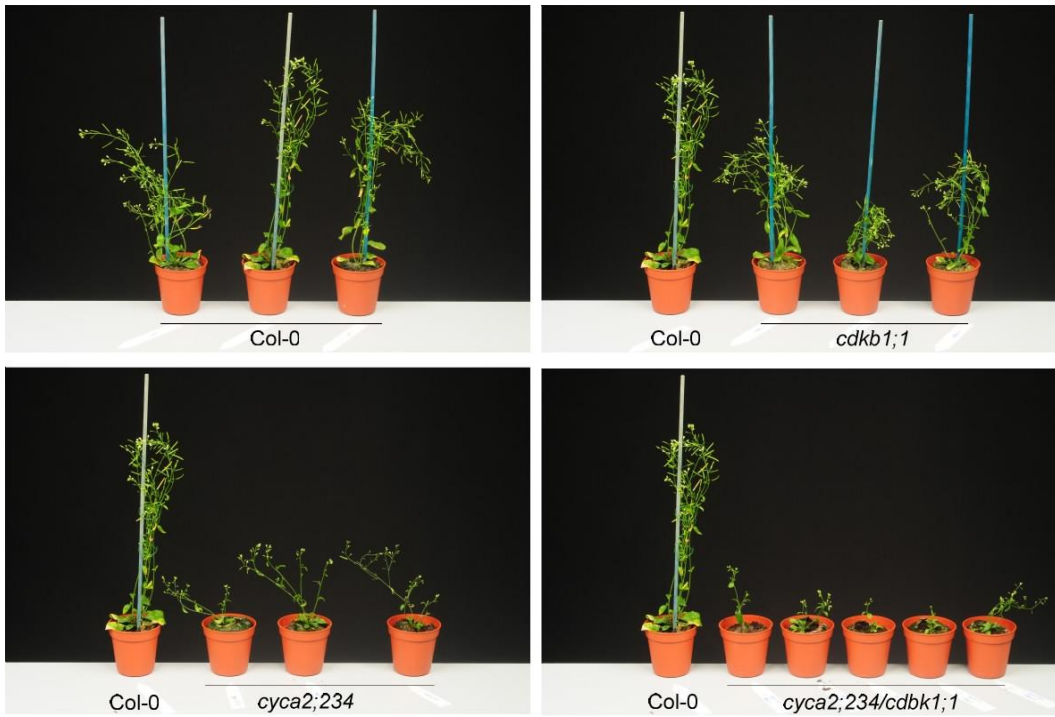


Figure 4.16. Overview picture of Col-0, *cdkb1;1*, *cyca2;234*, and *cyca2;234 cdkb1;1* mutant combinations at the stage of flowering.

4.3.6 FLP and MYB88 regulate the timely repression of *CYCA2;3* during terminal guard cell differentiation

While for *CYCA2;1* and *CYCA2;4* no stomatal expression could be observed (Fig. 4.17), *CYCA2;3* expression along with *CDKB1;1* and *CYCA2;2*, was induced in late GMCs, remained high in young guard cells, but was strongly reduced or did even disappear in mature stomata (Fig. 4.18A). Together with previously identified mutants that have supernumerary guard cells in stomatal complexes (Lai *et al.*, 2005; Ohashi-Ito and Bergmann, 2006), the observed decline in cell-cycle gene expression at the end of stomatal development hints at the existence of an active repression mechanism. Loss-of-function mutations in two MYELOBLASTOSIS (MYB) transcription factors, FOUR LIPS/MYB124 (FLP hereafter) and its paralogue MYB88 induce clusters of four or more guard cells (Lai *et al.*, 2005). Loss-of-function in the basic helix-loop-helix protein FAMA (Ohashi-Ito and Bergmann, 2006) also results in cell clusters, but unlike those of *flp myb88*, without guard cell identity. The apparent independence from the stomata differentiation process renders FLP and MYB88 as potential candidate *CYCA2* repressors, the more because they are expressed at roughly the same stages of stomatal development as *CYCA2;2*, and *CYCA2;3* (Fig. 4.18A).

To determine whether *CYCA2* expression is required for the extra divisions found in *flp myb88*, and/or *fama* backgrounds, we generated *cyca2;234 fama-1* quadruple and *cyca2;234 flp-7 myb88* quintuple mutants. The *cyca2;234 fama-1* plants did not show any SGCs, instead they formed clusters of cells that lacked guard cell identity; however, these clusters had fewer cells than *fama-1* suggesting that *fama-1* is only partly epistatic to *cyca2;234* (Fig. 4.19). By contrast, the formation of stomatal clusters in a *flp-7 myb88 cyca2;234* background was completely suppressed (Fig. 4.18B), demonstrating that *CYCA2* gene products are required for the *flp-7 myb88* stomatal phenotype and that FLP and MYB88 might represent transcriptional regulators of *CYCA2* expression. In *flp-1 myb88* stomata, *CYCA2;3* promoter activity remained high after the GMC division (Fig. 4.18C), suggesting that FLP and MYB88 repress *CYCA2;3* promoter activity; it is possible that FLP and MYB88 regulate expression of the

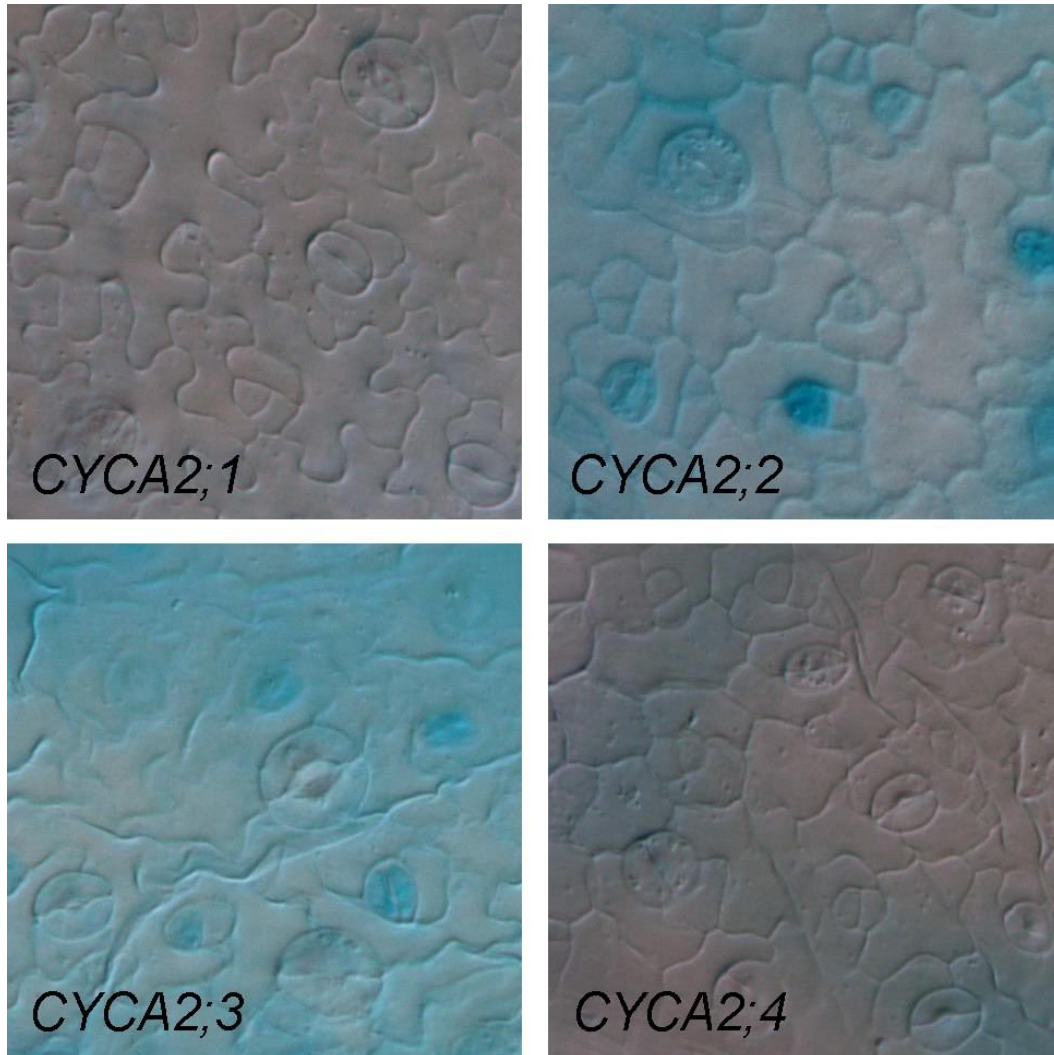


Figure 4.17. Expression pattern of CYCA2s in the stomatal lineage. While *CYCA2;2* and *CYCA2;3* are strongly expressed in the stomatal lineage, no *CYCA2;1* and *CYCA2;4* could be detected in these cells. The shadow of GUS staining seen in *CYCA2;4* is staining of underlying vascular tissues.

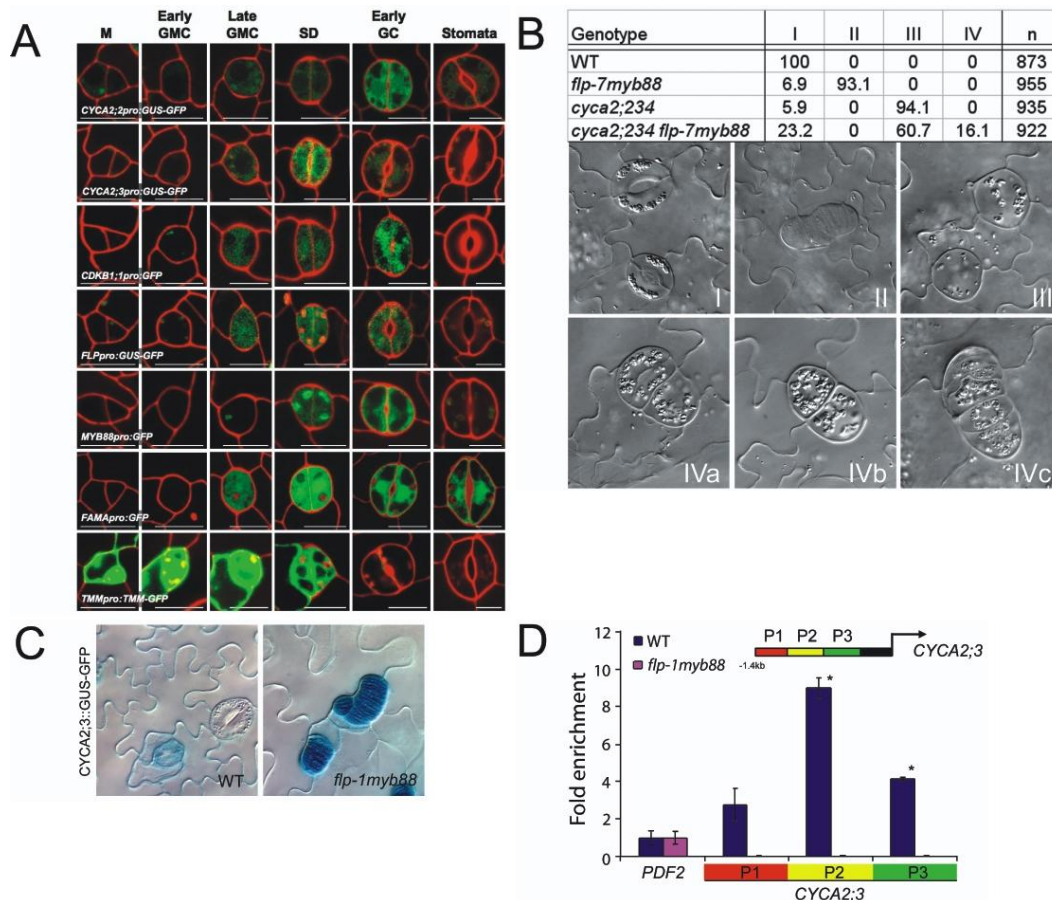


Figure 4.18. FLP/MYB124 and MYB88 are direct repressors of *CYCA2;3* expression during guard mother cell (GMC) division. (A) Expression analysis of transcriptional promoter:reporter fusions (except for TMM::TMM:GFP (TOO MANY MOUTHS (TMM) translational fusion). *FLP*, *MYB88*, and *FAMA*, which encode transcription factors, are expressed in late GMCs, during symmetric division, and in young guard cells. *TMM* expression marks an earlier phase of stomatal development. *CYCA2;2*, *CYCA2;3*, and *CDKB1;1* are expressed at similar stages to *FLP*, *MYB88*, and *FAMA*. Each meristemoid (M) develops into a GMC. Late GMCs have thickened end walls that are usually bisected by the symmetric division (SD) that produces two young guard cells (GCs). The latter undergo further morphogenesis including stomatal pore formation. (B) Chart showing frequencies of different stomatal phenotypes in WT, *flp-7 myb88*, *cyca2;234*, and in *cyca2;234 flp-7 myb88*. Stomata in the WT are normal by definition (type I stomata). In *flp-7 myb88*, many stomata are arranged in clusters (type II), while in *cyca2;234* SGCs (type III) predominate. In a *cyca2;234 flp-7 myb88* quintuple mutant, most stomata are single-celled (type III), but some small clusters of stomata next to apparent SGCs are present (type IV), suggesting a ‘fusion’ phenotype (IVa-c). (C) *CYCA2;3::GUS:GFP* in WT and in *flp-1 myb88*. *CYCA2;3::GUS:GFP* GUS levels are low or absent from mature guard cells in WT plants, and strongly expressed in *flp-1 myb88* stomatal clusters. (D) ChIP-qPCR on three fragments upstream (-1.4 kb) of the translational start of *CYCA2;3* (P1-P3). PCR conducted on ChIPed DNA samples from 10-DAG WT and *flp-1 myb88* shoots using FLP/MYB88 antibody. *PROTEIN PHOSPHATASE 2A SUBUNIT A3* was used as a negative control. The positions for PCR products in *CYCA2;3* promoter are indicated. Strongest, specific binding was observed for P2. The error bars indicate the standard error from two biological replicates. Asterisk denotes a statistically significant difference ($P < 0.05$).

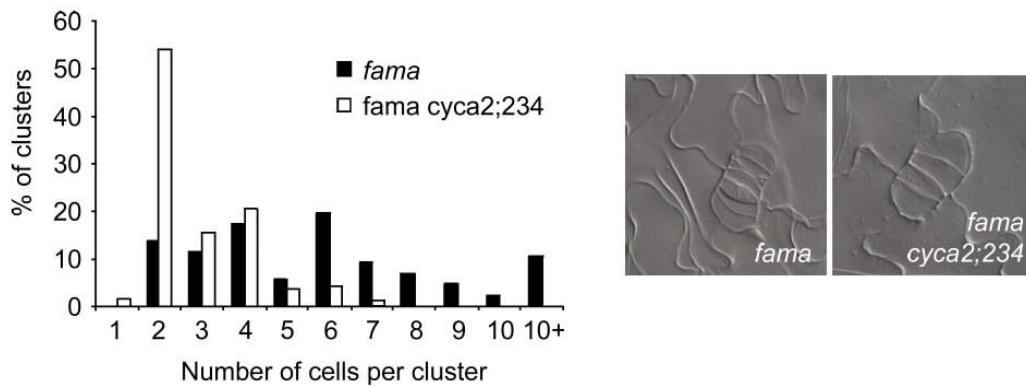


Figure 4.19. Genetic interaction between *fama* and *cyca2;234*. Frequency distribution of number of cells per cluster in *fama* and *fama cyca2;234* in mature cotyledons. The number of cells per cluster is dramatically reduced by *cyca2;234* mutation, but does not give rise to *cyca2;234* SGCs. Note that these cells do not have any stomatal identity since *FAMA* is required for a guard cell fate.

other *CYCA2* genes. To test if the effect of FLP and MYB88 on *CYCA2;3* expression was direct, we performed ChIP-qPCR using polyclonal antibodies raised against FLP and MYB88 (Xie *et al.*, 2010). In the WT, *CYCA2;3* promoter chromatin fragments were enriched after ChIP, while these were lost in *flp-1 myb88* mutants (Fig. 4.18D), demonstrating a specific, direct interaction of FLP and MYB88 with *CYCA2;3* chromatin. Thus, FLP and MYB88 appear to restrict *CYCA2;3* transcription after GMC division via direct interaction with its promoter.

4.4 DISCUSSION

4.4.1 *CYCA2*s modulate the G2-to-M transition

Several findings led to the initial assumption that plant A-type cyclins function in S-phase and in the G2-to-M transition, in analogy to the animal and yeast cell-cycle model. These findings include *CYCA2* expression patterns in synchronized suspension cells (Menges *et al.*, 2005; Reichheld *et al.*, 1996; Shaul *et al.*, 1996), their ability to rescue the growth of yeast cyclin mutants (Setiady *et al.*, 1995), and their ability to induce *Xenopus* oocyte maturation (Renaudin *et al.*, 1994). In addition, the ectopic expression of plant cyclins is sufficient to drive cells into mitosis (Boudolf *et al.*, 2009; Imai *et al.*, 2006).

Recently, it was shown that engineered yeast cells arrested in G2 are able to skip mitosis and re-acquire a G1 status when CDK activity is low (Coudreuse and Nurse, 2010). Therefore, if *CYCA2*s affect mitotic CDK activity, one could expect ectopic endoreduplication and reduced proliferation in the absence of *CYCA2* function. Previously, single mutants in *cyca2;1* and *cyca2;3* were shown to have increased levels of endoreduplication (Imai *et al.*, 2006; Yoshizumi *et al.*, 2006). Consistent with these data, we found that *cyca2* triple mutants displayed greatly increased endoreduplication levels, reduced cell proliferation in developing leaves and G2-phase arrest of GMCs resulting in SGCs with 4C DNA levels. Together, these data demonstrate that *CYCA2*s contribute to the CDK activity that is required for mitosis.

In animal systems, it is well established that B-type cyclins in complex with a CDK act as MITOSIS-PROMOTING FACTOR (MPF). MPF activity is further regulated by A-type cyclins through effects on transcription, activation, localization and stability (Lindqvist *et al.*, 2009). In plants, ectopic expression of *CYCB1;2* in differentiated cell types such as trichomes was sufficient to trigger ectopic cell divisions, suggesting a MPF-like function of CYCBs in plants (Schnittger *et al.*, 2002). Using an *in planta* synchronized cell cycle-inducible system, we found that the onset of B-type cyclin expression was delayed in *cyca2* triple mutants. Thus, mitotic entry involves the sequential activity of CYCA2-CDK and CYCB-CDK complexes.

4.4.2 Tissue specificity and redundancy among CYCA2s

Each cell type and tissue, within complex organs such as developing leaves, needs custom-tailored cell-cycle regulation for the organ to reach its typical size and shape. This complexity is reflected in the large number of cell-cycle regulatory genes in plants. In *Arabidopsis*, four *CYCA2* genes are encoded in its genome. Each individual *CYCA2* shows its own particular expression patterns across developing organs, displaying tissue- and cell type-specific expression, such as in vascular tissues and the stomatal lineage. Their expression patterns also show variable degrees of overlap in certain tissues, suggesting local redundancies. Striking examples are the vascular expression of *CYCA2;1* and *CYCA2;4* and the stomatal expression of *CYCA2;2* and *CYCA2;3*. In both tissues, the individual genes contribute locally to proliferation in a specific tissue or cell type.

Besides the expression-pattern-dependent redundancy, the mutant analyses revealed differential contributions of individual *CYCA2*s to proliferation. The analysis of the phenotypes of different triple mutants allowed the estimation of their relative importance for specific processes. In the case of root meristem size, lateral root formation, endoreduplication, and stomatal development, *CYCA2;3* seemed to be most relevant; during stomatal formation, only single *cyca2;3* mutants resulted in SGC formation. Moreover, in combination with *cyca2;3*, other *cyca2* mutations synergistically enhanced the frequency of SGC formation.

Observed differences in penetrance can be explained in part by tissue-specific expression and relative expression levels. However, our study does not allow us to exclude effects of protein stability and differences in biochemical properties as additional regulatory mechanisms.

4.4.3 Developmental control over cell cycle through repression of *CYCA2*

Proliferation and differentiation are largely mutually exclusive processes. While some cells exit the cell cycle after mitosis and remain in G1-phase, other differentiating cells undergo several rounds of a modified cell cycle, in which the G2-to-M phase transition is omitted and only DNA synthesis occurs (endoreduplication). In animals, some developmental programs coordinate cell-cycle exit during differentiation through transcription-factor activity (Buttitta and Edgar, 2007; Myster and Duronio, 2000). One strategy is to induce CDK inhibitory proteins, while another is to repress cell-cycle activating proteins. Interestingly, the transcription of A-type cyclins is often actively repressed during differentiation processes (James *et al.*, 2006; Li and Vaessin, 2000; Martinez *et al.*, 2006; Pan *et al.*, 2010; Sebastian *et al.*, 2009). In plants, it is not known how developmental signals can modulate the switch between a full cell cycle and the endocycle or cell-cycle exit during differentiation. Previously, INCREASED LEVEL OF POLYPLOIDY1 was found to act as repressor of *CYCA2* expression (Yoshizumi *et al.*, 2006). Here, we show that FLP and MYB88 repress *CYCA2;3* expression during cell-cycle exit in differentiating guard cells. This mechanism resembles the PROSPERO-dependent mechanism in *Drosophila* that links neuronal lineage development with the transcriptional regulation of cell-cycle regulatory genes (Li and Vaessin, 2000).

Mutations that affect *CYCA2* function display higher than normal ploidy levels (Imai *et al.*, 2006; Yoshizumi *et al.*, 2006), whereas *CYCA2;3* overexpression strongly suppresses endoreduplication (Boudolf *et al.*, 2009; Imai *et al.*, 2006), indicating that *CYCA2* levels are major negative determinants of endoreduplication in leaves. Early stages of leaf development involve high proliferation rates, while later stages gradually switch to differentiation-associated endoreduplication and cell expansion (Beemster *et al.*, 2006; Donnelly *et al.*,

1999). Interestingly, *CYCA2;3* expression is rapidly repressed during the switch from proliferation to endoreduplication in differentiating leaves (Imai *et al.*, 2006). Similarly, antagonizing auxin signalling also enhances endoreduplication via reduced *CYCA2;3* expression (Ishida *et al.*, 2010). However, it remains to be seen whether this effect is directly mediated by differentiation-induced transcription factors and how auxin is involved in this.

Stomatal development ends after a single symmetric division of a GMC, each of whose daughter cells terminally differentiate into individual guard cells (Bergmann and Sack, 2007). Mutants in the stomatal transcription factors FLP and MYB88 do not stop dividing after the GMC has divided, even though guard cell identity markers are expressed (Lai *et al.*, 2005). We found that downregulation of *CYCA2;3* after the first GMC division, normally seen in wild-type plants, was absent in *flp myb88* double mutants. Direct interaction with *CYCA2;3* promoter chromatin corroborate that FLP and MYB88 act as direct repressors of *CYCA2;3* expression in guard cells. Similarly, the expression of an interacting CDK (Boruc *et al.*, 2010b; Boudolf *et al.*, 2009), *CDKB1;1* was also shown to be directly repressed by FLP and MYB88 (Xie *et al.*, 2010). These data are consistent with a model in which FLP and MYB88 enforce cell-cycle exit during terminal guard cell differentiation by direct repression of *CYCA2/CDKB1;1* kinase complexes. This mechanism ensures that stomata consist of only two guard cells, a condition required for their proper functioning as adjustable air valves.

CHAPTER 5: TRANSCRIPTIONAL CONTROL OF EARLY VEIN EXPRESSION OF *CYCA2;1* AND *CYCA2;4* IN *ARABIDOPSIS* LEAVES ⁴

5.1 INTRODUCTION

In most multicellular organisms, transport functions are provided by specialized tissue networks. In animals, the formation of most of these networks is highly stereotyped, suggesting tight genetic control (Lu and Werb, 2008; Metzger and Krasnow, 1999). By contrast, the formation of vein networks in plant leaves is both reproducible and variable: reproducible because all parts of the leaf are supplied by veins; variable because the exact positions of these veins are unpredictable (Berleth *et al.*, 2000; Sachs, 1989). These seemingly conflicting properties suggest a self-organizing patterning mechanism that integrates vein formation with leaf growth (Dengler and Kang, 2001; Sachs, 1989). The molecular details of this patterning mechanism are still unclear, but varied evidence supports a decisive function for the transport and transduction of the plant signal auxin in vein formation. Veins form along paths of maximum transport and transduction of the auxin signal (Donner *et al.*, 2009; Mattsson *et al.*, 2003; Sawchuk *et al.*, 2007; Scarpella *et al.*, 2006; Wenzel *et al.*, 2007; Chapter 2), application of auxin to leaf primordia induces formation of new veins (Jost, 1942; Sachs, 1989; Scarpella *et al.*, 2006), and inhibition of auxin transport during leaf development dramatically alters vein patterns (Mattsson *et al.*, 1999; Sieburth, 1999). In agreement with these observations, genetic defects in auxin transport or signal transduction lead to characteristic defects in vein patterns (Alonso-Peral *et al.*, 2006; Garrett *et al.*, 2012; Krogan *et al.*, 2012; Mattsson *et al.*, 1999; Przemec *et al.*, 1996). While a role for signals other than auxin in vein

⁴ A version of this chapter has been published. Copyright 2012, with permission from Elsevier. Reprinted from *Mechanisms of Development*, 2013, T. J. Donner and E. Scarpella, Transcriptional control of early vein expression of *CYCA2;1* and *CYCA2;4* in *Arabidopsis* leaves, volume 130, pages 14-24, doi: <http://dx.doi.org/10.1016/j.mod.2012.07.002>

Conceived and designed the experiments: TJD, ES. Performed the experiments: TJD. Analyzed the data: TJD, ES. Wrote the paper: TJD, ES.

I generated the data that gave rise to figures: 5.1, 5.2, 5.3, 5.4, 5.5, and 5.6.

patterning is by no means excluded, the patterning process terminates with the onset of expression of the *ARABIDOPSIS THALIANA HOMEBOX8 (ATHB8)* and *SHORT ROOT (SHR)* genes in files of isodiametric subepidermal cells of the leaf ('ground' cells) (Gardiner *et al.*, 2011; Kang and Dengler, 2004; Scarpella *et al.*, 2004; Chapter 3). Only ground cells expressing these genes will in fact elongate into procambial cells: the precursors of all mature vascular cell types (Esau, 1965; Kang and Dengler, 2004; Sawchuk *et al.*, 2007; Scarpella *et al.*, 2004).

Identification of the *cis*-regulatory elements required to initiate gene expression at stages prior to procambium differentiation could provide insight into the gene regulatory networks that control vein patterning. However, few genes have been identified whose expression is initiated at 'preprocambial' stages of vein development (*e.g.*, Carland and Nelson, 2004; Carland and Nelson, 2009; Ckurshumova *et al.*, 2011; Donner *et al.*, 2009; Gardiner *et al.*, 2010; Gardiner *et al.*, 2011; Kang and Dengler, 2004; Konishi and Yanagisawa, 2007; Sawchuk *et al.*, 2007; Scarpella *et al.*, 2004; Scarpella *et al.*, 2006; Wenzel *et al.*, 2007; Chapters 2 and 3). Moreover, information on the regulatory elements required for preprocambial expression is thus far only available for *ATHB8*, whose preprocambial expression depends on a TGTCTG motif that is bound by the AUXIN RESPONSE FACTOR5/MONOPTEROS (MP hereafter) transcription factor (Donner *et al.*, 2009; Chapter 2).

The *CYCLIN A2;1 (CYCA2;1)* and *CYCLIN A2;4 (CYCA2;4)* genes of *Arabidopsis thaliana* are expressed in veins and are redundantly required for vein cell proliferation (Bursens *et al.*, 2000; Imai *et al.*, 2006; Vanneste *et al.*, 2011; Chapter 4). Here we show that *CYCA2;1* and *CYCA2;4* are expressed at preprocambial stages of vein development. Further, we show that preprocambial expression of *CYCA2;1* and *CYCA2;4* depends, respectively, on a 76- and 77-bp *cis*-regulatory element. Finally, we find that these regulatory elements contain, respectively, one and three putative transcription-factor binding sites that are conserved in sister species of *Arabidopsis thaliana*. Our results suggest that regulatory elements of different structures encode preprocambial expression.

5.2 MATERIALS AND METHODS

5.2.1 Vector construction

The *CYCA2;1* (AT5G25380) and *CYCA2;4* (AT1G80370) transcriptional fusions were generated with gene-specific primers (Table 5.1) and recombined into pFYTAG (Zhang *et al.*, 2005).

5.2.2 Plant material and growth conditions

The origin and nature of the ATHB8::HTA6:EYFP, *CYCA2;1*::HTA6:EYFP, *CYCA2;4*::HTA6:EYFP, ATHB8::ECFP-Nuc, and UBQ10::EGFP:LTI6B lines are in Table 5.2. Seeds were sterilized and germinated, and seedlings and plants were grown and transformed as described in Section 2.2.2. For each construct, the progeny of 6-14 independent single-insertion transgenic lines were selected and analyzed as in Gardiner *et al.* (2011; Chapter 3).

5.2.3 Microscopy and image analysis

Dissected leaves were mounted and imaged as described in section 2.2.3. Image brightness and contrast were adjusted through linear stretching of the histogram in ImageJ (National Institutes of Health, <http://rsb.info.nih.gov/ij>). Signal colocalization was visualized as in (Sawchuk *et al.*, 2008). Images were cropped in Adobe Photoshop 7.0 (Adobe Systems Incorporated, San Jose, CA, USA) and were labeled and assembled into figures in Canvas 8.0 (ACD Systems International Inc., Seattle, WA, USA).

5.2.4 Bioinformatics

Sequences were retrieved in January 2012 with Phytozome v8.0 (Goodstein *et al.*, 2012) (<http://www.phytozome.net/>) and aligned with mVISTA (Frazer *et al.*, 2004) (<http://genome.lbl.gov/vista/index.shtml>) using LAGAN option (Brudno *et al.*, 2003) with 6-bp calculation window, 4-bp consensus width, and 100% conservation identity. Putative transcription-factor binding sites were identified with AGRIS (Davuluri *et al.*, 2003) (<http://arabidopsis.med.ohiostate.edu/RGNet/>), Athamap (Steffens *et al.*, 2004)

Table 5.1. Sequences of primers used in this study.

Construct Name	Primers	Coordinates	Size (bp)
<i>CYCA2;1</i> (AT5G25380)			
[-1523,-20)::YFPnuc	5'-ggggacaagtttgatacaaaaaagcaggcttagtaaacactttgttagcc 5'-ggggaccactttgtacaagaaagctgggtcactccactgattcaacaag	[-1523,-20]	1504
[-1042,-20)::YFPnuc	5'-ggggacaagtttgatacaaaaaagcaggcttttggtgactatgttctc 5'-ggggaccactttgtacaagaaagctgggtcactccactgattcaacaag	[-1042,-20]	1023
[-525,-20)::YFPnuc	5'-ggggacaagtttgatacaaaaaagcaggctcgtctctcgtttgatcgtg 5'-ggggaccactttgtacaagaaagctgggtcactccactgattcaacaag	[-525,-20]	506
[-943,-20)::YFPnuc	5'-ggggacaagtttgatacaaaaaagcaggctgtccaatgggcttttaggttatg 5'-ggggaccactttgtacaagaaagctgggtcactccactgattcaacaag	[-943,-20]	924
[-866,-20)::YFPnuc	5'-ggggacaagtttgatacaaaaaagcaggctgaatagagcgcgtaacgg 5'-ggggaccactttgtacaagaaagctgggtcactccactgattcaacaag	[-866,-20]	847
[-847,-20)::YFPnuc	5'-ggggacaagtttgatacaaaaaagcaggcttgattagatctccaatt 5'-ggggaccactttgtacaagaaagctgggtcactccactgattcaacaag	[-847,-20]	828
[-781,-20)::YFPnuc	5'-ggggacaagtttgatacaaaaaagcaggctgtcagaaccactctgcacttac 5'-ggggaccactttgtacaagaaagctgggtcactccactgattcaacaag	[-781,-20]	762

[-717,-20)::YFPnuc	5'-ggggacaagtttgacaaaaagcaggctcaaagtcactttctcttttc 5'-ggggaccactttgtacaagaaagctgggtcactccactgattcaacaag	[-717,-20]	698
[-646,-20)::YFPnuc	5'-ggggacaagtttgacaaaaagcaggctacaaaatcccgcctcacgc 5'-ggggaccactttgtacaagaaagctgggtcactccactgattcaacaag	[-646,-20]	627
<i>CYCA2;4</i> (AT1G80370)			
[-1483,-1)::YFPnuc	5'-ggggacaagtttgacaaaaagcaggctactattcctctctctatcg 5'-ggggaccactttgtacaagaaagctgggtgattgaaaccctttgacac	[-1483,-1]	1483
[-1003,-1)::YFPnuc	5'-ggggacaagtttgacaaaaagcaggctaaagcgaattgactataacc 5'-ggggaccactttgtacaagaaagctgggtgattgaaaccctttgacac	[-1003,-1]	1003
[-565,-1)::YFPnuc	5'-ggggacaagtttgacaaaaagcaggctcagaagaaattgatctagtcg 5'-ggggaccactttgtacaagaaagctgggtgattgaaaccctttgacac	[-565,-1]	565
[-1905,-1)::YFPnuc	5'-ggggacaagtttgacaaaaagcaggctgaaacgggttcttaagtttctac 5'-ggggaccactttgtacaagaaagctgggtgattgaaaccctttgacac	[-1905,-1]	1905
[-1855,-1)::YFPnuc	5'-ggggacaagtttgacaaaaagcaggctgtgtagaatttatggatggattc 5'-ggggaccactttgtacaagaaagctgggtgattgaaaccctttgacac	[-1855,-1]	1855
[-1814,-1)::YFPnuc	5'-ggggacaagtttgacaaaaagcaggctgagtccaataagcattaagg 5'-ggggaccactttgtacaagaaagctgggtgattgaaaccctttgacac	[-1814,-1]	1814

[-1644,-1)::YFPnuc	5'-ggggacaagttgtacaaaaagcaggcttggaggaaatctttcttcaaac 5'-ggggaccactttgtacaagaaagctgggtgattgaaaccctttgacac	[-1644,-1]	1644
[-1568,-1)::YFPnuc	5'-ggggacaagttgtacaaaaagcaggcttgaatagccacgctgttactg 5'-ggggaccactttgtacaagaaagctgggtgattgaaaccctttgacac	[-1568,-1]	1568

Table 5.2. Origin and nature of lines.

Line	Origin	Nature
ATHB8::HTA6:EYFP	Sawchuk <i>et al.</i> , 2007	Transcriptional fusion of <i>ATHB8</i> (AT4G32880; -1997 to -1) with a translational fusion between <i>HISTONE 2A (HTA6)</i> and enhanced yellow fluorescent protein (EYFP) (Zhang <i>et al.</i> , 2005)
CYCA2;1::HTA6:EYFP	Vanneste <i>et al.</i> , 2011 (Chapter 4)	Transcriptional fusion of <i>CYCA2;1</i> (AT5G25380; -1828 to -20) to HTA6:EYFP (Zhang <i>et al.</i> , 2005)
CYCA2;4::HTA6:EYFP	Vanneste <i>et al.</i> , 2011 (Chapter 4)	Transcriptional fusion of <i>CYCA2;4</i> (AT1G80370; -1963 to -1) to HTA6:EYFP (Zhang <i>et al.</i> , 2005)
ATHB8::ECFP-Nuc	Sawchuk <i>et al.</i> , 2007	Transcriptional fusion of <i>ATHB8</i> (AT4G32880; -1997 to -1) driving a nuclear-localized enhanced cyan fluorescent protein (ECFP-Nuc) (Kubo <i>et al.</i> , 2005)
UBQ10::GFP:LTI6B	Sawchuk <i>et al.</i> , 2008	Transcriptional fusion of <i>UBIQUITIN10 (UBQ10)</i> (AT4G05320; -1516 to -1) with a translational fusion between enhanced green fluorescent protein (EGFP) and <i>LOW TEMPERATURE INDUCED6B (LTI6B)</i> (Cutler <i>et al.</i> , 2000)

(<http://www.athamap.de/>), Athena (O'Connor *et al.*, 2005) (<http://www.bioinformatics2.wsu.edu/cgi-bin/Athena/cgi/home.pl>), PLACE (Higo *et al.*, 1999) (<http://www.dna.affrc.go.jp/PLACE/>), Plant CARE (Lescot *et al.*, 2002) (<http://bioinformatics.psb.ugent.be/webtools/plantcare/html/>), and rVISTA 2.0 (Loots and Ovcharenko, 2004) (<http://rvista.dcode.org>) using the TRANSFAC professional V10.2 library for plants and 0.75.similarity matrix.

5.3 RESULTS AND DISCUSSION

5.3.1 Early vein expression of *CYCA2;1* and *CYCA2;4* in *Arabidopsis* leaves

The *CYCA2;1* and *CYCA2;4* genes of *Arabidopsis thaliana* are expressed in veins (Bursens *et al.*, 2000; Imai *et al.*, 2006; Vanneste *et al.*, 2011; Chapter 4), but their expression dynamics are unknown. We thus imaged expression of the *CYCA2;1::HTA6:EYFP* and *CYCA2;4::HTA6:EYFP* transcriptional fusions (*CYCA2;1* or *CYCA2;4* promoter driving expression of a nuclear yellow fluorescent protein) (Vanneste *et al.*, 2011; Chapter 4) during first leaf development, and compared it with that of the preprocambial reference gene expression marker *ATHB8::HTA6:EYFP* (Donner *et al.*, 2009; Sawchuk *et al.*, 2007; Chapter 2). The illustration in Fig. 5.1A defines vein-specific terminology to which we refer throughout this study.

In agreement with published observations (Donner *et al.*, 2009; Gardiner *et al.*, 2010; Gardiner *et al.*, 2011; Chapters 2 and 3), *ATHB8::HTA6:EYFP* was expressed in the midvein of the 1- and 2.5-days after germination (DAG) leaf primordium (Fig. 5.1B,C). *ATHB8::HTA6:EYFP* was additionally expressed in the first pair of vein loops at 3 DAG (Fig. 5.1D), in the second pair of vein loops and higher-order veins at 4 DAG (Fig. 5.1E), and in the third pair of vein loops at 5 DAG (Fig. 5.1F).

CYCA2;1::HTA6:EYFP was not expressed in subepidermal tissues of the 1-DAG leaf primordium (Fig. 5.1G) but was expressed in the lowermost domain of the midvein at 2 DAG (Fig. 5.1H). By 3 DAG, *CYCA2;1::HTA6:EYFP* expression had extended to the entire midvein, and *CYCA2;1::HTA6:EYFP* was additionally expressed in at least the lowermost domains of the first loops (Fig.

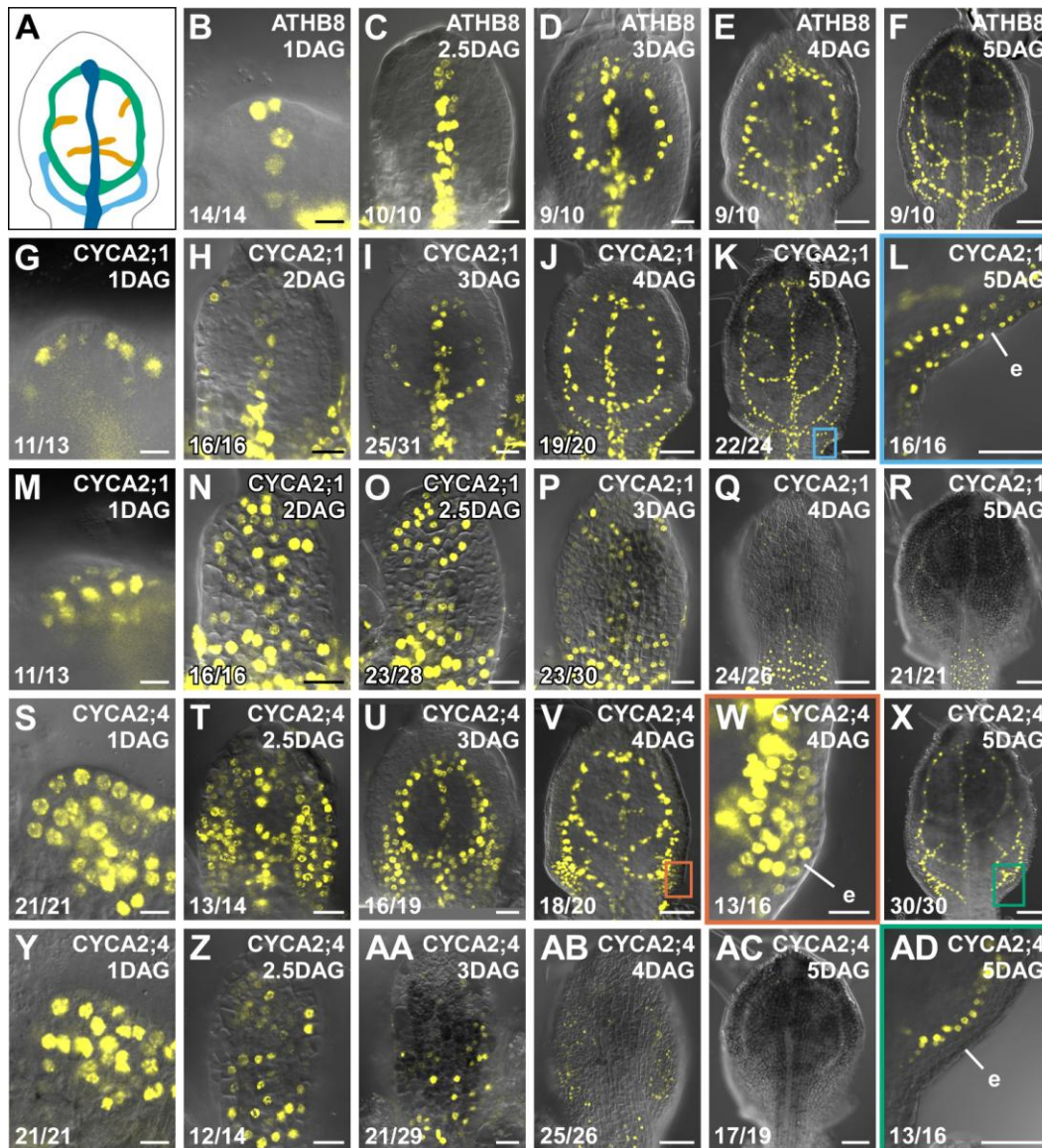


Figure 5.1. Expression of *CYCA2;1* and *CYCA2;4* in *Arabidopsis* leaf development. (A) Schematic of the vein pattern of the *Arabidopsis* first leaf 4 days after germination (DAG). Dark blue, midvein; green, first loops; light blue, second loops; orange, higher order veins. (B-AD) Overlay of confocal-laser-scanning and differential-interference-contrast microscopy images. First leaves. Yellow, HTA6:EYFP. Top right, genes and age in DAG; bottom left, fraction of samples showing the displayed features. (B,G,M,S,Y) Lateral view, abaxial (*i.e.*, ventral) side to the left. (C-F,H-L,N-R,T-X,Z-AD) Abaxial view. (B-L,S-X,AD) Subepidermal focal plane. (M-R,Y-AC) Epidermal focal plane. (L,W,AD) Details of regions boxed in K, V, and X, respectively. e, epidermis. Scale bars = 10 μ m (B,G,M,S,Y), 20 μ m (C,D,H,I,N-P,T,U,W,Z,AA), 50 μ m (E,J,L,Q,V,AB,AD), 75 μ m (F,K,R,X,AC).

5.1I). By 4 DAG, CYCA2;1::HTA6:EYFP expression had extended to the entire first loops (Fig. 5.1J). At this stage, CYCA2;1::HTA6:EYFP was additionally expressed in at least the lowermost domains of the second loops and in higher-order veins developing in the upper areas of the leaf (Fig. 5.1J). By 5 DAG, CYCA2;1::HTA6:EYFP expression had extended to the entire second and third loops and to higher-order veins developing in the lower areas of the leaf (Fig. 5.1K).

CYCA2;4::HTA6:EYFP was expressed near-ubiquitously in the 1-DAG leaf primordium (Fig. 5.1S). By 2.5 DAG, CYCA2;4::HTA6:EYFP expression had become restricted to the midvein and two broad, lateral domains (Fig. 5.1T). By 3 DAG, these broad domains of CYCA2;4::HTA6:EYFP expression had become restricted to the first loops in the upper areas of the leaf primordium but had remained broad in the lower areas of the leaf primordium (Fig. 5.1U). By 4 DAG, broad domains of CYCA2;4::HTA6:EYFP expression had become restricted to the second loops but had remained broad in the lowermost areas of the leaf (Fig. 5.1V,W). At this stage, CYCA2;4::HTA6:EYFP was additionally expressed in higher-order veins developing in the upper areas of the leaf, while expression in the midvein had started to decline (Fig. 5.1V). By 5 DAG, residual broad domains of CYCA2; 4::HTA6:EYFP expression had become restricted to the third loops (Fig. 5.1X,AD). At this stage, CYCA2;4::HTA6:EYFP was additionally expressed in higher-order veins developing in the lower areas of the leaf, while expression in the first loops had started to decline (Fig. 5.1X).

In addition to their expression in subepidermal cells, CYCA2;1::HTA6:EYFP and CYCA2;4::HTA6:EYFP were expressed in the epidermis. CYCA2;1::HTA6:EYFP was expressed in nearly all epidermal cells of the 1-DAG leaf primordium, though expression was weaker at the tip (Fig. 5.1G,M), but by 2 DAG CYCA2;1::HTA6:EYFP epidermal expression had become restricted to an hourglass-shaped domain (Fig. 5.1N). By 3 DAG, CYCA2;1::HTA6:EYFP epidermal expression had started to decline from the upper areas of the leaf primordium (Fig. 5.1I,O,P) and had become terminated in those areas of the leaf by 4 DAG (Fig. 5.1J,Q). CYCA2;1::HTA6:EYFP

epidermal expression persisted in the lower areas of the leaf until at least 5 DAG (Fig. 5.1K,L,R).

CYCA2;4::HTA6:EYFP was expressed near-ubiquitously in the epidermis of the 1-DAG leaf primordium (Fig. 5.1S,Y). By 2.5 DAG, CYCA2;4::HTA6:EYFP epidermal expression had started to decline from the upper areas of the leaf primordium (Fig. 5.1T,Z) and had become terminated in the upper half of the leaf primordium by 3 DAG (Fig. 5.1U,AA). By 4 DAG, CYCA2;4::HTA6:EYFP was only expressed in the epidermis of the lowermost and lateral areas of the leaf (Fig. 5.1V,W,AB), and by 5 DAG CYCA2;4::HTA6:EYFP epidermal expression had become terminated (Fig. 5.1X,AC,AD). In summary, as ATHB8::HTA6:EYFP, both CYCA2;1::HTA6:EYFP and CYCA2;4::HTA6:EYFP were expressed at early stages of vein development. Expression of CYCA2;1::HTA6:EYFP was initiated later than that of ATHB8::HTA6:EYFP, but expression domains of CYCA2;1::HTA6:EYFP were as narrow as those of ATHB8::HTA6:EYFP from early on. Expression domains of CYCA2;4::HTA6:EYFP were broad early on and only at later stages did they become restricted to narrow sites of vein formation. Finally, unlike ATHB8::HTA6:EYFP, both CYCA2;1::HTA6:EYFP and CYCA2;4::HTA6:EYFP were additionally expressed in the epidermis.

It is possible that expression of *CYCA2;1* and *CYCA2;4* is controlled by regions beyond the upstream non-coding sequences used here to monitor their expression. However, our data are consistent with patterns of transcript accumulation (Burssens *et al.*, 2000; de Almeida Engler *et al.*, 2009) or of activity of longer upstream non-coding regions (Imai *et al.*, 2006; Vanneste *et al.*, 2011; Chapter 4), suggesting that expression of our transcriptional fusions reports relevant features of the expression of *CYCA2;1* and *CYCA2;4*.

While expression of *CYCA2;1* defines a new type of early vein expression profile, expression dynamics of *CYCA2;4* closely resemble those of the PIN1 auxin transporter (Scarpella *et al.*, 2006; Wenzel *et al.*, 2007), whose function is required for vein patterning (Bilsborough *et al.*, 2011; Mattsson *et al.*, 1999; Okada *et al.*, 1991); this similarity may reflect the high mitotic activity of the cells

involved in the vein patterning process (Donnelly *et al.*, 1999; Kang and Dengler, 2002).

5.3.2 Expression of *CYCA2;1* and *CYCA2;4* at preprocambial stages of vein development

The seeming overlap in expression of *CYCA2;1::HTA6:EYFP*, *CYCA2;4::HTA6:EYFP*, and *ATHB8::HTA6:EYFP* in leaf development (Fig. 5.1) suggests that, as *ATHB8*, *CYCA2;1* and *CYCA2;4* are expressed at preprocambial stages of vein development. Cells at preprocambial stages are defined by (1) *ATHB8* expression and (2) isodiametric shape (Kang and Dengler, 2004; Scarpella *et al.*, 2004).

As previously shown (Vanneste *et al.*, 2011; Chapter 4), all the cells in the second loops of 4-DAG leaves that express *CYCA2;1::HTA6:EYFP* or *CYCA2;4::HTA6:EYFP* also express *ATHB8::ECFP-Nuc* (Fig. 5.2C,D). However, not all the cells expressing *ATHB8::ECFP-Nuc* express *CYCA2;1::HTA6:EYFP*: expression domains of *ATHB8::ECFP-Nuc* are longer than those of *CYCA2;1::HTA6:EYFP* (Fig. 5.2C). Further, not all the cells expressing *CYCA2;4::HTA6:EYFP* express *ATHB8::ECFP-Nuc*: expression domains of *CYCA2;4::HTA6:EYFP* are broader than those of *ATHB8::ECFP-Nuc* (Fig. 5.2D).

To test whether *CYCA2;1* and *CYCA2;4* are expressed in isodiametric cells, we imaged expression of *CYCA2;1::HTA6:EYFP* or *CYCA2;4::HTA6:EYFP* in the second loops of 4-DAG leaves ubiquitously expressing a plasma-membrane-localized green fluorescent protein (*UBQ10::EGFP:LTI6B*) (Sawchuk *et al.*, 2008). As *ATHB8::HTA6:EYFP* (Fig. 5.2E), both *CYCA2;1::HTA6:EYFP* and *CYCA2;4::HTA6:EYFP* were expressed in isodiametric subepidermal cells (Fig. 5.2F,G). In conclusion, expression of *CYCA2;1::HTA6:EYFP* and *CYCA2;4::HTA6:EYFP* in isodiametric cells expressing *ATHB8::ECFP-Nuc* suggests that both *CYCA2;1* and *CYCA2;4* are expressed at preprocambial stages of vein development.

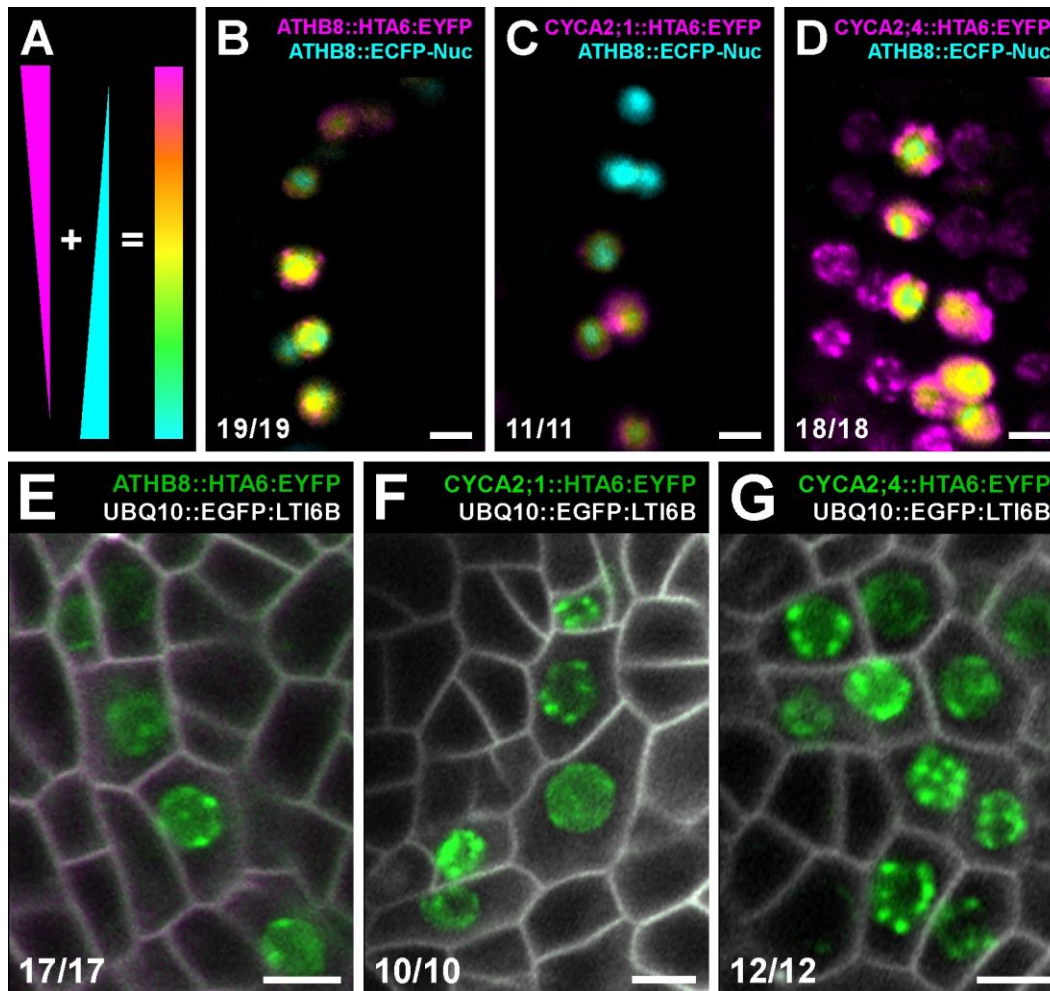


Figure 5.2. Stage-specific expression of *CYCA2;1* and *CYCA2;4* in vein development. (A–D) As illustrated in A, images in B–D are color-coded with a dual-channel look-up-table from cyan to magenta through green, yellow and red (Demandolx and Davoust, 1997): fluorescence in each detection channel was displayed in either cyan (*ATHB8::ECFP-Nuc*) or magenta (*ATHB8::HTA6:EYFP*, *CYCA2;1::HTA6:EYFP*, or *CYCA2;4::HTA6:EYFP*), and single-fluorophore images were merged using a differential operator. Preponderance of cyan signal over colocalized magenta signal is encoded in green, opposite in red, and colocalized cyan and magenta signals of equal intensity in yellow. (B–G) Confocal-laser-scanning microscopy images. Details of second loops of 4-DAG first leaves, abaxial view, subepidermal focal plane. Top right, markers; bottom left, fraction of samples showing the displayed features. Scale bars = 5 μm .

5.3.3 *Cis*-regulation of *CYCA2;1* preprocambial expression

We next asked what regulatory elements are required for preprocambial expression of *CYCA2;1*. To address this question, we generated three consecutive ~500-bp 5'-end deletions of the *CYCA2;1* promoter (Fig. 5.3A) and tested their ability to drive HTA6:EYFP expression in the second loops of 4-DAG leaves as cells in these veins are at preprocambial stages of development (Donner *et al.*, 2009; Gardiner *et al.*, 2010; Gardiner *et al.*, 2011) (Fig. 5.2). We designed all deletions so as to avoid interrupting putative transcription-factor binding sites as identified by searchable databases (see Section 5.2.4).

The *CYCA2;1* promoter fragment from -1042 to -20 relative to the start codon, [-1042,-20] hereafter, was the shortest fragment that drove expression in the second loops of 4-DAG leaves as the [-525,-20] fragment was unable to drive leaf expression at this developmental stage (Fig. 5.3B-E). These data suggest that the 517-bp region of the *CYCA2;1* promoter between -1042 and -525 is required for preprocambial expression. Thus, we generated six consecutive ~70-bp 5'-end deletions of this 517-bp region of the *CYCA2;1* promoter (Fig. 5.3A) and tested their ability to drive HTA6:EYFP expression in the second loops of 4-DAG leaves.

The [-943,-20] fragment of the *CYCA2;1* promoter was the shortest fragment that drove expression in the second loops of 4-DAG leaves as the [-866,-20] fragment drove expression only in the midvein and first loops at this developmental stage (Fig. 5.3F,H,J-M). The [-943,-20] fragment of the *CYCA2;1* promoter was also the shortest fragment that drove epidermal expression in 4-DAG leaves as the [-866,-20] fragment was unable to drive epidermal expression at this developmental stage (Fig. 5.3G,I). We conclude that the 77-bp regulatory element between -943 and -866 of the *CYCA2;1* promoter is required for both epidermal expression of *CYCA2;1* and expression of *CYCA2;1* at preprocambial stages of vein development.

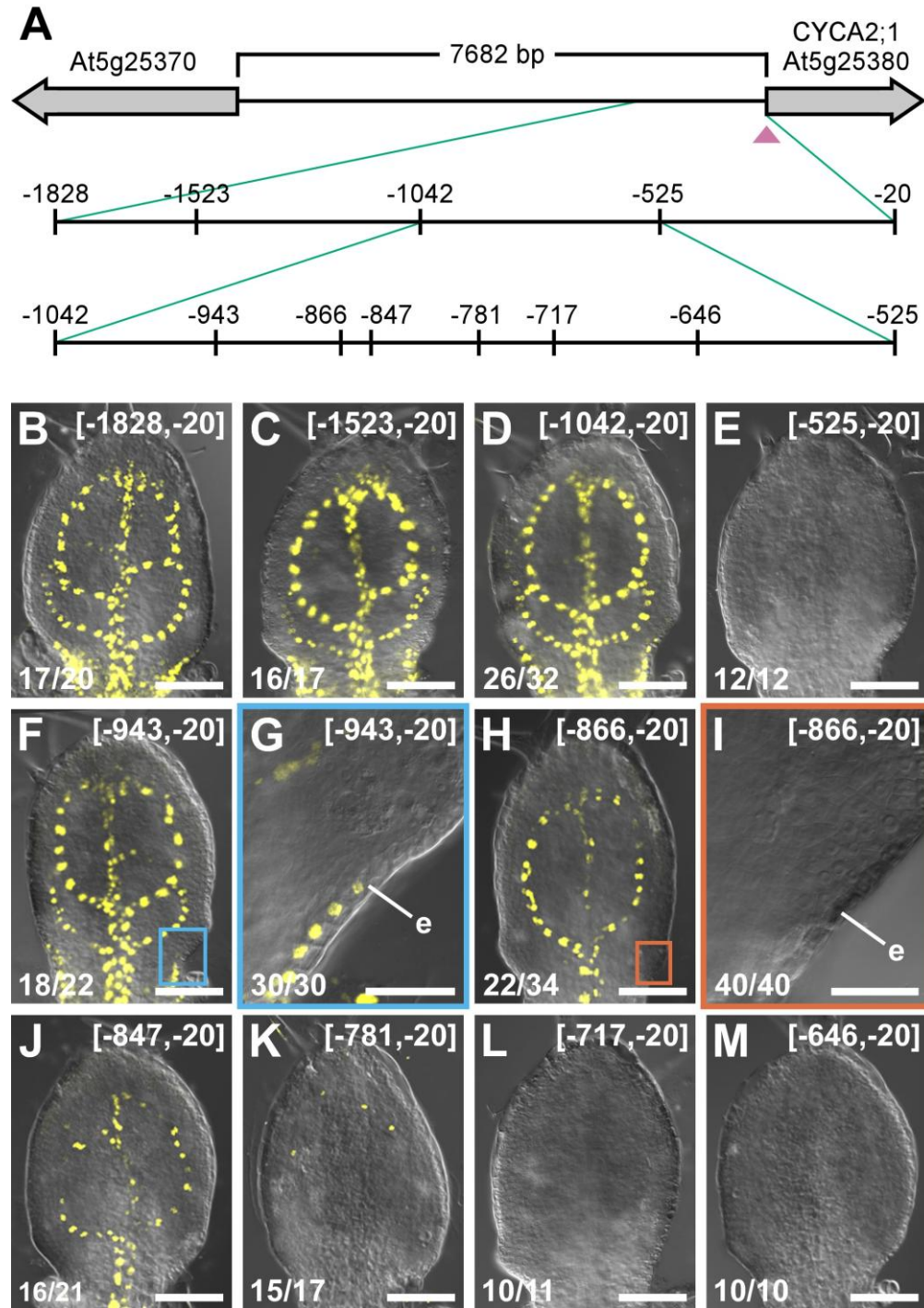


Figure 5.3. Deletion analysis of the *CYCA2;1* promoter. (A) Line diagram of the *CYCA2;1* promoter fragments used in this study. Grey arrows, genes; magenta triangle, predicted transcription-start site based on longest cDNA sequence available (NCBI Accession No.: NM_122447); numbers indicate position relative to the start codon (+1). (B–M) Overlay of confocal-laser-scanning and differential-interference-contrast microscopy images. First leaves 4 DAG, abaxial view, subepidermal focal plane. Yellow, HTA6:EYFP. Top right, promoter coordinates; bottom left, fraction of samples showing the displayed features. (G,I) Details of region boxed in F and H, respectively. e, epidermis. Scale bars = 50 μ m (B-F,H,J-M), 25 μ m (G,I).

5.3.4 *Cis*-regulation of *CYCA2;4* preprocambial expression

To identify regulatory elements required for preprocambial expression of *CYCA2;4*, we generated three consecutive ~500-bp 5'-end deletions of the *CYCA2;4* promoter (Fig. 5.4A) and tested their ability to drive HTA6:YFP expression in the second loops of 4-DAG leaves.

The [-1963,-1] fragment of the *CYCA2;4* promoter was the only fragment that drove expression in the second loops of 4-DAG leaves as the [-1483,-1] fragment only drove erratic expression at this developmental stage (Fig. 5.4B-E). These data suggest that the 480-bp region of the *CYCA2;4* promoter between -1963 and -1483 is required for preprocambial expression. Thus, we generated six consecutive ~80-bp 5'-end deletions of this 480-bp promoter region of the *CYCA2;4* promoter (Fig. 5.4A) and tested their ability to drive HTA6:YFP expression in the second loops of 4-DAG leaves.

The [-1644,-1] fragment of the *CYCA2;4* promoter was the shortest fragment that drove expression in the second loops of 4-DAG leaves as the [-1568,-1] fragment drove expression only in the midvein and first loops (Fig. 5.4I-K). Furthermore, the [-1644,-1] fragment of the *CYCA2;4* promoter was the shortest fragment that drove epidermal expression as the [-1568,-1] fragment was unable to drive epidermal expression at this developmental stage (Fig. 5.4I-K). We conclude that the 76-bp regulatory element between -1644 and -1568 of the *CYCA2;4* promoter is required for both epidermal expression of *CYCA2;4* and expression of *CYCA2;4* at preprocambial stages of vein development.

5.3.5 Conserved regulatory motifs in preprocambial elements of *CYCA2;1* and *CYCA2;4*

To identify evolutionarily conserved transcription-factor binding sites in the 77- and 76-bp regulatory elements of the *CYCA2;1* and *CYCA2;4* promoters that are required for preprocambial expression of the respective genes in *Arabidopsis thaliana*, we compared the sequences of these two elements with the sequences of the corresponding promoter regions in *Arabidopsis lyrata*, *Capsella rubella*, and

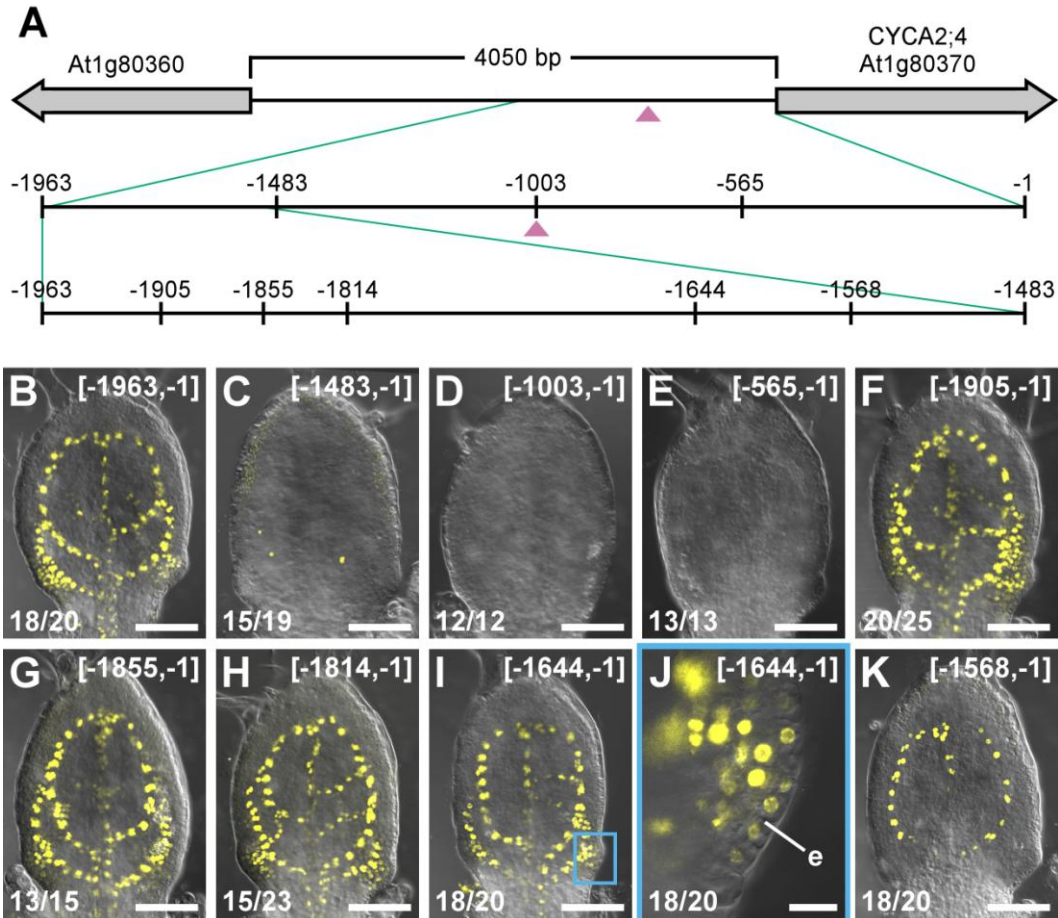


Figure 5.4. Deletion analysis of the *CYCA2;4* promoter. (A) Line diagram of the *CYCA2;4* promoter fragments used in this study. Grey arrows, genes; magenta triangle, predicted transcription-start site based on longest cDNA sequence available (NCBI Accession No.: NM_106686); numbers indicate position relative to the start codon (+1). (B-K) Overlay of confocal-laser-scanning and differential-interference-contrast microscopy images. First leaves 4 DAG, abaxial view, subepidermal focal plane. Yellow, HTA6:EYFP. Top right, promoter coordinates; bottom left, fraction of samples showing the displayed features. (J) Detail of region boxed in I. e, epidermis. Scale bars = 50 μ m (B-I,K), 25 μ m (J).

Thellungiella halophila: all the true-diploid species of the *Brassicaceae* family for which whole-genome sequence is available.

The *CYCA2;1* regulatory element contains a conserved, putative binding site for transcription factors of the DNA-BINDING WITH ONE ZINC FINGER (DOF) family (Yanagisawa, 2002) (Fig. 5.5A). The *CYCA2;4* regulatory element contains conserved, putative binding sites for three types of transcription factors: ARABIDOPSIS RESPONSE REGULATOR (ARR) (Muller and Sheen, 2007), DOF, and SILENCER-BINDING FACTOR-1 (SBF-1) (Lawton *et al.*, 1991) (Fig. 5.5B).

Expression data at tissue resolution are available for 13 of the 36 *Arabidopsis* DOF genes (Fornara *et al.*, 2009; Gardiner *et al.*, 2010; Gardner *et al.*, 2009; Imaizumi *et al.*, 2005; Konishi and Yanagisawa, 2007; Skirycz *et al.*, 2006; Skirycz *et al.*, 2007; Skirycz *et al.*, 2008; Ward *et al.*, 2005). Expression of all these 13 DOF genes overlaps with expression of *CYCA2;1* and *CYCA2;4*, and overexpression of OBP1, one such DOF genes, is sufficient to upregulate *CYCA2;1* expression (Skirycz *et al.*, 2008). Further, expression of at least six of the 11 *Arabidopsis* ARR transcription-factor genes overlaps with expression of *CYCA2;4* (Tajima *et al.*, 2004; Yokoyama *et al.*, 2007), and three of such ARR genes redundantly control root vascular development (Ishida *et al.*, 2008; Yokoyama *et al.*, 2007). Thus, it is possible that DOF and ARR transcription factors regulate preprocambial expression of *CYCA2;1* and *CYCA2;4*.

SBF-1 is a transcription factor closely related, or identical, to GT-1 (Lawton *et al.*, 1991). SBF-1 binds to the promoter of the bean *CHALCONE SYNTHASE15* (*CHS15*) gene and regulates light responsiveness of *CHS15* expression (Lawton *et al.*, 1991). High light intensity downregulates *CYCA2;4* expression (Blasing *et al.*, 2005; Covington and Harmer, 2007; Edwards *et al.*, 2006; Smith *et al.*, 2004), and it is possible that light responsiveness of *CYCA2;4* expression is mediated by GT-1-like transcription factors; however, no evidence is currently available that supports a role for GT-1 or related proteins in regulation

A

A. thaliana G|CC---AATGGGCTTTT-AGGTT-...-AT-GAAACGGTT-...-TAATC-...-AATGGGGCAC-...-TCAAA-...-TAGTA-...-AAGTAA-...-GGAA-...-CAG-...-ATGCCATA
A. lyrata TTTC---ATCAGGCTTTT-AGGTT-...-AT-GAAACGGTT-...-TAAGC-...-A-TGGGGCAC-...-TGAA-...-TAGTG-...-TAAGGA-...-GGAA-...-CAG-...-ATGCAATA
C. rubella TTGG---AATGGGCTTTTAAAGTT-...-ATTGAAACGGTT-...-TAATAT...AAATAGAGCAT-...-GTAACG...TTAGTAG...AAAGCAA-...-AGAAG...CAG-...-ACGTCAAA
T. halophila ATCCATTAATCGACTTTT-AGGCTC...GAT-AAAACAGTTG...TTGATCA...CTATGATGCACA...ATCAAA-...-ATGTA-...-AAGGAAT...TGAAA-...-CAGT...TATGCCTAC

DOF

CTTT

B

A. thaliana TGGTGGAATCTTTC---TTCAAATCTTCAAAATTTGAACAGAG-...-TTTTTGTA-...-ATTTAATCATTTTTATTTACCTTTGG--A
A. lyrata TGGTGGAATCTTTC---TTCAGATCTTCAAAATTTGAACAGAG-...-TTATGTA-...-GTTTAATCACTTTTATTTACCTTTGG--A
C. rubella TGGTGGAATCTTTCGTC---TTCAAATCTTAAAAATTTGAACAGAG...CCTTTTGTAT...AGTTAATCTTTTTTTTTTTTTTTTGTGCGA
T. halophila TGGTGGAATCTTTC---TTCAAACCTATAAAAATTTGAACAGAG-...-TT-TGCA-...-ATTTAATCAAATTTTATTCAACTTAA--A

ARR

AATCT

DOF

CTTT

SBF-1

TTAATC

Figure 5.5. Preprocambial regulatory elements of *CYCA2;1* and *CYCA2;4* in *Brassicaceae* species. (A,B) Sequence alignment of the 77- and 76-bp regulatory elements in the promoters of *CYCA2;1* (A) and *CYCA2;4* (B) that are required for preprocambial expression of the respective genes in *A. thaliana* (*CYCA2;1*: chromosome 5, position 8,814,287–8,814,363; *CYCA2;4*: chromosome 1, position 30,213,050–30,213,125) with corresponding regions in *A. lyrata* (*CYCA2;1*: scaffold 6, position 11,368,916–11,368,840; *CYCA2;4*: scaffold 2, position 19,070,399–19,070,326), *C. rubella* (*CYCA2;1*: scaffold 6, position 8,836,382–8,836,495; *CYCA2;4*: scaffold 2, position 13,910,768–13,910,641) and *T. halophila* (*CYCA2;1*: scaffold 2, position 3,660,221–3,661,993; *CYCA2;4*: scaffold 9, position 231,847–231,919). Orange highlight, sequence identity. Conserved, putative transcription-factor binding sites are below sequence alignment.

of tissue- or stage-specific expression. Moreover, mutation of a putative GT-1-binding site in the *ATHB8* promoter, which is active at preprocambial stages of vein development, has no effect on *ATHB8* expression (Donner *et al.*, 2009; Chapter 2).

It is of course possible that preprocambial expression of *CYCA2;1* and *CYCA2;4* depends on unknown motifs overlapping the 3' ends of the 77- and 76-bp regulatory elements or located in the evolutionarily conserved promoter regions where no known transcription-factor binding sites were identified. It is also possible that the regulatory motifs controlling preprocambial expression of *CYCA2;1* and *CYCA2;4* are highly degenerate or that the sequence of such regulatory motifs is conserved while the surrounding promoter context is not, as it occurs in some gene regulatory networks of plants and animals (Dowell, 2010; Moyroud *et al.*, 2011; Wilson and Odom, 2009). Finally, as shown for some animal genes (Carroll, 2005; Wray, 2007), it is possible that expression of *CYCA2;1* and *CYCA2;4* is not evolutionarily conserved, and thus preprocambial motifs may reside in non-conserved promoter regions. While it will be interesting to identify the transcription factors that bind to the preprocambial elements of *CYCA2;1* and *CYCA2;4*, our results already assist in defining the *cis*-regulatory inputs that specify early vein expression.

5.3.6 Transcriptional regulation of preprocambial expression

Preprocambial expression of *ATHB8* depends on a TGTCTG ARF-binding site (Donner *et al.*, 2009; Chapter 2). No core sequences of ARF-binding sites (TGTC) (Ulmasov *et al.*, 1997a) exist in the preprocambial elements of *CYCA2;1* and *CYCA2;4*, suggesting that preprocambial expression can be encoded in regulatory elements of different structures (Fig. 5.6). The different preprocambial elements may specify differences in expression of *ATHB8*, *CYCA2;1*, and *CYCA2;4*, such as the additional epidermal expression of *CYCA2;1* and *CYCA2;4*, the broad-to-narrow dynamic of *CYCA2;4* subepidermal expression, and the later initiation of *CYCA2;1* subepidermal expression. However, a similar diversity in structure of regulatory elements controlling co-expression has also been observed in gene regulatory networks of animals (*e.g.*, Brown *et al.*, 2007; Ramialison *et*

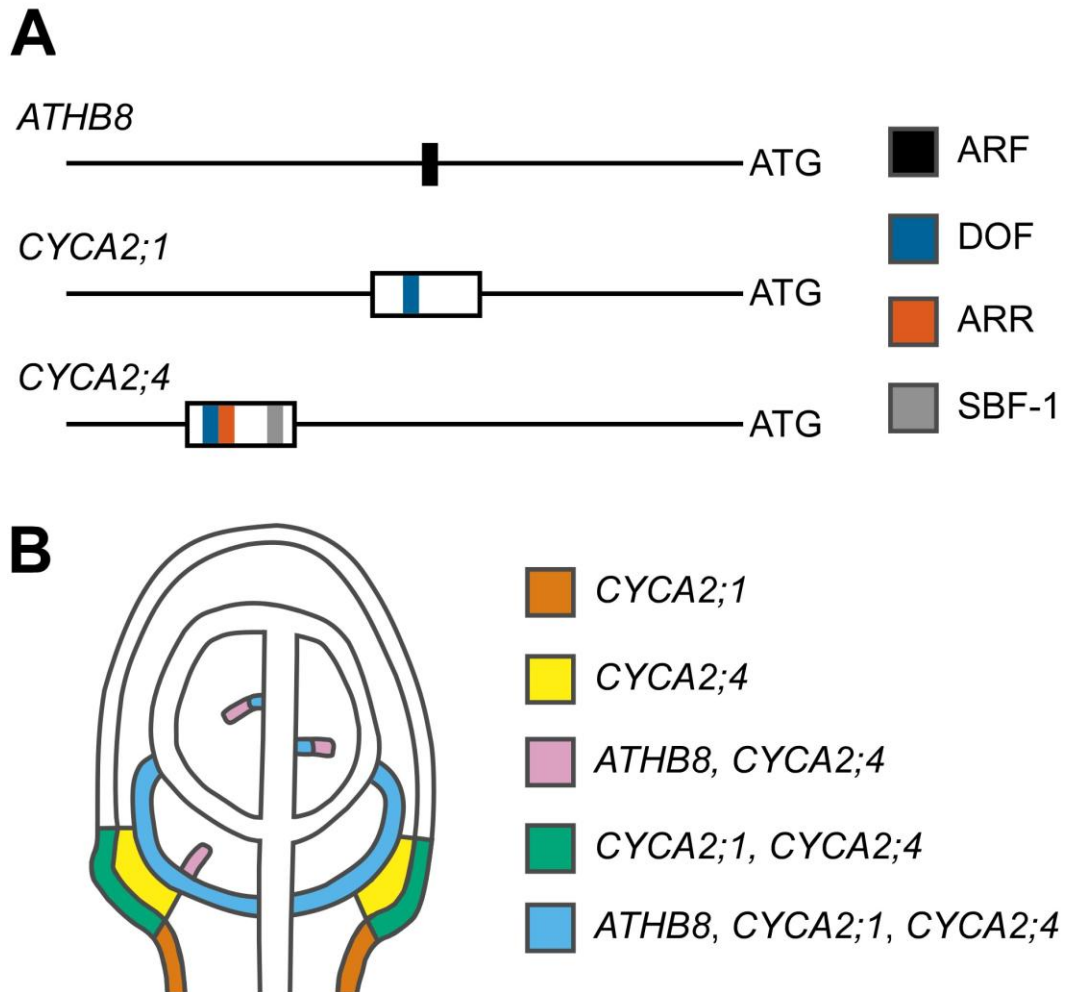


Figure 5.6. Transcriptional regulation of precambial expression. (A) Line diagrams of the promoters of *ATHB8*, *CYCA2;1*, and *CYCA2;4*. Boxes and vertical lines indicate precambial regulatory elements and transcription-factor binding sites, respectively. (B) Schematic of a 4-DAG first leaf illustrating the expression domains of *ATHB8*, *CYCA2;1*, and *CYCA2;4* that are specified by the regulatory elements in (A).

al., 2012; Zinzen *et al.*, 2009) and may represent an inherent property of the *cis*-regulatory code, a property that defies the expectation that common design underlies co-regulation.

CHAPTER 6: CONCLUSIONS AND PERSPECTIVES

Plant vascular tissues transport signals that coordinate the development of new roots with that of new shoot organs and that direct the development of the non-vascular cells that surround vascular strands (Berleth and Sachs, 2001). Therefore, understanding the mechanisms controlling vascular strand formation could provide an entry point to understand how the formation of plant organs and tissue patterns is coordinated and integrated. In this context, leaves are a convenient system as vascular networks are formed *de novo* during leaf development and vascular strand formation is reiterated throughout leaf development (Nelson and Dengler, 1997).

Isodiametric, polygonal cells that will elongate into procambial cells, the precursors of all mature vascular cell types (Esau 1943; Esau, 1965; Foster, 1952), switch on expression of ‘preprocambial’ genes such as *ARABIDOPSIS THALIANA HOMEBOX8 (ATHB8)* (Kang and Dengler, 2004; Scarpella *et al.*, 2004), and the correlation between domains of preprocambial gene expression and sites of vascular strand formation persists upon experimental manipulation (Alonso-Peral *et al.*, 2006; Carland and Nelson, 2004; Cnops *et al.*, 2006; Gardiner *et al.*, 2010; Gardiner *et al.*, 2011; Hou *et al.*, 2010; Koizumi *et al.*, 2000; Petricka and Nelson, 2007; Pineau *et al.*, 2005; Pullen *et al.*, 2010; Robles *et al.*, 2010; Scarpella *et al.*, 2006; Chapter 3). Therefore, the events that control formation of leaf vascular strands likely occur before onset of expression of preprocambial genes, and the factors that regulate preprocambial gene expression may also control formation of leaf vascular strands. If this were the case, the identification of regulatory elements required for preprocambial gene expression and of the transcription factors that bind to these elements could inform on the gene regulatory networks that control formation of leaf vascular strands.

Our results suggest that different regulatory elements and transcription factors are required for preprocambial gene expression, and are consistent with auxin being a ‘master regulator’ of gene expression at early stages of leaf vascular development.

6.1 REGULATORY ELEMENTS REQUIRED FOR GENE EXPRESSION AT EARLY STAGES OF LEAF VASCULAR DEVELOPMENT

Expression of *SHORT-ROOT (SHR)*, *CYCLIN A2;1 (CYCA2;1)*, and *CYCLIN A2;4 (CYCA2;4)* is initiated at preprocambial stages of leaf vascular development (Gardiner *et al.*, 2011; Kang and Dengler, 2004; Scarpella *et al.*, 2004; Vanneste *et al.*, 2011; Chapters 3 and 4). Furthermore, different regulatory elements seem to be required for preprocambial expression of *ATHB8*, *CYCA2;1*, and *CYCA2;4*: a TGTCTG Auxin Response Element (ARE) is required for *ATHB8* preprocambial expression (Donner *et al.*, 2009; Chapter 2); a 76-bp region containing a putative binding site for transcription factors of the DNA-BINDING WITH ONE ZINC FINGER (DOF) family is required for *CYCA2;1* preprocambial expression (Donner and Scarpella, 2013; Chapter 5); and a 77-bp region containing putative binding sites for transcription factors of the DOF, ARABIDOPSIS RESPONSE REGULATOR (ARR), and SILENCER-BINDING FACTOR-1 (SBF-1) families is required for *CYCA2;4* preprocambial expression (Donner and Scarpella, 2013; Chapter 5).

The same regulatory elements are often assumed to control the transcription of co-expressed genes (Niehrs and Pollet, 1999); however, different regulatory elements seem to be required for the preprocambial expression of *ATHB8*, *CYCA2;1*, and *CYCA2;4*. This discrepancy could reflect spatial or temporal differences in the expression of these genes. For example, *CYCA2;1* expression is initiated at preprocambial stages of leaf vascular development, but *CYCA2;1* is additionally expressed in the leaf epidermis (Donner and Scarpella, 2013; Vanneste *et al.*, 2011; Chapters 4 and 5); and the same regulatory region that is required for preprocambial expression of *CYCA2;1* is also required for epidermal expression of *CYCA2;1* (Donner and Scarpella, 2013; Chapter 5). On the other hand, *ATHB8* expression is restricted to developing vascular strands (Donner *et al.*, 2009; Kang and Dengler, 2004; Scarpella *et al.*, 2004; Chapter 2), and the regulatory element that is required for *ATHB8* preprocambial expression is not required for any other aspect of *ATHB8* expression (Donner *et al.*, 2009; Chapter 2). Furthermore, preprocambial expression of *CYCA2;1* is initiated later

than preprocambial expression of *ATHB8* (Donner and Scarpella, 2013; Chapter 5).

Therefore, it is possible that the different regulatory elements we have identified in the promoters of *ATHB8*, *CYCA2;1*, and *CYCA2;4* are required for different spatial or temporal aspects of the expression of these genes. However, it seems difficult to reconcile this hypothesis with the finding that expression of *ATHB8* and *SHR* is initiated in the same cells at the same time and yet the *SHR* promoter lacks the TGTCTG Auxin Response Element (ARE) that is required for preprocambial expression of *ATHB8* (Donner *et al.*, 2009; Gardiner *et al.*, 2011; Chapters 2 and 3). This finding would thus seem to suggest that different regulatory elements indeed control preprocambial gene expression, a redundancy in the regulatory code that has also been observed in animals (*e.g.*, Brown *et al.*, 2007; Ramialison *et al.*, 2008; Ramialison *et al.*, 2012; Zinzen *et al.*, 2009). On the other hand, this redundancy in the regulatory code could simply be apparent and reflect the co-existence of distinct regulatory pathways, each controlling a distinct cellular function. For example, as vascular cells develop, they acquire both an elongated shape and the ability to transport solutes (Esau, 1965; Taiz and Zeiger, 2006), two properties that could be under the control of distinct regulatory pathways. Different preprocambial regulatory elements in the promoters of *ATHB8* and *SHR* could thus reflect participation of *ATHB8* and *SHR* in such distinct regulatory pathways and cellular functions. Alternatively, expression of *ATHB8* and *SHR* could be controlled by the same regulatory pathway, and the presence of different preprocambial regulatory elements in the promoters of these genes may reflect promiscuity in the sequence that is recognized by the same transcription factor. The TGTCTG element in the *ATHB8* promoter is bound by the AUXIN RESPONSE FACTOR (ARF) protein MONOPTEROS (MP) (Donner *et al.*, 2009; Chapter 2). *In vitro*, ARFs bind most strongly to TGTCTC elements, but changes to the nucleotide in position 5 and/or 6 of this sequence are tolerated, suggesting that TGTC is the minimal sequence required for ARF binding (Ulmasov *et al.*, 1997a; Ulmasov *et al.*, 1997b; Ulmasov *et al.*, 1999b), a finding that is consistent with results of *in vivo* chromatin immunoprecipitation

assays (Donner *et al.*, 2009; Schlereth *et al.*, 2010; Walcher and Nemhauser, 2011; Zhao *et al.*, 2010; Chapter 2). There is no TGTCTG sequence in the *SHR* promoter, but there are 16 TGTC sequences, including two TGTCTC sequences. Therefore, it is possible that an ARE is required for preprocambial expression of *SHR*, though the sequence of this regulatory element would be different from that of the ARE that is required for preprocambial expression of *ATHB8*.

While the TGTCTG element in the *ATHB8* promoter is required for the expression of *ATHB8* at preprocambial stages of leaf vascular development (Donner *et al.*, 2009; Chapter 2), it is unlikely that the presence of this element in a promoter is sufficient to confer preprocambial gene expression. The TGTCTG sequence is present in the most proximal 500-bp promoter of approximately 5000 *Arabidopsis* genes, but some of these genes, such as *CAPRICE*, *WAG1*, and *PHOTOTROPIN2*, are not expressed in vascular strands (Koshino-Kimura *et al.*, 2005; Schellman *et al.*, 2002; Sherr, 2012); some others, such as *CYCA2;1*, are expressed at early stages of leaf vascular development, but the TGTCTG sequence in their promoters is not required for this aspect of expression (Donner and Scarpella, 2013; Chapter 5). The lack of correlation between the presence of a TGTCTG sequence in a gene's promoter and the gene's expression at early stages of leaf vascular development is consistent with the finding that not all putative AREs are bound by ARFs *in vivo* (Cole *et al.*, 2009; Inukai *et al.*, 2005; Schlereth *et al.*, 2010). While it is currently unclear why only a subset of AREs are actually bound by ARFs, this finding may reflect the influence of sequences flanking a putative ARE on ARF binding. In fact, mutation of the sequences flanking an ARE affect the strength of the ARE-ARF interaction *in vitro* (Ulmasov *et al.*, 1995; Ulmasov *et al.*, 1997a; Ulmasov *et al.*, 1997b). Alternatively, additional regulatory elements could be required for TGTCTG elements to drive preprocambial gene expression; these additional elements could be bound by other ARFs or by transcription factors that belong to other families. ARF dimers bind more strongly to AREs than ARF monomers (Hardtke *et al.*, 2004; Li *et al.*, 2011; Scacchi *et al.*, 2010; Ulmasov *et al.*, 1999a; Ulmasov *et al.*, 1999b; Vernoux *et al.*, 2011); promoter regions bound by ARFs *in vivo* often contain

multiple AREs (Cole *et al.*, 2009; Okushima *et al.*, 2007; Scacchi *et al.*, 2010; Schlereth *et al.*, 2010); and the size of the region protected by ARFs in DNase I foot-printing assays is consistent with DNA binding by ARF dimers (Ulmasov *et al.*, 1997a). If, at least in some cases, ARFs bound DNA as dimers, one would expect the spacing between AREs to be critical for ARF-dimer binding. The synthetic auxin-responsive promoter DR5 is a multimer of TGTCTC AREs that are separated by a CCTTT sequence (Ulmasov *et al.*, 1997b). The DR5 promoter drives reporter gene expression at preprocambial stages of leaf vascular development (Mattsson *et al.*, 2003), but the activity of this promoter depends on the correct spacing of the AREs, consistent with the hypothesis that ARFs can bind to AREs as dimers (Ulmasov *et al.*, 1997a; reviewed in Guilfoyle *et al.*, 1998). ARFs can also form dimers with transcription factors that belong to other families, suggesting the formation of inter-family transcriptional complexes (Scacchi *et al.*, 2010; Shin *et al.*, 2007; Varaud *et al.*, 2011). If ARFs participate in such inter-family transcriptional complexes, the promoters that are the targets of the function of these complexes should contain regulatory elements for both transcription factor families. The *SMALL AUXIN-UP RNA15* (*SAUR15*) gene of *Arabidopsis* is expressed throughout the leaf, including in vascular strands, and a TGTCTG element in the *SAUR15* promoter that is bound by MP is required for responsiveness to auxin and brassinosteroids (Gil and Green, 1997; Walcher and Nemhauser, 2011). Both *SAUR15* expression and MP-binding to the *SAUR15* TGTCTG element require the binding of BRASSINOSTEROID INSENSITIVE1-ETHYL METHANESULFONATE SUPPRESSOR1 (*BES1*) to a brassinosteroid response element in the *SAUR15* promoter, suggesting a possible interaction between MP and *BES1* in the regulation of *SAUR15* expression (Walcher and Nemhauser, 2011). Finally, it is possible that the lack of correlation between the presence of a TGTCTG sequence in a gene's promoter and the gene's expression at early stages of leaf vascular development is the result of spatial inaccessibility of the TGTCTG element by an ARF. Structural analysis of the DNA-binding domain of ARFs suggests that it interacts with the major groove of the DNA double helix (Yamasaki *et al.*, 2004); therefore, if a TGTCTG element were

located within the minor groove, ARFs might be unable to access and bind to the element.

In conclusion, available evidence suggests that the dependency of preprocambial expression of different genes on different regulatory elements reflects spatial or temporal differences in the expression of these genes or redundancy in the regulatory pathways controlling their expression. Further, at least for auxin responsive promoters, the presence of sequences thus far identified as required for preprocambial gene expression in a gene's promoter seems insufficient to predict the gene's preprocambial expression.

6.2 TRANSCRIPTION FACTORS REQUIRED FOR GENE EXPRESSION AT EARLY STAGES OF LEAF VASCULAR DEVELOPMENT

The regulatory elements required for preprocambial expression of *ATHB8*, *CYCA2;1*, and *CYCA2;4* implicate transcription factors of different families—ARF, DOF, ARR, and SBF-1—in the regulation of gene expression at preprocambial stages of leaf vascular development (Donner and Scarpella, 2013; Donner *et al.*, 2009; Chapters 2 and 5; Section 6.1). As transcription factors can typically bind to variations of an optimal sequence, it is possible that a single family of transcription factors binds to the different regulatory elements required for preprocambial expression of *ATHB8*, *CYCA2;1*, and *CYCA2;4*; however, none of the transcription factors of the ARF, DOF, ARR, and SBF-1 families seem to have sufficient flexibility in their binding specificity for this to be a likely scenario (Lawton *et al.*, 1991; Sakai *et al.*, 2000; Ulmasov *et al.*, 1997a; Ulmasov *et al.*, 1997b; Ulmasov *et al.*, 1999b; Yanagisawa and Schmidt, 1999). Thus, different transcription factor families are likely to control preprocambial gene expression during leaf vascular development.

That different transcription factor families may be implicated in regulation of preprocambial gene expression could reflect the co-existence in vascular cells of distinct regulatory pathways, each controlling a distinct cellular function, for example cell elongation or solute transport (Esau *et al.*, 1965; Taiz and Zeiger, 2010; Section 6.1). Alternatively, it could reflect the existence of distinct

regulatory pathways, each controlling the same cellular function, thus ensuring that such function is still supplied if either the upstream transcription factors or the regulatory elements to which they bind becomes mutated. In any case, the different transcription factors that regulate preprocambial gene expression could be controlled by a common ‘master regulator’ of vascular gene expression, and perhaps vascular development. Candidate molecules for such a regulator would be expected to integrate vascular strand formation with organ and organismal development, a requirement that is reminiscent of the functions of auxin (Berleth and Sachs, 2001; Berleth *et al.*, 2000; Capron *et al.*, 2009; Sachs, 2000; Chapter 1). However, for auxin to be considered a ‘master regulator’ of vascular gene expression, evidence should exist that suggests that auxin controls the expression of *ATHB8*, *SHR*, *CYCA2;1*, and *CYCA2;4* as well as that of their upstream regulators. This seems to be the case for *ATHB8*: *ATHB8* expression is auxin-inducible (Baima *et al.*, 1995; Donner *et al.*, 2009; Mattsson *et al.*, 2003; Chapter 2); it is down-regulated by loss of *MP* function and gain of *BDL/IAA12* function (Ckurshumova *et al.*, 2011; Donner *et al.*, 2009; Mattsson *et al.*, 2003; Schlereth *et al.*, 2010; Chapter 2); and up-regulated by gain of *MP* function (Donner *et al.*, 2009; Garrett *et al.*, 2012; Krogan *et al.*, 2012; Mattsson *et al.*, 2003; Chapter 2). Moreover, preprocambial expression of *ATHB8* is regulated by an ARE that is bound directly by *MP* (Donner *et al.*, 2009; Chapter 2). As *ATHB8* expression, *SHR* expression is down-regulated by loss of *MP* function (Ckurshumova *et al.*, 2011), and the *SHR* promoter contains several putative AREs (Section 6.1). As *ATHB8* expression, *CYCA2;1* expression is induced by auxin (Burssens *et al.*, 2000). Finally, as expression of *ATHB8* and *SHR*, expression of *CYCA2;4* is down-regulated by loss of *MP* function and gain of *IAA14/SOLITARY ROOT* function (Ckurshumova *et al.*, 2011; Vanneste *et al.*, 2005). It thus seems that expression of all of these four preprocambial genes is controlled by auxin; can we say the same of their presumed upstream regulators? Expression of *MP* is up-regulated by auxin (Lau *et al.*, 2011; Wenzel *et al.*, 2007). Expression of four of the 37 *DOF* genes of *Arabidopsis* is down-regulated by loss of *MP* function or gain of *BDL/IAA12* function (Ckurshumova *et al.*, 2011; Schlereth *et al.*, 2010),

and expression at least nine *DOF* genes are up-regulated by auxin (Kang and Singh, 2000, Paponov *et al.*, 2008; Winter *et al.*, 2007). Unlike expression of *MP* and *DOF*s, however, expression of *ARR* genes does not seem to be regulated by auxin (Paponov *et al.*, 2008; Winter *et al.*, 2007). Finally, *SBF-1* has not yet been cloned, but it is thought to be related to *GT-1*, which does not seem to be controlled by auxin (Winter *et al.*, 2007).

In summary, available evidence suggests that expression of at least some preprocambial genes and their upstream regulators is controlled by auxin, which is consistent with the hypothesis that auxin is a ‘master regulator’ of vascular gene expression.

6.3 FUNCTIONS OF GENES EXPRESSED AT EARLY STAGES OF LEAF VASCULAR DEVELOPMENT

If auxin were a ‘master regulator’ of not only vascular gene expression but also vascular development, the functions of *ATHB8*, *SHR*, *CYCA2;1*, and *CYCA2;4* and of their upstream regulators—members of the ARF, DOF, ARR, and SBF-1 families of transcription factors—would be expected to overlap with the functions of auxin in vascular development.

Positions of sites of vascular strand formation during leaf development are exquisitely sensitive to inhibition of polar auxin transport (Mattson *et al.*, 1999; Sieburth, 1999); however, this sensitivity is greatly reduced at stages of vascular development prior to the differentiation of procambial cells (Mattsson *et al.*, 1999). In the *athb8* mutant, PIN1 expression and vein patterning are more sensitive to defects induced by auxin transport inhibition (Donner *et al.*, 2009; Chapter 2). Therefore, it is possible that one of the functions of *ATHB8* is to reduce sensitivity of preprocambial cells to variations in auxin transport that may occur during normal leaf development, thus stabilizing positions of sites of vascular strand formation. If that were so, how could *ATHB8* do that? One possibility is that *ATHB8* negatively regulates molecules that act as endogenous inhibitors of auxin transport. Consistent with this possibility, overexpression of *microRNA165*, which degrades transcripts of *ATHB8* and of the other class III

HOMEODOMAIN-LEUCINE ZIPPER (HD-ZIPIII) genes, leads to an increase in flavonoids (Zhou *et al.*, 2007), which have been shown to act as inhibitors of polar auxin transport (Jacobs and Rubery, 1988; reviewed in Peer and Murphy, 2007; Taylor and Grotewold, 2005). Alternatively, as PIN1 polarity determines the direction of auxin transport (Wisniewksa *et al.*, 2006), *ATHB8* could stabilize the positions of sites of vascular strand formation during leaf development by stabilizing PIN1 polarity. Expression of PINOID (PID), a serine-threonine kinase that can phosphorylate PIN1 thus changing its polarity (Friml *et al.*, 2004), subsides in presumptive vascular cells (Benjamins *et al.*, 2001; Michniewicz *et al.*, 2007; Sherr, 2012), where *ATHB8* expression is initiated (Kang and Dengler, 2004; Scarpella *et al.*, 2004). Consistent with PID function in regulation of PIN1 polarity, *pid* mutants have defects in leaf vascular patterns that resemble those of *pin1* mutants (Hou *et al.*, 2010; Kleine-Vehn *et al.*, 2009; Sherr, 2012). Thus, it is possible that *ATHB8*, redundantly with other *HD-ZIPIII* genes, down-regulates PID expression in preprocambial cells, thus stabilizing PIN1 polarity and positions of sites of vascular strand formation during leaf development. As PIN1 polarity is stabilized by auxin (Paciorek *et al.*, 2005), and as mutants defective in auxin synthesis display reductions in vascular strand formation (Cheng *et al.*, 2006), one other possibility is that *ATHB8* stabilizes PIN1 polarity, and thus positions of sites of vascular strand formation, during leaf development by promoting auxin synthesis in preprocambial cells. The *HD-ZIPIII* gene *INTERFASCICULAR FIBERLESS1/REVOLUTA (REV* hereafter) regulates the expression of genes encoding auxin synthesis enzymes (Brandt *et al.*, 2012). Because *HD-ZIPIII* genes are functionally redundant with one another (Carlsbecker *et al.*, 2010; Miyashima *et al.*, 2011; Prigge *et al.*, 2005), it is possible that *ATHB8*, as *REV*, regulates auxin synthesis, thus stabilizing PIN1 polarity and positions of sites of vascular strand formation during leaf development. Of course, it is also possible that *ATHB8* stabilizes positions of sites of vascular strand formation during leaf development by yet another mechanism or that the sensitivity of PIN1 expression and vein patterning to auxin transport

inhibition in *athb8* results from the feedback on leaf vascular patterning of defects at later stages of *athb8* vascular development (Donner *et al.*, 2009; Chapter 2).

In both roots and leaves, the *SHR* gene is expressed in vascular cells, but the SHR protein is also expressed in the layer of non-vascular cells that surrounds vascular strands (Gardiner *et al.*, 2011; Helariutta *et al.*, 2000; Nakajima *et al.*, 2001; Chapter 3), a cell layer that will differentiate into the endodermis in the root and the bundle-sheath in the leaf (Esau, 1965). In the root, the SHR protein is synthesized in the cells of the vascular strand and moves to the surrounding cell layer to control endodermis formation (Benfey *et al.*, 1993; Helariutta *et al.*, 2000; Nakajima *et al.*, 2001). Therefore, it is possible that SHR is synthesized in the cells of vascular strands of the leaf and moves to the cell layer that surrounds each vascular strand to control bundle-sheath formation. Available evidence suggests that *SHR* expression is regulated by auxin signaling (Ckurshumova *et al.*, 2011; Sections 6.1 and 6.2). Both *SHR* and the auxin-response transcription factor MP are expressed in root vascular cells (Bureau *et al.*, 2010; Helariutta *et al.*, 2000; Schlereth *et al.*, 2010), and both *mp* and *shr* mutants lack the endodermis (Benfey *et al.*, 1993; Berleth and Jurgens, 1993). Thus, it is possible that MP controls endodermis formation by activating *SHR* expression in root vascular cells. Because *mp* leaves lack bundle-sheath cells (Przemeck *et al.*, 1996), it is tempting to speculate that MP controls bundle-sheath formation by a similar mechanism.

In animals, *CYCA2* genes have been shown to regulate the progression of S-phase and the transition from G2-to-M phases during cell division (Pines and Hunter; reviewed in Fung and Poon, 2005; Wolgemuth, 2011), which is consistent with leaf defects of *Arabidopsis* plants burdened by mutation of all four *CYCA2* genes—fewer cells, increased polyploidy, and smaller leaves (Vanneste *et al.*, 2011; Chapter 4)—and with *CYCA2* expression in the leaf (Donner and Scarpella, 2013; Vanneste *et al.*, 2011; Chapters 4 and 5), which resembles leaf expression of the mitotic cyclin gene *CYCBI;1*, expression which identifies sites of cell division during leaf development (Donnelly *et al.*, 1999; Kang and Dengler, 2002). *CYCA2* genes are required for the formation of leaf serrations and vascular proliferation at leaf hydathodes (Vanneste *et al.*, 2011; Chapter 4). Leaf serrations

and leaf hydathodes are associated with auxin response maxima (Aloni *et al.*, 2003; Barkoulous *et al.*, 2008; Billsborough *et al.*, 2011; Mattsson *et al.*, 2003; Scarpella *et al.*, 2006); auxin positively regulates expression of *CYCA2;1* (Bursens *et al.*, 2000; Sections 6.1 and 6.2); *CYCA2;4* expression is reduced in auxin signaling mutants (Ckurshumova *et al.*, 2011; Vanneste *et al.*, 2005); and, as *cyca2* quadruple-mutants, auxin signaling mutants have fewer, polyploid cells (Ishida *et al.*, 2010). Thus, it is possible that one of the functions of auxin in leaf development is to promote cell division by activation of *CYCA2* expression. Consistent with this possibility, expression of *CYCA2* genes (Bursens *et al.*, 2000; Donner and Scarpella, 2013; Imai *et al.*, 2006; Vanneste *et al.*, 2011; Chapters 4 and 5) resembles expression of the auxin-response transcription factor MP (Donner *et al.*, 2009; Wenzel *et al.*, 2007; Chapter 2). A tight relationship between auxin signaling and cell division is also suggested by the interaction between *mp* and *altered meristem program1/constitutive morphogenesis2/hauptling/multifolia/primordia timing* (*amp1* hereafter) (Chaudhury *et al.*, 1993; Hou *et al.*, 1993; Mayer *et al.*, 1991; Mordhorst *et al.*, 1998; Vidaurre *et al.*, 2007). *amp1* mutants have enlarged shoot apical meristems and undergo extra cell-divisions near the base of the embryo (Saibo *et al.*, 2007; Vidaurre *et al.*, 2007), whereas *mp* mutants have reduced shoot apical meristems and fail to undergo key cell divisions at the base of the embryo (Berleth and Jurgens, 1993; Vidaurre *et al.*, 2007), suggesting that cell division is repressed by *AMP1* and promoted by *MP*. Moreover, the partial suppression of *mp* defects by *amp1* suggests that *AMP1* and *MP* oppose one another's function in the regulation of cell division (Vidaurre *et al.*, 2007). Thus, *MP* could promote leaf and vascular development by releasing cells from *AMP1*-mediated repression of division. It would be interesting to test whether the opposing functions of *MP* and *AMP1* on cell division and leaf and vascular development are mediated by *CYCA2* genes.

The functions of transcription factors of the ARF, DOF, and ARR families also seem to overlap with the functions of auxin in vascular development. ARFs effect auxin-responsive gene expression (Mockaitis and Estelle, 2008; Chapter 1), and *mp* mutants show defects in vascular strand differentiation (Donner *et al.*,

2009; Przemeck *et al.*, 1996; Chapters 1 and 2). A DOF binding site is required for the auxin responsiveness of the expression of a tobacco gene (Baumann *et al.*, 1999), and overexpression of a *DOF* gene in *Arabidopsis* leads to expanded zones of vascular tissue differentiation (Guo *et al.*, 2009). Finally, three *ARR* genes redundantly control vascular tissue development (Ishida *et al.*, 2008; Yokoyama *et al.*, 2007).

In conclusion, available evidence suggests that functions of at least some preprocambial genes and their upstream regulators overlap with the functions of auxin in leaf vascular development, which is consistent with the hypothesis that auxin is a ‘master regulator’ of vascular development. On the other hand, the evidence currently available is scarce and thus the speculative nature of the derived conclusions should be emphasized. Nevertheless, my research has generated both a conceptual and experimental framework for the gene regulatory networks that control expression at early stages of leaf vascular development that could be used as a starting-point to dissect the mechanisms that control leaf vascular development.

BIBLIOGRAPHY

Aloni, R., Schwalm, K., Langhans, M., and Ullrich, C. I. (2003). Gradual shifts in sites of free-auxin production during leaf-primordium development and their role in vascular differentiation and leaf morphogenesis in *Arabidopsis*. *Planta* **216**: 841-853.

Alonso, J. M., Stepanova, A. N., Leisse, T. J., Kim, C. J., Chen, H., Shinn, P., Stevenson, D. K., Zimmerman, J., Barajas, P., Cheuk, R., Gadrinab, C., Heller, C., Jeske, A., Koesema, E., Meyers, C. C., Parker, H., Prednis, L., Ansari, Y., Choy, N., Deen, H., Geralt, M., Hazari, N., Hom, E., Karnes, M., Mulholland, C., Ndubaku, R., Schmidt, I., Guzman, P., Aguilar-Henonin, L., Schmid, M., Weigel, D., Carter, D. E., Marchand, T., Risseuw, E., Brogden, D., Zeko, A., Crosby, W. L., Berry, C. C., and Ecker, J. R. (2003). Genome-wide insertional mutagenesis of *Arabidopsis thaliana*. *Science* **301**: 653-657.

Alonso-Peral, M. M., Candela, H., del Pozo, J. C., Martinez-Laborda, A., Ponce, M. R., and Micol, J. L. (2006). The *HVE/CAND1* gene is required for the early patterning of leaf venation in *Arabidopsis*. *Development* **133**: 3755-3766.

Bailey-Serres, J., Sorenson, R., and Juntawong, P. (2009). Getting the message across: cytoplasmic ribonucleoprotein complexes. *Trends Plant Sci.* **14**: 443-453.

Baima, S., Nobili, F., Sessa, G., Lucchetti, S., Ruberti, I., and Morelli, G. (1995). The expression of the *ATHB-8* homeobox gene is restricted to provascular cells in *Arabidopsis thaliana*. *Development* **121**: 4171-4182.

Baima, S., Possenti, M., Matteucci, A., Wisman, E., Altamura, M. M., Ruberti, I., and Morelli, G. (2001). The *Arabidopsis* *ATHB-8* HD-ZIP protein acts as a differentiation-promoting transcription factor of the vascular meristems. *Plant Physiol.* **126**: 643-655.

Barkoulas, M., Hay, A., Kougioumoutzi, E., and Tsiantis, M. (2008). A developmental framework for dissected leaf formation in the *Arabidopsis* relative *Cardamine hirsuta*. *Nat Genet.* **40**: 1136-1141.

Beeckman, T., Przemeck, G. K. H., Stamatiou, G., Lau, R., Terryn, N., Rycke, R. D., Inze, D., and Berleth, T. (2002). Genetic complexity of *CELLULOSE SYNTHASE A* gene function in *Arabidopsis* embryogenesis. *Plant Physiol.* **130**: 1883-1893.

Beemster, G. T. S., Vercruyse, S., De Veylder, L., Kuiper, M., and Inzé, D. (2006). The *Arabidopsis* leaf as a model system for investigating the role of cell cycle regulation in organ growth. *J Plant Res.* **119**: 43-50.

Belostotsky, D. A. and Sieburth, L. E. (2009). Kill the messenger: mRNA decay and plant development. *Curr Opin Plant Biol.* **12**: 96-102.

Benhamed, M., Martin-Magniette, M., Taconnat, L., Bitton, F., Servet, C., De Clercq, R., De Meyer, B., Buyschaert, C., Rombauts, S., Villarroel, R., Aubourg, S., Beynon, J., Bhalerao, R. P., Coupland, G., Grissem, W., Menke, F. L. H., Weisshaar, B., Renou, J., Zhou, D., and Hilson, P. (2008). Genome-scale *Arabidopsis* promoter array identifies targets of the histone acetyltransferase GCN5. *Plant J.* **56**: 493-504.

Benjamins, R., Quint, A., Weijers, D., Hooykaas, P., and Offringa, R. (2001). The PINOID protein kinase regulates organ development in *Arabidopsis* by enhancing polar auxin transport. *Development* **128**: 4057-4067.

Benkova, E., Michniewicz, M., Sauer, M., Teichmann, T., Seifertova, D., Jurgens, G., and Friml, J. (2003). Local, efflux-dependent auxin gradients as a common module for plant organ formation. *Cell* **115**: 591-602.

Bergmann, D. C. and Sack, F. D. (2007). Stomatal development. *Annu Rev Plant Biol.* **58**:163-181.

Berleth, T. and Jurgens, G. (1993). The role of the *MONOPTEROS* gene in organizing the basal body region of the *Arabidopsis* embryo. *Development* **118**: 575-587.

Berleth, T., Mattsson, J., and Hardtke, C. S. (2000). Vascular continuity and auxin signals. *Trends Plant Sci.* **5**: 387-393.

Berleth, T. and Sachs, T. (2001). Plant morphogenesis: long-distance coordination and local patterning. *Curr Opin Plant Biol.* **4**: 57-62.

Bilsborough, G. D., Runions, A., Barkoulas, M., Jenkins, H. W., Hasson, A., Galinha, C., Laufs, P., Hay, A., Prusinkiewicz, P., and Tsiantis, M. (2011). Model for the regulation of *Arabidopsis thaliana* leaf margin development. *Proc Natl Acad Sci U S A.* **108**: 3424-3429.

Birnbaum, K., Shasha, D. E., Wang, J. Y., Jung, J. W., Lambert, G. M., Galbraith, D. W., Benfey, P. N. (2003). A gene expression map of the *Arabidopsis* root. *Science* **302**: 1956-1960.

Blasing, O. E., Gibon, Y., Günther, M., Hohne, M., Morcuende, R., Osuna, D., Thimm, O., Usadel, B., Scheible, W., and Stitt, M. (2005). Sugars and circadian regulation make major contributions to the global regulation of diurnal gene expression in *Arabidopsis*. *Plant Cell* **17**: 3257-3281.

- Bolle, C.** (2004). The role of GRAS proteins in plant signal transduction and development. *Planta* **218**: 683-692.
- Bolle, C., Koncz, C., and Chua, N.** (2000). PAT1, a new member of the GRAS family, is involved in PHYTOCHROME A signal transduction. *Genes Dev.* **14**: 1269-1278.
- Boruc, J., Mylle, E., Duda, M., De Clercq, R., Rombauts, S., Geelen, D., Hilson, P., Inzé, D., Van Damme, D., and Russinova, E.** (2010a). Systematic localization of the *Arabidopsis* core cell cycle proteins reveals novel cell division complexes. *Plant Physiol.* **152**: 553-565.
- Boruc, J., Van den Daele, H., Hollunder, J., Rombauts, S., Mylle, E., Hilson, P., Inze, D., De Veylder, L., and Russinova, E.** (2010b). Functional modules in the *Arabidopsis* core cell cycle binary protein-protein interaction network. *Plant Cell* **22**: 1264-1280.
- Boudolf, V., Lammens, T., Boruc, J., Van Leene, J., Van Den Daele, H., Maes, S., Van Isterdael, G., Russinova, E., Kondorosi, E., Witters, E., De Jaeger, G., Inze, D., and De Veylder, L.** (2009). CDKB1;1 forms a functional complex with CYCA2;3 to suppress endocycle onset. *Plant Physiol.* **150**: 1482-1493.
- Boudolf, V., Barroco, R., de Almeida Engler, J., Verkest, A., Beeckman, T., Naudts, M., Inze, D., and De Veylder, L.** (2004). B1-type cyclin-dependent kinases are essential for the formation of stomatal complexes in *Arabidopsis thaliana*. *Plant Cell* **16**: 945-955.
- Boyes, D. C., Zayed, A. M., Ascenzi, R., McCaskill, A. J., Hoffman, N. E., Davis, K. R., and Grolach, J.** (2001). Growth stage-based phenotypic analysis of *Arabidopsis*: a model for high throughput functional genomics in plants. *Plant Cell* **13**: 1499-1510.
- Brandt, R., Salla-Martret, M., Bou-Torrent, J., Musielak, T., Stahl, M., Lanz, C., Ott, F., Schmid, M., Greb, T., Schwarz, M., Choi, S., Barton, M. K., Reinhart, B. J., Liu, T., Quint, M., Palauqui, J., Martinez-Garcia, J. F., and Wenkel, S.** (2012). Genome-wide binding-site analysis of REVOLUTA reveals a link between leaf patterning and light-mediated growth responses. *Plant J.* **72**: 31-42.
- Brown, C. D., Johnson, D. S., and Sidow, A.** (2007). Functional architecture and evolution of transcriptional elements that drive gene co-expression. *Science* **317**: 1557-1560.

- Brownfield, L., Hafidh, S., Borg, M., Sidorova, A., Mori, T., and Twell, D.** (2009). A plant germline-specific integrator of sperm specification and cell cycle progression. *PLoS Genet.* **5**: e1000430. doi: 10.1371/journal.pgen.1000430.
- Brudno, M., Do, C. B., Cooper, G. M., Kim, M. F., Davydov, E., NISC Comparative Sequencing Program, Green, E. D., Sidow, A., and Batzoglou, S.** (2003). LAGAN and multi-LAGAN: efficient tools for large-scale multiple alignment of genomic DNA. *Genome Res.* **13**: 721-731.
- Burssens, S., de Almeida Engler, J., Beeckman, T., Richard, C., Shaul, O., Ferreira, P., Van Montagu, M., and Inze, D.** (2000). Developmental expression of the *Arabidopsis thaliana* *CYCA2;1* gene. *Planta* **211**: 623-631.
- Buttitta, L. A. and Edgar, B. A.** (2007). Mechanisms controlling cell cycle exit upon terminal differentiation. *Curr Opin Cell Biol.* **19**: 697-704.
- Candela, H., Martinez-Laborda, A., and Micol, J. L.** (1999). Venation pattern formation in *Arabidopsis thaliana* vegetative leaves. *Dev Biol.* **205**: 205-216.
- Capron, A., Chatfield, S., Provart, N., and Berleth, T.** (2009). Embryogenesis: pattern formation from a single cell. *The Arabidopsis Book* e0126.
- Carland, F. M., Fujioka, S., and Nelson, T. M.** (2010). The sterol methyltransferases SMT1, SMT2, and SMT3 influence *Arabidopsis* development through non-brassinosteroid products. *Plant Physiol.* **153**: 741-756.
- Carland, F. M. and Nelson, T. M.** (2004). *COTYLEDON VASCULAR PATTERN2*-mediated inositol (1,4,5) triphosphate signal transduction is essential for closed venation patterns of *Arabidopsis* foliar organs. *Plant Cell* **16**: 1263-1275.
- Carland, F. M. and Nelson, T. M.** (2009). CVP2- and CVL1-mediated phosphoinositide signaling as a regulator of the ARF GAP SFC/VAN3 in establishment of foliar vein patterns. *Plant J.* **59**: 895-907.
- Carlsbecker, A., Lee, J., Roberts, C. J., Dettmer, J., Lehesranta, S., Zhou, J., Lindgren, O., Moreno-Risueno, M. A., Vaten, A., Thitamadee, S., Campilho, A., Sebastian, J., Bowman, J. L., Helariutta, Y., and Benfey, P. N.** (2010). Cell signalling by *microRNA165/6* directs gene dose-dependent root cell fate. *Nature* **465**: 316-321.
- Caro, E., Castellano, M. M., and Gutierrez, C.** (2007). A chromatin link that couples cell division to root epidermis patterning in *Arabidopsis*. *Nature* **447**: 213-217.

- Carroll, S. B.** (2005). Evolution at two levels: on genes and form. *PLoS Biol* **3**: e245.
- Chaudhury, A. M., Letham, S., Craig, S., and Dennis, E. S.** (1993). *amp1* - a mutant with high cytokinin levels and altered embryonic pattern, faster vegetative growth, constitutive photomorphogenesis, and precocious flowering. *Plant J.* **4**: 907-916.
- Cheng, Y., Dai, X., and Zhao, Y.** (2006). Auxin biosynthesis by the YUCCA flavin monooxygenases controls the formation of floral organs and vascular tissues in *Arabidopsis*. *Genes Dev.* **20**: 1790-1799.
- Ckurshumova, W., Koizumi, K., Chatfield, S. P., Sanchez-Buelna, S. U., Gangaeva, A. E., McKenzie, R., and Berleth, T.** (2009). Tissue-specific GAL4 expression patterns as a resource enabling targeted gene expression, cell type-specific transcript profiling, and gene function characterization in the *Arabidopsis* vascular system. *Plant Cell Physiol.* **50**: 141-150.
- Ckurshumova, W., Scarpella, E., Goldstein, R. S., and Berleth, T.** (2011). Double-filter identification of vascular-expressed genes using *Arabidopsis* plants with vascular hypertrophy and hypotrophy. *Plant Sci.* **181**: 96-104.
- Clough, S. J. and Bent, A.F.** (1998). Floral dip: a simplified method for *Agrobacterium*-mediated transformation of *Arabidopsis thaliana*. *Plant J.* **16**: 735-743.
- Cnops, G., Neyt, P., Raes, J., Petrarulo, M., Nelissen, H., Malenica, N., Luschnig, C., Tietz, O., Ditengou, F., Palme, K., Azmi, A., Prinsen, E., and Van Lijsebettens, M.** (2006). The *TORNADO1* and *TORNADO2* genes function in several patterning processes during early leaf development in *Arabidopsis thaliana*. *Plant Cell* **18**: 852-866.
- Cole, M., Chandler, J., Weijers, D., Jacobs, B., Comelli, P., and Werr, W.** (2009). DORNROSCHEN is a direct target of the auxin response factor MONOPTEROS in the *Arabidopsis* embryo. *Development* **136**: 1643-1651.
- Coudreuse, D. and Nurse, P.** (2010). Driving the cell cycle with a minimal CDK control network. *Nature* **468**: 1074-1079.
- Covington, M. F. and Harmer, S. L.** (2007). The circadian clock regulates auxin signaling and responses in *Arabidopsis*. *PLoS Biol.* **5**: e222.
- Cutler, S. R., Ehrhardt, D. W., Griffiths, J. S., and Somerville, C. R.** (2000). Random GFP::cDNA fusions enable visualization of subcellular structures in cells of *Arabidopsis* at a high frequency. *Proc Natl Acad Sci U S A.* **97**: 3718-3723.

- Davuluri, R. V., Sun, H., Palaniswamy, S. K., Matthews, N., Molina, C., Kurtz, M., and Grotewold, E.** (2003). AGRIS: *Arabidopsis* Gene Regulatory Information Server, an information resource of *Arabidopsis* cis-regulatory elements and transcription factors. *BMC Bioinformatics* **4**: 25.
- de Almeida Engler, J., De Veylder, L., De Groot, R., Rombauts, S., Boudolf, V., De Meyer, B., Hemerly, A., Ferreira, P., Beeckman, T., Karimi, M., Hilson, P., Inze, D., and Engler, G.** (2009). Systematic analysis of cell-cycle gene expression during *Arabidopsis* development. *Plant J.* **59**: 645-660.
- De Veylder, L., Beeckman, T., and Inze, D.** (2007). The ins and outs of the plant cell cycle. *Nat Rev Mol Cell Biol.* **8**: 655-665.
- del Pozo, J. C., Boniotti, M. B., and Gutierrez, C.** (2002). *Arabidopsis* E2F_c functions in cell division and is degraded by the ubiquitin-SCF^{AtSKP2} pathway in response to light. *Plant Cell* **14**: 3057-3071.
- Dello Ioio, R., Linhares, F. S., Scacchi, E., Casamitjana-Martinez, E., Heidstra, R., Costantino, P., and Sabatini, S.** (2007). Cytokinins determine *Arabidopsis* root-meristem size by controlling cell differentiation. *Curr Biol.* **17**: 678-682.
- Demandolx, D. and Davoust, J.** (1997). Multicolour analysis and local image correlation in confocal microscopy. *J Microsc.* **185**: 21-36.
- Dengler, N. G. and Kang, J.** (2001). Vascular patterning and leaf shape. *Curr Opin Plant Biol.* **4**: 50-56.
- Dewitte, W., Riou-Khamlichi, C., Scofield, S., Healy, J. M. S., Jacquard, A., Kilby, N. J., and Murray, J. A. H.** (2003). Altered cell cycle distribution, hyperplasia, and inhibited differentiation in *Arabidopsis* caused by the D-type cyclin CYCD3. *Plant Cell* **15**: 79-92.
- Dewitte, W., Scofield, S., Alcasabas, A. A., Maughan, S. C., Menges, M., Braun, N., Collins, C., Nieuwland, J., Prinsen, E., Sundaresan, V., and Murray, J. A. H.** (2007). *Arabidopsis* CYCD3 D-type cyclins link cell proliferation and endocycles and are rate-limiting for cytokinin responses. *Proc Natl Acad Sci U S A.* **104**: 14537-14542.
- Deyholos, M. K., Cavaness, G. F., Hall, B., King, E., Punwani, J., Van Norman, J., and Sieburth, L. E.** (2003). VARICOSE, a WD-domain protein, is required for leaf blade development. *Development* **130**: 6577-6588.
- Deyholos, M. K., Corder, G., Beebe, D., and Sieburth, L. E.** (2000). The *SCARFACE* gene is required for cotyledon and leaf vein patterning. *Development* **127**: 3205-3213.

- Dharmasiri, N., Dharmasiri, S., and Estelle, M.** (2005a). The F-box protein TIR1 is an auxin receptor. *Nature* **435**: 441-445.
- Dharmasiri, N., Dharmasiri, S., Weijers, D., Lechner, E., Yamada, M., Hobbie, L., Ehrismann, J. S., Jurgens, G., and Estelle, M.** (2005b). Plant development is regulated by a family of auxin receptor F-box proteins. *Dev Cell* **9**: 109-119.
- Di Laurenzio, L., Wysocka-Diller, J., Malamy, J. E., Pysh, L., Helariutta, Y., Freshour, G., Hahn, M. G., Feldmann, K. A., and Benfey, P. N.** (1996). The *SCARECROW* gene regulates an asymmetric cell division that is essential for generating the radial organization of the *Arabidopsis* root. *Cell* **86**: 423-433.
- Dill, A., Jung, H., and Sun, T.** (2001). The DELLA motif is essential for gibberellin-induced degradation of RGA. *Proc Natl Acad Sci U S A.* **98**: 14162-14167.
- Dill, A. and Sun, T.** (2001). Synergistic derepression of gibberellin signaling by removing RGA and GAI function in *Arabidopsis thaliana*. *Genetics* **159**: 777-785.
- Donnelly, P. M., Bonetta, D., Tsukaya, H., Dengler, R. E., and Dengler, N. G.** (1999). Cell cycling and cell enlargement in developing leaves of *Arabidopsis*. *Dev Biol.* **215**: 407-419.
- Donner, T. J. and Scarpella, E.** (2013). Transcriptional control of early vein expression of *CYCA2;1* and *CYCA2;4* in *Arabidopsis* leaves. *Mech Dev.* **130**: 14-24.
- Donner, T. J., Sherr, I., and Scarpella, E.** (2009). Regulation of preprocambial cell state acquisition by auxin signaling in *Arabidopsis* leaves. *Development* **136**: 3235-3246.
- Donner, T. J., Sherr, I., and Scarpella, E.** (2010). Auxin signal transduction in *Arabidopsis* vein formation. *Plant Signal Behav.* **5**: 70-72.
- Dowell, R. D.** (2010). Transcription factor binding variation in the evolution of gene regulation. *Trends Genet.* **26**: 468-475.
- Edwards, K. D., Anderson, P. E., Hall, A., Salathia, N. S., Locke, J. C. W., Lynn, J. R., Straume, M., Smith, J. Q., and Millar, A. J.** (2006). *FLOWERING LOCUS C* mediates natural variation in the high-temperature response of the *Arabidopsis* circadian clock. *Plant Cell* **18**: 639-650.

Erickson, R. O. (1976). Modeling of plant growth. *Annu Rev Plant Physiol.* **27**: 407-434.

Esau, K. (1943). Origin and development of primary vascular tissues in plants. *Bot Rev.* **9**: 125-206.

Esau, K. (1965). *Plant Anatomy*. New York, NY, USA: John Wiley.

Fang, R. X., Nagy, F., Sivasubramaniam, S., and Chua, N. (1989). Multiple *cis*-regulatory elements for maximal expression of the cauliflower mosaic virus 35S promoter in transgenic plants. *Plant Cell* **1**: 141-150.

Fisher, D. L. and Nurse, P. (1996). A single fission yeast mitotic cyclin B p34^{cdc2} kinase promotes both S-phase and mitosis in the absence of G₁ cyclins. *EMBO J.* **15**: 850-860.

Fode, B., Siemsen, T., Thurow, C., Weigel, R., and Gatz, C. (2008). The *Arabidopsis* GRAS protein SCL14 interacts with class II TGA transcription factors and is essential for the activation of stress-inducible promoters. *Plant Cell* **20**: 3122-3135.

Fornara, F., Panigrahi, K. C. S., Gissot, L., Sauerbrunn, N., Ruhl, M., Jarillo, J. A., and Coupland, G. (2009). *Arabidopsis* DOF transcription factors act redundantly to reduce *CONSTANS* expression and are essential for a photoperiodic flowering response. *Dev Cell* **17**: 75-86.

Foster, A. S. (1952). Foliar venation in angiosperms from an ontogenetic standpoint. *Am J Bot.* **39**: 752-766.

Frazer, K. A., Pachter, L., Poliakov, A., Rubin, E. M., and Dubchak, I. (2004). VISTA: computational tools for comparative genomics. *Nucleic Acids Res.* **32**: W273-W279.

Friml, J., Vieten, A., Sauer, M., Weijers, D., Schwarz, H., Hamann, T., Offringa, R., and Jurgens, G. (2003). Efflux-dependent auxin gradients establish the apical-basal axis of *Arabidopsis*. *Nature* **426**: 147-153.

Friml, J., Yang, X., Michniewicz, M., Weijers, D., Quint, A., Tietz, O., Benjamins, R., Ouwerkerk, P. B. F., Ljung, K., Sandberg, G., Hooykaas, P. J. J., Palme, K., and Offringa, R. (2004). A PINOID-dependent binary switch in apical-basal PIN polar targeting directs auxin efflux. *Science* **306**: 862-865.

Fu, X., Richards, D. E., Fleck, B., Xie, D., Burton, N., and Harberd, N. P. (2004). The *Arabidopsis* mutant *sleepy1*^{gar2-1} protein promotes plant growth by increasing the affinity of the SCF^{S^{LY}1} E3 ubiquitin ligase for DELLA protein substrates. *Plant Cell* **16**: 1406-1418.

- Fung, T. K. and Poon, R. Y. C.** (2005). A roller coaster ride with the mitotic cyclins. *Semin Cell Dev Biol.* **16**: 335-342.
- Gallagher, K. L., Paquette, A. J., Nakajima, K., and Benfey, P. N.** (2004). Mechanisms regulating SHORT-ROOT intercellular movement. *Curr Biol.* **14**: 1847-1851.
- Gardiner, J., Donner, T. J., and Scarpella, E.** (2011). Simultaneous activation of *SHR* and *ATHB8* expression defines switch to preprocambial cell state in *Arabidopsis* leaf development. *Dev Dyn.* **240**: 261-270.
- Gardiner, J., Sherr, I., and Scarpella, E.** (2010). Expression of *DOF* genes identifies early stages of vascular development in *Arabidopsis* leaves. *Int J Dev Biol.* **54**: 1389-1396.
- Gardner, M. J., Baker, A. J., Assie, J., Poethig, R. S., Haseloff, J. P., and Webb, A. A. R.** (2009). GAL4 GFP enhancer trap lines for analysis of stomatal guard cell development and gene expression. *J Exp Bot.* **60**: 213-226.
- Garrett, J. J. T., Meents, M. J., Blackshaw, M. T., Blackshaw, L. C., Hou, H., Styranko, D. M., Kohalmi, S. E., and Schultz, E. A.** (2012). A novel, semi-dominant allele of *MONOPTEROS* provides insight into leaf initiation and vein pattern formation. *Planta* **236**: 297-312.
- Geldner, N., Anders, N., Wolters, H., Keicher, J., Kornberger, W., Muller, P., Delbarre, A., Ueda, T., Nakano, A., and Jurgens, G.** (2003). The *Arabidopsis* GNOM ARF-GEF mediates endosomal recycling, auxin transport, and auxin-dependent plant growth. *Cell* **112**: 219-230.
- Gil, P. and Green, P. J.** (1997). Regulatory activity exerted by the *SAUR-AC1* promoter region in transgenic plants. *Plant Mol Biol.* **34**: 803-808.
- Goodstein, D. M., Shu, S., Howson, R., Neupane, R., Hayes, R. D., Fazo, J., Mitros, T., Dirks, W., Hellsten, U., Putnam, N., and Rokhsar, D. S.** (2012). Phytozome: a comparative platform for green plant genomics. *Nucleic Acids Res.* **40**: D1178-D1186.
- Greb, T., Clarenz, O., Schafer, E., Muller, D., Herrero, R., Schmitz, G., and Theres, K.** (2003). Molecular analysis of the *LATERAL SUPPRESSOR* gene in *Arabidopsis* reveals a conserved control mechanism for axillary meristem formation. *Genes Dev.* **17**: 1175-1187.
- Gubler, F., Raventos, D., Keys, M., Watts, R., Mundy, J., and Jacobsen, J. V.** (1999). Target genes and regulatory domains of the GAMYB transcriptional activator in cereal aleurone. *Plant J.* **17**: 1-9.

Guenot, B., Bayer, E., Kierzkowski, D., Smith, R. S., Mandel, T., Zadnikova, P., Benkova, E., and Kuhlemeier, C. (2012). PIN1-independent leaf initiation in *Arabidopsis*. *Plant Physiol.* **159**: 1501-1510.

Guilfoyle, T. J. and Hagen, G. (2001). Auxin response factors. *J. Plant Growth Regul.* **20**: 281-291.

Guilfoyle, T. J. and Hagen, G. (2007). Auxin response factors. *Curr Opin Plant Biol.* **10**: 453-460.

Guilfoyle, T. J. and Hagen, G. (2012). Getting a grasp on domain III/IV responsible for Auxin Response Factor-IAA protein interactions. *Plant Sci.* **190**: 82-88.

Guilfoyle, T. J., Hagen, G., Ulmasov, T., and Murfett, J. (1998). How does auxin turn on genes? *Plant Physiol.* **118**: 341-347.

Hadfi, K., Speth, V., and Neuhaus, G. (1998). Auxin-induced developmental patterns in *Brassica juncea* embryos. *Development* **125**: 879-887.

Hamann, T., Benkova, E., Baurle, I., Kientz, M., and Jurgens, G. (2002). The *Arabidopsis* *BODENLOS* gene encodes an auxin response protein inhibiting MONOPTEROS-mediated embryo patterning. *Genes Dev.* **16**: 1610-1615.

Hamann, T., Mayer, U., and Jurgens, G. (1999). The auxin-insensitive *bodenlos* mutation affects primary root formation and apical-basal patterning in the *Arabidopsis* embryo. *Development* **126**: 1387-1395.

Hardtke, C. S. and Berleth, T. (1998). The *Arabidopsis* gene *MONOPTEROS* encodes a transcription factor mediating embryo axis formation and vascular development. *EMBO J.* **17**: 1405-1411.

Hardtke, C. S., Ckurshumova, W., Vidaurre, D. P., Singh, S. A., Stamatiou, G., Tiwari, S. B., Hagen, G., Guilfoyle, T. J., and Berleth, T. (2004). Overlapping and non-redundant functions of the *Arabidopsis* auxin response factors *MONOPTEROS* and *NONPHOTOTROPIC HYPOCOTYLA*. *Development* **131**: 1089-1100.

Haseloff, J. P. (1999). GFP variants for multispectral imaging of living cells. *Methods Cell Biol.* **58**: 139-151.

Helariutta, Y., Fukaki, H., Wysocka-Diller, J., Nakajima, K., Jung, J., Sena, G., Hauser, M., and Benfey, P. N. (2000). The *SHORT-ROOT* gene controls radial patterning of the *Arabidopsis* root through radial signaling. *Cell* **101**: 555-567.

- Higo, K., Ugawa, Y., Iwamoto, M., and Korenaga, T.** (1999). Plant *cis*-acting regulatory DNA elements (PLACE) database: 1999. *Nucleic Acids Res.* **27**: 297-300.
- Himanen, K., Boucheron, E., Vanneste, S., de Almeida Engler, J., Inze, D., and Beeckman, T.** (2002). Auxin-mediated cell cycle activation during early lateral root initiation. *Plant Cell* **14**: 2339-2351.
- Himanen, K., Vuylsteke, M., Vanneste, S., Vercruyse, S., Boucheron, E., Alard, P., Chriqui, D., Van Montagu, M., Inzé, D., and Beeckman, T.** (2004). Transcript profiling of early lateral root initiation. *Proc Natl Acad Sci U S A.* **101**: 5146-5151.
- Hirota, A., Kato, T., Fukaki, H., Aida, M., and Tasaka, M.** (2007). The auxin-regulated AP2/EREBP gene *PUCHI* is required for morphogenesis in the early lateral root primordium of *Arabidopsis*. *Plant Cell* **19**: 2156-2168.
- Hobbie, L., McGovern, M., Hurwitz, L. R., Pierro, A., Liu, N. Y., Bandyopadhyay, A., and Estelle, M.** (2000). The *axr6* mutants of *Arabidopsis thaliana* define a gene involved in auxin response and early development. *Development* **127**: 23-32.
- Hou, H., Erickson, J., Meservy, J., and Schultz, E. A.** (2010). *FORKED1* encodes a PH domain protein that is required for PIN1 localization in developing leaf veins. *Plant J.* **63**: 960-973.
- Hou, Y., von Arnim, A. G., and Deng, X.** (1993). A new class of *Arabidopsis* constitutive photomorphogenic genes involved in regulating cotyledon development. *Plant Cell* **5**: 329-339.
- Imai, K. K., Ohashi, Y., Tsuge, T., Yoshizumi, T., Matsui, M., Oka, A., and Aoyama, T.** (2006). The A-type cyclin CYCA2;3 is a key regulator of ploidy levels in *Arabidopsis* endoreduplication. *Plant Cell* **18**: 382-396.
- Imaizumi, T., Schultz, T. F., Harmon, F. G., Ho, L. A., and Kay, S. A.** (2005). FKF1 F-box protein mediates cyclic degradation of a repressor of *CONSTANS* in *Arabidopsis*. *Science* **309**: 293-297.
- Inoue, T., Higuchi, M., Hashimoto, Y., Seki, M., Kobayashi, M., Kato, T., Tabata, S., Shinozaki, K., and Kakimoto, T.** (2001). Identification of CRE1 as a cytokinin receptor from *Arabidopsis*. *Nature* **409**: 1060-1063.
- Inukai, Y., Sakamoto, T., Ueguchi-Tanaka, M., Shibata, Y., Gomi, K., Umemura, I., Hasegawa, Y., Ashikari, M., Kitano, H., and Matsuoka, M.** (2005). *CROWN ROOTLESS1*, which is essential for crown root formation in rice,

- is a target of an auxin response factor in auxin signaling. *Plant Cell* **17**: 1387-1396.
- Inze, D. and De Veylder, L.** (2006). Cell cycle regulation in plant development. *Annu Rev Genet.* **40**: 77-105.
- Ishida, K., Yamashino, T., Yokoyama, A., and Mizuno, T.** (2008). Three type-B response regulators, ARR1, ARR10, and ARR12, play essential but redundant roles in cytokinin signal transduction throughout the life cycle of *Arabidopsis thaliana*. *Plant Cell Physiol.* **49**: 47-57.
- Ishida, T., Adachi, S., Yoshimura, M., Shimizu, K., Umeda, M., and Sugimoto, K.** (2010). Auxin modulates the transition from the mitotic cycle to the endocycle in *Arabidopsis*. *Development* **137**: 63-71.
- Ito, T., Sakai, H., and Meyerowitz, E. M.** (2003). Whorl-specific expression of the *SUPERMAN* gene of *Arabidopsis* is mediated by *cis*-elements in the transcribed region. *Curr Biol.* **13**: 1524-1530.
- Jackson, V.** (1978). Studies on histone organization in the nucleosome using formaldehyde as a reversible cross-linking agent. *Cell* **15**: 945-954.
- Jacobs, M. and Rubery, P. H.** (1988). Naturally occurring auxin transport regulators. *Science* **241**: 346-349.
- James, C. G., Woods, A., Underhill, T. M., and Beier, F.** (2006). The transcription factor *ATF3* is upregulated during chondrocyte differentiation and represses cyclin D1 and A gene transcription. *BMC Mol Biol.* **7**: 30.
- Jeffrey, P. D., Russo, A. A., Polyak, K., Gibbs, E., Hurwitz, J., Massague, J., Pavletich, N. P.** (1995). Mechanism of CDK activation revealed by the structure of a cyclinA-CDK2 complex. *Nature* **376**: 313-320.
- Jost, L.** (1942). Uber Gefassbrucken. *Zeitsch Bot.* **38**: 161-215.
- Kang, H. and Singh, K. B.** (2000). Characterization of salicylic acid-responsive, *Arabidopsis* DOF domain proteins: overexpression of *OBP3* leads to growth defects. *Plant J.* **21**: 329-339.
- Kang, J. and Dengler, N. G.** (2002). Cell cycling frequency and expression of the homeobox gene *ATHB-8* during leaf vein development in *Arabidopsis*. *Planta* **216**: 212-219.
- Kang, J. and Dengler, N.** (2004). Vein pattern development in adult leaves of *Arabidopsis thaliana*. *Int J Plant Sci* **165**: 231-242.

- Kang, J., Mizukami, Y., Wang, H., Fowke, L., and Dengler, N. G.** (2007). Modification of cell proliferation patterns alters leaf vein architecture in *Arabidopsis thaliana*. *Planta* **226**: 1207-1218.
- Kepinski, S. and Leyser, O.** (2005). The *Arabidopsis* F-box protein TIR1 is an auxin receptor. *Nature* **435**: 446-451.
- Kinsman, E. A. and Pyke, K. A.** (1998). Bundle sheath cells and cell-specific plastid development in *Arabidopsis* leaves. *Development* **125**: 1815-1822.
- Kleine-Vehn, J., Huang, F., Naramoto, S., Zhang, J., Michniewicz, M., Offringa, R., and Friml, J.** (2009). PIN auxin efflux carrier polarity is regulated by PINOID kinase-mediated recruitment into GNOM-independent trafficking in *Arabidopsis*. *Plant Cell* **21**: 3839-3849.
- Klucking, E. P.** (1992). *Leaf venation patterns*. Berlin: J. Cramer.
- Koff, A., Giordano, A., Desai, D., Yamashita, K., Harper, J. W., Elledge, S., Nishimoto, T., Morgan, D. O., Franza, B. R., and Roberts, J. M.** (1992). Formation and activation of a Cyclin E-cdk2 complex during the G₁ phase of the human cell cycle. *Science* **257**: 1689-1694.
- Koizumi, K., Naramoto, S., Sawa, S., Yahara, N., Ueda, T., Nakano, A., Sugiyama, M., and Fukuda, H.** (2005). VAN3 ARF-GAP-mediated vesicle transport is involved in leaf vascular network formation. *Development* **132**: 1699-1711.
- Koizumi, K., Sugiyama, M., and Fukuda, H.** (2000). A series of novel mutants of *Arabidopsis thaliana* that are defective in the formation of continuous vascular network: calling the auxin signal flow canalization hypothesis into question. *Development* **127**: 3197-3204.
- Konishi, M. and Yanagisawa, S.** (2007). Sequential activation of two *DOF* transcription factor gene promoters during vascular development in *Arabidopsis thaliana*. *Plant Physiol Biochem.* **45**: 623-629.
- Koshino-Kimura, Y., Wada, T., Tachibana, T., Tsugeki, R., Ishiguro, S., and Okada, K.** (2005). Regulation of *CAPRICE* transcription by MYB proteins for root epidermis differentiation in *Arabidopsis*. *Plant Cell Physiol.* **46**: 817-826.
- Krecek, P., Skupa, P., Libus, J., Naramoto, S., Tejos, R., Friml, J., and Zazimalova, E.** (2009). The PIN-FORMED (PIN) protein family of auxin transporters. *Genome Biol.* **10**: 249.
- Krogan, N. T., Ckurshumova, W., Marcos, D., Caragea, A. E., and Berleth, T.** (2012). Deletion of *MP/ARF5* domains III and IV reveals a requirement for

- AUX/IAA* regulation in *Arabidopsis* leaf vascular patterning. *New Phytol.* **194**: 391-401.
- Kubo, M., Udagawa, M., Nishikubo, N., Horiguchi, G., Yamaguchi, M., Ito, J., Mimura, T., Fukuda, H., and Demura, T.** (2005). Transcription switches for protoxylem and metaxylem vessel formation. *Genes Dev.* **19**: 1855-1860.
- Kwon, C. S., Hibara, K., Pfluger, J., Bezhani, S., Metha, H., Aida, M., Tasaka, M., and Wagner, D.** (2006). A role for chromatin remodeling in regulation of *CUC* gene expression in the *Arabidopsis* cotyledon boundary. *Development* **133**: 3223-3230.
- Lai, L. B., Nadeau, J. A., Lucas, J., Lee, E., Nakagawa, T., Zhao, L., Geisler, M., and Sack, F. D.** (2005). The *Arabidopsis* R2R3 MYB proteins FOUR LIPS and MYB88 restrict divisions late in the stomatal cell lineage. *Plant Cell* **17**: 2754-2767.
- Larson, P. R.** (1975). Development and organization of the primary vascular system in *Populus deltoides* according to phyllotaxy. *Am J Bot.* **62**: 1084-1099.
- Lau, S., De Smet, I., Kolb, M., Meinhardt, H., and Jurgens, G.** (2011). Auxin triggers a genetic switch. *Nat Cell Biol.* **13**: 611-615.
- Lauber, M. H., Waizenegger, I., Steinmann, T., Schwarz, H., Mayer, U., Hwang, I., Lukowitz, W., and Jurgens, G.** (1997). The *Arabidopsis* KNOLLE protein is a cytokinesis-specific syntaxin. *J Cell Biol.* **139**: 1485-1493.
- Lawton, M. A., Dean, S. M., Dron, M., Kooter, J. M., Kragh, K. M., Harrison, M. J., Yu, L., Tanguay, L., Dixon, R. A., and Lamb, C. J.** (1991). Silencer region of a chalcone synthase promoter contains multiple binding sites for a factor, SBF-1, closely related to GT-1. *Plant Mol Biol.* **16**: 235-249.
- Lee, D. J., Park, J. W., Lee, H. W., and Kim, J.** (2009). Genome-wide analysis of the auxin-responsive transcriptome downstream of *iaa1* and its expression analysis reveal the diversity and complexity of auxin-regulated gene expression. *J Exp Bot.* **60**: 3935-3957.
- Lee, J., Colinas, J., Wang, J. Y., Mace, D., Ohler, U., and Benfey, P. N.** (2006). Transcriptional and posttranscriptional regulation of transcription factor expression in *Arabidopsis* roots. *Proc Natl Acad Sci U S A.* **103**: 6055-6060.
- Lee, M., Kim, B., Song, S., Heo, J., Yu, N., Lee, S. A., Kim, M., Kim, D. G., Sohn, S. O., Lim, C. E., Chang, K. S., Lee, M. M., and Lim, J.** (2008). Large-scale analysis of the *GRAS* gene family in *Arabidopsis thaliana*. *Plant Mol Biol.* **67**: 659-670.

- Lee, S., Cheng, H., King, K. E., Wang, W., He, Y., Hussain, A., Lo, J., Harberd, N. P., and Peng, J.** (2002). Gibberellin regulates *Arabidopsis* seed germination via *RGL2*, a *GAI/RGA*-like gene whose expression is up-regulated following imbibition. *Genes Dev.* **16**: 646-658.
- Leroy, O., Hennig, L., Breuninger, H., Laux, T., and Kohler, C.** (2007). Polycomb group proteins function in the female gametophyte to determine seed development in plants. *Development* **134**: 3639-3648.
- Lescot, M., Dehais, P., Thijs, G., Marchal, K., Moreau, Y., Van de Peer, Y., Rouze, P., and Rombauts, S.** (2002). PlantCARE, a database of plant *cis*-acting regulatory elements and a portal to tools for *in silico* analysis of promoter sequences. *Nucleic Acids Res.* **30**: 325-327.
- Levesque, M. P., Vernoux, T., Busch, W., Cui, H. C., Wang, J. Y., Blilou, I., Hassan, H., Nakajima, K., Matsumoto, N., Lohmann, J. U., Scheres, B., and Benfey, P. N.** (2006). Whole-genome analysis of the SHORT-ROOT developmental pathway in *Arabidopsis*. *PLoS Biology* **4**: e143.
- Li, H., Johnson, P., Stepanova, A., Alonso, J. M., and Ecker, J. R.** (2004). Convergence of signaling pathways in the control of differential cell growth in *Arabidopsis*. *Dev Cell* **7**: 193-204.
- Li, H., Xu, L., Wang, H., Yuan, Z., Cao, X., Yang, Z., Zhang, D., Xu, Y., and Huang, H.** (2005). The putative RNA-dependent RNA polymerase *RDR6* acts synergistically with *ASYMMETRIC LEAVES1* and 2 to repress *BREVIPEDICELLUS* and *microRNA165/166* in *Arabidopsis* leaf development. *Plant Cell* **17**: 2157-2171.
- Li, J., Bush, J., Xiong, Y., Li, L., and McCormack, M.** (2011). Large-scale protein-protein interaction analysis in *Arabidopsis* mesophyll protoplasts by split firefly luciferase complementation. *PLoS ONE* **6**: e27364.
- Li, J., Dai, X., and Zhao, Y.** (2006). A role for *AUXIN RESPONSE FACTOR19* in auxin and ethylene signaling in *Arabidopsis*. *Plant Physiol.* **140**: 899-908.
- Li, L. and Vaessin, H.** (2000). Pan-neural Prospero terminates cell proliferation during *Drosophila* neurogenesis. *Genes Dev.* **14**: 147-151.
- Li, Y., Liu, Z. B., Shi, X., Hagen, G., and Guilfoyle, T. J.** (1994). An auxin-inducible element in soybean *SAUR* promoters. *Plant Physiol.* **106**: 37-43.
- Lindqvist, A., Rodriguez-Bravo, V., and Medema, R. H.** (2009). The decision to enter mitosis: feedback and redundancy in the mitotic entry network. *J Cell Biol.* **185**: 193-202.

- Liu, C., Xu, Z., and Chua, N.** (1993). Auxin polar transport is essential for the establishment of bilateral symmetry during early plant embryogenesis. *Plant Cell* **5**: 621-630.
- Liu, Z., Ulmasov, T., Shi, X., Hagen, G., and Guilfoyle, T. J.** (1994). Soybean *GH3* promoter contains multiple auxin-inducible elements. *Plant Cell* **6**: 645-657.
- Long, J. A., Ohno, C., Smith, Z. R., and Meyerowitz, E. M.** (2006). TOPLESS regulates apical embryonic fate in *Arabidopsis*. *Science* **312**: 1520-1523.
- Loots, G. G. and Ovcharenko, I.** (2004). rVISTA 2.0: evolutionary analysis of transcription factor binding sites. *Nucleic Acids Res.* **32**: W217-W221.
- Lorrain, S., Lin, B., Auriac, M. C., Kroj, T., Saindrenan, P., Nicole, M., Balague, C., and Roby, D.** (2004). VASCULAR ASSOCIATED DEATH1, a novel GRAM domain-containing protein, is a regulator of cell death and defense responses in vascular tissues. *Plant Cell* **16**: 2217-2232.
- Louis, J.** (1935). L'ontogenese du systeme conducteur dans la pousse feuillée des Dicotyles et des Gymnospermes. *La Cellule* **44**: 87-172.
- Lu, P. and Werb, Z.** (2008). Patterning mechanisms of branched organs. *Science* **322**: 1506-1509.
- Mahonen, A. P., Bonke, M., Kauppinen, L., Riikonen, M., Benfey, P. N., and Helariutta, Y.** (2000). A novel two-component hybrid molecule regulates vascular morphogenesis of the *Arabidopsis* root. *Genes Dev.* **14**: 2938-2943.
- Malamy, J. E. and Benfey, P. N.** (1997). Organization and cell differentiation in lateral roots of *Arabidopsis thaliana*. *Development* **124**: 33-44.
- Marrocco, K., Thomann, A., Parmentier, Y., Genschik, P., and Criqui, M. C.** (2009). The APC/C E3 ligase remains active in most post-mitotic *Arabidopsis* cells and is required for proper vasculature development and organization. *Development* **136**: 1475-1485.
- Martinez, A. M., Colomb, S., Dejardin, J., Bantignies, F., and Cavalli, G.** (2006). Polycomb group-dependent *Cyclin A* repression in *Drosophila*. *Genes Dev.* **20**: 501-513.
- Martin-Trillo, M., Lazaro, A., Poethig, R. S., Gomez-Mena, C., Pineiro, M. A., Martinez-Zapater, J. M., and Jarillo, J. A.** (2006). *EARLY IN SHORT DAYS1 (ESD1)* encodes ACTIN-RELATED PROTEIN6 (AtARP6), a putative component of chromatin remodeling complexes that positively regulates FLC accumulation in *Arabidopsis*. *Development* **133**: 1241-1252.

- Mason, M. G., Li, J., Mathews, D. E., Kieber, J. J., and Schaller, G. E.** (2004). Type-B response regulators display overlapping expression patterns in *Arabidopsis*. *Plant Physiol.* **135**: 927-937.
- Matsushime, H., Roussel, M. F., Ashmun, R. A., and Sherr, C. J.** (1991). COLONY-STIMULATING FACTOR1 regulates novel cyclins during the G1 phase of the cell cycle. *Cell* **65**: 701-713.
- Mattsson, J., Ckurshumova, W., and Berleth, T.** (2003). Auxin signaling in *Arabidopsis* leaf vascular development. *Plant Physiol.* **131**: 1327-1339.
- Mattsson, J., Sung, Z. R., and Berleth, T.** (1999). Responses of plant vascular systems to auxin transport inhibition. *Development* **126**: 2979-2991.
- Mayer, U., Buttner, G., and Jurgens, G.** (1993). Apical-basal pattern formation in the *Arabidopsis* embryo: studies on the role of the *GNOM* gene. *Development* **117**: 149-162.
- Mayer, U., Torres-Ruiz, R. A., Berleth, T., Misera, S., and Jurgens, G.** (1991). Mutations affecting body organization in the *Arabidopsis* embryo. *Nature* **353**: 402-407.
- Melaragno, J. E., Mehrotra, B., and Coleman, A. W.** (1993). Relationship between endopolyploidy and cell size in epidermal tissue of *Arabidopsis*. *Plant Cell* **5**: 1661-1668.
- Menges, M., de Jager, S. M., Gruissem, W., and Murray, J. A. H.** (2005). Global analysis of the core cell cycle regulators of *Arabidopsis* identifies novel genes, reveals multiple and highly specific profiles of expression, and provides a coherent model for plant cell cycle control. *Plant J.* **41**: 546-566.
- Metzger, R. J. and Krasnow, M. A.** (1999). Genetic control of branching morphogenesis. *Science* **284**: 1635-1639.
- Michniewicz, M., Zago, M. K., Abas, L., Weijers, D., Schweighofer, A., Meskiene, I., Heisler, M. G., Ohno, C., Zhang, J., Huang, F., Schwab, R., Weigel, D., Meyerowitz, E. M., Luschnig, C., Offringa, R., and Friml, J.** (2007). Antagonistic regulation of PIN phosphorylation by PP2A and PINOID directs auxin flux. *Cell* **130**: 1044-1056.
- Miyashima, S., Koi, S., Hashimoto, T., and Nakajima, K.** (2011). Non-cell-autonomous *microRNA165* acts in a dose-dependent manner to regulate multiple differentiation status in the *Arabidopsis* root. *Development* **138**: 2303-2313.
- Mockaitis, K. and Estelle, M.** (2008). Auxin receptors and plant development: a new signaling paradigm. *Annu Rev Cell Dev Biol.* **24**: 55-80.

Mordhorst, A. P., Voerman, K. J., Hartog, M. V., Meijer, E. A., van Went, J., Koornneef, M., and de Vries, S. C. (1998). Somatic embryogenesis in *Arabidopsis thaliana* is facilitated by mutations in genes repressing meristematic cell divisions. *Genetics* **149**: 549-563.

Morgan, D. O. (1995). Principles of CDK regulation. *Nature* **374**: 131-134.

Morgan, D. O. (1997). CYCLIN-DEPENDENT KINASES: engines, clocks, and microprocessors. *Annu Rev Cell Dev Biol.* **13**: 261-291.

Motokura, T. and Arnold, A. (1993). Cyclin D and oncogenesis. *Curr Opin Genet Dev.* **3**: 5-10.

Moyroud, E., Minguet, E. G., Ott, F., Yant, L., Pose, D., Monniaux, M., Blanchet, S., Bastien, O., Thevenon, E., Weigel, D., Schmid, M. and Parcy, F. (2011). Prediction of regulatory interactions from genome sequences using a biophysical model for the *Arabidopsis* LEAFY transcription factor. *Plant Cell* **23**: 1293-1306.

Muller, B. and Sheen, J. (2007). Advances in cytokinin signaling. *Science* **318**: 68-69.

Mustroph, A., Zanetti, M. E., Jang, C. J. H., Holtan, H. E., Repetti, P. P., Galbraith, D. W., Girke, T., and Bailey-Serres, J. (2009). Profiling transcriptomes of discrete cell populations resolves altered cellular priorities during hypoxia in *Arabidopsis*. *Proc Natl Acad Sci U S A.* **106**: 18843-18848.

Myster, D. L. and Duronio, R. J. (2000). Cell cycle: to differentiate or not to differentiate? *Curr Biol.* **10**: R302-R304.

Nagaki, K., Talbert, P. B., Zhong, C. X., Dawe, R. K., Henikoff, S., and Jiang, J. (2003). Chromatin immunoprecipitation reveals that the 180-bp satellite repeat is the key functional DNA element of *Arabidopsis thaliana* centromeres. *Genetics* **163**: 1221-1225.

Nagpal, P., Ellis, C. M., Weber, H., Ploense, S. E., Barkawi, L. S., Guilfoyle, T. J., Hagen, G., Alonso, J. M., Cohen, J. D., Farmer, E. E., Ecker, J. R. and Reed, J. W. (2005). Auxin response factors ARF6 and ARF8 promote jasmonic acid production and flower maturation. *Development* **132**: 4107-4118.

Nakajima, K., Sena, G., Nawy, T., and Benfey, P. N. (2001). Intercellular movement of the putative transcription factor SHR in root patterning. *Nature* **413**: 307-311.

- Nakamura, R. L., McKendree Jr., W. L., Hirsch, R. E., Sedbrook, J. C., Gaber, R. F., and Sussman, M. R.** (1995). Expression of an *Arabidopsis* potassium channel gene in guard cells. *Plant Physiol.* **109**: 371-374.
- Naramoto, S., Sawa, S., Koizumi, K., Uemura, T., Ueda, T., Friml, J., Nakano, A., and Fukuda, H.** (2009). Phosphoinositide-dependent regulation of VAN3 ARF-GAP localization and activity essential for vascular tissue continuity in plants. *Development* **136**: 1529-1538.
- Nelson, T. M. and Dengler, N. G.** (1997). Leaf vascular pattern formation. *Plant Cell* **9**: 1121-1135.
- Niehrs, C. and Pollet, N.** (1999). Synexpression groups in eukaryotes. *Nature* **402**: 483-487.
- Normanly, J.** (2010). Approaching cellular and molecular resolution of auxin biosynthesis and metabolism. *Cold Spring Harb Perspect Biol.* **2**: a001594.
- O'Connor, T. R., Dyreson, C., and Wyrick, J. J.** (2005). Athena: a resource for rapid visualization and systematic analysis of *Arabidopsis* promoter sequences. *Bioinformatics* **21**: 4411-4413.
- Ohashi-Ito, K. and Bergmann, D. C.** (2006). *Arabidopsis* FAMA controls the final proliferation/differentiation switch during stomatal development. *Plant Cell* **18**: 2493-2505.
- Okada, K., Ueda, J., Komaki, M. K., Bell, C. J., and Shimura, Y.** (1991). Requirement of the auxin polar transport system in early stages of *Arabidopsis* floral bud formation. *Plant Cell* **3**: 677-684.
- Okushima, Y., Overvoorde, P. J., Arima, K., Alonso, J. M., Chan, A., Chang, C., Ecker, J. R., Hughes, B., Lui, A., Nguyen, D., Onodera, C., Quach, H., Smith, A., Yu, G., and Theologis, A.** (2005). Functional genomic analysis of the *AUXIN RESPONSE FACTOR* gene family members in *Arabidopsis thaliana*: unique and overlapping functions of *ARF7* and *ARF19*. *Plant Cell* **17**: 444-463.
- Okushima, Y., Fukaki, H., Onoda, M., Theologis, A., and Tasaka, M.** (2007). *ARF7* and *ARF19* regulate lateral root formation via direct activation of *LBD/ASL* genes in *Arabidopsis*. *Plant Cell* **19**: 118-130.
- Ouwerkerk, P. B. F., Trimborn, T. O., Hilliou, F., and Memelink, J.** (1999). Nuclear factors GT-1 and 3AF1 interact with multiple sequences within the promoter of the *TDC* gene from Madagascar periwinkle: GT-1 is involved in UV light-induced expression. *Mol Gen Genet.* **261**: 610-622.

Paciorek, T., Zazimalova, E., Ruthardt, N., Petrasek, J., Stierhof, Y., Kleine-Vehn, J., Morris, D. A., Emans, N., Jurgens, G., Geldner, N. and Friml, J. (2005). Auxin inhibits endocytosis and promotes its own efflux from cells. *Nature* **435**: 1251-1256.

Palma, K., Zhao, Q., Cheng, Y. T., Bi, D., Monaghan, J., Cheng, W., Zhang, Y., and Li, X. (2007). Regulation of plant innate immunity by three proteins in a complex conserved across the plant and animal kingdoms. *Genes Dev.* **21**: 1484-1493.

Pan, J., Nakade, K., Huang, Y., Zhu, Z., Masuzaki, S., Hasegawa, H., Murata, T., Yoshiki, A., Yamaguchi, N., Lee, C., Yang, W., Tsai, E., Obata, Y. and Yokoyama, K. K. (2010). Suppression of cell-cycle progression by Jun dimerization protein (JDP2) involves downregulation of cyclin-A2. *Oncogene* **29**: 6245-6256.

Paponov, I. A., Paponov, M., Teale, W., Menges, M., Chakrabortee, S., Murray, J. A. H., and Palme, K. (2008). Comprehensive transcriptome analysis of auxin responses in *Arabidopsis*. *Mol Plant* **1**: 321-337.

Payne, R. W. (2010). *Genstat Release 13 Reference Manual, Part 3: Procedure Library PL21*. Oxford, UK: VSN International.

Payton, M. and Coats, S. (2002). Cyclin E2, the cycle continues. *Int J Biochem Cell Biol.* **34**: 315-320.

Peer, W. A. and Murphy, A. S. (2007). Flavonoids and auxin transport: modulators or regulators? *Trends Plant Sci.* **12**: 556-563.

Peng, J., Carol, P., Richards, D. E., King, K. E., Cowling, R. J., Murphy, G. P., and Harberd, N. P. (1997). The *Arabidopsis* *GAI* gene defines a signaling pathway that negatively regulates gibberellin responses. *Genes Dev.* **11**: 3194-3205.

Petersson, S. V., Johansson, A. I., Kowalczyk, M., Makoveychuk, A., Wang, J. Y., Moritz, T., Grebe, M., Benfey, P. N., Sandberg, G., and Ljung, K. (2009). An auxin gradient and maximum in the *Arabidopsis* root apex shown by high-resolution cell-specific analysis of IAA distribution and synthesis. *Plant Cell* **21**: 1659-1668.

Petrasek, J. and Friml, J. (2009). Auxin transport routes in plant development. *Development* **136**: 2675-2688.

Petrasek, J., Mravec, J., Bouchard, R., Blakeslee, J. J., Abas, M., Seifertova, D., Wisniewska, J., Tadele, Z., Kubes, M., Covanova, M., Dhonukshe, P., Skupa, P., Benkova, E., Perry, L., Krecek, P., Lee, O. R., Fink, G. R., Geisler,

- M., Murphy, A. S., Luschnig, C., Zazimalova, E., and Friml, J.** (2006). PIN proteins perform a rate-limiting function in cellular auxin efflux. *Science* **312**: 914-918.
- Petricka, J. J. and Nelson, T. M.** (2007). *Arabidopsis* nucleolin affects plant development and patterning. *Plant Physiol.* **144**: 173-186.
- Pineau, C., Freydier, A., Ranocha, P., Jauneau, A., Turner, S., Lemonnier, G., Renou, J., Tarkowski, P., Sandberg, G., Jouanin, L., Sundberg, B., Boudet, A., Goffner, D., and Pichon, M.** (2005). *hca*: an *Arabidopsis* mutant exhibiting unusual cambial activity and altered vascular patterning. *Plant J.* **44**: 271-289.
- Pines, J. and Hunter, T.** (1990). Human cyclin A is adenovirus E1A-associated protein p60 and behaves differently from cyclin B. *Nature* **346**: 760-763.
- Ponnusamy, S., Alderson, N. L., Hama, H., Bielawski, J., Jiang, J. C., Bhandari, R., Snyder, S. H., Jazwinski, S. M., and Ogretmen, B.** (2008). Regulation of telomere length by fatty acid elongase 3 in yeast: involvement of inositol phosphate metabolism and Ku70/80 function. *J Biol Chem.* **283**: 27514-27524.
- Prigge, M. J., Otsuga, D., Alonso, J. M., Ecker, J. R., Drews, G. N., and Clark, S. E.** (2005). Class III HOMEODOMAIN-LEUCINE ZIPPER gene family members have overlapping, antagonistic, and distinct roles in *Arabidopsis* development. *Plant Cell* **17**: 61-76.
- Przemeck, G. K. H., Mattsson, J., Hardtke, C. S., Sung, Z. R., and Berleth, T.** (1996). Studies on the role of the *Arabidopsis* gene *MONOPTEROS* in vascular development and plant cell axialization. *Planta* **200**: 229-237.
- Pullen, M., Clark, N., Zarinkamar, F., Topping, J., and Lindsey, K.** (2010). Analysis of vascular development in the *hydra* sterol biosynthetic mutants of *Arabidopsis*. *PLoS ONE* **5**: e12227.
- Pysh, L. D., Wysocka-Diller, J. W., Camilleri, C., Bouchez, D., and Benfey, P. N.** (1999). The *GRAS* gene family in *Arabidopsis*: sequence characterization and basic expression analysis of the *SCARECROW-LIKE* genes. *Plant J.* **18**: 111-119.
- Ramialison, M., Bajoghli, B., Aghaallaei, N., Ettwiller, L., Gaudan, S., Wittbrodt, B., Czerny, T., and Wittbrodt, J.** (2008). Rapid identification of PAX2/5/8 direct downstream targets in the otic vesicle by combinatorial use of bioinformatics tools. *Genome Biol.* **9**: R145.

- Ramialison, M., Reinhardt, R., Henrich, T., Wittbrodt, B., Kellner, T., Lowy, C. M., and Wittbrodt, J.** (2012). *Cis*-regulatory properties of medaka synexpression groups. *Development* **139**: 917-928.
- Raven, J. A.** (1975). Transport of indoleacetic acid in plant cells in relation to pH and electrical potential gradients, and its significance for polar IAA transport. *New Phytol.* **74**: 163-172.
- Reed, J. W.** (2001). Roles and activities of AUX/IAA proteins in *Arabidopsis*. *Trends Plant Sci.* **6**: 420-425.
- Reichheld, J., Chaubet, N., Shen, W. H., Renaudin, J., and Gigot, C.** (1996). Multiple A-type cyclins express sequentially during the cell cycle in *Nicotiana tabacum* BY2 cells. *Proc Natl Acad Sci U S A.* **93**: 13819-13824.
- Renaudin, J., Colasanti, J., Rime, H., Yuan, Z., and Sundaresan, V.** (1994). Cloning of four cyclins from maize indicates that higher plants have three structurally distinct groups of mitotic cyclins. *Proc Natl Acad Sci U S A.* **91**: 7375-7379.
- Rhoades, M. W., Reinhart, B. J., Lim, L. P., Burge, C. B., Bartel, B., and Bartel, D. P.** (2002). Prediction of plant microRNA targets. *Cell* **110**: 513-520.
- Robles, P., Fleury, D., Candela, H., Cnops, G., Alonso-Peral, M. M., Anami, S., Falcone, A., Caldana, C., Willmitzer, L., Ponce, M. R., Van Lijsebettens, M. and Micol, J. L.** (2010). The *RON1/FRY1/SAL1* gene is required for leaf morphogenesis and venation patterning in *Arabidopsis*. *Plant Physiol.* **152**: 1357-1372.
- Rosso, M. G., Li, Y., Strizhov, N., Reiss, B., Dekker, K., and Weisshaar, B.** (2003). An *Arabidopsis thaliana* T-DNA mutagenized population (GABI-Kat) for flanking sequence tag-based reverse genetics. *Plant Mol Biol.* **53**: 247-259.
- Rouse, D., Mackay, P., Stirnberg, P., Estelle, M., and Leyser, O.** (1998). Changes in auxin response from mutations in an AUX/IAA gene. *Science* **279**: 1371-1373.
- Rubery, P. H. and Sheldrake, A. R.** (1974). Carrier-mediated auxin transport. *Planta* **118**: 101-121.
- Sablowski, R. W. M. and Meyerowitz, E. M.** (1998). A homolog of *NO APICAL MERISTEM* is an immediate target of the floral homeotic genes *APETALA3/PISTILLATA*. *Cell* **92**: 93-103.
- Sachs, T.** (1975). The control of the differentiation of vascular networks. *Ann Bot.* **39**: 197-204.

- Sachs, T.** (1981). The control of the patterned differentiation of vascular tissues. *Adv Bot Res.* **9**: 151-262.
- Sachs, T.** (1989). The development of vascular networks during leaf development. *Curr Top Plant Biochem Physiol.* **8**: 168-183.
- Sachs, T.** (1991). Cell polarity and tissue patterning in plants. *Development Suppl.* **1**: 83-93.
- Saibo, N. J. M, Vriezen, W. H., De Grauwe, L., Azmi, A., Prinsen, E., and Van Der Straeten, D.** (2007). A comparative analysis of the *Arabidopsis* mutant *amp1-1* and a novel weak *amp1* allele reveals new functions of the AMP1 protein. *Planta* **225**: 831-842.
- Sakai, H., Aoyama, T., and Oka, A.** (2000). *Arabidopsis* ARR1 and ARR2 response regulators operate as transcriptional activators. *Plant J.* **24**: 703-711.
- Satyanarayana, A. and Kaldis, P.** (2009). Mammalian cell-cycle regulation: several Cdks, numerous cyclins and diverse compensatory mechanisms. *Oncogene* **28**: 2925-2939.
- Sauer, M., Balla, J., Luschnig, C., Wisniewska, J., Reinohl, V., Friml, J., and Benkova, E.** (2006). Canalization of auxin flow by AUX/IAA-ARF-dependent feedback regulation of PIN polarity. *Genes Dev.* **20**: 2902-2911.
- Sawa, S., Ohgishi, M., Goda, H., Higuchi, K., Shimada, Y., Yoshida, S., and Koshiba, T.** (2002). The *HAT2* gene, a member of the *HD-ZIP* gene family, isolated as an auxin inducible gene by DNA microarray screening, affects auxin response in *Arabidopsis*. *Plant J.* **32**: 1011-1022.
- Sawchuk, M. G., Donner, T. J., Head, P., and Scarpella, E.** (2008). Unique and overlapping expression patterns among members of photosynthesis-associated nuclear gene families in *Arabidopsis*. *Plant Physiol.* **148**: 1908-1924.
- Sawchuk, M. G., Head, P., Donner, T. J., and Scarpella, E.** (2007). Time-lapse imaging of *Arabidopsis* leaf development shows dynamic patterns of procambium formation. *New Phytol.* **176**: 560-571.
- Scacchi, E., Salinas, P., Gujas, B., Santuari, L., Krogan, N., Ragni, L., Berleth, T., and Hardtke, C. S.** (2010). Spatio-temporal sequence of cross-regulatory events in root meristem growth. *Proc Natl Acad Sci U S A.* **107**: 22734-22739.
- Scarpella, E., Francis, P., and Berleth, T.** (2004). Stage-specific markers define early steps of procambium development in *Arabidopsis* leaves and correlate

termination of vein formation with mesophyll differentiation. *Development* **131**: 3445-3455.

Scarpella, E., Marcos, D., Friml, J., and Berleth, T. (2006). Control of leaf vascular patterning by polar auxin transport. *Genes Dev.* **20**: 1015-1027.

Scarpella, E., Rueb, S., and Meijer, A. H. (2003). The *RADICLELESS1* gene is required for vascular pattern formation in rice. *Development* **130**: 645-658.

Schellmann, S., Schnittger, A., Kirik, V., Wada, T., Okada, K., Beermann, A., Thumfahrt, J., Jurgens, G., and Hulskamp, M. (2002). *TRIPTYCHON* and *CAPRICE* mediate lateral inhibition during trichome and root hair patterning in *Arabidopsis*. *EMBO J.* **21**: 5036-5046.

Schlereth, A., Moller, B., Liu, W., Kientz, M., Flipse, J., Rademacher, E. H., Schmid, M., Jurgens, G., and Weijers, D. (2010). *MONOPTEROS* controls embryonic root initiation by regulating a mobile transcription factor. *Nature* **464**: 913-916.

Schnittger, A., Schobinger, U., Stierhof, Y., and Hulskamp, M. (2002). Ectopic B-type cyclin expression induces mitotic cycles in endoreduplicating *Arabidopsis* trichomes. *Curr Biol.* **12**: 415-420.

Schubert, D., Primavesi, L., Bishopp, A., Roberts, G., Doonan, J., Jenuwein, T., and Goodrich, J. (2006). Silencing by plant *POLYCOMB*-group genes requires dispersed trimethylation of histone H3 at lysine 27. *EMBO J.* **25**: 4638-4649.

Schuetz, M., Berleth, T., and Mattsson, J. (2008). Multiple *MONOPTEROS*-dependent pathways are involved in leaf initiation. *Plant Physiol.* **148**: 870-880.

Sebastian, S., Sreenivas, P., Sambasivan, R., Cheedipudi, S., Kandalla, P., Pavlath, G. K., and Dhawan, J. (2009). *MLL5*, a trithorax homolog, indirectly regulates H3K4 methylation, represses cyclin A2 expression, and promotes myogenic differentiation. *Proc Natl Acad Sci U S A.* **106**: 4719-4724.

Setiady, Y. Y., Sekine, M., Hariguchi, N., Yamamoto, T., Kouchi, H., and Shinmyo, A. (1995). Tobacco mitotic cyclins: cloning, characterization, gene expression, and functional assay. *Plant J.* **8**: 949-957.

Shaner, N. C., Campbell, R. E., Steinbach, P. A., Giepmans, B. N. G., Palmer, A. E., and Tsien, R. Y. (2004). Improved monomeric red, orange, and yellow fluorescent proteins derived from *Discosoma* sp. red fluorescent protein. *Nat Biotechnol.* **22**: 1567-1572.

Shaul, O., Mironov, V., Burssens, S., Van Montagu, M., and Inze, D. (1996). Two *Arabidopsis* cyclin promoters mediate distinctive transcriptional oscillation in synchronized tobacco BY-2 cells. *Proc Natl Acad Sci U S A.* **93**: 4868-4872.

Sherr, I. (2012). Regulation of auxin transport in *Arabidopsis* leaf vascular development. (M.Sc. thesis). Retrieved from <http://era.library.ualberta.ca/public/view/item/uuid:aef9c4b2-e568-4f8f-bcb9-a3d5ef8b27e5> on November 20, 2012.

Shevell, D. E., Leu, W., Gillmor, C. S., Xia, G., Feldmann, K. A., and Chua, N. (1994). *EMB30* is essential for normal cell division, cell expansion, and cell adhesion in *Arabidopsis* and encodes a protein that has similarity to *Sec7*. *Cell* **77**: 1051-1062.

Shin, R., Burch, A. Y., Huppert, K. A., Tiwari, S. B., Murphy, A. S., Guilfoyle, T. J., and Schachtman, D. P. (2007). The *Arabidopsis* transcription factor MYB77 modulates auxin signal transduction. *Plant Cell* **19**: 2440-2453.

Sieburth, L. E. (1999). Auxin is required for leaf vein pattern in *Arabidopsis*. *Plant Physiol.* **121**: 1179-1190.

Sieburth, L. E., Muday, G. K., King, E. J., Benton, G., Kim, S., Metcalf, K. E., Meyers, L., Seamen, E., and Van Norman, J. M. (2006). *SCARFACE* encodes an ARF-GAP that is required for normal auxin efflux and vein patterning in *Arabidopsis*. *Plant Cell* **18**: 1396-1411.

Silverstone, A. L., Ciampaglio, C. N., and Sun, T. (1998). The *Arabidopsis* *RGA* gene encodes a transcriptional regulator repressing the gibberellin signal transduction pathway. *Plant Cell* **10**: 155-169.

Skirycz, A., Jozefczuk, S., Stobiecki, M., Muth, D., Zanor, M., Witt, I., and Mueller-Roeber, B. (2007). Transcription factor AtDOF4;2 affects phenylpropanoid metabolism in *Arabidopsis thaliana*. *New Phytol.* **175**: 425-438.

Skirycz, A., Radziejwoski, A., Busch, W., Hannah, M. A., Czeszejko, J., Kwasniewski, M., Zanor, M. I., Lohmann, J. U., De Veylder, L., Witt, I., and Mueller-Roeber, B. (2008). The DOF transcription factor OBP1 is involved in cell cycle regulation in *Arabidopsis thaliana*. *Plant J.* **56**: 779-792.

Skirycz, A., Reichelt, M., Burow, M., Birkemeyer, C., Rolcik, J., Kopka, J., Zanor, M. I., Gershenzon, J., Strnad, M., Szopa, J., Mueller-Roeber, B., and Witt, I. (2006). DOF transcription factor AtDof1.1 (OBP2) is part of a regulatory network controlling glucosinolate biosynthesis in *Arabidopsis*. *Plant J.* **47**: 10-24.

Smale, S. T. and Kadonaga, J. T. (2003). The RNA polymerase II core promoter. *Annu Rev Biochem.* **72**: 449-479.

Smith, S. M., Fulton, D. C., Chia, T., Thorneycroft, D., Chapple, A., Dunstan, H., Hylton, C., Zeeman, S. C., and Smith, A. M. (2004). Diurnal changes in the transcriptome encoding enzymes of starch metabolism provide evidence for both transcriptional and posttranscriptional regulation of starch metabolism in *Arabidopsis* leaves. *Plant Physiol.* **136**: 2687-2699.

Song, S., Hofhuis, H., Lee, M. M., and Clark, S. E. (2008). Key divisions in the early *Arabidopsis* embryo require POL and PLL1 phosphatases to establish the root stem cell organizer and vascular axis. *Dev Cell* **15**: 98-109.

Souter, M., Topping, J., Pullen, M., Friml, J., Palme, K., Hackett, R., Grierson, D., and Lindsey, K. (2002). *hydra* mutants of *Arabidopsis* are defective in sterol profiles and auxin and ethylene signaling. *Plant Cell* **14**: 1017-1031.

Sozzani, R., Cui, H., Moreno-Risueno, M. A., Busch, W., Van Norman, J. M., Vernoux, T., Brady, S. M., Dewitte, W., Murray, J. A. H., and Benfey, P. N. (2010). Spatiotemporal regulation of cell-cycle genes by SHORTROOT links patterning and growth. *Nature* **466**: 128-132.

Steffens, N. O., Galuschka, C., Schindler, M., Bulow, L., and Hehl, R. (2004). AthaMap: an online resource for *in silico* transcription factor binding sites in the *Arabidopsis thaliana* genome. *Nucleic Acids Res.* **32**: D368-D372.

Steinmann, T., Geldner, N., Grebe, M., Mangold, S., Jackson, C. L., Paris, S., Galweiler, L., Palme, K., and Jurgens, G. (1999). Coordinated polar localization of auxin efflux carrier PIN1 by GNOM ARF GEF. *Science* **286**: 316-318.

Steynen, Q. J. and Schultz, E. A. (2003). The *FORKED* genes are essential for distal vein meeting in *Arabidopsis*. *Development* **130**: 4695-4708.

Suzuki, T., Miwa, K., Ishikawa, K., Yamada, H., Aiba, H., and Mizuno, T. (2001). The *Arabidopsis* sensor His-kinase, AHK4, can respond to cytokinins. *Plant Cell Physiol.* **42**: 107-113.

Szemenyei, H., Hannon, M., and Long, J. A. (2008). TOPLESS mediates auxin-dependent transcriptional repression during *Arabidopsis* embryogenesis. *Science* **319**: 1384-1386.

Taiz, L. and Zeiger, E. (2010). *Plant Physiology*. Sunderland, MA, USA: Sinauer Associates, Inc.

Tajima, Y., Imamura, A., Kiba, T., Amano, Y., Yamashino, T., and Mizuno, T. (2004). Comparative studies on the type-B response regulators revealing their

distinctive properties in the His-to-Asp phosphorelay signal transduction of *Arabidopsis thaliana*. *Plant Cell Physiol.* **45**: 28-39.

Takahashi, I., Kojima, S., Sakaguchi, N., Umeda-Hara, C., and Umeda, M. (2010). Two *Arabidopsis* cyclin A3s possess G1 cyclin-like features. *Plant Cell Rep.* **29**: 307-315.

Tan, X., Calderon-Villalobos, L. I. A., Sharon, M., Zheng, C., Robinson, C. V., Estelle, M., and Zheng, N. (2007). Mechanism of auxin perception by the TIR1 ubiquitin ligase. *Nature* **446**: 640-645.

Taylor, L. P. and Grotewold, E. (2005). Flavonoids as developmental regulators. *Curr Opin Plant Biol.* **8**: 317-323.

Telfer, A. and Poethig, R. S. (1994). Leaf development in *Arabidopsis*. In *Arabidopsis* (ed. Meyerowitz, E. M. and Somerville, C. R.), pp. 379-401. Cold Spring Harbor, NY, USA: Cold Spring Harbor Laboratory Press.

Tian, C., Muto, H., Higuchi, K., Matamura, T., Tatematsu, K., Koshiba, T., and Yamamoto, K. T. (2004). Disruption and overexpression of *AUXIN RESPONSE FACTOR8* gene of *Arabidopsis* affect hypocotyl elongation and root growth habit, indicating its possible involvement in auxin homeostasis in light condition. *Plant J.* **40**: 333-343.

Tiwari, S. B., Hagen, G., and Guilfoyle, T. J. (2003). The roles of auxin response factor domains in auxin-responsive transcription. *Plant Cell* **15**: 533-543.

Torres-Galea, P., Huang, L., Chua, N., and Bolle, C. (2006). The GRAS protein SCL13 is a positive regulator of phytochrome-dependent red light signaling, but can also modulate phytochrome A responses. *Mol Gen Genomics* **276**: 13-30.

Tsuchisaka, A. and Theologis, A. (2004). Unique and overlapping expression patterns among the *Arabidopsis* *1-AMINO-CYCLOPROPANE-1-CARBOXYLATE SYNTHASE* gene family members. *Plant Physiol.* **136**: 2982-3000.

Tyler, L., Thomas, S. G., Hu, J., Dill, A., Alonso, J. M., Ecker, J. R., and Sun, T. (2004). DELLA proteins and gibberellin-regulated seed germination and floral development in *Arabidopsis*. *Plant Physiol.* **135**: 1008-1019.

Ueki, S. and Citovsky, V. (2000). Intercellular RNA transport in plants. *Curr Top Plant Biol.* **2**: 167-179.

Ulmasov, T., Hagen, G., and Guilfoyle, T. J. (1997a). ARF1, a transcription factor that binds to auxin response elements. *Science* **276**: 1865-1868.

Ulmasov, T., Hagen, G., and Guilfoyle, T. J. (1999a). Activation and repression of transcription by auxin response factors. *Proc Natl Acad Sci U S A.* **96**: 5844-5849.

Ulmasov, T., Hagen, G., and Guilfoyle, T. J. (1999b). Dimerization and DNA binding of auxin response factors. *Plant J.* **19**: 309-319.

Ulmasov, T., Liu, Z., Hagen, G., and Guilfoyle, T. J. (1995). Composite structure of auxin response elements. *Plant Cell* **7**: 1611-1623.

Ulmasov, T., Murfett, J., Hagen, G., and Guilfoyle, T. J. (1997b). AUX/IAA proteins repress expression of reporter genes containing natural and highly active synthetic auxin response elements. *Plant Cell* **9**: 1963-1971.

Vandepoele, K., Raes, J., De Veylder, L., Rouze, P., Rombauts, S., and Inze, D. (2002). Genome-wide analysis of core cell cycle genes in *Arabidopsis*. *Plant Cell* **14**: 903-916.

Vanneste, S., Coppens, F., Lee, E., Donner, T. J., Xie, Z., Van Isterdael, G., Dhondt, S., De Winter, F., De Rybel, B., Vuylsteke, M., De Veylder, L., Friml, J., Inze, D., Grotewold, E., Scarpella, E., Sack, F., Beemster, G. T. S., and Beeckman, T. (2011). Developmental regulation of *CYCA2s* contributes to tissue-specific proliferation in *Arabidopsis*. *EMBO J.* **30**: 3430-3441.

Vanneste, S., De Rybel, B., Beemster, G. T. S., Ljung, K., De Smet, I., Van Isterdael, G., Naudts, M., Iida, R., Gruissem, W., Tasaka, M., Inze, D., Fukaki, H., and Beeckman, T. (2005). Cell cycle progression in the pericycle is not sufficient for SOLITARY ROOT/IAA14-mediated lateral root initiation in *Arabidopsis thaliana*. *Plant Cell* **17**: 3035-3050.

Varaud, E., Brioude, F., Szecsi, J., Leroux, J., Brown, S., Perrot-Rechenmann, C., and Bendahmane, M. (2011). AUXIN RESPONSE FACTOR8 regulates *Arabidopsis* petal growth by interacting with the bHLH transcription factor BIGPETALp. *Plant Cell* **23**: 973-983.

Vernoux, T., Brunoud, G., Farcot, E., Morin, V., Van den Daele, H., Legrand, J., Oliva, M., Das, P., Larrieu, A., Wells, D., Guedon, Y., Armitage, L., Picard, F., Guyomarc'h, S., Cellier, C., Parry, G., Koumproglou, R., Doonan, J. H., Estelle, M., Godin, C., Kepinski, S., Bennett, M., De Veylder, L., and Traas, J. (2011). The auxin signalling network translates dynamic input into robust patterning at the shoot apex. *Mol Syst Biol.* **7**: 508.

Wagner, D. and Meyerowitz, E. M. (2002). SPLAYED, a novel SWI/SNF ATPase homolog, controls reproductive development in *Arabidopsis*. *Curr Biol.* **12**: 85-94.

- Walcher, C. L. and Nemhauser, J. L.** (2012). Bipartite promoter element required for auxin response. *Plant Physiol.* **158**: 273-282.
- Wang, H., Jones, B., Li, Z., Frasse, P., Delalande, C., Regad, F., Chaabouni, S., Latche, A., Pech, J. C., and Bouzayen, M.** (2005a). The tomato *AUX/IAA* transcription factor *IAA9* is involved in fruit development and leaf morphogenesis. *Plant Cell* **17**: 2676-2692.
- Wang, J., Wang, L., Mao, Y., Cai, W., Xue, H., and Chen, X.** (2005b). Control of root cap formation by microRNA-targeted AUXIN RESPONSE FACTORS in *Arabidopsis*. *Plant Cell* **17**: 2204-2216.
- Ward, J. M., Cufu, C. A., Denzel, M. A., and Neff, M. M.** (2005). The DOF transcription factor OBP3 modulates phytochrome and cryptochrome signaling in *Arabidopsis*. *Plant Cell* **17**: 475-485.
- Weijers, D., Sauer, M., Meurette, O., Friml, J., Ljung, K., Sandberg, G., Hooykaas, P., and Offringa, R.** (2005). Maintenance of embryonic auxin distribution for apical-basal patterning by PIN-FORMED-dependent auxin transport in *Arabidopsis*. *Plant Cell* **17**: 2517-2526.
- Weijers, D., Schlereth, A., Ehrismann, J. S., Schwank, G., Kientz, M., and Jurgens, G.** (2006). Auxin triggers transient local signaling for cell specification in *Arabidopsis* embryogenesis. *Dev Cell* **10**: 265-270.
- Wen, C. and Chang, C.** (2002). *Arabidopsis RGL1* encodes a negative regulator of gibberellin responses. *Plant Cell* **14**: 87-100.
- Wenzel, C. L., Schuetz, M., Yu, Q., and Mattsson, J.** (2007). Dynamics of *MONOPTEROS* and PIN-FORMED1 expression during leaf vein pattern formation in *Arabidopsis thaliana*. *Plant J.* **49**: 387-398.
- Wildwater, M., Campilho, A., Perez-Perez, J. M., Heidstra, R., Blilou, I., Korthout, H., Chatterjee, J., Mariconti, L., Gruitsem, W., and Scheres, B.** (2005). The *RETINOBLASTOMA-RELATED* gene regulates stem cell maintenance in *Arabidopsis* roots. *Cell* **123**: 1337-1349.
- Wilmoth, J. C., Wang, S., Tiwari, S. B., Joshi, A. D., Hagen, G., Guilfoyle, T. J., Alonso, J. M., Ecker, J. R., and Reed, J. W.** (2005). NPH4/ARF7 and ARF19 promote leaf expansion and auxin-induced lateral root formation. *Plant J.* **43**: 118-130.
- Wilson, M. D. and Odom, D. T.** (2009). Evolution of transcriptional control in mammals. *Curr Opin Genet Dev.* **19**: 579-585.

- Wisniewska, J., Xu, J., Seifertova, D., Brewer, P. B., Ruzicka, K., Blilou, I., Rouquie, D., Benkova, E., Scheres, B., and Friml, J.** (2006). Polar PIN localization directs auxin flow in plants. *Science* **312**: 883.
- Worley, C. K., Zenser, N., Ramos, J., Rouse, D., Leyser, O., Theologis, A., and Callis, J.** (2000). Degradation of AUX/IAA proteins is essential for normal auxin signalling. *Plant J.* **21**: 553-562.
- Wray, G. A.** (2007). The evolutionary significance of *cis*-regulatory mutations. *Nat Rev Genet.* **8**: 206-216.
- Xie, Z., Lee, E., Lucas, J. R., Morohashi, K., Li, D., Murray, J. A. H., Sack, F. D., and Grotewold, E.** (2010). Regulation of cell proliferation in the stomatal lineage by the *Arabidopsis* MYB FOUR LIPS via direct targeting of core cell cycle genes. *Plant Cell* **22**: 2306-2321.
- Xu, J., Hofhuis, H., Heidstra, R., Sauer, M., Friml, J., and Scheres, B.** (2006). A molecular framework for plant regeneration. *Science* **311**: 385-388.
- Yamasaki, K., Kigawa, T., Inoue, M., Tateno, M., Yamasaki, T., Yabuki, T., Aoki, M., Seki, E., Matsuda, T., Tomo, Y., Hayami, N., Terada, T., Shirouzu, M., Osanai, T., Tanaka, A., Seki, M., Shinozaki, K., and Yokoyama, S.** (2004). Solution structure of the B3 DNA binding domain of the *Arabidopsis* cold-responsive transcription factor RAV1. *Plant Cell* **16**: 3448-3459.
- Yanagisawa, S.** (2002). The DOF family of plant transcription factors. *Trends Plant Sci.* **7**: 555-560.
- Yanagisawa, S. and Schmidt, R. J.** (1999). Diversity and similarity among recognition sequences of DOF transcription factors. *Plant J.* **17**: 209-214.
- Yokoyama, A., Yamashino, T., Amano, Y., Tajima, Y., Imamura, A., Sakakibara, H., and Mizuno, T.** (2007). Type-B ARR transcription factors, ARR10 and ARR12, are implicated in cytokinin-mediated regulation of protoxylem differentiation in roots of *Arabidopsis thaliana*. *Plant Cell Physiol* **48**: 84-96.
- Yoshizumi, T., Tsumoto, Y., Takiguchi, T., Nagata, N., Yamamoto, Y. Y., Kawashima, M., Ichikawa, T., Nakazawa, M., Yamamoto, N., and Matsui, M.** (2006). INCREASED LEVEL OF POLYPLOIDY1, a conserved repressor of *CYCLINA2* transcription, controls endoreduplication in *Arabidopsis*. *Plant Cell* **18**: 2452-2468.
- Yu, Y., Steinmetz, A., Meyer, D., Brown, S., and Shen, W.** (2003). The tobacco A-type cyclin, *Nicta;CYCA3;2*, at the nexus of cell division and differentiation. *Plant Cell* **15**: 2763-2777.

- Zhang, C., Gong, F. C., Lambert, G. M., and Galbraith, D. W.** (2005). Cell type-specific characterization of nuclear DNA contents within complex tissues and organs. *Plant Methods* **1**: 7.
- Zhao, Z., Andersen, S. U., Ljung, K., Dolezal, K., Miotk, A., Schultheiss, S. J., and Lohmann, J. U.** (2010). Hormonal control of the shoot stem-cell niche. *Nature* **465**: 1089-1092.
- Zhou, G., Kubo, M., Zhong, R., Demura, T., and Ye, Z.** (2007). Overexpression of *miR165* affects apical meristem formation, organ polarity establishment, and vascular development in *Arabidopsis*. *Plant Cell Physiol.* **48**: 391-404.
- Zinzen, R. P., Girardot, C., Gagneur, J., Braun, M., and Furlong, E. E. M.** (2009). Combinatorial binding predicts spatio-temporal *cis*-regulatory activity. *Nature* **462**: 65-70.